To the Graduate Council:

I am submitting herewith a dissertation written by James Charles Conklin entitled "Thermophoretic Transport of Particles That Act as Volumetric Heat Sources in Natural Convection Flow." I have examined the final copy of this dissertation for form and content and recommend that it be accepted in partial fulfillment of the requirements for the degree of Doctor of Philosophy, with a major in Mechanical Engineering.

Robert J. Krane

Robert J. Krane, Major Professor

We have read this dissertation
and recommend its acceptance:

Accepted for the Council:

C. W. Minkel

Vice Provost
and Dean of The Graduate School

# THERMOPHORETIC TRANSPORT OF PARTICLES THAT ACT AS VOLUMETRIC HEAT SOURCES IN NATURAL CONVECTION FLOW

A Dissertation

Presented for the

Doctor of Philosophy

Degree

The University of Tennessee, Knoxville

James Charles Conklin

August 1989

## ACKNOWLEDGMENTS

I expressly acknowledge my major professor, Dr. R. J. Krane of the Department of Mechanical and Aerospace Engineering in the College of Engineering at The University of Tennessee. His extensive knowledge of thermal-flow sciences is impressive and his professorial enthusiasm is inspiring. I acknowledge the guidance of Drs. S. A. Hodge and T. S. Kress of the Oak Ridge National Laboratory, who suggested the topic of this dissertation and provided partial funding from December 1983 to March 1985 from the Severe Accident Sequence Analysis program of the Nuclear Regulatory Commission. I acknowledge with gratitude my supervisor at the Oak Ridge National Laboratory, Mr. S. J. Ball, for his support and forbearance during my doctoral program.

## ABSTRACT

The natural convection boundary layer with suspended heat generating aerosol particles adjacent to a cooled, isothermal, vertical wall was investigated for the following circumstances: laminar and turbulent flow, large temperature differences between the wall and the fluid, stable thermal stratification far from the wall, and fluid participation in thermal radiation heat transfer. The deposition of aerosol particles by thermophoresis was investigated.

A scaling analysis showed the negligible effect inside the boundary layer of the particulate heat source strengths of practical interest. Only the temperature of the fluid far from the wall is affected appreciably by the heat sources. The scaled boundary layer differential equations are transformed to a nonsimilarity form for numerical solution using two different methods.

An expression for the ratio of mass transfer to heat transfer coefficients was developed to simplify the computation of thermophoretic particle deposition at the wall for the case of constant temperature conditions far from the wall. Variable thermophysical property effects for the three gases of steam, air, and hydrogen were investigated. A dimensionless ratio of transfer coefficients for large temperature differences and turbulent flow was computed as a product of the laminar constant property results and a ratio of the known thermophysical properties at the wall and far from the wall. An approximation of the laminar constant property results for all three gases is developed in terms of the known wall and fluid temperatures, Prandtl number, and a thermophoretic constant. This allows particle deposition to be computed from a known heat transfer coefficient without explicitly solving the particle conservation equation.

Very low heat source strengths result in a quadratic vertical temperature distribution far from the wall. As a result of this thermal stratification in the freestream, particle movement from outside the boundary layer toward the wall is blocked from reaching the wall at a point approximately halfway down the wall due to detraining outflow.

Thermophoretic particle deposition in the presence of participating thermal radiation was investigated using the diffusion or Rosseland approximation. A decreased temperature gradient caused by an increase in the effective thermal conductivity results in decreased thermophoretic particle deposition.

## TABLE OF CONTENTS

CHAPTER PAGE

CHAPTER PAGE

## LIST OF TABLES

## LIST OF FIGURES

FIGURE PAGE

# CHAPTER 1

## INTRODUCTION

Natural convection flows occur in many types of industrial systems, whether as an intended method of heating or cooling a fluid or structure or as a result of abnormal operation. This dissertation investigates a class of natural convection flows that may occur as a result of a severe accident at a nuclear power reactor. These flows are of practical interest because they must be understood by reactor designers and operators. They are also of academic interest because of the many unusual phenomena that arise due to the extreme conditions under which these flows would take place.

During a reactor accident, natural convection will occur in the steam next to the vertical walls of the reactor vessel. These natural convection flows are similar to those that occur next to a cooled vertical flat plate. The presence of radioactive particles in the fluid, however, is likely in accident circumstances. These particles transfer their radioactive decay energy to the fluid in the form of volumetric heating due to the beta rays and to the confining structures by gamma radiation. The analysis of the gamma ray energy transfer was beyond the scope of this dissertation. The volumetric heating due to the beta rays results in an additional term in the energy equation. Also, the temperature difference between the reactor vessel wall and the fluid is large, such that the effect of variable thermophysical properties of the fluid must be considered in the governing equations. The turbulent nature of the resulting flows is also considered.

Another unusual aspect of these flows is the transport of the radioactive particles to the wall by thermally induced forces. The movement of particles down a temperature gradient in the fluid is called thermophoresis. Thermophoretic movement of the radioactive particles makes the volumetric heat source a function of position from the wall, since the concentration of particles decreases as the wall was approached. The heat generated by a particle is assumed to be entirely absorbed by the constant temperature wall after deposition and, therefore, to no longer affect the flow. The presence of thermophoresis requires the analyst to account for particle conservation as well as energy conservation.

Certain aspects of the flows of interest here have been studied by others both experimentally and analytically. All of the phenomena mentioned above, however, had not been simultaneously present in any flow previously investigated. It is doubtful that a laboratory experiment could be devised to encompass all the effects included in this problem. The results for fluid temperature profiles, wall heat transfer, and wall particle flux computed in this investigation are compared with the experimental results of other investigations on the individual aspects of this problem.

The desired results of this investigation are simplified relationships for the rates of heat transfer and particle deposition appropriate for the conditions in the upper section of a Boiling Water Reactor (BWR) that has undergone a severe accident. The parameters investigated include:

1. Large wall-to-fluid temperature differences on the order of the fluid temperature.
2. A range of volumetric heat source strengths up to 5 $kW/m^3$.
3. A range of spherical particle sizes from 0.1 μm to 10.0 μm in diameter.

# CHAPTER 2

# MOTIVATION AND DESCRIPTION OF THE RESEARCH

## 2.1. Introduction

During certain severe accident conditions in a boiling water reactor (BWR), there will be no net flow out of or into the reactor vessel. During this period, forced convection induced by a rise in the reactor core pressure due to nuclear decay heating will move steam from the core to the upper plenum of the reactor vessel. This steam will contain radioactive fission products entrained in the flow as volatile species, noble gases, and aerosols. The fission product radioactive decay energy is transferred directly by gamma radiation into the walls of the confining reactor internals and by beta radiation locally to the fluid in the immediate vicinity of the fission product. This fission product may itself be an aerosol, or may be adsorbed on an inert aerosol particle. The fate of these fission products is of paramount importance for reactor safety studies, as the health and safety of the public requires isolation of these fission products from the environment.

This research investigated the natural convection flow adjacent to the reactor vessel inside wall during the period when the flow is essentially quiescent in the upper section of the reactor vessel. The steam adjacent to the reactor vessel inner wall contains aerosol heat sources suspended as particles, with the steam having a temperature significantly higher than that of the reactor vessel wall. The colder wall induces a downward, possibly turbulent, natural convection flow and establishes a temperature gradient normal to the wall that causes the aerosol particles to migrate toward the wall by the mechanism of thermophoresis. This particle movement establishes a particle concentration gradient, which in turn, establishes a non-uniform distribution of the volumetric heat source strength in the boundary layer adjacent to the reactor vessel wall. The heat source strength of each particle is assumed to remain constant over the relatively short time scale of interest for the fluid, on the order of minutes, as compared to the relatively long time scale for radioactive decay, which is on the order of hours.

## 2.2. Geometry

The actual Boiling Water Reactor (BWR) upper pressure vessel geometry is somewhat complicated since it includes such structures as the steam dryers, as shown in Figure 2-1. Thus, a simplified geometry consisting of a vertical, isothermal flat plate of fixed height, which is immersed in a semi-infinite fluid containing heat generating particles, was used for this investigation. The use of this simple geometry enabled the investigation to focus on the interactions between the various phenomena of interest in the flow without the added problems inherent in modeling a complicated geometry. A drawing of the simplified flow geometry appears in Figure 2-2. Flow in only two dimensions lengthwise and normal to the wall was considered.

A length of three meters was chosen as the characteristic plate height for this analysis. This is a typical axial distance along the vessel wall from the upper vessel head flange to where the steam separators are located, as shown on Figure 2-1.

The approximation of the interior wall of the cylindrical reactor vessel by a flat plate is reasonable due to the large radius of curvature (3.2 m) in a horizontal plane and the relatively thin boundary layer thickness. The laminar flow velocity boundary layer thickness was estimated from $\delta/L = Gr^{-1/4}$ (Jaluria, 1980). At a Rayleigh number of $2\times10^{9}$, representing the transition from laminar to turbulent natural convective flow regimes, the boundary layer thickness is on the order of 14 mm for a characteristic length of 3 m. A "thermal microscale" applicable for turbulent natural convection boundary layers is estimated from the relationship $\delta/L = Gr^{-1/3}$ (Arpaci, 1986). At a turbulent Grashof number of $5\times10^{12}$, computed for steam conditions of 6.9 MPa and 1000°C and wall temperature of 300°C, the turbulent thermal microscale is approximately 0.17 mm for the same characteristic length of 3 m. Therefore, laminar flow conditions set an upper limit for an estimate of boundary layer thickness. The distance from the vessel wall to the nearest structure, the steam dryer shroud, is 500 mm which justifies the semi-infinite fluid assumption.

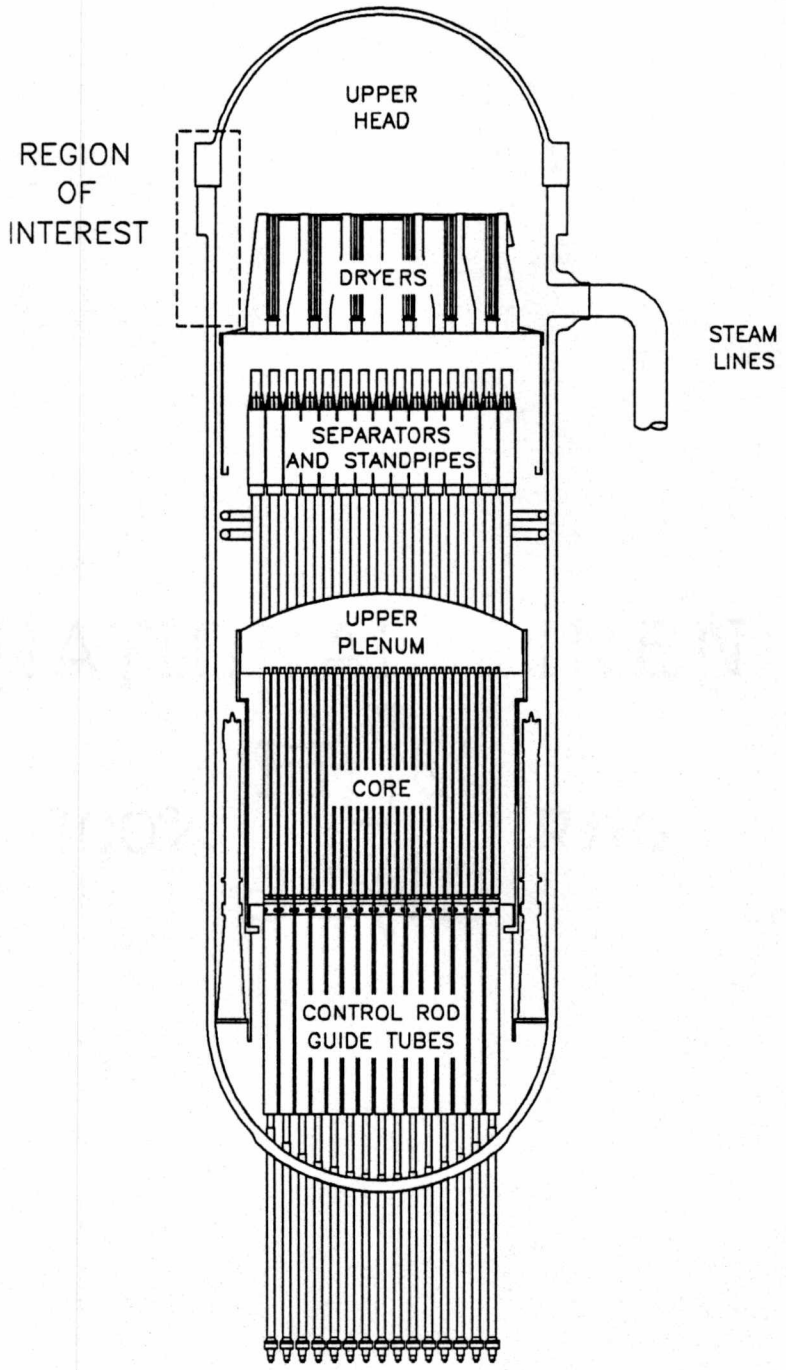


Figure 2-1. Boiling Water Reactor Internals.

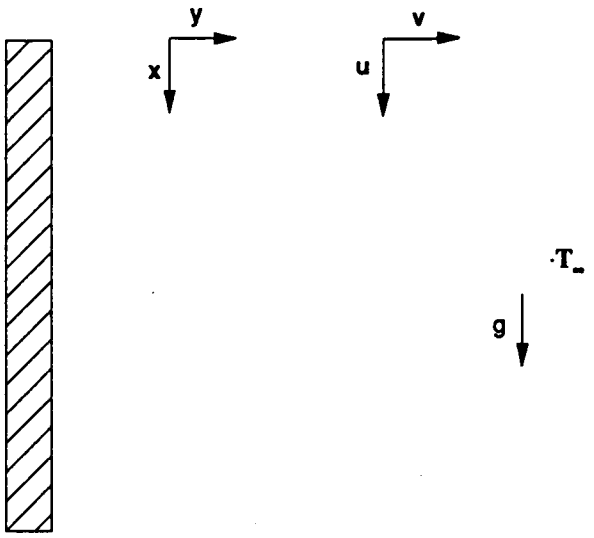


Semi-infinite Newtonian fluid containing particles, each acting as a heat source with a strength of $\gamma$ watts, where $T_\infty > T_w$.

Thick, vertical flat plate of finite length $L$ and at an isothermal temperature of $T_w$

Figure 2-2. Flow Geometry.

The reactor vessel wall temperature was set to 300°C, with steam conditions on the order of 1000°C and 6.9 MPa. These steam conditions are representative of a newtonian fluid with a molecular Prandtl number on the order of unity (Keenan et al., 1969; Kreith, 1973). The assumption of constant vessel wall temperature is justified by the scaling arguments is given in Appendix D. These arguments consider the relative heat capacities of the reactor vessel wall and the steam. The reactor vessel wall temperature will increase, but at a much slower rate than that of the steam, even though the steam contains entrained volumetric heat sources. Hodge (1988) estimates that an upper limit estimate of the volumetric strength of the heat sources is 5 kW/m$^3$.

### 2.3. Variable Thermophysical Fluid Properties

Most published investigations of natural convection flow make use of the Boussinesq approximation to simplify the analysis. The Boussinesq approximation neglects all property variations except that of the density in the body force term in Newton's second law. Because the difference between the initial wall temperature and the fluid temperature is large and on the order of the absolute temperature of the steam, $\Delta T/T = O(1)$, the Boussinesq approximation is invalid for the flows of interest. For these flows, variations of the thermophysical properties with temperature were considered.

### 2.4. Fluid Temperature Distributions Far from the Wall

Only thermally stable conditions in the fluid outside of the boundary layer were considered. Specifically, two cases in which the fluid temperature outside of the boundary layer increases with height, or is constant with respect to height, are of interest in this investigation. The first case is that of completely quiescent fluid with entrained heat sources. According to Sparrow et al. (1963), the temperature profile under these conditions is quadratic with respect to distance along the plate. Sparrow et al. (1963) defined a Rayleigh number $Ra^*$, based upon the internal heat source strength $Q$, that has the form:

$$Ra^* = \frac{g\beta Q L^5}{\alpha \nu k}. \qquad (2-1)$$

Sparrow et al. (1963) stated that the upper limit for stability is a Rayleigh number of 37 325. This upper limit on the ability of the fluid outside of the boundary layer to remain stable sets the upper limit on the heat source strength in the boundary layer that is applicable for this first case.

A second possible temperature distribution in the fluid outside of the boundary layer is that of a constant temperature. According to Sparrow et al. (1963), this implies a non-zero velocity in the freestream. Greene (1982) performed an experiment with a volumetrically heated pool of aqueous electrolyte and observed a boundary layer next to a cooled wall that he claimed was typical of a laminar natural convection boundary layer. Greene, however, did not address the non-zero freestream velocity circumstances when presenting his analysis. Subsequent analysis performed in the present investigation and presented in Section 5.3.1 shows that the heat transfer at the vertical wall for Greene's experimental circumstances was not applicable for the flows of interest of this present work.

However, for a case comparable to that of Greene where the Richardson number, defined as the ratio of the Grashof number to the square of the Reynolds number, is on the order of 500, Kikuchi et al. (1986) show that the temperature perturbations in the fluid due to turbulent fluctuations far from the walls in an enclosed volumetrically heated cavity are less than 10% of the difference in wall temperatures. Hence, they show that this negligible, but non-zero, freestream velocity has little effect upon the heat transferred to the wall by natural convection.

### 2.5. Aerosol Transport with Thermophoresis

According to Wichner et al. (1984), approximately 8 kg of aerosol would be produced upon a reactor vessel failure. The volume of a typical large BWR is 600 $m^3$. If the aerosol was distributed uniformly throughout the reactor vessel, assuming that the aerosol is composed of mostly the reactor vessel structural material of steel which has a density of 7800 $kg/m^3$, and assuming that the aerosol particles have a diameter of one micrometer, the number of particles per unit volume would be $3.25 \times 10^{12}$ $m^{-3}$. Since the density of steam is 11.8 $kg/m^3$ at the conditions of 6.9 MPa and 1000°C, the number of

particles per unit mass of steam is $2.75\times10^{11}$ kg$^{-1}$. Thus, the volumetric fraction of the particles is $1.7\times10^{-6}$ and, as shown in Appendix D, the presence of aerosol particles does not significantly affect the conservation of mass equation, the equation for Newton's Second Law, or the conservation of energy equation when these equations are written for the fluid alone.

The aerosol particles are assumed to be spherical in shape with diameters on the order of 1 μm. Knudsen numbers in the range from $0 < Kn < 0.25$ were investigated. The Knudsen number is defined as the ratio of the mean free path of the fluid to the particle radius. Only monodisperse (i.e., one diameter) aerosols were modeled. A range of particle diameters from 0.1 μm to 10.0 μm (Wright and Arwood, 1987) was considered. The assumption of monodisperse spherical particles was made for the same reasons as was the simplified geometry of the flat plate, that is, to focus the analysis on the interactions of thermophoretic particle transport with the fluid and the wall, rather than the complicated interactions between different shapes and sizes of particles. Also, this assumption was used to help reduce the particle conservation equation to a convenient form, as is shown in Appendix D.

The thermophoretic coefficient, $K$, depends on the thermal conductivities of both the particle and the fluid and on the Knudsen number. A derivation of an expression for $K$, based upon the analysis by Brock (1962), is presented in Appendix C. Talbot et al. (1980) presented comparisons of theoretical and experimental results for thermophoretic velocities using different values of the thermophoretic coefficient $K$. Since no existing correlation for $K$ appears to be best for the aerosols under investigation, a range of values for $K$ on the order of unity was used (Epstein et al., 1985).

### 2.6. Turbulence Modeling

A very large body of information has been developed for turbulent flows. The emphasis in this particular investigation was not to develop a new turbulence model, but to utilize and modify as required an existing model of turbulence to investigate the effects of turbulence on heat and mass transfer to the wall. Accordingly, a simple turbulence model, based on Prandtl's mixing length hypothesis (Launder and Spalding,

1972) with an algebraic closure for the mixing length was employed. The computed results for heat transfer of the model are compared to experimental results for heat transfer in a turbulent natural convection boundary layer flow to ensure that the turbulence model yields reasonable results for heat transfer.

The turbulence model was assumed to remain essentially unaffected by the presence of the particles. A dimensionless "stopping distance parameter" for turbulent particle pipe flow, $S^+$, was derived by McCoy and Hanratty (1977). This parameter can also be interpreted as the dimensionless relaxation time for a particle initially moving at the shear friction velocity to be brought to zero velocity by Stokes drag. This parameter has the form:

$$S^+ = \frac{d_P^2 u^{*2} \rho_P}{18 \nu^2 \rho_f}. \qquad (2-2)$$

McCoy and Hanratty (1977) analyzed experimental particle deposition data and concluded that particles with a dimensionless stopping distance less than 0.15 followed the laminar streamlines near the wall with no inertial deposition on the wall. The dimensionless stopping distance was $10^{-6}$ for a particle with 1 μm diameter at a Grashof number of $10^{12}$ in steam. With such a small stopping distance, the particles were assumed to follow the turbulent eddies.

The dimensional stopping distance for a particle to be brought to rest from the shear friction velocity by Stokes drag is given by the expression (McCoy and Hanratty, 1977):

$$\text{Stokes stopping distance} = \frac{d_P^2}{18} \frac{\rho_P u^*}{\mu_f} = S^+ \frac{\nu}{u^*}. \qquad (2-3)$$

For a 10 μm diameter particle in a flow with a Grashof number of $10^{12}$, the Stokes stopping distance given by equation (2-4) is approximately 2 μm, or one-fifth the particle diameter. This distance is much smaller than the turbulent laminar sublayer, which is

on the order of 200 μm (George and Capp, 1979). Because of this small Stokes stopping distance, the particles will not penetrate the laminar sublayer adjacent to the wall due to inertial forces. *Thus, inertial deposition is neglected.*

Rouhiainen and Stachiewicz (1970) present an analysis for particle deposition from turbulent flows where a shear-flow-induced lift force also moved particles to the wall through the laminar sublayer from a turbulent core. This lift force is due to the Magnus effect caused by particle movement in a shear stress gradient as analyzed by Saffman (1965). The shear stress gradient causes the spherical particle to spin, which would induce movement towards the wall for particles moving parallel to the wall and moving faster than the fluid. Boothroyd (1971) presented an expression for the ratio of the lift force to the Stokes drag force, which has the form:

$$\frac{F_{lift}}{F_{Stokes}} = 0.171\, d_P \left(\frac{1}{\nu}\frac{du}{dy}\right)^{1/2}. \qquad (2-4)$$

For particles with a diameter of 1 μm in a flow with a Grashof number of $10^{12}$, the ratio given by equation (2-2) is $2\times10^{-3}$, which indicates that any movement due to the Magnus effect lift force would be quickly damped by the Stokes drag force. This ratio would be even smaller for lower Grashof number flows. *Thus, particle deposition by the Magnus effect is neglected.*

The simple turbulence model is based upon a two-layer, or two-zone, postulate as presented by Cebeci and Khattab (1975). The natural convection velocity boundary layer is divided into two regions; the inner region where friction and buoyant effects are important, and the outer region where friction and inertial effects are important. A model presented by Reynolds (1978) is used for the near wall region and a model based upon Prandtl's hypothesis (Schlichting, 1979) for turbulent free jets is used for the outer region. Different expressions were investigated in each zone for the turbulent Prandtl number $Pr_t$, representing the ratio of the turbulent diffusivity of momentum to the turbulent diffusivity of thermal energy, and for the turbulent Schmidt number $Sc_t$, representing the ratio of the turbulent diffusivity of momentum to the turbulent diffusivity of the particles.

### 2.7. Gamma and Thermal Radiation Modeling

In the flows of interest in this investigation, there is both gamma radiation emitted from the radioactive decay of the fission products and thermal radiation emitted from the steam molecules. Due to the differing radiation absorption characteristics of steam at the stated conditions of 6.9 MPa and 1000°C, the gamma radiation passes through the boundary layer with little absorption, while the thermal radiation energy emitted by the steam molecules is absorbed immediately by an adjacent molecule in the boundary layer.

The gamma energy given off by the fission products of interest is in the range of 16 femtojoule to 160 femtojoule (0.1 MeV to 1.0 MeV) (Etherington, 1958). The intensity of the gamma radiation is attenuated at an exponential rate, which is dependent on the path length and the absorption coefficient. The absorption coefficient is dependent on the nuclear absorption process and the specific fluid. The gamma radiation is attenuated according to the following expression:

$$\frac{I}{I_\infty} = \exp(-\mu\delta)\,. \qquad (2-5)$$

The absorption coefficient for the 16 fJ (0.1 MeV) gamma rays has the largest value of 1.8 $m^{-1}$ (El-Wakil, 1962) in steam at the stated conditions. For the laminar boundary layer thickness of 14 mm, the gamma radiation is attenuated by a factor of 2.5%, with 97.5% of the lowest energy gamma rays passing through the boundary layer and being absorbed in the reactor wall. As the absorption coefficient decreases with an increase in gamma energy, even less of the high energy gamma rays are absorbed in the boundary layer. Thus, the gamma radiation from the particles is assumed to not significantly heat the fluid in the boundary layer.

The molecules of steam absorb and emit thermal radiation at infrared wavelengths. A measure of the participating gas radiation heat transfer (Sparrow and Cess, 1966) is the dimensionless optical thickness $\tau$, which is defined as $\tau = \kappa L$, where $\kappa$ is an absorption coefficient and $L$ is a path length. The absorption coefficient of steam is

dependent upon wavelength. For the stated steam conditions, the absorption coefficient varies from 220 $m^{-1}$ for the Planck mean absorption coefficient to 15 400 $m^{-1}$ for the Rosseland mean absorption coefficient (Abu-Romia and Tien, 1967). For the laminar boundary layer thickness of 14 mm, the optical thickness varies from 3.3 (Planck mean) to 235 (Rosseland mean). Thus, the optically thick, or Rosseland, assumption is justified under these circumstances.

The optically thick assumption makes an analogy between radiation heat transfer and a diffusion process such as conduction heat transfer. Sparrow and Cess (1966) used this analogy with conduction heat transfer and developed an analysis for forced convection heat transfer from a non-reflecting, diffusely emitting and absorbing (black) flat plate. Sparrow and Cess (1966) developed a parameter, $M$, that represents the ratio of conduction heat transfer and radiation heat transfer in the optically thick limit. $M$ has the form:

$$M = \frac{k\kappa}{4\sigma T_{\infty}^3}. \qquad (2-6)$$

For the stated steam conditions, this parameter varies from $6\times10^{-4}$ to $4.4\times10^{-2}$, indicating that radiation heat transfer is an important heat transfer mode in the flows of interest here. Thus, the procedure used by Sparrow and Cess (1966) for the optically thick radiation heat transfer from a participating gas to a black flat plate was used in this investigation.

The value of the emissivity of the flat plate has little effect on the heat transfer to the wall for large optical depths. Viskanta and Grosch (1962b) analyzed for the effect of surface emissivity on simultaneous conduction and radiation heat transfer for a participating gas between two flat plates for various values of the parameter $M$ and the optical depth. For an optical depth of 10.0 and an $M$ parameter value of 0.01, the difference between the computed plate heat flux values was less than 9% for plate emissivity values of 1.0 and 0.5. This range of emissivity values is applicable to the steel reactor vessel wall of the BWR. For the larger optical depths in this problem, the surface emissivity has less effect on the heat transfer results.

# CHAPTER 3

# LITERATURE SURVEY

The categories of the published literature concerning this investigation were arbitrarily defined as follows:

1. Laminar and turbulent natural convection flow with constant thermophysical properties for isothermal flat plates.
2. Variable property effects on natural convection flows.
3. Natural convection flows in a thermally stratified fluid.
4. Aerosol transport by combined convection and thermophoresis.
5. Turbulence modeling.
6. The effects of volumetric heat sources on natural convection.
7. Numerical methods.
8. Natural convection with participating gas thermal radiation.

The literature surveyed in these categories is described in the following subsections.

## 3.1. Investigations Based on the Assumption of Constant Thermophysical Properties

Although the physical conditions of interest in this investigation require consideration of variable thermophysical properties, situations where the wall overheat ratio, defined as $\lambda = (T_w - T_\infty)/T_\infty$, is less than 0.1 may also occur. Since the methods developed in this investigation should be applicable for low wall overheat ratios, heat transfer results based on the assumption of constant thermophysical properties are also surveyed in this subsection.

An important pioneering work on the laminar natural convection flow on a vertical, isothermal flat plate is that of Schmidt and Beckmann (1930). This work presents an analysis and experimental results for the laminar natural convection of air over a vertical, isothermal flat plate. A very useful heat transfer correlation from their work has the form:

$$Nu = H(Pr)Ra^{1/4}, \qquad (3-1)$$

where $H(Pr)$ is a function of the Prandtl number only.

This particular correlation, verified by Eckert and Soehngen (1948), is important, since any numerical method used to compute natural convection heat transfer for the stated conditions of laminar flow over an isothermal flat plate in a constant temperature freestream must compare well with this relationship.

Ostrach (1953) formally extended the laminar analysis from fundamental considerations, showed that the flow was of a boundary-layer nature for large Grashof numbers, and presented a similarity solution. Ostrach also presented a table of numerical solutions for the dimensionless heat transfer and viscous shear at the wall for a large range of Prandtl numbers (0.01 to 1000.0).

Ede (1967) presents a comprehensive review of the theoretical analysis and experimental data for the heat transfer in natural convection flows over vertical flat plates and vertical circular cylinders. Ede observed that Ostrach's similarity solution predicts reasonably well the heat transfer results for Rayleigh numbers from $10^6$ to $10^8$. The Ostrach solution underpredicts the heat transfer, however, for Rayleigh numbers higher than $10^8$ and lower than $10^6$.

Churchill and Usagi (1972) present a correlation of the form of equation (3-1) based on an analysis of various experimental results over a wide range of Prandtl numbers. The coefficient $H(Pr)$ in this correlation has the form:

$$H(Pr) = \frac{0.503}{[1. + (0.492/Pr)^{9/16}]^{4/9}} \quad . \qquad (3-2)$$

Bayley (1955) presents an integral analysis of turbulent natural convection, using assumptions of turbulent velocity and temperature profiles within the natural convection boundary layer. Bayley did not employ the Prandtl mixing length hypothesis, since in a natural convection flow the turbulent diffusivity computed with this model would be zero at the velocity maximum, which is physically unrealistic. Bayley used a constant value for turbulent diffusivity of seven times the kinematic viscosity, ($\nu_t = 7\nu$), integrated

the assumed (polynomial) velocity and temperature profiles across the boundary layer, and developed the following expression for the mean Nusselt number, which is valid for Rayleigh number flows between $2\times10^9$ and $10^{12}$:

$$Nu = 0.10\,Ra^{1/3}. \qquad (3-3)$$

Bayley showed that this correlation compared favorably with the experimental data for air available to him at the time.

Saunders (1939) experimentally investigated the turbulent heat transfer from a vertical plate in water and presented the following correlation for Rayleigh numbers greater than $10^{10}$:

$$Nu = 0.17Ra^{1/3}. \qquad (3-4)$$

For a similar geometry in air, Warner and Arpaci (1968) present results in agreement with equation (3-4), while similar experiments by Cheesewright (1968) and Seibers et al. (1985) present results that are in better agreement with equation (3-3). Saunders (1939) also performed experiments in air and presents the identical correlation, equation (3-3), for turbulent heat transfer from a flat plate as did Bayley (1955).

### 3.2. Investigations Based on the Assumption of Variable Thermophysical Properties

The Boussinesq approximation, commonly used in natural convection flows, neglects all property variations except for density differences in the body force term of Newton's Second Law. Gray and Giorgini (1976) mathematically expanded the variable properties in the equations of motion in terms of the independent state variables of temperature and pressure. They determined the limits of applicability for the Boussinesq assumption for these independent variables in terms of a reference set of thermophysical properties for the specified fluid of interest. All of the dependent and independent variables in the equations of motion were scaled by appropriate reference quantities in order to identify the relative magnitudes of the physical effects represented

by these terms. Natural convection in a horizontal fluid layer of thickness $L$ and temperature difference $\Delta T$ was considered. Distances were scaled by the length $L$. Temperature differences were scaled by $\Delta T$. The velocity was scaled by the term $U_c = (g\beta\Delta TL)^{1/2}$, which is the maximum velocity that might be expected to occur in the boundary layer (Jaluria, 1980). The dynamic pressure was scaled by $\rho U_c^2$. The differences in pressure at different elevations were scaled by $\rho_0 gL$. For this investigation, the upper limit for applicability of the Boussinesq approximation based on the plate height is not a limiting factor. The requirement that the ratio of the difference between the wall and freestream fluid temperatures to the absolute temperature of the fluid be much less than unity, however, is violated. Under the conditions of interest in the present work, this ratio is of the order of 0.5. Thus, the Boussinesq approximation is not valid for this work and the effects of variable thermophysical properties must be taken into account.

A comprehensive summary of the analytical and experimental work on temperature dependent thermal properties was reported by Kakaç et al. (1985). A comparison between forced and natural convection results shows that viscosity variations for liquids with moderate and large Prandtl numbers (except water) cause the major effect upon heat transfer. The variability of the isobaric volumetric expansion coefficient, $\beta$, of water also has a significant effect on the heat transfer.

Acoustic phenomena may be neglected when the Boussinesq approximation is used. Stated differently, the energy contained in a pressure wave is negligible with respect to the energy contained in the convective motion of the fluid when this approximation is valid. Neglecting acoustic phenomena greatly simplifies the differential equations and is computationally desirable. Gray and Giorgini (1976) developed a criterion that specifically addresses the pressure work term in the energy conservation equation that accounts for the acoustic energy. This criterion states that when the dimensionless term given by

$$\left(\frac{\beta g L}{C}\right)\left(\frac{T_\infty}{T_w - T_\infty}\right) \qquad (3-5)$$

has an absolute value less than 0.1, acoustic phenomena may be neglected. For the conditions of interest here, this term (3-5) is on the order of $5\times10^{-6}$ and, thus, the criterion is readily satisfied.

Gray and Giorgini (1976) specifically allow for the unsteady terms to remain in the equations for Newton's Second Law and conservation of energy. They, however, did not include volumetric heat sources in their analysis. This topic is discussed further in Section 3.6, which deals with the effects of volumetric heat sources.

Sparrow and Gregg (1958) utilized a Howarth-Dorodnitsyn transformation and obtained a similarity solution to the problem of an isothermal flat plate in laminar natural convection flow with variable properties. The effects of variable properties appear in the governing equations in terms of the dimensionless ratios of properties given by:

$$\left(\frac{\rho\mu}{\rho_w\mu_w}\right), \quad \left(\frac{\rho k}{\rho_w k_w}\right), \quad \text{and} \quad \frac{C}{C_w}. \tag{3-6}$$

In the limiting case of constant properties, these ratios are all equal to unity and the governing equations are all reduced to their familiar forms.

Sparrow and Gregg (1958) investigated the effects of varying these property ratios, which were either constant or functions of the similarity variable (the Chapman-Rubesin approximation), for a number of gases and for mercury. Their results indicate that the effect of variable properties on laminar natural convection is relatively small and that reasonably good results can be obtained by evaluating the volumetric expansion coefficient as the reciprocal of the freestream temperature (an approximation which holds exactly for an ideal gas) and the remaining properties at the film temperature.

Sparrow and Gregg (1958) developed a reference temperature procedure by comparing the results of a variable property analysis to that of a constant property analysis. This reference temperature has the form:

$$T_r = T_w - a(T_w - T_\infty), \tag{3-7}$$

where $a$ is a constant evaluated for a particular fluid. For the idealized gases that were investigated, the value of $a$ is 0.38. For mercury, the value of $a$ is 0.30.

Minkowycz and Sparrow (1976) evaluated the heat transfer from an isothermal vertical plate in steam under variable property conditions. They report a value of 0.46 for the constant $a$ of equation (3-7).

Cairnie and Harrison (1982) also used a Howarth-Dorodnitsyn transformation and a numerical solution technique that can utilize tabular values of temperature dependent properties, as well as the Chapman-Rubesin approximation. They performed experiments for a hot flat plate in air at atmospheric pressure. In these experiments, they measured the axial velocity distribution in the boundary layer with a laser Doppler anemometer and the temperature distribution with fine wire thermocouples. They obtained good agreement between their experimental and numerical results for a constant Chapman-Rubesin approximation for properties evaluated at the film temperature.

Thus, there is ample evidence that the effects of variable thermophysical properties are not strong for the laminar natural convection flow of gases. However, these effects are more important for liquids, especially liquids near the critical point, and in turbulent flows.

Seibers (1979) computed strong effects due to variable properties on turbulent natural convection flows over an isothermal vertical flat plate in air. Seibers evaluated the thermophysical properties at the film temperature, defined as the average of the wall and ambient fluid temperatures, and found heat transfer rates at least 50% greater for flows with large temperature differences than heat transfer rates computed from correlations developed from flows having lower Grashof numbers and smaller temperature differences.

Clausing (1983) gives the results of several experiments in turbulent natural convection from a vertical flat plate at high temperature differences for gaseous air and nitrogen at cryogenic temperatures. His results show approximately 30% higher heat transfer for a wall-to-ambient temperature ratio of 1.75 with the properties evaluated at the ambient temperature as compared to a constant property analysis. He also presents

results showing 60% higher heat transfer for a wall to ambient temperature ratio of 1.75 with the properties evaluated at the film temperature as compared to a constant property analysis. He concludes that the structure of the turbulent boundary layer is dependent on ambient temperature conditions, since the laminar sublayer adjacent to the solid boundary will have a large temperature gradient and that most of the fluid inside the boundary layer is at conditions close to the ambient fluid conditions. Thus, the thermophysical properties should be evaluated at conditions close to ambient conditions.

Seibers et al. (1983; 1985) report additional results for turbulent natural convection in air for a vertical flat plate at constant temperature at high wall overheat ratios, which is defined as $\lambda = (T_w - T_\infty)/T_\infty$. They evaluated the thermophysical properties of air at the temperature far from the wall of the test section and correlated the experimental results with the relationship:

$$Nu = 0.098\, Gr^{1/3} \left(\frac{T_w}{T_\infty}\right)^{-0.14} . \qquad (3-8)$$

The results of Seibers et al. (1985) disagree with those of Clausing (1983) in that the corrections for the effect of variable properties show opposite trends. Equation (3-8) predicts a decrease in the heat transfer coefficient for a specified Grashof number evaluated at the temperature far from the wall as the ratio of wall temperature to free-stream temperature increases. Clausing's correlation, however, predicts an increase in the heat transfer coefficient as the wall temperature ratio increases. The reasons for this disagreement are not known.

### 3.3. Investigations of Thermal Stratification on Natural Convection Boundary Layer Flows

Thermal stratification may occur when volumetric heat sources exist in the fluid far from the reactor vessel walls. The present research investigated stably stratified flows only.

Jaluria (1985) developed the criterion for stable thermal stratification in a natural convection flow. He also discusses some of the practical aspects of experimentally obtaining a stably stratified freestream under steady-state conditions.

Fujii et al. (1974) present an analysis of the nonsimilar natural convection flow on an isothermal plate in laminar flow in a fluid with a power law temperature stratification. A finite-difference solution is compared to a perturbation solution, with good agreement at the third level of perturbation. The finite difference solution is compared with experimental results for water. The authors claim good agreement between temperature and velocity results, although the accuracy of the velocity measurement was stated to be somewhat low.

Chen and Eichhorn (1976) give an analysis for a constant temperature flat plate with linear thermal stratification. The local nonsimilarity method of Sparrow et al. (1972) was used, along with a shooting method with least squares correction, to numerically solve the coupled equations. Experimental Nusselt number results for a fluid with a Prandtl number from 5.5 to 7.5 and a Rayleigh number from $1.7\times10^6$ to $3.2\times10^7$ are presented and compared to the computed results and the results of a series solution from an earlier paper by Eichhorn (1969). The series solution shows good agreement with the experimentally determined Nusselt number for small values of the stratification parameter, which represents small perturbations from the unstratified case. The first and second level of truncation solutions from the local nonsimilarity method also show good agreement; however, only the second level of truncation shows good agreement with the experimentally measured values of the Nusselt number for large values of the stratification parameter, which represents a significant level of departure from isothermal conditions.

No references were found on experimental or analytical investigations of turbulent natural convection flow on an isothermal, vertical flat plate in a stably-stratified environment.

### 3.4. Aerosol Transport by Combined Convection and Thermophoresis

The small particles of interest in the present work are aerosols on the order of one micrometer in diameter which are generated by a nuclear reactor accident in which melting of the nuclear core is postulated. The particles in the boundary layer adjacent to the internal structures will move by convection and thermophoresis. The references that describe the phenomenon of thermophoresis will be presented first, followed by a presentation of the references that describe the effects of combined convection and thermophoresis on particulate transport in fluid flow.

Thermophoresis is a physical phenomenon by which small particles suspended in a gas are moved by a force generated by a temperature gradient in a direction down the temperature gradient. Thermophoresis arises in many applications. In a kerosene lantern, for example, soot particles move through the hot gas stream and are deposited on the relatively cool glass wall by thermophoresis. Talbot et al. (1980) observed thermophoresis while measuring flow velocities in heated geometries with a laser Doppler velocimeter, which requires seeding the flow with small particles. Rosner and Seshadri (1981) present examples of thermophoretic deposition of combustion byproducts on cooled gas turbine blades and heat exchanger surfaces. Simpkins et al. (1979) identify thermophoresis as the dominant physical mechanism for deposition of glass layers with differing optical indices of refraction during the manufacture of the optical fibers used in telecommunications. Very detailed descriptions of the mechanics of aerosols, including thermophoresis, appear in Hidy and Brock (1970) and Waldmann and Schmitt (1966). Loyalka (1983) presents a review of the current methods for aerosol transport analysis used in nuclear reactor safety research, specifically including thermophoresis.

Maxwell (Kennard, 1938) was the first to attempt to describe the physical principles of thermophoresis while investigating the radiometer effect. Talbot (1980) presents a summary paper of the analyses and of the experimental measurements for thermophoresis. Talbot divides thermophoresis into three categories which depend upon the Knudsen number. The Knudsen number, *Kn*, is defined as the ratio of the

mean free path of the gas to a characteristic dimension of the particle, generally the radius. The three Knudsen number regimes are the free molecular, for which $Kn >> 1$, the transition, for which $Kn = O(1)$, and the slip, for which $0 < Kn < 0.25$. *The slip flow Knudsen number regime is of interest in the present work.*

Epstein (1929) was the first to obtain a relationship for thermophoretic velocity in terms of the fluid properties and imposed temperature gradient by deriving an expression for the thermophoretic force and equating it to the Stokes drag force of a single sphere in an infinite fluid. The Epstein relationship successfully predicted a thermophoretic velocity for situations where the thermal conductivity of the gas was significantly greater than that of the particle. However, the Epstein relationship does not predict a sufficiently large thermophoretic velocity for sodium chloride particles in air as reported by Schadt and Cadle (1961) and Derjaguin et al. (1966), for which the thermal conductivity of the particles is greater than that of the gas. *For the conditions of interest of the present investigation, the thermal conductivity of the aerosol particles (steel) will be much greater than the thermal conductivity of the gas (steam).*

Brock (1962) improved on the Epstein relationship with a hydrodynamic analysis by assuming that the Navier-Stokes fluid equations and the Fourier law of thermal conduction are valid in the fluid surrounding a spherical particle and that the Fourier law of thermal conduction is valid inside the particle. Brock applied matching boundary conditions for the heat flux, temperature jump, thermal slip, and velocity slip at the surface of the spherical particle. The resultant thermal force was equated to the Stokes drag force, as modified by Basset (1888) to include flow slip at low Knudsen numbers, resulting in a relationship for thermophoretic velocity. This relationship also underpredicts the measured thermophoretic velocities of high thermal conductivity particles, but not as much as does the Epstein relationship (Talbot et al., 1980). With improved values for temperature jump, thermal slip, and velocity slip coefficients, the Brock relationship reasonably predicts the thermophoretic velocity for Knudsen numbers less than 0.1 (Talbot et al., 1980). The procedure used by Brock is outlined in Appendix C as part of an analysis to show that the presence of a volumetric heat source in the spherical particle does not affect the thermophoretic coefficient $K$.

Dwyer (1967) utilized higher order kinetic theory to approximate the continuum equations and boundary conditions, computing the thermal force with the thirteen-moment equations of Grad. This procedure, similar to that of Sone (1972), yields reasonable results for particles with relatively low thermal conductivities as compared to that of the gas. Dwyer's analysis, however, predicts a reversal in the thermophoretic force (i.e., in the direction of the thermal gradient) for particles with relatively high thermal conductivities in the slip flow regime. Talbot et al. (1980) state that this reversal in the thermal force is due to a property of the thirteen-moment equations where normal stresses arise from heat transfer normal to the interface. This "negative thermophoresis" should be measurable but has not been experimentally verified (Talbot, 1980; Fuchs, 1982).

Derjaguin and Yalamov (1965), as emended by Derjaguin and Yalamov (1966), applied irreversible thermodynamics and Onsager's reciprocity relations to an aerosol simulated by a porous wall and obtained an expression for thermophoretic velocity similar to that of Brock (1962), with a value of the thermal slip coefficient twice that of Brock's.

Kousaka et al. (1976) describe a method, called an "ultramicroscope method," for measurement of thermophoretic velocities in the slip regime and discuss desirable conditions for accurate determination of the thermophoretic velocity. Experimental results are presented for three aerosols with particle thermal conductivities approximately ten times that of the gas. The measured velocities have better agreement with the predicted velocities of Derjaguin and Yalamov (1966) than those of Brock (1962).

Bakanov and Roldughin (1979) amplified both the hydrodynamic analysis by Brock (1962) and the thermodynamic analysis by Derjaguin and Yalamov (1965). Bakanov and Roldughin claim to obtain improved thermophoretic velocity relationships using both methods. Curiously, they offered no comparisons with experimental data.

Fuchs (1982) describes an experimental method that employs a Millikan cell with a heated upper plate and a cooled lower plate that is presently used to measure thermophoretic velocities. Fuchs also describes and criticizes another method, called the "jet method," for measuring thermophoretic velocity. Fuchs compares measured

velocities for sodium chloride particles in air to the predicted velocities from a few of the theoretically derived expressions. Good agreement with any one velocity correlation over the range of Knudsen numbers from 0.06 to 0.3 is not obtained. Fuchs specifically states that "negative thermophoresis" is not observed. Fuchs also states that data for Knudsen numbers below 0.06 is lacking.

Goldhirsch and Ronis (1983a) also used irreversible thermodynamics in an attempt to explain thermophoresis over the range of Knudsen numbers from the slip regime to the free-molecular regime. They show that the Soret effect could be described as thermophoresis of molecules. Goldhirsch and Ronis (1983b) further extended their analysis to low gas and particle densities. They claim that the main processes responsible for thermophoresis occur close to the surface of a particle and are of a nonhydrodynamic nature. The thermal conductivity of the particle does not appear in their expression for thermophoretic velocity. They claim good agreement with experimental data for particles of both low and high thermal conductivities. Their functional relationship for thermophoretic velocity is given by a quite complicated expression.

Soga (1986) analysed a linearized version of the gas kinetic theory equations with a singular perturbation method to obtain a relationship for the thermophoretic velocity that is applicable for small Knudsen numbers. He compared the results of his expression with those of Brock (1962), Derjaguin and Yalamov (1966), and with the experimental results of Jacobson and Brock (1965). He concluded that Brock's formula with corrected slip coefficients, as well as that of Derjaguin and Yalamov, overpredicts the thermal force for low Knudsen numbers and that the magnitude of the thermal force is sensitive to the energy accommodation coefficient.

Reed and Morrison (1973) present an analysis for the transient motion response of a spherical particle in the slip flow regime to a suddenly applied temperature gradient. They developed the following expression for a relaxation time to steady-state motion:

$$\frac{\text{thermal force}}{\text{relaxation time}} = \frac{\rho_p r_p^2}{\mu_f}. \qquad (3-9)$$

For the conditions of interest to this present work, this thermal force relaxation time for a particle with a diameter of 10 μm is on the order of $4\times10^{-3}$ s, much shorter than the time period of interest which is on the order of minutes. Smaller diameter particles will have a shorter thermal force relaxation time.

Prodi and Tampieri (1988) also present another characteristic time for the transient temperature response of the aerosol in an answer to the critique of Fuchs (1982) concerning the accuracy of the "jet method" for measuring thermophoretic velocity. A scaling analysis of this thermal response characteristic time to the time for a particle to move the distance of one diameter due to the thermal force at steady-state conditions is presented in Appendix C. It is shown there that for the circumstances of this present work, the effects due to transient energy storage in the particle on thermophoretic velocity are negligible. Thus, *transient thermophoretic effects will be neglected in the present work.*

The previous references postulate a model of a single sphere in an infinite fluid, in which a modified Stokes drag force is equated to a thermophoretic force in order to obtain an expression for the thermophoretic velocity. Reed and Morrison (1974) used a hydrodynamic analysis in the zero Knudsen number limit to account for velocity field perturbations due to the presence of another sphere or a wall. Their analysis predicts an increase in drag force due to the presence of another sphere. The correction, however, is negligible for dilute suspensions. The analysis, similar to that of Brenner (1961), that accounts for the presence of a wall normal to the sphere velocity also shows an increase in drag as the wall is approached. This increase in drag begins when the distance between the sphere and the wall is less than five diameters and is substantial only when this distance is less than one diameter. This result indicates that the thermophoretic velocity will decrease as the sphere approaches the wall if the thermal force remains unchanged. Reed and Morrison (1975) extend their analysis to include the effects of the wall for the thermal force on the spherical particle. They show that the thermal force on the particle increases as the distance between the wall and the particle decreases. However, the thermophoretic velocity does not increase, since the hydrodynamic drag also increases as the wall is approached and the thermophoretic velocity is

a result of balancing these two forces. The particle velocity must be zero at the wall, so there must be a decrease in thermophoretic velocity as the wall is approached. According to Reed and Morrison (1975), the decrease in thermophoretic velocity becomes noticeable for the conditions of this investigation when the particle is approximately one diameter from the wall. Kanki et al. (1985) also extended this analysis by Reed and Morrison by accounting for thermal slip around the particle. They concluded that the sphere will decrease in velocity as the wall is approached due to increased drag, as it must, and that the thermal force will increase as the wall is approached, becoming infinite at the wall which holds the particle against the wall.

The method of matched asymptotic expansions was used for forced convection laminar flow inside a long tube by Walker et al. (1979) and for forced convection laminar flow along a planar surface by Gökoglu and Rosner (1986) to estimate the relative thickness of the Brownian diffusion layer with respect to the thermal boundary layer thickness. Both references show that in the absence of thermophoresis, the relative thickness of the Brownian layer is on the order of $Sc^{-1/3}$ and that in the presence of thermophoresis, the relative thickness of the Brownian layer is on the order of $Sc^{-1}$. With an estimate of the thickness of the laminar natural convection thermal boundary layer of $\delta_{thermal}/L = Pr^{-1/2}\, Gr^{-1/4}$ (Jaluria, 1980), the ratio of the thickness of the Brownian diffusion layer to the particle diameter in the presence of thermophoresis is given by:

$$\frac{\delta_{Brownian}}{d_P} = \frac{L}{d_P} Pr^{-1/2}\, Gr^{-1/4}\, Sc^{-1}. \qquad (3-10)$$

For the laminar flow conditions of interest in this investigation, the Grashof number is on the order of $10^9$, the Schmidt number is on the order of $10^4$, the Prandtl number is 0.8, the particle diameter is on the order of $10^{-6}$ m, and a characteristic length for the overall flow geometry is 3 m. Based on these values, equation (3-10) gives a value of $\delta_{Brownian}/d_P \approx 2$. The thickness of the Brownian diffusion layer is therefore of the order of the criterion for wall effects on thermophoresis developed by Reed and Morrison (1975). Thus, *the wall effect on thermophoretic velocity will affect the particle flux*

deposited on the wall to the extent that Brownian diffusion *affects the particle flux for the conditions of interest in this investigation.* The effect of Brownian diffusion is shown to be negligible for the conditions of interest of this investigation in Section 5.6.

Hales et al. (1972) used a similarity variable formulation of the boundary layer equations for laminar natural convection heat transfer along a vertical isothermal wall and included the effect of thermophoresis for free molecule (i.e., $Kn >> 1$) conditions. An iterative technique with a hybrid analog-digital computer was used for solution. An approximate analysis is used to develop an estimate for the deposited particle flux at the wall. Two limiting conditions of zero thermophoresis and zero Brownian diffusion were postulated. The relation for deposition of particles in the zero Brownian diffusion case was expressed in terms of the Schmidt number, which is of questionable utility since the Schmidt number is dependent on the value of the Brownian diffusion coefficient.

Hales et al. (1972) also made an admittedly imperfect analogy between heat and mass transfer to derive an approximate relationship for particle deposition, including Brownian diffusion and (apparently) thermal convection effects. According to their speculative correlation for turbulent natural convection flow, particle deposition increases with distance along the plate. They raised the question of whether inertia or thermophoresis is the dominant mechanism for particle movement to the wall. Byers and Calvert (1969) had already addressed this question and, using both analysis and experiment, showed that thermophoresis is the dominant mechanism for particulate movement in forced convection flow in a tube for particles with diameters on the order of one micrometer.

Mills and Wassel (1975) consider aerosol transport in a natural convection laminar boundary layer adjacent to an either heated or cooled isothermal vertical wall. A similarity transformation is used to reduce the boundary layer equations to ordinary differential equations. The nonlinear similarity equations are linearized, then solved with an unspecified implicit finite difference technique. The results presented for the heated wall case are incorrect, since no "dust free zone" appears. The total exclusion of dust from a zone around a heated surface was first noticed by Tyndall in 1870 (Waldmann and Schmitt, 1966). Recent experimental evidence (Talbot et al., 1980) also confirms

the existence of a layer with a total absence of particles adjacent to a heated surface. The correlation for cooled surfaces is of questionable utility since the particle Schmidt number appears in the formulation for the wall particle flux.

Goren (1977) used a similarity transformation for variable-property forced convection boundary layer flow over a flat plate at a uniform temperature to compute the rate of thermophoretic particle deposition. Goren shows that the deposited particle concentration is independent of boundary layer run length for the specific value of the dimensionless thermophoretic coefficient equal to the reciprocal of the Prandtl number.

Rosner and Fernandez de la Mora (1982) consider the thermophoretic drift of particles across a forced convection turbulent boundary layer on an aerodynamically smooth cooled surface for the application of gas turbines. The various terms in the governing equations are Reynolds averaged, as is demonstrated in Appendix B. An additional averaged term results, analogous to apparent turbulent viscosity, that is called "eddy thermophoresis." This additional Reynolds-averaged term results from the simultaneous fluctuation of the particle concentration and the thermophoretic velocity. Rosner and Fernandez de la Mora (1982) neglect eddy thermophoresis within the boundary layer based on the argument that near the wall where the thermophoretic velocity is high, the turbulence is small and that away from the wall where the turbulence is high, the thermophoretic velocity is small. They further argue that in boundary layer analysis, the turbulence term arising from the convective terms in the conservation equation is generally much larger than any other turbulence terms. No experimental evidence that would verify the existence of eddy thermophoresis is apparent.

Mills et al. (1984) consider laminar forced convection of air over an isothermal flat plate with transpiration at the surface. They develop a correlation for particle mass deposition at the wall that is claimed to account for the coupling between thermophoresis and convection. The effect of surface transpiration appears as a ratio of heat flux at zero transpiration to that with surface transpiration. Gökoglu (1987) indicates errors in this analysis and comments that for surface blowing, the reduction in particle wall deposition is much greater than the reduction in heat transfer because the very thin concentration boundary layer is more sensitive to blowing than is the relatively thick

thermal boundary layer. Because of the errors in the analysis of Mills et al. (1984), their resultant formulation is of questionable use, but the intent of the work, which is to develop simple methods for predicting particle deposition rates, is quite valid.

Epstein et al. (1985) used a local nonsimilarity transformation to extend Goren's laminar flow analysis for deposition of particles to turbulent natural convective flows adjacent to a vertical flat plate. Epstein et al. (1985) show, although not as clearly as does Goren, that the deposited particle concentration is constant along the plate length when the thermophoretic coefficient is equal to the reciprocal of the Prandtl number. This analysis of Epstein et al. (1985) is of a preliminary nature because it employs the local similarity method for the numerical solution; that is, the first level of truncation is used with little justification other than that of avoiding the numerical difficulties encountered when using the higher levels of truncation. One very interesting observation of Epstein et al. (1985) is that the effective thermophoretic particle concentration at the wall is essentiality identical for laminar and turbulent natural convection flows having an identical Prandtl number, identical thermophoretic coefficient $K$, and identical ratio of wall-to-freestream temperature ratio, $T_w/T_\infty$. Since a direct analogy between wall particle concentration and wall temperature may be postulated under these conditions, this leads to the possibility of a direct relationship between the rate of particle deposition and the rate of heat transfer, independent of the fluid flow regime, but (perhaps) dependent on the fluid Prandtl number, the thermophoretic coefficient $K$, and the ratio of wall to freestream temperatures.

Batchelor and Shen (1985) theoretically analyzed the thermophoretic deposition of particles in forced laminar flow to cold surfaces. They show mathematically that if the particles come from a region with uniform concentration and temperature, the concentration at any point in the flow will be constrained between limits determined by problem parameters. Based on this analysis, they developed an expression for the particle concentration at the isothermal cold wall due to thermophoresis in terms of the wall temperature ratio $T_w/T_\infty$ and the product of the thermophoretic coefficient $K$ and the Prandtl number. They compared their expression to the numerical results for two

nonsimilarity flows and found good agreement for small wall-to-fluid temperature differences. They claim that, if caution is used, this expression can be applied to the computation of the rate of particle deposition, if the fluid properties and the values of the wall and freestream temperatures are known.

### 3.5. Turbulence Modeling

The heat transfer effects due to turbulence in natural convection, like those due to turbulence in forced convection, are generally computed using empirically based models. The empiricism is generally necessary due to the inherent complexity of turbulent flows. The Navier-Stokes equations are applicable at any point in a flowing fluid, and, therefore, are (in principle) appropriate for the computation of turbulent flows. However, the smallest scale of the turbulence would require the computation and storage of such a great deal of information that these computations are presently beyond the capabilities of existing computers. Furthermore, some estimates (Anderson et al., 1984) suggest that the practical computation of turbulent flows using the Navier-Stokes equations may *always* remain beyond the capabilities of existing computers. Since the overall heat transfer and pressure loss characteristics are all that are desired (or measured) for a physical apparatus, an averaging procedure is normally performed to simplify the modeling of turbulent flows.

In experiments on natural convection flows with a constant wall temperature, the typical measurements have included the mean turbulent velocity profile and mean temperature profile in the boundary layer. Such experiments include those by Lock and Trotter (1968), Cheesewright (1968), Cheesewright and Ierokiopitis (1982), Hoogendoorn and Euser (1978), Vliet and Liu (1969), and Warner and Arpaci (1968). Based partly upon these experimental data, George and Capp (1979) and Kutateladze (1976) postulated two regions of flow in a natural convection boundary layer: an inner region where viscous and thermal conduction effects are important and an outer region where inertial or convective effects are important.

Since direct computation of turbulent flows using the Navier-Stokes equations is impossible, the formulation of the governing equations is usually accomplished by a time-averaging procedure in which the flow variables are written as a sum of a time averaged mean component and a fluctuating component. Upon substitution of the flow variables written in this form into the Navier-Stokes equations, certain terms may be reduced to zero by time averaging methods (Tennekes and Lumley, 1972; White, 1974). Yang and Aung (1985) performed this procedure and obtained a set of equations very similar to the laminar flow equations for the mean flow quantities with the addition of one term in each conservation equation representing the effects of the time-averaged fluctuating components. The details of this averaging procedure and the resultant equations are presented in Appendix B. For the Newton's Second Law equation, an additional term appears that represents the apparent turbulent shear stress. An additional term also appears in the energy conservation equation that represents apparent transport of thermal energy by turbulent diffusion.

Guceri and Farouk (1985), as well as Reynolds and Cebeci (1978), described three methods of modeling the apparent turbulent shear stress. The first was stress-equation (Reynolds stress) modeling where a differential equation is written, using the Navier-Stokes equations, for each component of turbulent stress (Bradshaw, 1978), which results in a larger system of coupled differential equations to be solved. The second is large-eddy modeling where time-averaging is done only on a sub-domain of the flow field. The third method is eddy diffusivity modeling where the turbulent stresses are related to the rate of mean fluid strain through an apparent turbulent viscosity as shown in equation (B-10) in Appendix B. To and Humphrey (1986) present the results of the two different numerical turbulence models of an algebraic stress model and a two-equation eddy diffusivity model for computation of the natural convection flow on a heated, vertical flat plate. As described in Chapter 4, Section 1.3, simpler models for eddy diffusivity perform acceptably well under certain circumstances. The large-eddy and Reynolds-stress models were not used here because they are prohibitively expensive and yet do not yield more accurate results than simpler models.

The eddy diffusivity approach was initially proposed by Boussinesq (1877). In this approach, an apparent turbulent eddy viscosity is defined as the ratio of the apparent turbulent shear stress to the mean rate of strain in the fluid, in a manner analogous to the definition of molecular viscosity. An effective turbulent thermal conductivity is defined in a similar manner. The turbulent Prandtl number is defined as the ratio of the turbulent diffusivity of momentum to the turbulent diffusivity of thermal energy. Prandtl (1925) proposed an algebraic, or "zero-equation," relationship for the eddy viscosity by using an analogy to the model of molecular viscosity taken from the kinetic theory of gases. A so-called mixing length must be determined algebraically for this model.

Prandtl (1942) also hypothesized that the scale of the turbulent eddies moving in a direction transverse to the main flow direction in a free turbulent flow, such as that in a jet emanating from an orifice into a calm fluid, is of the same order of magnitude as the width of the mixing zone. Prandtl based this hypothesis on the experimental observations of Reichardt (1941).

Prandtl (1945) also proposed a formulation of the turbulent viscosity as a product of the square root of the turbulent kinetic energy and the mixing length. In this model, the turbulent kinetic energy, which is defined as the sum of the squares of the fluctuating components, is determined by the solution of a transport equation and the mixing length determined as in the zero-equation model. This additional equation introduces another transport equation into the coupled set of equations, thereby increasing the complexity of the model. However, the turbulent viscosity for this one-equation model, similar to that of the zero-equation model, vanishes at the velocity maximum, which is physically unrealistic. There is no apparent physical mechanism to explain a zero turbulent viscosity at the maximum of the mean velocity. Miyamoto et al. (1982) present experimental measurements of the turbulent natural convection boundary layer where zero turbulent viscosity is observed well inside the mean velocity maximum.

Mason and Seban (1974) utilized this one-equation model, with the mixing length near the wall based upon the van Driest (1957) formulation near the wall and the mixing length far from the wall assumed to be a constant value. They present results for

velocity profiles and heat transfer that are in agreement with the experimental results of Vliet and Liu (1969), but not with those of Cheesewright (1968). Cheesewright and Ierokiopitis (1982), however, acknowledge a discrepancy in the heat balance in the earlier data of Cheesewright.

Jones and Launder (1972) formulated a two-equation model for the eddy viscosity with one differential equation written for the turbulent kinetic energy and another for the turbulent dissipation rate. Guceri and Farouk (1985), as well as Yang and Aung (1985), present additional transport equations for these quantities. Guceri and Farouk (1985) claim that zero-equation models are best suited for boundary layer flows, while two-equation models can be successfully applied to both internal and external flows. Guceri and Farouk present the results of their computations in the form of comparisons with experimental data for natural convection flows on a horizontal cylinder and in a horizontal cylindrical annulus.

Cebeci and Khattab (1975) present numerical results computed with a zero-equation model. In a manner similar to that of Mason and Seban (1974), two different values were used for the mixing length. An expression for turbulent Prandtl number based on the molecular Prandtl number (Cebeci and Smith, 1974) was also used. Cebeci and Katthab (1975) obtained reasonably good agreement with the experimental data of other investigations for the local heat transfer, the temperature profile, and the velocity profile in turbulent natural convection flow on a vertical flat plate, even though the zero-equation model predicts that the turbulent viscosity is zero at the maximum point in the natural convection velocity profile.

Kato et al. (1968) used an integral technique with a zero-equation model that does not predict a zero turbulent viscosity at the velocity peak. Reasonably good agreement with experimental results is shown for heat transfer as well as velocity and temperature profiles. However, the turbulent viscosity model used was originally developed for forced turbulent flow with no apparent modification for turbulent natural convection. Their turbulence model near the wall is similar to those of Mason and Seban (1974) and Cebeci and Khattab (1975), but differs from these models in the outer region far from the wall.

Bayley (1955) also used an integral method to compute natural convection heat transfer from an isothermal, vertical flat plate, using a turbulent viscosity equal to seven times the kinematic viscosity. Subsequent experimental investigations in air (Warner and Arpaci, 1968; Seibers et al., 1985) have shown the validity of Bayley's correlation for heat transfer, even though Bayley used a crude turbulence model. Apparently, for natural convection heat transfer, sufficiently accurate heat transfer results may be obtained with simple turbulence models.

### 3.6. The Effects of Volumetric Heat Sources on Natural Convection Flows

Volumetric heat sources entrained in a fluid may have an effect on either natural or forced convection. Volumetric heat sources can be observed in industrial processes such as those involving exothermic chemical reactions, storage of liquid or gaseous nuclear wastes, and nuclear reactor design and safety analysis.

The presence of a volumetric heat source adds a nonhomogeneous term into the equation for conservation of energy. A similarity solution may be possible if the source term is of an appropriate functional form (Gebhart et al., 1988), but in general, the velocity and temperature profiles do not display similarity-type behavior. Natural convection flows in fluids containing heat sources have been investigated for a variety of geometries. A large number of experimental results are reported in a survey paper by Kulacki and Richards (1985). The majority of these investigations consider enclosed cavities having spatially uniform volumetric heat generation with various thermal boundary conditions.

Gebhart et al. (1988) determined the necessary conditions for a volumetric heat source in a boundary layer to result in a similarity solution: the heat source must be a function of distance from the wall and decrease to zero at the edge of the boundary layer for a similarity solution to exist. Gebhart et al. (1988) also state that the flow due to a volumetric heat source uniformly distributed throughout the fluid, including both a fluid region near the wall and a fluid region far from the wall, may not be representative of boundary layer flow.

Chu (1955) developed an analysis for thermoacoustic waves generated by heat addition, stating that the heat source must vary in time for pressure waves to be generated. The time scale for variation of the heat sources considered in the present research is on the order of hours, the approximate time period of radioactive decay for the fission products. Rehm and Baum (1978) scaled the governing equations of motion, including the effect of a time-variant heat source but neglected viscous and thermal conduction effects. Their scaled equations show that in flows with fast heat addition, such as laser heating, acoustic waves must be considered, while for those with slow heat addition, such as combustion, acoustic waves can be neglected. Paolucci (1982) elaborated upon the Rehm and Baum (1978) work by including the viscous and thermal conduction terms in the governing equations.

Paolucci (1982) specifically addressed the situation in which large time-dependent thermal gradients exist as well as combustion heat sources. Paolucci develops the following criterion, $H$, to quantify fast and slow heat addition:

$$H = \frac{QL}{\rho_c U_c^3}. \qquad (3-11)$$

$H$ represents the ratio of the energy added by the heat source to the energy arising from fluid motion. According to Paolucci, the acoustic effects due to heat source addition need only be considered if $H$ is on the order of $Ma^2$ or less, where $Ma$ is the Mach number, which is defined as the ratio of a characteristic velocity to the sonic velocity. For the conditions of this investigation, $H$ is on the order of 10 and, therefore, since the Mach number is on the order of $10^{-2}$, acoustic phenomena due to the addition of heat are negligible.

de Boer (1984) analyzed the effect of a heat source in natural convection flows. He defines the nondimensional depth to be the ratio of the physical depth $L$ to the hydrostatic depth, $P/\rho g$, such that a "shallow fluid" has a nondimensional depth much less than one and a "deep fluid" has a nondimensional depth of order one. de Boer also defines a nondimensional heat source strength as:

$$\begin{matrix}\text{nondimensional} \\ \text{heat source strength}\end{matrix} = \frac{(\beta Q/\rho C)^{2/3}(L/g)^{1/3}}{\beta T}. \qquad (3-12)$$

A "weakly heated fluid" has a nondimensional heat source strength much less than one and a "strongly heated fluid" has a nondimensional heat source strength of order one. For the conditions of interest for the present research, the nondimensional depth is on the order of $5\times10^{-5}$ and the nondimensional heat source strength is on the order of $10^{-3}$. de Boer shows that only in fluids that are both strongly heated and deep would acoustic phenomena be non-negligible. Therefore, *according to the criteria of de Boer, thermoacoustic wave phenomena are neglected in this investigation.* The scaling analysis in Appendix D also supports the neglect of acoustic pressure wave phenomena.

Sparrow et al. (1963) analyzed the stability of a fluid with uniform internal heating that is confined between two horizontal plates. A relationship showing the dependence of stability on the Rayleigh number was derived for the onset of fluid motion that occurs wherever a negative temperature gradient (temperature decreasing with increasing height) exists somewhere in the fluid. They also observed that when a temperature gradient is positive everywhere between the two plates, the fluid is stable and quiescent. For the case of two plates at the same temperature, when the Rayleigh number based on the internal heat source strength and the plate spacing exceeds 37 325, an instability occurs.

Jones (1974) analyzed the effects of an exothermic reaction in a horizontal cylinder of gas with isothermal walls. For this case, if the gas reacts according to the Arrhenius relationship, the heat liberated by the reaction is exponentially dependent upon the temperature. Jones used a stream function-vorticity formulation with a finite-difference numerical solution technique. Good qualitative agreement with the experimental results of others is shown for a gas enclosed in a spherical vessel.

Cairnie et al. (1981) studied the effects of a combustible chemical species in a laminar natural convection flow adjacent to a heated flat plate. Experiments for a range of conditions up to ignition onset were performed. The temperature in the boundary

layer was measured with a traversing thermocouple probe. The boundary layer equations were derived including the effect of chemical self-heating. Chemical self-heating is defined as heating by a volumetric source that is dependent upon species concentration and temperature. No self-heating was observed below a plate temperature of 540 K, but effects on the temperature field due to variable thermal properties were observed. Comparison of the computed and measured results is not satisfactory. The lack of a satisfactory comparison is claimed to be due to the chemical modeling.

Kee et al. (1976) considered the natural convection flow with heat sources inside a cylinder with a constant wall temperature. They nondimensionalized the governing equations of motion such that the geometrical term of the aspect ratio ($L/d$) of the cylinder appears explicitly. A stream function-vorticity formulation was used with a finite-difference numerical solution technique to compute the streamlines and temperature distribution of the fluid inside the cylinder. The temperature profiles were experimentally investigated inside a cylinder containing tritium, a radioactive gas assumed to give up its decay energy in a manner that gives volumetric heating. The volumetric heat source strength was increased by increasing the gas pressure. As the heat source strength was increased, the maximum temperature increased and the point of its occurrence moved upwards along the cylinder centerline. Although the variations in the measured temperatures are within the normal limits of experimental error, the measured temperatures corresponding to the lowest of three values of heat source strength are lower than the values predicted by numerical analysis. This discrepancy might be attributed to some of the radioactive decay energy of tritium being radiated directly to the walls of the cylinder, in addition to being absorbed and serving locally throughout the fluid as a heat source.

Bergholtz (1980) considered a rectangular enclosure completely filled with a newtonian fluid containing uniformly distributed heat sources. The enclosure was cooled at the sides with isothermal walls at the same temperature, and insulated at the top and bottom. Bergholtz found that a sufficiently strong heat source causes two physically distinct regions of flow to occur: a central core upflow and boundary layer downflows at the cooled vertical walls. The temperature distribution of the core flow is stably and

strongly stratified, due to the upward convection of heat. The stable thermal stratification also allows the wall boundary layers to entrain fluid at the top and to detrain fluid at the bottom of the enclosure in order to maintain conservation of mass. Assuming bilateral symmetry along the vertical axis of the enclosure, the equations were considered separately in the two regions of the central core and the wall boundary layer. In the core upflow region, the viscous effects due to the wall were neglected in the Newton's Second Law equation and the conductive transport of energy was neglected in the conservation of energy equation. In the wall boundary layer region, the heat generation effects were neglected, due to the assumption of a thin boundary layer. The equations for the two regions were coupled together by requiring the global conservation of mass and energy at any given position along the vertical axis of the enclosure. Numerical integration and iteration were necessary to obtain a solution with this method. Bergholtz's method presents an alternative approach for considering a solution domain which might require a large number of mesh points for a finite-difference solution and, therefore, be unnecessarily expensive to solve. No experimental comparisons were presented.

Randall and Sesonske (1959) used an approximate integral technique to integrate the boundary layer equations for a cooled vertical flat plate for laminar flow in a semi-infinite fluid. A constant volumetric heat source was postulated to exist only in the natural convection boundary layer and not in the fluid far from the plate. Their computed results indicate that the presence of heat sources decreases the boundary layer thickness with a resulting increase in heat transfer coefficient as compared to a natural convection flow that does not contain heat sources and which has the same temperature difference between the flat plate and the fluid far from the plate.

Greene (1982) performed an experiment with a rectangular pool of aqueous electrolyte with one isothermal wall instrumented with thermocouples. A uniform volumetric heat source was established by imposing an alternating current across the pool. The pool was open to the atmosphere at the top and insulated at the bottom and vertical boundaries except for the one isothermal vertical wall which was instrumented with thermocouples. The temperature distribution along the vertical centerline of the fluid

in the pool was also measured with thermocouples. Two regions of flow were observed: a uniform temperature upflow in the center of the pool and a boundary layer downflow near the isothermal test wall. Greene varied the heat source strength up to the point of pool boiling and measured the heat flux to the wall. The remainder of the heat generated within the fluid was removed by convection and evaporation at the open upper surface of the pool. He developed a correlation for heat transfer to the vertical wall based on heat source strength. The boundary layer flow down the vertical wall was laminar in all cases, although instabilities characteristic of transition to turbulence appeared at the higher heat source strengths near the threshold of pool boiling. He claims that to within the limits of experimental accuracy, the observed flows adjacent to the wall exhibit behavior similar to the laminar natural convection flow on an isothermal wall in a semi-infinite fluid that does not contain heat sources. This claim, however, is questionable since fluid must detrain from the boundary layer near the bottom of Greene's enclosure with a subsequent horizontal outward velocity which cannot possibly exist for a vertical flat plate in a semi-infinite fluid.

Steinberner and Reineke (1978) present numerical and experimental heat transfer results for a closed rectangular cavity having isothermal walls and which is heated with a uniform volumetric heat source generated in the aqueous electrolyte. They present results for three heat strength source levels, but do not present any detailed temperature measurements or a compilation of Nusselt and Rayleigh numbers as did Greene (1982). For the upper portion of the vertical wall, the reported results are representative of laminar flow in a constant temperature fluid with a Prandtl number of five. The volumetric heat source strengths in these experiments were on the order of one kilowatt per cubic meter, approximately two orders of magnitude lower than the heat source strengths of Greene (1982). Steinberner and Reineke (1978) present a Nusselt number correlation that apparently does little more than restate the conservation of energy relation and is not presented here.

Two observations on the results presented by Steinberner and Reineke (1978) are of note. First, the measured Nusselt numbers are noticeably lower than those predicted by the correlation of Saunders (1939), which appears in this work as equation (3-4).

Second, for the highest heat source strength, the Nusselt number increases noticeably with increasing length along the wall. This is just the opposite of the trend for the other two heat source strengths. A stationary secondary vortex is apparently generated at the highest value of heat source strength in the lower, turbulent portion of the vertical boundary layer. This vortex should not occur in the boundary layer flow over a vertical flat plate in a quiescent fluid.

Kikuchi et al. (1986) performed a series of experiments in a rectangular box that enclosed a volumetrically heated fluid. Their box was cooled on both horizontal surfaces, which results in different flow patterns than those expected in the present work. However, they present detailed temperature measurements showing that the magnitude of the temperature perturbations due to turbulent fluctuations in the core flow region away from the boundaries was less than 10% of the temperature difference between the walls. In the absence of references investigating the specific conditions of interest for the present research, this work of Kikuchi et al. (1986) presents the approximate conditions of the temperature fluctuations far from the walls due to a sufficiently strong heat source.

### 3.7. Numerical Methods

The fully-coupled system of nonlinear partial differential equations that govern the flows of interest here is a formidable challenge to solve. Closed-form analytical solutions are not presently available. Therefore, approximate numerical methods must be employed in order to solve this set of equations. Two major methods of numerical analysis are finite difference techniques and finite element techniques. Roache (1972), Patankar (1980), Anderson et al. (1984), and Jaluria and Torrance (1986), and many others present the general topic of finite difference methods. Baker (1983) presents finite element method techniques for numerical solution of the governing equations for fluid flow of interest here. A complete list of the references on the numerical solution of the governing partial differential equations would undoubtedly be too extensive for

inclusion in this work. Thus, only the references that are of direct interest will be cited. Appendix A presents a detailed discussion of the numerical methods used in this investigation.

Solution, either analytical or numerical, is usually facilitated if partial differential equations can be reduced by appropriate transformations, called similarity variable transformations, to ordinary differential equations. Dresner (1983) and Hansen (1964) present methods for deriving similarity variable transformations and present solutions of transformed equations representative of many problems in physics and engineering. Most notable for this present work are the solutions of boundary-layer problems. If the system of governing partial differential equations of the boundary-layer equations can be transformed by a similarity variable into an equivalent set of ordinary differential equations, the form of these transformed differential equations and bounding conditions is classified as a two-point boundary-value problem (Burden et al., 1981). Keller (1976) published a monograph that presents different methods for numerical solution of such two-point boundary-value problems. Because of the wealth of analysis and experience that appears in the literature in solving this type of problem, a similarity solution of a transformed partial differential equation is desirable.

Unfortunately, such physical considerations as transverse curvature, linearly stratified temperature boundary conditions, and surface transpiration can prohibit obtaining a similarity solution. Use of a transformation variable in this case simply transforms one set of partial differential equations to another set of partial differential equations having a different appearance. For example, the set of turbulent flow boundary-layer equations for this work appear as equations (4-11), (4-16), (4-17), and (4-18). Upon defining a stream function in equation (4-31), the variable transformations of equations (4-32) and (4-33), and the nondimensionalizations of equations (4-34) through (4-37), the deceptively simple set of boundary-layer differential equations is transformed into the apparently complex equations (4-40), (4-41), and (4-42). This set of equations, which are called "nonsimilar" because of the appearance of streamwise partial derivatives, is no longer a two-point boundary-value problem and other means of obtaining solutions must be used.

Two different numerical schemes are used in the present work to solve the governing system of differential equations. The first method used is the method of local nonsimilarity, developed by Sparrow et al. (1972). This method transforms the nonsimilar partial differential equations into an approximately equivalent set of ordinary differential equations, so that solution techniques for two-point boundary-value problems can be used. Two solution techniques used in the present work are a "shooting" scheme with a least-squares correction as developed by Nachtsheim and Swigert (1965) and the finite-difference procedure developed by Lentini and Pereyra (1977) that employs the trapezoidal rule with deferred corrections.

The second method of solution that is used is a finite-difference scheme developed by Keller (1978), called the "Keller Box" method. This method, initially developed for solving parabolic partial differential equations (Keller, 1971), was easily adapted for the purposes of this present work. The Keller Box scheme can allow variable mesh spacing with second-order accuracy and can also incorporate mathematically singular behavior at the endpoints. The Keller Box scheme can be formulated in terms of the original, untransformed variables, as well as the nonsimilar equations. Keller (1978) remarks that even defining a stream function is unnecessary with the Box method.

Of special interest here is the investigation of Fairweather and Vedha-Nayagam (1987). They present the solutions of five published boundary-layer problems with three publicly available computer software packages specifically designed to solve two-point boundary-value problems governed by ordinary differential equations. These software packages are based on the following numerical techniques: a finite-difference method that implements the trapezoidal rule with deferred corrections, a spline collocation method, and a multiple shooting method. In some cases, the results from the three methods differed with the published results, but not with each other. In other cases, one or more of the methods failed to yield a solution. In general, the software packages are shown to provide powerful numerical analysis methods that are easily implemented for the solution of boundary-layer problems. One of these software packages used by

Fairweather and Vedha-Nayagam (1987), DVCPR (IMSL, 1982) which implements the method of Lentini and Pereyra (1977), is used for some of the solutions obtained with the method of local nonsimilarity.

### 3.8. Natural Convection with Participating Gas Thermal Radiation

Participating gas radiation heat transfer can play an important role in many practical flows, such as combustion processes. Computation of the radiative heat flux in a fluid in which the gas molecules emit and absorb radiant thermal energy can be quite complicated and involved. Not only is the emission process highly nonlinear due to its dependence on the fourth power of the fluid temperature, but also the absorptivity and emissivity of the gas are frequency dependent. Reference texts, such as those by Sparrow and Cess (1966), Özisik (1973), and Siegel and Howell (1981), discuss the complexity of analytically describing gas radiation and pose some limiting assumptions that have been useful in developing engineering models of such phenomena.

Participating gas radiation heat transfer has been reviewed in detail by Viskanta (1966), who also derives the complex integral relationships that govern the transport of radiant thermal energy. Two approximations based upon the absorption characteristics of the gas and the geometry of the flow were developed. These are the optically thin approximation, in which the gas is assumed to emit but not absorb energy, and the optically thick approximation, where the gas is assumed to absorb thermal radiation in the immediate vicinity of the location at which it was emitted. The optically thick approximation is also known as the diffusion, or the Rosseland, approximation, which was developed for use in astrophysics (Rosseland, 1936). The Rosseland approximation changes the integral relationship for the heat flux in a participating gas into a differential relationship that resembles those governing a diffusion process, such as conduction heat transfer.

Several forced and natural convection flows have been investigated using these two approximate models of participating gas radiation. The results of these investigations show that the overall effect of participating gas radiation heat transfer is to increase the total rate of heat transfer, as compared to convection heat transfer alone under the same

conditions. However, the fractions of the total heat transferred by the individual radiation and convection components for any particular fluid vary depending on the values of the thermal emissivity of the wall and also on the ratio of wall and fluid temperatures.

Viskanta and Grosh (1962a) used a similarity transformation and the Rosseland approximation to investigate forced convection boundary layer flows over a wedge. For a hot wall, the convective portion of the total heat transferred decreased below that computed for nonparticipating heat transfer. For a cooled wall, the convective portion of the total transferred heat decreased as the ratio of wall temperature to fluid temperature varied from 1.0 to 0.5 due to a decreased temperature gradient at the wall. For a cooled wall with a ratio of wall to fluid temperature less than 0.5, the convective portion of the total transferred heat increases over that due to radiation alone. Viskanta (1966) claimed that this increased convective heat transfer at low wall temperature ratios was due to the participating radiation acting as if an effective heat source were adjacent to the wall, where it can induce additional convective movement in the fluid.

Viskanta and Grosh (1962b) analyzed simultaneous conduction and radiation heat transfer to include the effect of surface emissivity on surface heat transfer. They did not use the Rosseland approximation. Instead, they used the method of successive approximations to solve the integral equations governing the nonlinear transmission of radiant energy. They present results in terms of the optical depth $\tau$, the surface emissivity $\varepsilon$, and the parameter $M$ of equation (2-6). For the optical depths of interest in this investigation, which are in the range of $\tau > 1$, and for radiation with negligible conduction, i.e. $M = 0$, the computed total heat transfer shows a noticeable decrease only for values of the surface emissivity less than 0.5, as compared to the heat transfer from a black surface for which $\varepsilon = 1$. For the optically thin case, a significant decrease in heat transfer for any surface emissivity less than one is shown. Thus, *for the present investigation, as long as the reactor vessel inside wall has an emissivity greater than 0.5, the effect of surface emissivity on heat transfer to the wall from a participating gas will be neglected.*

Cess (1966) utilized the method of matched asymptotic expansions to analyze "small" participating gas radiation effects in a gray nonscattering gas in natural convection along a vertical plate, which was assumed to have a wall emissivity of one. Cess predicts an increase in convection heat transfer for small gas radiation effects. An elaboration of Cess' solution appeared in Aziz and Na (1984). The complexity of the analysis of a problem in participating gas heat transfer can be examined in this reference.

Novotny and Yang (1967) presented an analysis of optically thick boundary layers, using matched asymptotic expansions. Small temperature differences were assumed so that the emissive power of the gas could be linearized with respect to temperature. The two specific cases of Blasius flow over a flat plate and free convective flow about a horizontal cylinder were investigated. Novotny and Yang employed an inner layer in which the reciprocal of the optical thickness is used as an expansion parameter. Their apparent intent was to address the effects of assuming the Rosseland approximation near a wall upon heat transfer. Their Rosseland approximation model does not consider radiation either reflected or emitted from a bounding surface.

Novotny and Yang (1967), as well as Audunson and Gebhart (1972), state that the diffusion approximation fails when the distance from the wall is less than one photon mean free path, which is defined as the reciprocal of the absorption coefficient. Novotny and Yang choose this distance of the photon mean free path as the outer edge of the inner layer and the inner edge of the outer layer in their matched asymptotic solution method. They report that in the limit of large optical thickness, the total heat flux is correctly determined due to the constant value of heat flux across this inner layer. However, the temperature gradient in the inner layer immediately adjacent to the wall was not correctly determined except for the case of relatively small participating radiation effects.

Arpaci (1968) utilized an approximate integral method to analyze the effects of participating gas radiation heat transfer on the natural convection boundary layer on a

flat plate in a stagnant radiating gas for both optically thin and optically thick approximations. The overall heat transfer from the plate is shown to increase as either the optical thickness, wall emissivity, or the ratio of the wall temperature to the fluid temperature increases. No comparisons with experimental results were reported.

England and Emery (1969) used the optically thin approximation to analyze the effect of participating gas radiation heat transfer on natural convection adjacent to a constant heat flux vertical flat plate. Comparisons with experiments in air and carbon dioxide showed good agreement with the results of their analytical model. For the conditions of their analysis, the radiation effects due to the participating medium were small and of the same magnitude as effects due to variable thermophysical properties in laminar natural convection flow.

Kennedy and Paszkowskyj (1970) used both the optically thick and optically thin approximations to analyze the effect of participating gas radiation heat transfer on natural convection from a heated vertical flat plate with unit emissivity. The radiation heat flux term was not linearized so that the analysis can be applied to cases in which there are large temperature differences between the wall and the fluid. The Boussinesq approximation was used in the formulation of the problem. The Boussinesq approximation was acknowledged to possibly yield inaccurate results at large wall to fluid temperature differences. As the optical depth increases, nonlinear radiation coupling effects significantly increase the total heat transfer from a heated plate as compared to the heat transfer computed assuming a linearized radiation heat flux. The cooled wall case was not analyzed for nonlinear radiation effects.

Audunson and Gebhart (1972) reported the results of an analytical and experimental investigation for ammonia at optically thin conditions adjacent to a constant heat flux wall. Three values of wall emissivity were used. Good comparisons between the analytical and experimental results were found over the ranges of parameters investigated. The heat transfer increased by as much as 40% over that for the case of no participating radiation. Increasing the wall emissivity increases the rates of both the radiative and the total heat transferred from the plate. The results of the convective and radiative processes were claimed to be independent and were superimposed.

Novotny et al. (1974) used a local nonsimilarity method to analyze the effects of linear radiation in ammonia, which is a non-gray gas. The nonsimilarity parameter was defined as a function of the gas band absorptivity characteristics. The differences between the higher levels of truncation for the nonsimilarity method increase as the values of wall emissivity increase. An increase in gas pressure results in a decrease in the ratio of the overall rate of heat transfer to the rate of convective heat transfer for ammonia.

Venkateshan and Krishna Prasad (1979) also present a matched asymptotic expansion solution for forced laminar compressible boundary layers using the diffusion approximation for the outer solution and the optically thin assumption for the inner solution. To the leading order of approximation, the radiation slip method yields the same results as the more complicated solution obtained with the method of matched asymptotic expansions. The radiation slip method, as developed by Deissler (1964), extends the diffusion approximation for finite optical depths to include the radiative effects of a bounding surface by allowing a temperature discontinuity at the surface, analogous to the temperature jump condition in a rarefied flow.

Kim and Viskanta (1984) utilize a band approximation for the non-gray emissive and absorptive effects of steam at high pressures and temperatures for forced convection flow in a tube. Their results show that for low flow conditions, the convective portion of the total heat transfer is greatly overpredicted if the interaction between convection and radiation is neglected.

Galuska et al. (1986) formulated a similarity solution for the optically thick boundary layer flow of a non-Newtonian power law fluid with a large Prandtl number. A thickening of the thermal and velocity boundary layers is predicted due to the effect of participating gas radiation, with the non-Newtonian fluids having thicker boundary layers than the Newtonian. The temperature gradient in all cases decreases as the parameter representing the level of radiative participation is increased.

# CHAPTER 4

# ANALYSIS

## 4.1. Introduction

The objective of the present work is to develop a numerical model for predicting the thermophoretic deposition of particles in a natural convection flow on a vertical flat plate. This model is to be used to obtain simplified correlations for the rates of heat transfer and particle deposition in the flows of interest. Thus, the mathematical modeling of the mechanisms of Brownian diffusion, thermophoresis, and convective transport that govern the deposition of particles is presented below.

This chapter presents the formulation of the governing equations and boundary conditions that describe the movement of fluid, thermal energy, and particles in a natural convection flow near a vertical cold wall. Since turbulent fluid flow conditions are possible, the modeling of the turbulence is also described. The appropriate nondimensionalization of the governing equations and their boundary conditions is also discussed. Relationships for the heat transfer and thermophoretic particle deposition are developed so that the model can be validated by comparison of computed results with results previously published by other investigators.

An expression, called the dimensionless ratio of transfer coefficients, is developed which correlates the thermophoretic deposition of particles and the heat transferred to the surface. For certain flow circumstances of interest, the governing equation for conservation of particles has an exact analytical solution in closed form. The nature of this exact solution is shown in detail so that computed values for the ratio of transfer coefficients can be compared to exact results. Bounding limits on the ratio of transfer coefficients are derived and then used to develop an approximate expression for the ratio of transfer coefficients in terms of known parameters.

## 4.2. Development of the Governing Equations

### 4.2.1. The governing equations and their boundary conditions

The governing equations and boundary conditions that describe the flows of interest here were developed using the results of the scaling analysis given in Appendix D and the formulation for the turbulence modeling shown in Appendix B.

The equations governing the natural convection flows of interest are those of conservation of mass, Newton's Second Law, and the conservation of energy for a compressible, newtonian fluid. The Stokes hypothesis for bulk viscosity, as developed by Pai (1956) and Batchelor (1967), is employed, since no specific value for the second coefficient of viscosity appeared to be better than Stoke's hypothesis (White, 1974). These equations are written in cartesian tensor notation as follows:

$$\frac{\partial \rho}{\partial t}+\frac{\partial(\rho u_j)}{\partial x_j} = 0\,, \tag{4-1}$$

$$\rho\frac{Du_i}{Dt} = \rho F_i+\frac{\partial}{\partial x_j}\left[\mu\left(\frac{\partial u_i}{\partial x_j}+\frac{\partial u_j}{\partial x_i}\right)\right]-\frac{2}{3}\frac{\partial}{\partial x_i}\left(\mu\frac{\partial u_j}{\partial x_j}\right)-\frac{\partial P}{\partial x_i}\,, \tag{4-2}$$

and

$$\rho C\frac{DT}{Dt} = (\beta T)\frac{DP}{Dt}+\frac{\partial}{\partial x_j}\left(k\frac{\partial T}{\partial x_j}\right)+Q-\frac{\partial}{\partial x_j}(q_{r_j})+\mu\left[\frac{\partial u_i}{\partial x_j}\left(\frac{\partial u_i}{\partial x_j}+\frac{\partial u_j}{\partial x_i}\right)-\frac{2}{3}\left(\frac{\partial u_j}{\partial x_j}\right)^2\right]. \tag{4-3}$$

The boundary conditions for these equations are zero fluid velocity at the wall, zero fluid velocity far away from the wall, and specified temperatures at the wall and in the fluid far away from the wall. These boundary conditions are given by the expressions:

$$u(x,0) = v(x,0) = u(x,\infty) = 0\,, \tag{4-4}$$

$$T(x,0) = T_w\,, \quad \text{and} \quad T(x,\infty) = T_\infty(x)\,. \tag{4-5}$$

The governing equation for the conservation of particles, which was originally given by Hidy and Brock (1970) and is developed by a scaling analysis of the total mass conservation equation in Appendix D, has the form:

$$\frac{D(\rho N)}{Dt} - \frac{\partial}{\partial x_j}(\rho N V_{Tj}) = \frac{\partial}{\partial x_j}\left[\rho \mathcal{D} \frac{\partial N}{\partial x_j}\right], \qquad (4-6)$$

where $\mathcal{D}$ is the coefficient for Brownian diffusion of the particles and $V_T$ is called the thermophoretic velocity of the particles. The thermophoretic velocity normal to the plate is related to the temperature gradient as follows (Goren, 1977):

$$V_T = -K \frac{\nu}{T} \frac{\partial T}{\partial y}, \qquad (4-7)$$

where $K$ is called the thermophoretic coefficient. $K$ depends on the thermal conductivities of both the particle and the fluid and on the Knudsen number. A detailed discussion of thermophoresis and the thermophoretic coefficient $K$ appears in Appendix C. For the conditions of interest in the present work, a range of values for $K$ on the order of unity was used.

In order to prescribe the boundary condition for particle concentration at the wall, introductory remarks about the physics of Brownian diffusion are included here. A successful theory of Brownian motion was published by Einstein in 1905 (Kennard, 1938). In Einstein's theory the random motion of pollen grains on the surface of water first noticed by Brown in 1828 (Kennard, 1938) can be explained as a diffusion process, such as the conduction of heat in solid materials or the movement of the molecules of one chemical species through another. Hidy and Brock (1970) show that Fick's law of diffusion is applicable to the Brownian movement of particles suspended in a fluid. For the purposes of the present work, a "perfectly absorbing wall" is postulated such that any aerosol particle immediately adjacent to the wall will stick to it and, therefore, be removed from the fluid. Hence, the particle concentration in the fluid immediately adjacent to the wall will be zero due to the movement of particles to the perfectly absorbing wall by Brownian diffusion. The boundary condition far from the wall for the equation of conservation of particulate matter in the flow, equation (4-6), is a specified concentration, $N_\infty$, far from the wall. These two boundary conditions are given by

$$N(x,0) = 0 \qquad \text{and} \qquad N(x,\infty) = N_\infty . \qquad (4-8)$$

Since the Brownian diffusion coefficient, $\mathcal{D}$, for this problem is quite small and is of the order of $10^{-11}$ $m^2/s$ (Hidy, 1984), Brownian diffusion will be an important mechanism for particle movement only in a very thin layer immediately adjacent to the wall (Walker et al., 1979). The scaling analysis of Appendix D affirms this situation for the conditions of interest in the present work. Walker et al. (1979) present an analysis using the method of matched asymptotic expansions that shows that the ratio of the Brownian diffusion layer thickness, $\delta_B$, to the thermal boundary layer thickness, $\delta_T$, is of the order of the inverse of the Schmidt number, or $\delta_B/\delta_T = Sc^{-1}$. They also show that the flux of particles that moves to the wall can be approximated with an error of the order of $Sc^{-1}$ by evaluating the particle flux at the outer edge of the Brownian layer.

Since the particle flux to the wall is desired, the particle concentration inside the Brownian layer need not be computed for the case where the particle flux to the wall in the Brownian diffusion layer is essentially equal to the thermophoretic flux at the edge of the Brownian layer. When the effects of Brownian diffusion on particle transport to the wall are negligible, the boundary condition at the wall of zero particle concentration due to Brownian diffusion is replaced with a relationship between the particle concentration gradient and the apparent particle concentration at the edge of the Brownian layer, which is located at a distance $\delta_B$ from the wall. Neglecting Brownian diffusion and convective movement at the edge of the Brownian layer, and considering only thermophoretic transport adjacent to the wall, reduces equation (4-6) to the following relationship which is evaluated at the edge of the Brownian layer:

$$\frac{\partial N(x,\delta_B)}{\partial y} - \frac{N(x,\delta_B)}{T(x,\delta_B)}\frac{\partial T(x,\delta_B)}{\partial y} = 0 . \qquad (4-9)$$

Equation (4-9) will be used as a boundary condition at the edge of the Brownian layer, instead of the value of zero for the particle concentration at the wall which is applicable for a perfectly absorbing wall.

As shown in Appendix D, the governing equations (4-1), (4-2), (4-3), and (4-6) are scaled to identify the nondimensional parameters of interest. As shown by the scaling

analysis of Appendix D, the transient response of the fluid conservation equations is much faster than the transient response of the solid wall. Therefore, the transient terms in the fluid conservation equations are neglected.

### 4.2.2. The boundary layer form of the governing equations

As shown in Appendix D, equations that govern the flow are simplified to the boundary layer equations for steady-state flow. The buoyancy force term in Newton's Second Law, which is given by equation (D-97), is that due to a gravitational body force acting in the negative $x$-direction as shown on Figure 2-2. The thermal radiation flux term in the equation for conservation of energy is written in a form that satisfies the optically thick assumption and is given as (Sparrow and Cess, 1966):

$$q_y = -\frac{16\sigma T^3}{3\kappa}\frac{\partial T}{\partial y}. \qquad (4-10)$$

Thus, the boundary layer forms of the governing equations, equations (D-96) through (D-99), are given by:

conservation of fluid mass

$$\frac{\partial}{\partial x}(\rho u)+\frac{\partial}{\partial y}(\rho v) = 0, \qquad (4-11)$$

Newton's Second Law

$$\rho u\frac{\partial u}{\partial x}+\rho v\frac{\partial u}{\partial y} = g(\rho_\infty-\rho)+\frac{\partial}{\partial y}\left(\mu\frac{\partial u}{\partial y}\right), \qquad (4-12)$$

conservation of energy

$$\rho u C\frac{\partial T}{\partial x}+\rho v C\frac{\partial T}{\partial y} = \frac{\partial}{\partial y}\left[\left(k+\frac{16\sigma T^3}{3\kappa}\right)\frac{\partial T}{\partial y}\right]+Q, \qquad (4-13)$$

and conservation of particles

$$\frac{\partial}{\partial x}(\rho u N)+\frac{\partial}{\partial y}[\rho N(v+V_T)] = \frac{\partial}{\partial y}\left(\rho\mathcal{D}\frac{\partial N}{\partial y}\right). \qquad (4-14)$$

Note that the Boussinesq approximation has not been made and that none of the thermophysical properties have been assumed to be constant.

### 4.3. Formulation of the turbulence model

#### 4.3.1. The time-averaged forms of the boundary layer equations

Equations (4-11), (4-12), (4-13), and (4-14) were time-averaged in the usual manner (Yang and Aung, 1985) as is shown in Appendix B. For example, the velocity component $u$ was assumed to consist of a time-averaged component $\bar{u}$ and a fluctuating component $u'$, or

$$u = \bar{u} + u'. \tag{4-15}$$

Similar formulations were used for the remaining flow variables. Substitution into the governing equations, followed by time-averaging, allowed identification of terms that represent the effects of the fluctuating turbulent flow variables. The turbulent viscosity, thermal conductivity, and particle diffusivity are identified in the governing equations by the subscript $t$ as follows :

$$\rho u\frac{\partial u}{\partial x}+\rho v\frac{\partial u}{\partial y} = g(\rho_\infty-\rho)+\frac{\partial}{\partial y}\left[(\mu+\mu_t)\frac{\partial u}{\partial y}\right], \tag{4-16}$$

$$\rho uC\frac{\partial T}{\partial x}+\rho vC\frac{\partial T}{\partial y} = \frac{\partial}{\partial y}\left[\left(k+k_t+\frac{16\sigma T^3}{3\kappa}\right)\frac{\partial T}{\partial y}\right]+Q, \tag{4-17}$$

and

$$\frac{\partial}{\partial x}(\rho uN)+\frac{\partial}{\partial y}[\rho N(v+V_T)] = \frac{\partial}{\partial y}\left[\rho(\mathcal{D}+\mathcal{D}_t)\frac{\partial N}{\partial y}\right]. \tag{4-18}$$

A large body of information has been developed for turbulent flows. The emphasis in this particular investigation was not on developing a new model of turbulence. Instead, the approach adopted here was to utilize and modify, if necessary, an existing model of turbulence to investigate the effects of turbulence on the heat and mass transfer to the wall. Accordingly, an ad hoc turbulence model with an algebraic closure

for the turbulent diffusivity was employed. The turbulence model was verified by comparing the computed results for heat transfer to the wall with experimental results, as discussed in Section 5.2.

The turbulence model was based upon a two-layer, or two-zone, postulate as presented by Cebeci and Khattab (1975). In this model, the natural convection velocity boundary layer is assumed to be divided into two regions: the inner region where viscous and buoyant effects are important and the outer region where viscous and inertial effects are important. A turbulent diffusivity relationship reported by Reynolds (1978) was used near the wall and a constant value of turbulent diffusivity based on the boundary layer thickness was used for the outer region. Different expressions were investigated in each zone for the turbulent Prandtl number, which represents the ratio of the turbulent diffusivity of momentum to the turbulent diffusivity of thermal energy, and for the turbulent Schmidt number, which represents the ratio of the turbulent diffusivity of momentum to the turbulent diffusivity of the particles.

Cebeci and Khattab (1975) based their use of two zones on an analogy with forced convection. They postulated that near the wall the fluid velocity and temperature profiles would be influenced primarily by the presence of the wall in a manner similar to that in the inner wall region in of a forced convection turbulent flow. They postulated that in an outer region far from the wall, the flow would be influenced by viscous and inertial forces in a fashion similar to that of the wake region in a turbulent forced convection channel flow. The turbulent diffusivity at any given distance from the wall is simply determined as the minimum value calculated using the expressions for the turbulent diffusivities in these two zones. The point at which the inner turbulent diffusivity first exceeds the outer turbulent diffusivity is designated as the dividing point between the inner and outer regions.

These two regions were observed experimentally, although in a qualitative way, by Lock and Trotter (1968) and Kutateladze (1976). These investigators commented that eddies appear to be damped near the wall and that the turbulent diffusivity in the outer region resembles that of a turbulent free jet. Since a simple turbulence model was desired, algebraic relationships were used to specify the turbulence quantities in each

region. Following the practice of Cebeci and Khattab (1975), the turbulent diffusivity at any given point in the boundary layer is taken to be the lesser of the computed values for the inner region turbulent diffusivity and the outer region turbulent diffusivity. The final selection of the turbulence model used in each region, which is reported in Chapter 5, was based on comparison of results computed with the competing models with experimental data. The various models of the turbulent viscosities in the inner and outer regions that were considered in this investigation are reviewed below.

### 4.3.2. The near wall region

Plumb and Kennedy (1977) adopted a two-equation model for turbulent viscosity and analyzed turbulent natural convection from a heated flat plate. Their computed results show good agreement with the experimental data of Bayley (1955), Cheesewright (1968), and Vliet and Liu (1969). Plumb and Kennedy claim that very near the wall, the apparent turbulent viscosity should have a cubic dependence on the distance from the wall. White (1974) presents an analysis that shows the apparent turbulent viscosity to have a cubic dependence on the wall distance in forced convection flow. Different turbulence models employing algebraic closure were evaluated for this cubic wall distance dependence.

Two expressions for the apparent turbulent viscosity were considered for use in the present work. The first model was proposed by Kato et al. (1968) and has the form:

$$\frac{\mu_t}{\mu} = 0.4y^+[1-\exp(-0.0017y^{+2})] \,. \qquad (4-19)$$

Equation (4-19) may be rewritten as:

$$\frac{\mu_t}{\mu} = 0.4y^+\left\{1-\exp\left[-\left(\frac{y^+}{A^+}\right)^2\right]\right\}, \qquad (4-20)$$

where $A^+$ is the standard form of the van Driest damping coefficient (Kays and Crawford, 1980), and $y^+$ is the standard form of the dimensionless distance from the wall in turbulent forced convection flow in which the distance from the wall is normalized by the

friction velocity and the kinematic viscosity. For the model of Kato et al. (1968), as presented in equation (4-19), $A^+$ is equal to 24.25. Kato et al. (1968) present no analysis or reference to support either this relationship or this numerical value of $A^+$. They do claim, however, that away from the wall, the turbulent viscosity distribution of equation (4-19) is proportional to $y^+$, as it is in forced convection, while very near the wall it is proportional to $y^{+3}$. This near wall behavior can be recovered mathematically by expanding the exponential function in a Taylor series and retaining the lowest order term. No physical explanation was presented by Kato et al. (1968) for the cubic dependence used in their model, although an explanation is presented by White (1974) for a cubic dependence near the wall in forced turbulent flow.

The second turbulence model was proposed by Reynolds (1976) and has the form:

$$\frac{\mu_t}{\mu} = 0.4y^+\left\{1-\exp\left[-\left(\frac{y^+}{A^+}\right)\right]\right\}^2, \qquad (4-21)$$

where $A^+$, the van Driest damping layer dimensionless distance, is an empirically determined constant. Reynolds (1976) presents experimentally determined values of $A^+$ for forced convection flow with surface transpiration. This model of near wall turbulence also has a functional dependence on the cube of $y^+$ as the wall is approached.

Two other models of turbulence were considered for use in the present work, but were rejected for reasons discussed below. The model of Kays and Crawford (1980) was developed for a fluid in the near wall region and is based on the assumption of constant fluid shear stress across this region. This equation has the form:

$$\frac{\mu_t}{\mu} = 0.4y^+\left\{1-\exp\left[-\left(\frac{y^+}{A^+}\right)\right]\right\}. \qquad (4-22)$$

Although this model is similar in appearance to the previous relationship by Reynolds (1976) of equation (4-21), it does not have a cubic dependence on $y^+$ very near the wall, and was, therefore, not considered further.

The standard Prandtl mixing length model (Prandtl, 1925), with the van Driest (1956) damping modification to the mixing length as summarized by Kays and Crawford (1980), is expressed in the following form:

$$\frac{\mu_t}{\mu} = \rho l^2 \left| \frac{\partial \overline{u}}{\partial y} \right|, \tag{4-23}$$

where $l$ is the "mixing length" given as

$$l = 0.4y\left[1 - \exp\left(-\frac{y^+}{A^+}\right)\right]. \tag{4-24}$$

This turbulence model predicts zero turbulent viscosity at the velocity maximum, which is not physically realistic for natural convection flows as discussed in Section 3.5. Thus, the Prandtl mixing length model was not considered further for use in this analysis.

The selection of the near wall turbulence model was made after the outer region turbulence model was selected, since both regions interact with each other through a common interface at some point within the boundary layer.

#### 4.3.3. The outer region

Lock and Trotter (1968) experimentally observed the structure of a turbulent natural convection boundary layer. They comment that the turbulent eddy distribution in the outer region resembles that of a turbulent free jet. Accordingly, another hypothesis by Prandtl (1942), as described by Schlichting (1979) and Arpaci and Larsen (1984), is applicable for free turbulent flow and was adopted for use in the present analysis. This other Prandtl hypothesis has the form:

$$\frac{\mu_t}{\mu} = \aleph \frac{b}{\nu} \Delta U, \tag{4-24}$$

where $b$ is a mixing zone flow width, $\Delta U$ is the maximum expected difference in velocity, and $\aleph$ is a dimensionless empirical constant. For a turbulent natural convection

boundary layer, the mixing zone flow width is the boundary layer thickness. The expected maximum velocity difference is the characteristic velocity for natural convection, which is described by Jaluria (1980) and is shown in Section D.2.

Jaluria (1980) used a scaling argument that equates the work done by the buoyancy force acting in a streamwise distance to the change in kinetic energy of the fluid. This characteristic natural convection velocity is

$$u_c = \left(\frac{\Delta\rho}{\rho} g x\right)^{1/2} = \frac{\nu}{x}(Gr_x)^{1/2} = \frac{\nu}{L}(\xi Gr_L)^{1/2}. \qquad (4-25)$$

where $\xi = x/L$ is defined as the nondimensional streamwise distance.

For fluids with Prandtl numbers on the order of unity, Arpaci (1986) shows that a "thermal microscale" $\delta$ is appropriate for turbulent boundary layers and that $\delta$ is proportional to the reciprocal of the cube root of the Grashof number, or

$$\delta = L Gr_L^{-1/3}. \qquad (4-26)$$

Substitution of equations (4-25) and (4-26) into the outer region eddy diffusivity relationship given by equation (4-24) yields the expression:

$$\frac{\mu_t}{\mu} = \aleph \xi^{1/2} Gr_L^{1/6}. \qquad (4-27)$$

This relationship indicates that the turbulent viscosity in the outer region increases as the square root of the axial distance from the leading edge of the surface. Equation (4-27), however, predicts a constant turbulent viscosity, or equivalently, constant turbulent shear stress, across the outer region of the turbulent boundary layer. This is not physically correct, since at some point far enough from the wall, the fluid must be quiescent in natural convection flow. Thus, in accordance with the experimental observations by Lock and Trotter (1968) of intermittent turbulence bursts and with the analysis presented in White (1974), the outer region turbulent diffusivity relationship of equation (4-27) was modified by multiplying it by the intermittency factor

$\gamma$ of Klebanoff (1955). This factor, which was originally determined from experimental observations of a boundary layer over a flat plate in turbulent forced convection flow, has the form:

$$\gamma = \left[1 + 5\left(\frac{y}{\delta}\right)^6\right]^{-1}. \qquad (4-28)$$

The Klebanoff intermittancy factor, which is empirically determined, predicts a smooth transition from a finite value of turbulent shear stress in the outer layer to a value asymptotically approaching zero turbulent shear stress at the apparent edge of the turbulent boundary layer, as it must for either forced or free convection. The effect of random fluctuations of the apparent turbulent shear stress, which is called "intermittancy," beyond the apparent boundary layer thickness can be observed in equation (4-28) at the edge of the boundary layer, where $\gamma$ is equal to 1/6 and not zero. As observed by Klebanoff (1955) for turbulent forced convection flows and by Lock and Trotter (1968) for turbulent natural convection flows, the edge of the turbulent boundary layer varies in a random fashion, unlike laminar convection.

Thus, the distribution of the eddy diffusivity of momentum in the outer region is approximated by the relationship

$$\frac{\mu_t}{\mu} = \aleph \xi^{1/2} Gr_L^{1/6} \gamma, \qquad (4-29)$$

where the constant $\aleph$ remains to be determined.

#### 4.3.4. Eddy diffusivities of heat and particles

A turbulent Prandtl number and a turbulent Schmidt number are defined as:

$$Pr_t = \frac{\varepsilon_M}{\varepsilon_H} \quad \text{and} \quad Sc_t = \frac{\varepsilon_M}{\varepsilon_P}. \qquad (4-30)$$

Many investigators (Tyldesley and Silver, 1968; Reynolds, 1978; Kays and Crawford, 1980) have attempted to determine the values of these quantities. These quantities

can be expected, like the turbulent diffusivity of momentum, to not only be dependent on the molecular properties of the fluid, but also the flow circumstances as well. Different functional relationships have been proposed in which $Pr_t$ varies as the eddy diffusivity, as the dimensionless distance from the wall, or is constant. None of these models has shown a clear superiority over the others. All of the models, however, seem to predict a turbulent Prandtl number on the order of unity. Accordingly, *a constant turbulent Prandtl number of one was used in the present work.*

Although not as many investigations were found for the values of the turbulent Schmidt number, the same trend was noticed as that for the Prandtl number in that no one correlation for turbulent Schmidt number is clearly better than any other. All of these correlations predict turbulent Schmidt numbers on the order of unity (Tyldesley and Silver, 1968). The value of the dimensionless particle stopping distance $S^+$, which is discussed in Section 2.5, is on the order of $10^{-6}$. Thus, since $S^+$ was also shown to be a dimensionless relaxation time when the particle is decelerated to zero velocity from the friction velocity by Stokesian drag, the particle is assumed to move with no velocity slip relative to a turbulent eddy (due to inertial effects), and, therefore, *has a turbulent Schmidt number of one.*

### 4.4. Transformation of the Boundary Layer Problem to Nonsimilarity Form

Introducing a stream function suitable for compressible flows and the Howarth-Dorodnitzyn transformation (Goren, 1977) allows the governing equations and their boundary conditions to be transformed into a more convenient form. The stream function, $\psi(x,y)$, which is defined such that the continuity equation is satisfied identically, is given by:

$$\frac{\partial \psi}{\partial y} \equiv \frac{\rho}{\rho_r} u \qquad \text{and} \qquad \frac{\partial \psi}{\partial x} \equiv -\frac{\rho}{\rho_r} v \,, \tag{4-31}$$

where the subscript r denotes a reference condition.

The required dimensionless variables are now defined as:

$$\xi = \frac{x}{L} \equiv \begin{matrix}\text{dimensionless streamwise} \\ \text{spatial coordinate,}\end{matrix} \tag{4-32}$$

$$\eta = \frac{1}{L}\left(\frac{Gr_L}{4\xi}\right)^{1/4}\int_0^y \frac{\rho}{\rho_r}dy' \equiv \begin{matrix}\text{dimensionless cross-stream} \\ \text{spatial coordinate} \\ \text{(pseudosimilarity coordinate),}\end{matrix} \tag{4-33}$$

$$f(\xi,\eta) = \frac{1}{4\nu_r}\left(\frac{Gr_L}{4}\right)^{-1/4}\xi^{-3/4}\psi(x,y) \equiv \begin{matrix}\text{dimensionless} \\ \text{stream function,}\end{matrix} \tag{4-34}$$

$$\theta(\xi,\eta) = \frac{T(x,y)-T_\infty(x)}{T_w-T_{\infty,0}} \equiv \text{dimensionless temperature,} \tag{4-35}$$

$$n(\xi,\eta) = \frac{N(x,y)}{N_\infty} \equiv \begin{matrix}\text{dimensionless particle} \\ \text{concentration,}\end{matrix} \tag{4-36}$$

and

$$\lambda(\xi) = \frac{T_w-T_{\infty,0}}{T_\infty(x)} \equiv \text{wall overheat ratio.} \tag{4-37}$$

For thermally-stratified flows, the wall overheat ratio, $\lambda$, is a function of the dimensionless streamwise coordinate $\xi$, since the denominator of equation (4-37) will be a function of the streamwise distance and the numerator will not.

The definition of the participating gas thermal radiation parameter, $M$, which was defined in Section 2.6, is repeated here as

$$M = \frac{k\kappa}{4\sigma T_\infty^3}. \tag{4-38}$$

$M$ is the ratio of heat transfer by conduction to heat transfer by radiation in an optically thick medium (Sparrow and Cess, 1966).

An additional dimensionless group, called the Damköhler number (Catchpole and Fulford, 1986), is given by

$$Da = \frac{Q_r L^2}{k_r (T_w - T_{\infty,0})}. \qquad (4-39)$$

$Da$ is the ratio of the rate of volumetric heat generation to the rate of heat conduction.

Substitution of these dependent and independent variable transformations of equations (4-31) through (4-39) into the boundary layer equations, equations (4-16) through (4-18), results in a system of equations in nonsimilarity form. This procedure does not eliminate, but does lessen dependence on the streamwise variable. The resulting system of equations is given by:

$$\frac{\partial}{\partial \eta}\left[\left(1+\frac{\mu_t}{\mu}\right)\left(\frac{\rho\mu}{\rho_r\mu_r}\right)\frac{\partial^2 f}{\partial \eta^2}\right] + 3f\frac{\partial^2 f}{\partial \eta^2} - 2\left(\frac{\partial f}{\partial \eta}\right)^2 + \theta\left(\frac{T_{\infty,0}}{T_\infty}\right) = 4\xi\left(\frac{\partial f}{\partial \eta}\frac{\partial^2 f}{\partial \eta \partial \xi} - \frac{\partial^2 f}{\partial \eta^2}\frac{\partial f}{\partial \xi}\right), \qquad (4-40)$$

$$\frac{1}{Pr_r}\left(\frac{C_r}{C}\right)\frac{\partial}{\partial \eta}\left\{\left(\frac{\rho k}{\rho_r k_r}\right)\left[1+\frac{k_t}{k}+\frac{4}{3M}(1+\lambda\theta)^3\right]\frac{\partial \theta}{\partial \eta}\right\} + 3f\frac{\partial \theta}{\partial \eta} - 4\xi\frac{\partial f}{\partial \eta}\frac{\partial}{\partial \xi}\left(\frac{1}{\lambda}\right)$$

$$+\frac{Da}{Pr_r}\left(\frac{C_r}{C}\right)\left(\frac{4\xi}{Gr}\right)^{1/2} n = 4\xi\left(\frac{\partial f}{\partial \eta}\frac{\partial \theta}{\partial \xi} - \frac{\partial \theta}{\partial \eta}\frac{\partial f}{\partial \xi}\right), \qquad (4-41)$$

and

$$\frac{\partial}{\partial \eta}\left[\left(\frac{1}{Sc}+\frac{1}{Sc_t}\frac{\mu_t}{\mu}\right)\left(\frac{\rho\mu}{\rho_r\mu_r}\right)\frac{\partial n}{\partial \eta}\right] + 3f\frac{\partial n}{\partial \eta} + K\frac{\partial}{\partial \eta}\left[\left(\frac{\rho\mu}{\rho_r\mu_r}\right)\left(\frac{\lambda\frac{\partial \theta}{\partial \eta}}{1+\lambda\theta}\right)n\right]$$

$$= 4\xi\left(\frac{\partial f}{\partial \eta}\frac{\partial n}{\partial \xi} - \frac{\partial n}{\partial \eta}\frac{\partial f}{\partial \xi}\right). \qquad (4-42)$$

These equations (4-40),(4-41), and (4-42) are general in that all of the physical parameters of interest for the present work are represented. Since, however, the ratios of the thermophysical properties may be functions of the fluid temperature and the turbulence quantities are functions of the distance from the wall, the above set of equations is not complete. Constitutive relations for the thermophysical properties will be used that are appropriate for the conditions under investigation, such as all ratios of

properties being identically one for conditions where the thermophysical properties may be assumed as constant or such as equation (5-1) or the polynomial relations of Irvine and Liley (1984) for conditions where variable thermophysical properties must be considered. The ratios of the turbulence quantities will be given as equations (4-21) or (4-22) for the inner turbulent zone and equation (4-29) for the outer turbulent zone. The Prandtl number, Damköhler number, thermophoretic coefficient $K$, optically-thick radiation parameter $M$, and wall overheat ratio $\lambda$ must also be specified to complete the physical modeling.

The boundary conditions, including that for the Brownian diffusion layer at the wall, were also rewritten to give:

$$f(\xi,0)=\frac{\partial f(\xi,0)}{\partial\eta}=1-\theta(\xi,0)-\xi\frac{\partial\left(\frac{1}{\lambda}\right)}{\partial\xi}=n(\xi,0)=\frac{\partial f(\xi,\infty)}{\partial\eta}=\theta(\xi,\infty)=1-n(\xi,\infty)=0\,. \quad (4-43)$$

The ratio $T_{\infty,0}/T_{\infty}$ appearing in equation (4-40) arises when both variable thermophysical properties and a thermally-stratified freestream are included in the model. This ratio does not appear in the governing equations if the Boussinesq approximation is employed in the case of a thermally-stratified freestream temperature. The ratio $k_t/k$ that appears in equation (4-41) will be called the "effective turbulent thermal conductivity," analogous to the term for the effective turbulent viscosity, $\mu_t/\mu$, that appears in equations (4-40) and (4-42).

For convenience in the formulation of equations (4-40), (4-41), and (4-42), partial differentiation with respect to $\eta$ is denoted by a prime and partial differentiation with respect to $\xi$ is denoted by a subscript. Thus, equations (4-40), (4-41), and (4-42) can be written in the form:

$$\frac{\partial}{\partial\eta}\left[\left(1+\frac{\mu_t}{\mu}\right)\left(\frac{\rho\mu}{\rho_r\mu_r}\right)f''\right]+3ff''-2(f')^2+\theta\left(\frac{T_{\infty,0}}{T_{\infty}}\right)=4\xi(f'f'_{\xi}-f''f_{\xi})\,, \quad (4-44)$$

$$\frac{1}{Pr_r}\left(\frac{C_r}{C}\right)\frac{\partial}{\partial\eta}\left\{\left(\frac{\rho k}{\rho_r k_r}\right)\left[1+\frac{k_t}{k}+\frac{4}{3M}(1+\lambda\theta)^3\right]\theta'\right\}+3f\theta'-4\xi f'\frac{\partial}{\partial\xi}\left(\frac{1}{\lambda}\right)+\frac{Da}{Pr_r}\left(\frac{C_r}{C}\right)\left(\frac{4\xi}{Gr}\right)^{1/2}n$$

$$=4\xi(f'\theta_\xi-\theta' f_\xi)\,, \qquad (4-45)$$

and

$$\frac{\partial}{\partial\eta}\left[\left(\frac{1}{Sc}+\frac{1}{Sc_t}\frac{\mu_t}{\mu}\right)\left(\frac{\rho\mu}{\rho_r\mu_r}\right)n'\right]+3fn'+K\frac{\partial}{\partial\eta}\left[\left(\frac{\rho\mu}{\rho_r\mu_r}\right)\left(\frac{\lambda\theta'}{1+\lambda\theta}\right)n\right]=4\xi(f'n_\xi-n'f_\xi)\,. \qquad (4-46)$$

The above set of equations (4-44), (4-45), and (4-46) and their boundary conditions given by equation (4-43) are insufficient for solution of the problem, although the third-order differential equation (4-44) has three properly posed boundary conditions and the two second-order differential equations (4-45) and (4-46) each have two properly posed boundary conditions. To complete the physical modeling of the problem as appropriate for the conditions under investigation in Chapters 5 and 6 as described previously, the remaining quantities that need to be specified are: the constitutive relations for the ratios of thermophysical properties which may be functions of the dependent variable of temperature, the ratios of the turbulence quantities which will be functions of the distance from the wall, Prandtl number, Damköhler number, thermophoretic coefficient $K$, optically-thick radiation parameter $M$, and wall overheat ratio $\lambda$.

### 4.5. Further Considerations of the Brownian Diffusion Layer

The Schmidt number, $Sc$, for the specified problem is quite large. Using relationships presented in Hidy (1984), the Schmidt number is found to be of the order of $10^5$ for spheres having a diameter of 1 μm in steam at 6.9 MPa and 1000°C. The simultaneous solution of these equations will reveal that there is a particle concentration boundary layer adjacent to the wall that lies inside the velocity and temperature boundary layers. This "boundary layer within a boundary layer" is the region in which Brownian diffusion of the particles to the wall takes place.

The turbulent particle transport, which appears as the first term on the left-hand side of equation (4-46), tends to zero as the wall is approached, as does the convective particle transport. Therefore, immediately adjacent to the wall, the only mechanisms

available to move particles to the wall are Brownian diffusion and thermophoresis. Both of these transport processes act in a direction normal to the wall, and for a cooled wall, serve to remove any particles that enter the Brownian layer from the fluid. Since the objective of this analysis is to predict particle removal from the fluid immediately adjacent to the wall, the concentration profile inside of this Brownian diffusion boundary layer may not need to be determined. Including the Brownian diffusion boundary layer in the numerical solution scheme would require very small grid spacings next to the wall with a resultant increase in computational effort. It will be shown in Section 5.6 that detailed computation of the concentration profile in the Brownian layer is not necessary for determining the particle flux to the wall. The scaling analysis in Section D.2 also shows that particle transport by Brownian diffusion is negligible with respect to particle transport by thermophoresis.

The Brownian diffusion boundary layer can be resolved by rescaling the governing equations. Walker et al. (1979) analytically solved for the particle concentration in laminar tube flow with thermophoretic transport of small particles using the method of matched asymptotic expansions. The inner layer in their analytical model includes Brownian diffusion effects, but the outer layer does not. They show that the particle flux to the wall is approximated to the leading order of the expansion, $Sc^{-1}$, by the thermophoretic particle flux calculated at the inner edge of the outer layer solution. They also show that the ratio of the Brownian boundary layer thickness to the thermal boundary layer thickness is on the order of $Sc^{-1}$. Therefore, since the Schmidt number of interest here is on the order of $10^5$, the particle flux at the wall is essentially equal to the particle flux at the outer edge of the Brownian diffusion layer and the wall and the edge of the Brownian layer are effectively coincident with respect to the velocity and thermal boundary layers.

The boundary condition of zero particle concentration in the fluid at the wall is not applicable if the Brownian layer is neglected, since only Brownian diffusion can act very near the wall to remove all the particles from the fluid to the assumed perfectly absorbing wall. The Brownian layer boundary condition of zero particle concentration at the wall can be replaced with a relationship between the particle concentration,

particle concentration gradient, temperature, and temperature gradient at the wall as was done by Epstein et al. (1985). This boundary condition at the wall in the absence of Brownian diffusion is obtained by nondimensionalizing equation (4-9) and has the form:

$$n_w' - \frac{\lambda \theta_w'}{1+\lambda} n_w = 0 . \qquad (4-47)$$

For the steam conditions, particle material, and particle size of interest in this problem, the Stokes settling time for a particle to fall the characteristic length of 3 m is on the order of three days. This is well beyond the time scale of a few minutes which is of interest here for the present work. Thus, *the boundary condition of fixed particle concentration in the fluid outside the boundary layer is assumed to remain constant.*

### 4.6. The Numerical Solution

Two different numerical methods were used to solve the coupled boundary-value problem given by equations (4-44), (4-45), and (4-46) and their boundary conditions given by equations (4-43) and (4-47). The necessary constitutive relations for the ratios of thermophysical properties will be dependent on the modeled problem, as described in Section 5.1 and presented as equation (5-1), a polynomial relationship from Irvine and Liley (1984), or set to one for the case of constant thermophysical properties. The relations for the turbulence quantities as developed for equations (4-20), (4-21) and (4-29) will be determined in Section 5.2.

The first numerical solution method, called the local nonsimilarity method (Sparrow et al., 1970), was employed in conjunction with two other numerical solution techniques: a variant of the "shooting" method developed by Nachtsheim and Swigert (1965) and a finite difference technique developed by Lentini and Pereyra (1977). The second technique is a finite-difference procedure called the Keller Box method (Keller, 1976). Further description of these numerical methods is given in Appendix A. Both of

these methods were used, but not for all the cases computed in this study. The numerical results obtained with each of these methods are compared with each other in Chapter 5.

## 4.7. Development of Heat Transfer and Particle Deposition Correlations

### 4.7.1. The general forms of the desired correlations

Generally, the results of either an analytical or experimental investigation for heat or mass transfer are presented in the form of a correlation that relates the dimensionless parameters. For natural convection flows, the dimensionless heat transfer at the surface is usually presented in the form of a Nusselt number, *Nu*, which is correlated as a function of the Prandtl number, *Pr*, and either the Rayleigh number, *Ra*, or the Grashof number, *Gr*. The dimensionless mass transfer at a surface is usually presented as a Sherwood number, *Sh*, which is correlated as a function of the Schmidt number, *Sc*. The Schmidt number is defined as the ratio of the kinematic viscosity to a diffusion coefficient. Any appropriate diffusion coefficient may be used in the definition of the Schmidt number, which could be either the Brownian diffusion coefficient or an effective thermophoretic diffusion coefficient. Since the transport of particles by Brownian diffusion is negligible with respect to the transport of particles by thermophoresis in the flows of interest here, a particle mass transfer correlation in terms of the Schmidt number based on the Brownian diffusion coefficient is of questionable use and will not be employed. An effective thermophoretic diffusion coefficient will also not be employed here, since a simple relationship between the heat transfer and particle transfer is preferable for use in the present work.

The objective of this work is to develop simplified correlations for thermophoretic particle transport. The correlation for thermophoretic particle transport to the wall developed below is a nondimensionalized ratio of the heat transfer and the particle transfer at the wall. Since the heat transfer must be computed for nuclear reactor safety analysis, this ratio of heat transfer to particle transfer can then be easily used to predict the thermophoretic particle transfer to a cooled wall.

First, the correlations used to ensure that the methods employed in this work correctly predict the natural convection heat transfer from a vertical flat plate are described. Then the ratio of thermophoretic particle transfer to heat transfer at the wall is derived.

### 4.7.2. Correlations for the heat transfer to the wall

The dimensionless heat transfer to the wall is given by the Nusselt number, $Nu = hL/k$. The exact functional relationship between the Nusselt number and the Rayleigh number is dependent on whether the flow is laminar or turbulent, as is described in Sections 4.7.2.1 and 4.7.2.2 below. Comparisons of the heat transfer results computed in this work with previously published analytical and experimental results will be made in terms of the Nusselt number-Rayleigh number correlations.

#### 4.7.2.1. Heat transfer correlations for laminar flows

As found in the literature search described in Section 3.1, Schmidt and Beckmann (1930), Eckert and Soehngen (1948), Ostrach (1953), and Churchill and Usagi (1972) present the Nusselt number in laminar natural convection flow on an isothermal vertical plate as the product of a function of the Prandtl number and the fourth root of either the Rayleigh number or the Grashof number. The basis for comparing the results of laminar flow studies was defined for the purposes of this dissertation as the ratio of the local Nusselt number and the fourth root of the local Rayleigh number. This ratio, which is a function of the Prandtl number and is of the order of 0.5 for laminar flow (Jaluria, 1980), is given by the expression

$$\frac{Nu}{Ra^{1/4}} = H_l(Pr)\,. \qquad (4-48)$$

Churchill and Usagi (1972) analyzed the published heat transfer results of various investigators over a wide range of Prandtl numbers, including the asymptotic limiting solutions for zero and infinite Prandtl numbers presented by LeFevre (1956), and report a correlation in the form

$$\frac{Nu}{Ra^{1/4}} = H_l(Pr) = \frac{0.503}{[1.+(0.492/Pr)^{9/16}]^{4/9}} . \qquad (4-49)$$

Churchill and Chu (1975) claim that the relationship given by equation (4-49) is in general agreement with the experimental values reported by Ede (1967) for flows having Rayleigh numbers in the range of $10^5$ to $10^9$.

Comparisons of the laminar heat transfer results computed here to those appearing in the literature are shown in Chapter 5.

#### 4.7.2.2. Heat transfer correlations for turbulent flows

As reported in the literature search in Section 3.1, the heat transfer coefficient in turbulent natural convection flow from a vertical flat plate has been experimentally observed to be independent of the distance from the leading edge of the plate. This independence of the heat transfer coefficient on the distance from the leading edge is shown by the ratio of the Nusselt number and the cube root of the Rayleigh number. This ratio is written in the form:

$$\frac{Nu}{Ra^{1/3}} = H_t(Pr) , \qquad (4-50)$$

which will be used to present the results of turbulent flow calculations. Note that the local and mean Nusselt numbers are identical for turbulent flow.

For gases with Prandtl numbers of approximately 0.7 and Rayleigh numbers in the range of $10^9$ to $10^{12}$, the ratio given by equation (4-50) varies only slightly from 0.10 (Bayley, 1955) to 0.13 (McAdams, 1954), as reported by Clausing (1983). Extensive experimental data were generated by Seibers et al. (1983) for air at high wall temperature ratios (up to $T_w / T_\infty = 2.75$) that are of the same magnitude as that of interest here. Seibers developed a Nusselt number correlation of the form:

$$Nu = 0.098 Gr^{1/3} \left(\frac{T_w}{T_\infty}\right)^{-0.14} . \qquad (4-51)$$

This correlation was modified by substituting the identity $Gr = Ra/Pr$, where the value for the Prandtl number of air is 0.707 at the ambient conditions of Seibers et al. (1983). This modification was performed in order to present the results of Seibers et al. (1983) as the ratio of Nusselt number to the cube root of the Rayleigh number. This modified correlation of Seibers et al. (1983) is

$$\frac{Nu}{Ra^{1/3}} = 0.110\left(\frac{T_w}{T_\infty}\right)^{-0.14}. \qquad (4-52)$$

Saunders (1939) performed experiments with a vertical flat plate in water and air. The heat transfer results were presented in the form of equation (4-50). The ratio of $Nu/Ra^{1/3}$ is 0.17 for water ($Pr = 7.0$) and 0.10 for air ($Pr = 0.73$). Saunders also reports that the transition from laminar flow to turbulent flow occurs at a Rayleigh number of $2\times10^9$ for both air and water.

Comparison of the values of the ratio $Nu/Ra^{1/3}$ computed here to those found in the literature is given in Chapter 5.

### 4.7.3. Development of a correlation for thermophoretic deposition of particles on the wall

Computation of the rate of deposition of particles on a cold wall requires the solution of a system of coupled, nonlinear, partial differential equations. Solution of this coupled system of equations presents a formidable challenge. If the flux of particles deposited on the wall could be related to the heat flux by a simple relationship involving the various parameters in the problem, the computational effort could be reduced. Thus, a simplified correlation is developed below which relates the flux of particles deposited on the wall to the heat flux at the wall. In Chapter 6, this simplified correlation is shown to yield sufficiently accurate particle deposition fluxes at the wall for the flow conditions of interest here.

#### 4.7.3.1. Ratio of thermophoretic particle transfer to heat transfer at the wall

A heat transfer coefficient is commonly used in convective heat transfer analysis in order to simplify the presentation of results and the computation of the convective heat flux. A mass transfer coefficient is also commonly employed for the same purposes.

For the case of thermophoretic particle transfer, where the heat transfer acts to effect a transfer of particles, a correlation of the ratio of these two transfer coefficients would allow a straightforward computation of the flux of thermophoretically deposited particles from the value of the heat flux, which is more easily measured or computed.

The heat transfer coefficient is defined as the ratio of the heat flux to the wall and the difference between the temperature of the fluid far from the wall and the temperature at the wall. This may be written:

$$h_H = \frac{q_w}{T_\infty - T_w}, \tag{4-53}$$

where the heat flux to the wall is the conductive heat flux in the fluid immediately adjacent to the wall. Upon substitution of the Fourier Law of heat conduction in the fluid at the wall, given by

$$q_w = -k\left(\frac{\partial T}{\partial y}\bigg|_w\right), \tag{4-54}$$

the heat transfer coefficient is then given by

$$h_H = \frac{-k\left(\frac{\partial T}{\partial y}\Big|_w\right)}{T_\infty - T_w}. \tag{4-55}$$

The particle transfer coefficient is defined by the relation

$$h_P = \frac{j_p}{\rho_\infty N_\infty}, \tag{4-56}$$

where $j_P$ is the particle flux immediately adjacent to the wall and $\rho_\infty N_\infty$ is the volumetric particle concentration far from the wall. The particle flux to the wall is due to thermophoresis. For the present purposes, this flux is taken to be the product of the thermophoretic velocity and the particle concentration at the outer edge of the Brownian layer.

The actual particle velocity at the wall must, of course, be zero, but as described in Section 4.5, the particle flux at the wall is essentially equal to the particle flux at the outer edge of the Brownian diffusion layer where the particle velocity is nonzero. Since the outer edge of the Brownian diffusion layer is effectively at the wall when Brownian diffusion is neglected, the temperature gradient at the wall will be used in the expression for thermophoretic velocity at the outer edge of the Brownian diffusion layer. The thermophoretic particle flux at the wall is given by the expression

$$j_P = -\rho_w N_w K \frac{\nu_w}{T_w}\left(\frac{\partial T}{\partial y}\bigg|_w\right). \tag{4-57}$$

Therefore, the particle transfer coefficient is given by

$$h_P = -\frac{\rho_w N_w}{\rho_\infty N_\infty} K \frac{\nu_w}{T_w}\left(\frac{\partial T}{\partial y}\bigg|_w\right). \tag{4-58}$$

Forming the ratio of the two transfer coefficients yields

$$\frac{h_P}{h_H} = \frac{\rho_w N_w}{\rho_\infty N_\infty}\frac{T_\infty - T_w}{T_w} K \frac{\nu_w}{k_w}. \tag{4-59}$$

This term is multiplied by the product of the density and the specific heat of the fluid far from the wall, which are known quantities. Rewriting in terms of the dimensionless particle concentration at the wall and known parameters from the problem description gives

$$\rho_\infty C_\infty \frac{h_P}{h_H} = n_w\left(\frac{-\lambda}{1+\lambda}\right)(KPr_\infty)\left(\frac{\mu_w}{\mu_\infty}\frac{k_\infty}{k_w}\right), \tag{4-60}$$

where $\lambda$ is the wall overheat ratio defined in equation (4-37).

The expression of equation (4-60) will be called the dimensionless ratio of transfer coefficients. Observation reveals that the dimensionless ratio of transfer coefficients predicts zero particle transfer to the wall for the following limiting, albeit trivial, cases:

1. Zero wall overheat ratio ($\lambda$=0), which implies that no temperature difference exists to move the particle to the wall by thermophoresis.
2. Zero thermophoretic coefficient $K$, which implies no thermophoresis.
3. Vanishingly small Prandtl number, which implies an infinitely thick thermal boundary layer.

The above limiting cases are trivial for the purposes of the present investigation, since: (1) a zero wall overheat ratio would also imply no natural convection, (2) thermophoresis is indeed of interest, and (3) thermophoresis in fluids with very small Prandtl numbers (liquid metals) is beyond the scope of the work. If equation (4-60) did not, however, reduce to zero for these limiting cases, it would be immediately suspect.

Further inspection of equation (4-60) reveals that for gases such as air at atmospheric conditions, the effects of variable thermophysical properties on this relationship would be restricted primarily to the effective wall particle concentration, since the dynamic viscosity and thermal conductivity have an almost identical functional dependence upon temperature and the last term in parentheses on the right-hand side of equation (4-60) would have a value close to unity. However, the effects of variable thermophysical properties in equation (4-60) are much more important for steam at the high temperatures and pressures of interest in this investigation. For steam at a pressure of 6.9 MPa and a temperature far from the wall of 1273 K with a wall temperature of 623 K, the ratio of thermophysical properties $\mu_w k_\infty / \mu_\infty k_w$ that appears in the last term in parentheses in equation (4-60) has a value of 1.21.

Further inspection of the dimensionless ratio of coefficients reveals that it also represents a ratio of the energy transferred by thermophoresis to the wall and the energy transferred by convection to the wall. By substituting the definition of the particle transfer coefficient, $h_P$, of equation (4-56) and the definition of heat transfer coefficient, $h_H$, of equation (4-53) in the left-hand side of equation (4-60) results in the following expression:

$$\rho_\infty C_\infty \frac{h_P}{h_H} = \left(\frac{j_P}{q_w}\right)\left[\frac{C_\infty (T_\infty - T_w)}{N_\infty}\right]. \qquad (4-61)$$

The second term in brackets $C_\infty( T_\infty - T_w) / N_\infty$ on the right-hand side of equation (4-61) represents the enthalpy in the fluid, relative to the wall, per particle. This term, when multiplied by the particle flux deposited at the wall by thermophoresis, represents the energy in the fluid transferred to the wall by thermophoresis. Thus, the dimensionless ratio of transfer coefficients represents the ratio of energy transferred by thermophoresis to the energy transferred by convection at the wall.

Evaluation of the dimensionless ratio of transfer coefficients using equation (4-60) requires the solution of equation (4-46) in order to compute the effective wall particle concentration. Since the stated objective of the present work is to develop simplified particle deposition correlations, an approximation for this dimensionless ratio of transfer coefficients is developed that does not require the effective wall particle concentration to be calculated. This approximation is given in Section 6.1. In order to assess the accuracy of the solution methods used in this work, values for this dimensionless ratio of transfer coefficients are determined in the following section for nontrivial cases having a known solution. Also, in order to develop simplified correlations for particle deposition, expressions for the upper and lower bounds on the value of the dimensionless ratio of transfer coefficients are developed below.

### 4.8. Exact Solutions of the Particle Conservation Equation

In order to assess the accuracy of the solution methods employed in this work, exact solutions of the dimensionless particle conservation equation for nontrivial cases are determined in this section. Values for the dimensionless ratio of transfer coefficients are also determined for each of these exact solutions. The Brownian layer is neglected in all cases, where, as described in Section 4.5, the particle flux at the wall is essentially equal to the particle flux at the outer edge of the Brownian layer and the wall is essentially coincident with the outer edge of the Brownian layer.

There are at least four situations where the particle conservation equation has the exact form as the conservation of energy equation. The necessary conditions for the

occurrence of any of these situations are that there must not be any volumetric heat sources and that boundary conditions of uniform particle concentration and uniform temperature distribution must apply. With these restrictions, the four situations are:

1. Laminar flow with constant thermophysical properties.
2. Laminar flow with variable thermophysical properties.
3. Turbulent flow with constant thermophysical properties.
4. Turbulent flow with variable thermophysical properties.

For situations 2 and 4, the thermophysical properties are assumed to vary such that they can be written as functions of the pseudosimilarity variable $\eta$. For situations 1 and 3, the thermophysical properties are constant except where the variations in density give rise to a body force (the Boussinesq approximation).

For the first case of laminar flow with constant thermophysical properties, the equations representing the conservation of energy and the conservation of particles, which can be written as functions of a similarity variable (Goren, 1977), are given by:

$$K\frac{d}{d\eta}\left(\frac{\lambda\theta'}{1+\lambda\theta}n\right)+3fn' = 0 \qquad (4-62)$$

and

$$\frac{1}{Pr_r}\frac{d}{d\eta}(\theta')+3f\theta' = 0\,. \qquad (4-63)$$

Since the values of the thermophoretic coefficient, $K$, and the reference Prandtl number, $Pr_r$, are not functions of the pseudosimilarity variable $\eta$, equation (4-62) may be rewritten as:

$$\frac{1}{Pr_r}\frac{d}{d\eta}\left(\theta'\frac{\lambda n}{1+\lambda\theta}KPr_r\right)+3fn' = 0\,. \qquad (4-64)$$

By inspection of the term in parentheses in the left-hand side of equation (4-64) for $KPr_r$ equal to one, a solution of the form

$$\frac{n}{1+\lambda\theta} = 1 \qquad (4-65)$$

is admissible, which reduces the particle conservation equation, equation (4-62), to a form identical to that of the energy conservation equation, equation (4-63). The ratio in equation (4-65) must equal unity in order to meet the boundary condition at the edge of the boundary layer.

With the definition for the dimensionless temperature, $\theta$, in equation (4-35), the particle concentration predicted by equation (4-65) at the wall is $n_w = 1+\lambda$. Thus, the dimensionless ratio of transfer coefficients is equal to the negative value of the wall overheat ratio, or

$$\rho_\infty C_\infty \frac{h_P}{h_H} = -\lambda . \qquad (4-66)$$

For the second situation of interest, laminar flow with variable thermophysical properties, the thermal conductivity, dynamic viscosity, and specific heat of the fluid were all assumed to vary such that they can be written as functions of the pseudosimilarity variable. In this case, the equations governing the conservation of energy and the particle distribution may be written in similarity form (Goren, 1977) as:

$$K\frac{d}{d\eta}\left[\left(\frac{\rho\mu}{\rho_r\mu_r}\right)\frac{\lambda\theta'}{1+\lambda\theta}n\right]+3fn' = 0 \qquad (4-67)$$

and

$$\frac{1}{Pr_r}\frac{C_r}{C}\frac{d}{d\eta}\left[\left(\frac{\rho k}{\rho_r k_r}\right)\theta'\right]+3f\theta' = 0 . \qquad (4-68)$$

Since the values of the thermophoretic coefficient, $K$, and the reference Prandtl number, $Pr_r$, are not functions of the pseudosimilarity variable $\eta$, equation (4-67) may be rewritten as

$$\frac{1}{Pr_r}\frac{d}{d\eta}\left[\left(\frac{\rho\mu}{\rho_r\mu_r}\right)\theta'\frac{\lambda n}{1+\lambda\theta}KPr_r\right]+3fn' = 0 . \qquad (4-69)$$

Two additional assumptions about the variation of the thermophysical properties are necessary to obtain an exact solution of the particle concentration conservation

equation. First, the ratio $(k\,\mu_r/k_r\,\mu)$ must be constant and equal to one. Second, the specific heat $C$ must remain constant, such that the ratio $C_r/C$ is identically one. Under the conditions of constant specific heat, $KPr_r$ equal to unity, and identical functional dependence with respect to the similarity variable $\eta$ for both the dynamic viscosity and the thermal conductivity, equation (4-65) reduces the particle conservation equation, equation (4-67), to the energy conservation equation, equation (4-68). The dimensionless ratio of transfer coefficients also reduces to a value equal to the negative of the wall overheat ratio. These two assumptions about the variation of the thermophysical properties restrict this particular exact solution to constant Prandtl number fluids. Over the range of temperatures expected for the steam conditions of interest here, none of these assumptions are valid.

Analysis of the third situation for turbulent flow with constant properties is similar to the analyses for the laminar flow above. In this case, however, the problem cannot be recast in similarity form. Thus, the nonsimilar conservation equations for particle concentration in the absence of Brownian diffusion and for conservation of energy are given by:

$$\frac{\partial}{\partial\eta}\left(\frac{1}{Sc_t}\frac{\mu_t}{\mu}n'\right)+K\frac{\partial}{\partial\eta}\left(\frac{\lambda\theta'}{1+\lambda\theta}n\right)+3fn' = 4\xi(f'n_\xi - n'f_\xi) \qquad (4-70)$$

and

$$\frac{1}{Pr_r}\frac{\partial}{\partial\eta}\left[\left(1+\frac{k_t}{k}\right)\theta'\right]+3f\theta' = 4\xi(f'\theta_\xi - \theta'f_\xi) \qquad (4-71)$$

where the ratio of turbulent thermal conductivity to molecular thermal conductivity is replaced by defining the turbulent Prandtl number as

$$\frac{k_t}{k} = \frac{Pr_r\,\mu_t}{Pr_t\,\mu}. \qquad (4-72)$$

The conservation of energy equation for a turbulent flow, equation (4-71), now appears in the form

$$\frac{1}{Pr_r}\frac{\partial}{\partial\eta}\left[\left(1+\frac{Pr_r}{Pr_t}\frac{\mu_t}{\mu}\right)\theta'\right]+3f\theta' = 4\xi(f'\theta_\xi-\theta' f_\xi)\,. \qquad (4-73)$$

Similarly, the turbulent particle conservation equation for a turbulent flow, equation (4-70), is rearranged to give:

$$\frac{1}{Pr_r}\frac{\partial}{\partial\eta}\left[\frac{\lambda\theta'}{1+\lambda\theta}nKPr_r+\frac{Pr_r}{Sc_t}\frac{\mu_t}{\mu}n'\right]+3fn' = 4\xi(f'n_\xi-n' f_\xi)\,. \qquad (4-74)$$

By inspection of the bracketed term in the left-hand side of equation (4-74) when $KPr_r$ is equal to one, equation (4-65) with the assumption of a constant wall overheat ratio, which excludes thermal stratification, reduces the particle conservation equation to the form:

$$\frac{1}{Pr_r}\frac{\partial}{\partial\eta}\left[\left(1+\frac{Pr_r}{Sc_t}\frac{\mu_t}{\mu}\right)\theta'\right]+3f\theta' = 4\xi(f'\theta_\xi-\theta' f_\xi)\,. \qquad (4-75)$$

From inspection of the bracketed terms in the left-hand sides of equations (4-73) and (4-75), the turbulent Schmidt number must be equal to the turbulent Prandtl number in order for equation (4-65) to be an admissible solution of equation (4-74). This restriction is reasonable when the particle inertia is sufficiently small such that the particle moves with a turbulent eddy.

Extension of the analysis for the case of turbulent flow with variable thermophysical properties follows in the same fashion as the analysis for variable property laminar flow. The same restrictions for the laminar flow case on the functional variation of thermal conductivity and dynamic viscosity and the constant values for specific heat and Prandtl number apply to the turbulent flow case.

These four exact solutions will be used in Section 5.5.1 to ensure that the numerical methods used in the present investigation yield a correct value for the dimensionless ratio of transfer coefficients, which is equal to the negative of the wall overheat ratio, $-\lambda$, under the limiting assumptions for each particular situation.

### 4.9. Bounding Limits for the Ratio of Transfer Coefficients

In order to develop simplified correlations for particle deposition, expressions for the upper and lower bounds on the value of the dimensionless ratio of transfer coefficients given by equation (4-60) are derived below. As shown in the previous section, the dimensionless ratio of transfer coefficients reduces to the negative of the wall overheat ratio for the above four cases when the value of $KPr_t$ is one. Physical situations in which $KPr_t$ has a value of approximately one are not unknown (Batchelor and Shen, 1985). The dimensionless ratio of transfer coefficients, equation (4-60), approaches zero for the condition of either the thermophoretic coefficient or the Prandtl number approaching zero. An approximation for the dimensionless ratio of transfer coefficients would be useful for situations in which the product $KPr_t$ is between zero and one. First, a bounding upper limit for the effective wall particle concentration is determined.

Batchelor and Shen (1985) developed bounding limits on the wall particle concentration in terms of the temperature and the product $KPr_t$ for the general case of forced convection. A similar analysis for the specific case of constant property laminar natural convection flow from an isothermally cooled wall is developed below.

The reference state for the evaluation of the thermophysical properties was taken to be the fluid state far from the wall. As before, the differential equations governing particle concentration and energy conservation for laminar natural convection flow are given by:

$$K\frac{d}{d\eta}\left(\frac{\lambda\theta'}{1+\lambda\theta}n\right)+3fn' = 0 \qquad (4-76)$$

and

$$\theta''+3Pr_{\infty}f\theta' = 0\,. \qquad (4-77)$$

Taking the derivative in the particle concentration equation (4-76) and regrouping yields

$$\frac{n'}{n}\left(3f+K\frac{\lambda\theta'}{1+\lambda\theta}\right)+K\frac{\lambda\theta'}{1+\lambda\theta}\left(\frac{\theta''}{\theta'}-\frac{\lambda\theta'}{1+\lambda\theta}\right) = 0\,. \qquad (4-78)$$

Solving the energy conservation equation (4-77) for the second derivative of the temperature and substituting into equation (4-78) gives

$$\frac{n'}{n}\left(3f+K\frac{\lambda\theta'}{1+\lambda\theta}\right)-K\frac{\lambda\theta'}{1+\lambda\theta}\left(3Pr_{\infty}f+\frac{\lambda\theta'}{1+\lambda\theta}\right)=0. \qquad (4-79)$$

Equation (4-79) is now manipulated to obtain two different expressions. By adding and subtracting the term

$$3f\frac{\lambda\theta'}{1+\lambda\theta}, \qquad (4-80)$$

equation (4-79) can be reduced to the form:

$$\left(3f+K\frac{\lambda\theta'}{1+\lambda\theta}\right)\frac{d}{d\eta}\left[\ln\left(\frac{n}{1+\lambda\theta}\right)\right]=-(1-KPr_{\infty})3f\left(\frac{\lambda\theta'}{1+\lambda\theta}\right). \qquad (4-81)$$

Similarly, by adding and subtracting the term

$$Pr_{\infty}\left(K\frac{\lambda\theta'}{1+\lambda\theta}\right)^2 \qquad (4-82)$$

to equation (4-79), the following equation is obtained:

$$\left(3f+K\frac{\lambda\theta'}{1+\lambda\theta}\right)\frac{d}{d\eta}\left\{\ln\left[\frac{n}{(1+\lambda\theta)^{KPr}}\right]\right\}=K(1-KPr_{\infty})\left(\frac{\lambda\theta'}{1+\lambda\theta}\right)^2. \qquad (4-83)$$

The first term in parentheses on the left-hand side of equation (4-79) and equation (4-83),

$$3f+K\frac{\lambda\theta'}{1+\lambda\theta}, \qquad (4-84)$$

contains two terms that represent the motion of a particle. The first term represents the convective motion and the second term represents the thermophoretic motion. These terms are both positive in natural convection as long as no reverse flow, significant wall transpiration, or heat flux in the direction from the wall to the fluid occur.

The right-hand side of equation (4-81) is always less than or equal to zero. It is identically zero at the edge of the boundary layer. This condition requires the derivative of the natural logarithm term on the left-hand side to also be less than or equal to zero. This condition places a restriction on the argument of the logarithm term as the wall is approached. The behavior required of this argument as the wall is approached is determined below.

Using the chain rule of differential calculus, the derivative of the natural logarithm term in equation (4-81) is rewritten as

$$\frac{d}{d\eta}\left(\ln\frac{n}{1+\lambda\theta}\right)=\left[\frac{d\left(\ln\frac{n}{1+\lambda\theta}\right)}{d\left(\frac{n}{1+\lambda\theta}\right)}\right]\left[\frac{d\left(\frac{n}{1+\lambda\theta}\right)}{d\eta}\right]. \qquad (4-85)$$

Since the derivative of the natural logarithm with respect to its argument is always positive for real positive arguments (Abramowitz and Stegun, 1965), and the right-hand side of equation (4-81) is always less than or equal to zero, the following inequality must hold:

$$\frac{d}{d\eta}\left(\frac{n}{1+\lambda\theta}\right)\le 0. \qquad (4-86)$$

At the edge of the boundary layer, the dimensionless concentration is identically one and the dimensionless temperature is identically zero. Because of the inequality given by (4-86), the argument of the derivative term must increase monotonically as the wall is approached. At the wall, the following inequality must hold:

$$\frac{n_w}{1+\lambda}\ge 1. \qquad (4-87)$$

Similarly, the right-hand side of equation (4-83) is always greater than or equal to zero, having a value of zero at the edge of the boundary layer. This condition requires the derivative of the natural logarithm term to also be greater than or equal to zero. Employing the chain rule and using the fact that the derivative of the natural logarithm with respect to its argument is always positive, the following inequality must hold:

$$\frac{d}{d\eta}\left[\frac{n}{(1+\lambda\theta)^{KPr_\infty}}\right] \geq 0 . \qquad (4-88)$$

At the edge of the boundary layer, the argument of the derivative in the above inequality (4-88) must, by definition, be one. Because of the above inequality (4-88), the argument of the derivative must monotonically decrease as the wall is approached. Thus, the following inequality must hold at the wall:

$$\frac{n_w}{(1+\lambda)^{KPr_\infty}} \leq 1 . \qquad (4-89)$$

Combining inequalities (4-87) and (4-89) yields the following inequality for the bounds for the particle concentration due to thermophoresis at the wall:

$$(1+\lambda) \leq n_w \leq (1+\lambda)^{KPr_\infty} . \qquad (4-90)$$

These bounds were derived for the specific case of laminar, constant property natural convection flow. Thus, the applicability of these bounding limits to the other conditions of interest of this problem will now be addressed.

These bounds on the particle concentration at the wall were utilized to obtain bounds on the dimensionless ratio of transfer coefficients as given by equation (4-60). For the lower limit of wall particle concentration, the dimensionless ratio of transfer coefficients is given by

$$\rho_\infty C_\infty \left(\frac{h_P}{h_H}\right)_{\min} = -\lambda KPr_\infty \left(\frac{\mu_w k_\infty}{\mu_\infty k_w}\right) . \qquad (4-91)$$

Similarly, for the upper limit of wall particle concentration, the dimensionless ratio of transfer coefficients reduces to

$$\rho_\infty C_\infty \left(\frac{h_P}{h_H}\right)_{max} = (1+\lambda)^{(KPr_\infty - 1)}\left[-\lambda KPr_\infty \left(\frac{\mu_w}{\mu_\infty}\frac{k_\infty}{k_w}\right)\right]. \qquad (4-92)$$

A method for comparing the computed dimensionless ratio of transfer coefficients to the bounding limits was devised by modifying equation (4-92) to include a coefficient, $\omega$, in the exponent as follows:

$$\rho_\infty C_\infty \frac{h_P}{h_H} = (1+\lambda)^{\omega(KPr_\infty - 1)}\left[-\lambda KPr_\infty \left(\frac{\mu_w}{\mu_\infty}\frac{k_\infty}{k_w}\right)\right]. \qquad (4-93)$$

The coefficient $\omega$ in equation (4-93) will be a number between zero and one, which is computed with the results of the solution of the coupled system of equations (4-44), (4-45), and (4-46) for the circumstances of interest of this work. The coefficient $\omega$ can be considered as a measure of where the computed dimensionless ratio of transfer coefficients lies between the bounds given by equations (4-91) and (4-92). Thus, a value of $\omega$ equal to zero would represent the lower bound and a value of $\omega$ equal to one would represent the upper bound of the dimensionless ratio of transfer coefficients.

The computed values of $\omega$ are presented in Table 6-7 in Section 6.1 for steam at 6.9 MPa and 1000°C, air at atmospheric pressure and 1000°C, and hydrogen at atmospheric pressure and 1000°C. The value of $\omega$ varies from approximately 0.5 for a value of $KPr_\infty$ of unity and increases to almost 1.0 as $KPr_\infty$ approaches zero. Thus, the actual computed values for the dimensionless ratio of transfer coefficients are closer to the upper bound given by equation (4-92).

To develop an approximation for the dimensionless ratio of transfer coefficients, the first term in parentheses, $(1+\lambda)$, on the right-hand side of equation (4-92) is expanded using the binomial theorem to get

$$(1+\lambda)^{(KPr_\infty - 1)} = 1 + (KPr_\infty - 1)\lambda + \frac{1}{2}(KPr_\infty - 1)(KPr_\infty - 2)\lambda^2 + \cdots. \qquad (4-94)$$

The wall overheat ratio is approximately equal to -0.5 for many of the cases of interest of this problem. This value of $\lambda$ requires retaining at least three terms in the binomial expansion in order to obtain convergence when the ratio of transfer coefficients is equal to the upper limit. However, the actual value for the dimensionless ratio of transfer coefficients should be somewhere between the limits given by equations (4-91) and (4-92), as indicated by the value of the coefficient $\omega$ in equation (4-93).

A truncated series expansion of equation (4-94) will be shown in Section 6.1, to yield an approximation for the dimensionless ratio of transfer coefficients without the necessity of solving the particle conservation equation for the effective wall concentration, which appears in equation (4-60). Since all the terms in equation (4-94) are positive for a cooled wall with the product $KPr_-$ less than one, errors due to alternating signs should not be a concern when the series is truncated at an arbitrary number of terms.

# CHAPTER 5

# MATHEMATICAL AND PHYSICAL MODELING JUSTIFICATION

## 5.1. Introduction

The analytical model developed in this work depicts the natural convection boundary layer flow adjacent to an isothermal, vertical flat plate immersed in a newtonian fluid of infinite extent. This model includes a number of extremely complex phenomena, such as turbulence, variable property effects, the thermophoretic transport of particulate matter that acts as a volumetric heat source, thermal stratification in the ambient fluid, and participation of the fluid in an exchange of thermal radiation. Thus, the importance of validating as many aspects of the model as possible by comparison of the computed results with the published results of other investigations cannot be overly emphasized. As might have been anticipated, no single analytical or experimental investigation could be found in the open literature that includes *all* of the effects accounted for in the present work. This necessitates validation of the model in a piecemeal fashion by comparison of computed results with the results of a number of different investigations, each of which is essentially focused on an exploration of only one of the many effects included in the present model. The various investigations used to make these comparisons are listed in Table 5-1. All of these investigations, except those involving flows with volumetric heat sources, consider natural convection boundary layer flows on isothermal, vertical plates.

As was shown in Chapter 4, the results for laminar flows will be compared with those from other investigations by comparing values of the ratio $Nu/Ra^{1/4}$. Similarly, the ratio $Nu/Ra^{1/3}$ will be used for comparing the results for turbulent flows.

The remainder of this chapter is mainly comprised of the detailed comparisons between the results computed with the present model and those given in the investigations listed in Table 5-1. A discussion of the effect of neglecting the Brownian diffusion layer on the accuracy of the results is also presented. Finally, the chapter closes with a summary of the results of the validation process.

Table 5-1. Summary of Other Investigations Used To Validate the Present Analytical Model.

| Type of Flow | Investigations Used For Comparison |
|---|---|
| Laminar flow with constant properties | Ostrach (1953) |
| Laminar flow with variable properties | Sparrow and Gregg (1958)<br>Cairnie and Harrison (1982) |
| Laminar flow with a thermally stratified ambient fluid | Chen and Eichhorn (1972) |
| Laminar flow with participating thermal radiation | Kuiken (1969)<br>Kennedy and Paszkowskyj (1970) |
| Turbulent flow with constant properties | Bayley (1955) |
| Turbulent flow with variable properties | Seibers et al. (1985) |
| Flow with volumetric heat sources (open rectangular pool geometry) | Greene (1982) |
| Flow with thermophoretic deposition of particles | Goren (1977) |

The experimental portions, if any, of the investigations listed above in Table 5-1 consist of a heated plate in a relatively cold fluid, with the exceptions of Greene (1982), which considers a cold plate in a relatively warmer fluid, and Goren (1977), which considers both isothermally heated and cooled wall conditions. For the present work, the conditions of a cold wall and a relatively warm fluid are of interest, as described in Chapter 2. The differential equations describing the motion, equation (4-44), the conservation of energy, equation (4-45), and the conservation of particles, equation (4-46), that are presented and nondimensionalized in Chapter 2 are applicable in either heated or cooled wall conditions for the reasons described as follows.

The origin for the coordinate system as shown in Figure 2-2 (at the top of the plate leading edge) is specifically for the flow for fluids with a positive volumetric expansion coefficient, $\beta$, on a cooled wall. For a heated wall, the flow would start at the bottom

which would then be the origin for heated wall conditions. Thus, either upflow adjacent to a heated wall or downflow adjacent to a cooled wall can be accommodated with no change in the sign of the dimensionless term representing velocity, $f'$.

Because of the manner in which the dimensionless fluid temperature, $\theta$, is defined in equation (4-35) as a ratio of the temperature difference in the fluid and the temperature difference between the wall and the ambient fluid, a heated or cooled wall has no effect on the sign of $\theta$. Thus, any particular value of $\theta$ can be representative of either a heated or cooled wall.

With the definition of the wall overheat ratio, $\lambda$, in equation (4-37) as the ratio of the difference between the wall and ambient fluid temperatures to the ambient fluid temperature, a heated or cooled wall can be accommodated in the computation of the particle concentration. However, thermophoretic transport of particles to the wall can only exist for cooled wall conditions, since a heated wall will expel particles away from the wall (Goren, 1977) and result in a zone adjacent to the heated wall with no particles at all. Because of the sign of $\lambda$ for a heated wall is positive, the differential equation describing the transport of particles, equation (4-46), becomes singular at some point near the heated wall and is therefore inappropriate both mathematically and physically to compute the particle concentration in the particle-free zone of the fluid.

### 5.2. Comparison of Results for Laminar Flow

As may be seen in Table 5-1, the laminar flow results computed with the present model are validated by comparison with the results of: (a) Ostrach (1953) for constant-property flows, (b) Sparrow and Gregg (1958) for variable-property flows, (c) Chen and Eichhorn (1976) for flows with linearly-stratified ambient fluids, and (d) Kuiken (1969) and Kennedy and Paszkowskyj (1970) for flows in which the gas participates in the thermal radiation process. When necessary, the results of these other investigations were recalculated in terms of the parameter $Nu/Ra^{1/4}$ to provide a common basis for comparison.

### 5.2.1. Flows with constant thermophysical properties

Ostrach (1953) reports the results of a similarity solution for the natural convection boundary layer flow on a vertical flat plate immersed in an isothermal body of fluid for a range of Prandtl numbers from 0.01 to 1000. This range of Prandtl numbers encompasses all possible fluids of interest from liquid metals, such as mercury, to oils. Ostrach shows good agreement between his computed heat transfer results and the experimentally measured data of others.

Since the conditions of this problem reduce the governing equations and boundary conditions to similarity form, only the similarity, or first, level of truncation of the local nonsimilarity method was used to generate results for the purposes of comparison. The results computed using the Keller Box method, the similarity solution obtained using the shooting method of Nachtsheim and Swigert (1965), and the finite-difference results obtained with the method of Lentini and Pereyra (1977) are presented in Table 5-2 along with the published results of Ostrach (1953). The results obtained with the correlation of Churchill and Usagi (1972), equation (4-49) are also listed in Table 5-2.

Table 5-2. Values of the Ratio $Nu/Ra^{1/4}$ for Constant-Property Laminar Flows.

| Prandtl Number | Ostrach | Churchill and Usagi | Present Investigation | | |
|---|---|---|---|---|---|
| | | | Keller Box | Lentini-Pereyra | Nachtsheim-Swigert |
| 0.001 | — | 0.1055 | 0.1050 | 0.1054 | 0.1176 |
| 0.01 | 0.1816 | 0.1814 | 0.1801 | 0.1803 | 0.1802 |
| 0.72 | 0.3873 | 0.3868 | 0.3865 | 0.3873 | 0.3874 |
| 1.0 | 0.4010 | 0.4005 | 0.4001 | 0.4010 | 0.4010 |
| 2.0 | 0.4260 | 0.4259 | 0.4250 | 0.4259 | 0.4260 |
| 5.0 | — | 0.4521 | 0.4501 | 0.4509 | 0.4511 |
| 7.0 | — | 0.4597 | 0.4574 | 0.4580 | 0.4583 |
| 10.0 | 0.4650 | 0.4667 | 0.4641 | 0.4649 | 0.4649 |
| 100.0 | 0.4899 | 0.4922 | 0.4904 | 0.4900 | 0.4898 |
| 1000.0 | 0.4987 | 0.5000 | 0.5032 | 0.4986 | 0.4952 |

As shown in Table 5-2, the results computed with the three different numerical methods used in the present investigation agree quite well with the published results of Ostrach (1953) and of Churchill and Usagi (1972), with the single exception of the result computed with the Nachtsheim-Swigert technique for a Prandtl number of 0.001. In this case, the value of $Nu/Ra^{1/4}$ computed by the Nachtsheim-Swigert method is approximately 12% greater than the value of this parameter computed with the Churchill-Usagi correlation.

### 5.2.2. Flows with variable thermophysical properties

The results of two investigations for laminar flow with variable thermophysical properties were compared with the results obtained using the methods of this dissertation. Sparrow and Gregg (1958) present the results of a numerical solution of the differential equations describing the similarity flow of a gas postulated to have thermophysical properties that vary as a specified function of the ratio of wall temperature to the fluid temperature far from the isothermal wall. Cairnie and Harrison (1982) present results for an experimental investigation of the heat transfer from a vertical isothermal plate at a high temperature.

Sparrow and Gregg (1958) developed the differential equations for the laminar natural convection similarity flow from a vertical isothermal plate for a fluid with variable thermophysical properties. They present the computed results for a gas with postulated variations of the density, dynamic viscosity, and thermal conductivity of the following forms:

$$\frac{\rho\mu}{\rho_r\mu_r} = \frac{\rho k}{\rho_r k_r} = \left(\frac{T_w/T_\infty}{1+\lambda\theta}\right)^{1/4} \qquad (5-1)$$

where $\lambda$ is the wall overheat ratio defined in equation (4-37) and $\theta$ is the dimensionless fluid temperature as defined in equation (4-35). White (1974) calls the property ratio of $\rho\mu/\rho_r\mu_r$ in equation (5-1) the Chapman-Rubesin parameter, although Sparrow and Gregg do not. The Prandtl number and specific heat are assumed to be constant. These functional relationships are simplified idealizations for a real gas such as air. Sparrow

and Gregg computed results for a range of wall temperature ratios to develop a reference temperature method for gases as described in the literature search in Section 3.2. The computed values of the ratio $Nu/Ra^{1/4}$ for a fluid having a Prandtl number of 0.7 at various wall temperature ratios are presented in Table 5-3 along with the published results of Sparrow and Gregg (1958). The computed results from this investigation shown in Table 5-3 show good agreement with those of Sparrow and Gregg.

Table 5-3. Values of the Ratio $Nu/Ra^{1/4}$ for the Variable-Property Laminar Flows of Sparrow and Gregg.

| Wall Temperature Ratio | Sparrow and Gregg | Present Investigation | | |
|---|---|---|---|---|
| | | Keller Box | Lentini-Pereyra | Nachtsheim-Swigert |
| 4.0 | 0.4056 | 0.4042 | 0.4048 | 0.4052 |
| 3.0 | 0.4023 | 0.4013 | 0.4019 | 0.4023 |
| 2.5 | 0.4001 | 0.3992 | 0.3998 | 0.4002 |
| 2.0 | 0.3968 | 0.3964 | 0.3969 | 0.3973 |
| 1.0 | 0.3859 | 0.3853 | 0.3856 | 0.3861 |
| 0.75 | 0.3805 | 0.3796 | 0.3799 | 0.3805 |
| 0.5 | 0.3706 | 0.3706 | 0.3713 | 0.3714 |
| 0.33 | 0.3608 | 0.3604 | 0.3609 | 0.3612 |
| 0.25 | 0.3531 | 0.3526 | 0.3531 | 0.3533 |

Cairnie and Harrison (1982) also developed and presented differential equations for natural convection similarity flow of a fluid with variable thermophysical properties. They numerically solved these differential equations using the Keller Box method (Keller, 1978). The values for the variable density, dynamic viscosity, and thermal conductivity of air were approximated in two ways by Cairnie and Harrison: the first is a cubic spline fit to the published data of Mayhew and Rogers (1969), the second is where the Chapman-Rubesin property ratio parameter (White, 1974) as shown in equation (5-1) is arbitrarily set to a constant having the values of 1.0, 0.9, and 0.8. Cairnie and Harrison

also report the results of experiments in air at an ambient temperature of 295 K for a vertical flat plate at a number of different wall temperatures ranging from 674 K to 323 K.

The computed results for the ratio $Nu/Ra^{1/4}$ obtained using both the Keller Box and the Lentini-Pereyra numerical methods of this dissertation are presented in Table 5-4 for a wall temperature of 674 K with variable properties and the three constant values for the Chapman-Rubesin parameter, $\rho\mu/\rho_r\mu_r$. The air properties are the polynomial functions of temperature taken from Irvine and Liley (1984). The reference condition is that of ambient air at 295 K. The corresponding published results of Cairnie and Harrison in the form of the ratio $Nu/Ra^{1/4}$ are presented in Table 5-4. The values of this ratio computed using the present model show good agreement for all corresponding cases.

Table 5-4. Values of the Ratio $Nu/Ra^{1/4}$ for the Variable-Property Laminar Flows of Cairnie and Harrison.

| Variable property relation | Cairnie and Harrison | Present Investigation | |
|---|---|---|---|
| | | Keller Box | Lentini-Pereyra |
| Chapman-Rubesin parameter | | | |
| 0.8 | 0.4337 | 0.4311 | 0.4348 |
| 0.9 | 0.4089 | 0.4065 | 0.4101 |
| 1.0 | 0.3880 | 0.3880 | 0.3891 |
| Curve fit | 0.4368 | 0.4556 | 0.4763 |

Cairnie and Harrison (1982) also present experimental temperature data. Their measured temperature profile in the boundary layer is presented in Figure 5-1, where it is compared with the results computed using the Lentini-Pereyra method and the Keller Box method for variable properties and the three constant values of the Chapman-Rubesin parameter. The air properties used for these calculations were taken from Irvine and Liley (1984) and the reference condition was that of ambient air at 295 K. As can be seen in Figure 5-1, the computed results of both the Keller Box and the Lentini-Pereyra procedures for the case of variable properties show very good agreement with experimental data for the case of the ratio of wall temperature to ambient air temperature of 2.35. The computed results using the three different constant values of the Chapman-Rubesin parameter are also presented on Figure 5-1. The agreement with the experimental data is very good for some segments of the boundary layer but not for other segments for any particular value of the Chapman-Rubesin parameter. None of computations with the three values has as good an agreement with the experimental data over the entire thickness of the boundary layer as do the variable property computations.

The polynomial expressions (in temperature) for the air properties taken from Irvine and Liley (1984) are easily implemented into the computer code with no apparent penalty in computation time as compared to approximating the Chapman-Rubesin parameter as a constant over the boundary layer thickness. There is no advantage to using a constant Chapman-Rubesin parameter. There is, however, a slight disadvantage in that the accuracy of the solution obtained with a constant Chapman-Rubesin parameter is less than that obtained using the polynomial curve fits for the variable properties. This is easily seen in the comparison with the experimental data shown in Figure 5-1.

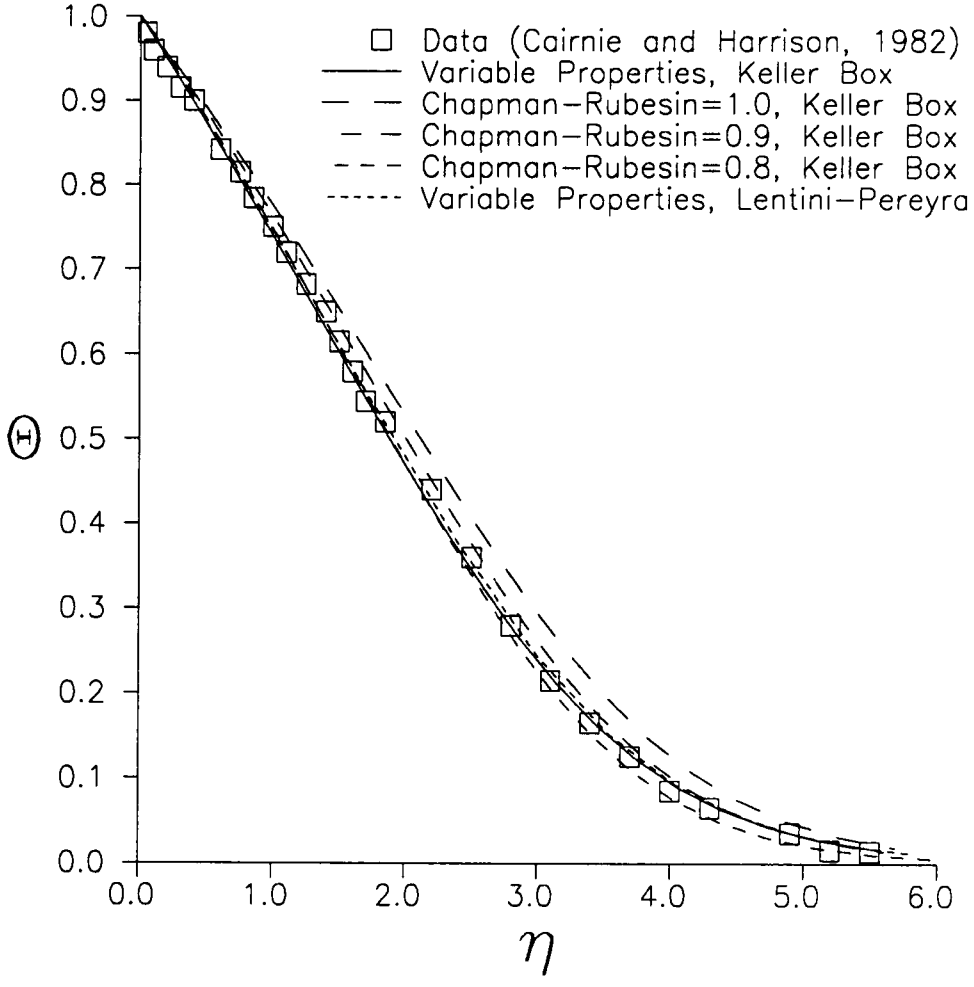


Figure 5-1. Dimensionless Temperature Profile for a Wall Temperature to Ambient Temperature Ratio of 2.35.

### 5.2.3. Flows with linear thermal stratification of the ambient fluid

Chen and Eichhorn (1976) report the results of an experimental and analytical investigation for laminar natural convection flow in a stable, thermally-stratified fluid. Jaluria (1980) presents an analysis of the necessary conditions for stable stratification to exist. A sufficient condition to ensure stable stratification is for the density to decrease with respect to height for systems in which the buoyancy force is due to gravity. Thus, for fluids with a positive isobaric coefficient of expansion, $\beta$, an increase of temperature with respect to height will yield a stable thermal stratification.

Chen and Eichhorn (1976) developed an analytical model for the boundary layer flow on an isothermal, vertical flat plate with a linearly-stratified ambient fluid. They found this flow to be nonsimilar. Thus, the method of local nonsimilarity was used along with the modified shooting method of Nachtsheim and Swigert for numerical solution of the coupled system of differential equations. Chen and Eichhorn computed results using the first-, second-, and third-level of truncation models. They presented their results from the second-level and third-level models for Prandtl numbers of 0.7 and 6.0. Sufficient agreement between the second- and third-level models was found, such that the results of the second-level model are sufficiently accurate. Chen and Eichhorn also performed an experiment in linearly, stably stratified water and found a favorable comparison between the overall heat transfer in their experimental apparatus to that obtained in their computations using the method of local nonsimilarity.

Raithby and Hollands (1978) applied their approximate integral method for heat transfer and show favorable comparisons between their computations and the experimental data and computed values of Chen and Eichhorn.

When implementing the method of local nonsimilarity, certain derivatives with respect to the streamwise nonsimilarity variable $\xi$ were retained by Chen and Eichhorn that were neglected in the original version of the method presented by Sparrow et al. (1970). These terms are identified in detail as shown in Appendix A.1.2. The inclusion or deletion of these terms caused some controversy in the literature. The studies by Coxson and Parks (1971) and Chen and Eichhorn (1976) claim that retention of these terms is preferable, while the studies by Sparrow (1971) and Rogers (1974) claim that

deletion of the terms is preferable. Thus, the effect of retaining or deleting these terms for the case of linear temperature stratification in the ambient fluid was investigated in the present work.

The solution of the nonsimilar boundary layer equations was obtained with each of the three different numerical methods used in this dissertation: the Keller Box, and the method on local nonsimilarity (second level of truncation model) with both the Lentini-Pereyra procedure and the modified shooting procedure of Nachtsheim and Swigert. For the method of local nonsimilarity, numerical solutions were obtained with and without the controversial terms. Little difference in computational effort and success in obtaining converged solutions was noticed for the method of Lentini and Pereyra. However, the Nachtsheim-Swigert method for the case of a Prandtl number of 0.7 with retention of the controversial terms failed to achieve convergence for the two highest values of streamwise coordinate, $\xi$, of 0.8 and 0.9.

The computed values of the ratio $Nu/Ra^{1/4}$ obtained using all of the numerical methods are presented in Table 5-5 for a Prandtl number of 0.7 and Table 5-6 for a Prandtl number of 6.0. These tables also contain the analogous results of Chen and Eichhorn for the purposes of comparison.

Inspection of Tables 5-5 and 5-6 shows that the agreement between the computed results of the Keller Box procedure and the method of local nonsimilarity is better when the controversial terms in the method of local nonsimilarity are included for most of the streamwise stations in Table 5-5 (with the exception of the streamwise stations at $\xi$ = 0.6, 0.7, and 0.8) and for *all* of the streamwise stations in Table 5-6. Indeed, for the case of a Prandtl number of 6.0, as shown in Table 5-6, the agreement between the method of local nonsimilarity including the controversial terms is within one percent of the value computed with the Keller Box procedure for all values of the streamwise spatial coordinate, $\xi$.

The agreement between the results from the local nonsimilarity method without the controversial terms and the results from the Keller Box method gradually improves until there is an approximately ten percent difference at the higher values of the streamwise spatial coordinate, $\xi$. Based upon these comparisons, the controversial

Table 5-5. Values of the Ratio $Nu/Ra^{1/4}$ for Laminar Flow with a Linearly-Stratified Ambient Fluid and a Prandtl Number of 0.7.

| | | Present Investigation | | | | |
|---|---|---|---|---|---|---|
| | | | Controversial Terms Deleted | | Controversial Terms Retained | |
| $\xi$ | Chen-Eichhorn | Keller Box | Lentini-Pereyra | Nachtsheim-Swigert | Lentini-Pereyra | Nachtsheim-Swigert |
| 0.0 | 0.3861 | 0.3860 | 0.3862 | 0.3861 | 0.3862 | 0.3861 |
| 0.1 | 0.3546 | 0.3550 | 0.3556 | 0.3555 | 0.3547 | 0.3546 |
| 0.2 | 0.3229 | 0.3235 | 0.3261 | 0.3261 | 0.3229 | 0.3229 |
| 0.3 | 0.2914 | 0.2920 | 0.2974 | 0.2974 | 0.2914 | 0.2914 |
| 0.4 | 0.2608 | 0.2603 | 0.2687 | 0.2687 | 0.2608 | 0.2608 |
| 0.5 | 0.2322 | 0.2281 | 0.2384 | 0.2384 | 0.2322 | 0.2322 |
| 0.6 | 0.2069 | 0.1952 | 0.2047 | 0.2047 | 0.2070 | 0.2070 |
| 0.7 | 0.1807 | 0.1611 | 0.1651 | 0.1652 | 0.1807 | 0.1807 |
| 0.8 | 0.1374 | 0.1248 | 0.1181 | 0.1181 | 0.1375 | — |
| 0.9 | 0.0754 | 0.0835 | 0.0630 | 0.0630 | 0.0753 | — |

Table 5-6. Values of the Ratio $Nu/Ra^{1/4}$ for Laminar Flow with a Linearly-Stratified Ambient Fluid and a Prandtl Number of 6.0.

| | | Present Investigation | | | | |
|---|---|---|---|---|---|---|
| | | | Controversial Terms Deleted | | Controversial Terms Retained | |
| $\xi$ | Chen-Eichhorn | Keller Box | Lentini-Pereyra | Nachtsheim-Swigert | Lentini-Pereyra | Nachtsheim-Swigert |
| 0.0 | 0.4551 | 0.4550 | 0.4552 | 0.4550 | 0.4552 | 0.4550 |
| 0.1 | 0.4148 | 0.4127 | 0.4167 | 0.4161 | 0.4151 | 0.4148 |
| 0.2 | 0.3735 | 0.3694 | 0.3772 | 0.3722 | 0.3735 | 0.3735 |
| 0.3 | 0.3304 | 0.3263 | 0.3366 | 0.3370 | 0.3297 | 0.3304 |
| 0.4 | 0.2860 | 0.2825 | 0.2949 | 0.2952 | 0.2851 | 0.2860 |
| 0.5 | 0.2405 | 0.2378 | 0.2512 | 0.2513 | 0.2398 | 0.2405 |
| 0.6 | 0.1941 | 0.1922 | 0.2054 | 0.2054 | 0.1935 | 0.1941 |
| 0.7 | 0.1468 | 0.1458 | 0.1573 | 0.1573 | 0.1464 | 0.1468 |
| 0.8 | 0.0988 | 0.0983 | 0.1071 | 0.1070 | 0.0985 | 0.0988 |
| 0.9 | 0.0499 | 0.0500 | 0.0546 | 0.0546 | 0.0496 | 0.0499 |

terms *should* be retained in the method of local nonsimilarity. Although this supposition is based on the results of only one case, that of linear temperature stratification, extension to other cases will be assumed as long as it is expedient to do so.

The results computed using the local nonsimilarity method with either numerical solution method agree with each other to the fourth significant digit for any given case, whether or not the controversial terms are retained. The published data from Chen and Eichhorn (1976) agree to the fourth significant digit with the results computed by including the terms, which was expected, since Chen and Eichhorn retained the terms in their computations. The computation time is on the order of a minute on a VAX 8600 at Oak Ridge National Laboratory for both the finite-difference procedure of Lentini and Pereyra (1977) and the modified shooting method of Nachtsheim and Swigert (1966). The programming effort, however, to develop the algorithmic coding for the Lentini-Pereyra procedure is much less than that for the Nachtsheim-Swigert modified shooting procedure. Thus, for reasons of simplicity the finite-difference procedure of Lentini and Pereyra is preferable when the method of local nonsimilarity is used.

The Keller Box method has been used by many investigators to solve the boundary layer differential equations. Although the development of the algorithmic computer coding is more involved than that for the Lentini-Pereyra procedure, the coding for the Keller Box method is still fairly straightforward to develop. The computation time is on the order of a few minutes on a desktop personal computer for all values of the streamwise coordinate, $\xi$, in Tables 5-5 and 5-6.

The dimensionless temperature and velocity profiles in a boundary layer flow with a linearly-stratified ambient fluid are presented in Figures 5-2 and 5-3. The results displayed in these figures were computed with both the Keller Box method and the Lentini-Pereyra method (with and without the controversial terms) for a Prandtl number of 0.7 at values of the streamwise coordinate, $\xi$, of 0.0, 0.2, 0.4, 0.6, and 0.8. As can be seen on Figure 5-2, temperature inversions in the outer regions of the boundary layer are computed by all of the methods for values of $\xi$ greater than zero. The temperature inversions computed by the Keller Box method are more prominent than those computed using the local nonsimilarity method. The temperature inversions for the case in

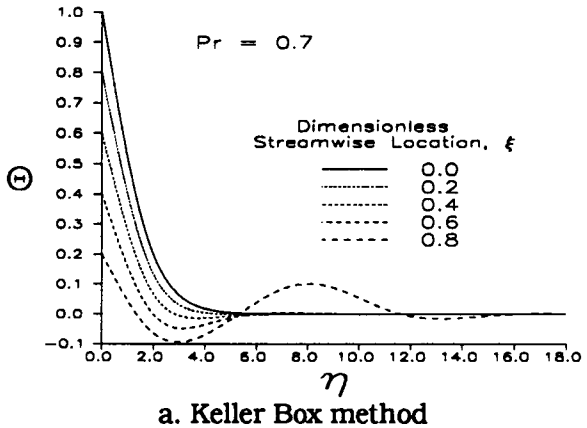


a. Keller Box method

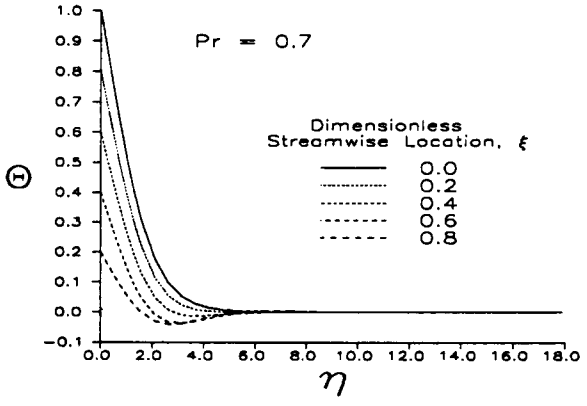


b. Lentini-Pereyra method (controversial terms deleted)

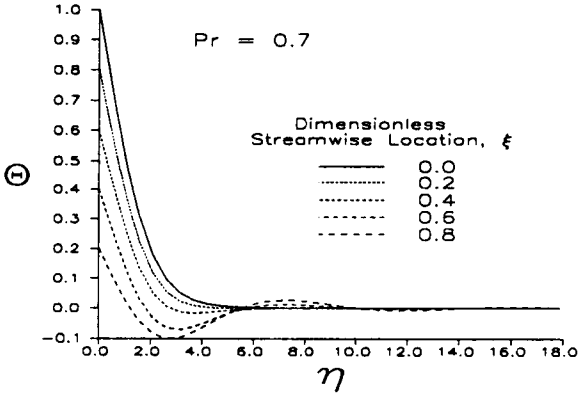


c. Lentini-Pereyra method (controversial terms retained)

Figure 5-2. Temperature Profiles for Laminar Flow in a Linearly-Stratified Fluid with a Prandtl Number of 0.7.

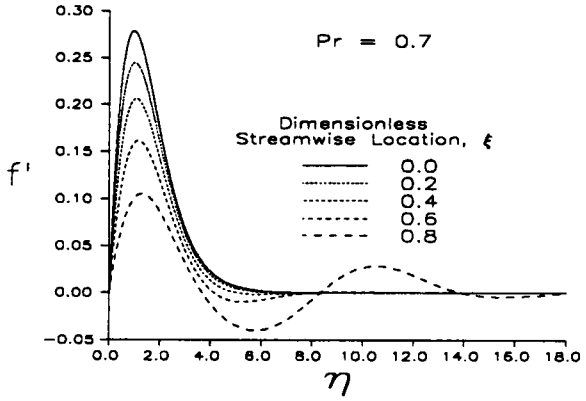


a. Keller Box method

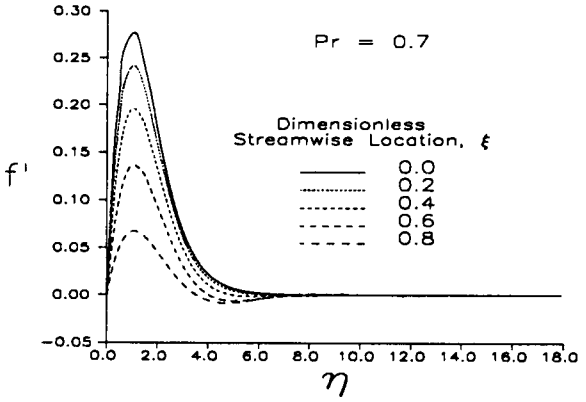


b. Lentini-Pereyra method (controversial terms deleted)

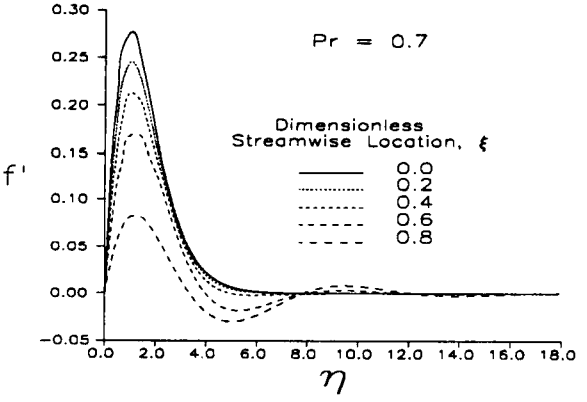


c. Lentini-Pereyra method (controversial terms retained)

Figure 5-3. Velocity Profiles for Laminar Flow in a Linearly-Stratified Fluid with a Prandtl Number of 0.7.

which the controversial terms are retained (Figure 5-2c) are more prominent than those in the case in which the controversial terms are deleted (Figure 5-2b). Velocity inversions are also evident in the outer portion of the boundary layer as shown in Figure 5-3. These inversions have the same trend with respect to the numerical solution method as do the temperature inversions; that is, more prominent velocity inversions are computed with the Keller Box method. Experimental data, which is presently lacking, is recommended to select one of the three numerical methods as the most accurate.

The dimensionless temperature and velocity profiles computed with from the Keller Box method for a Prandtl number of 6.0 are presented in Figures 5-4 and 5-5, respectively. The temperature and velocity inversions are not as prominent as those computed for a Prandtl number of 0.7.

Venkatachala and Nath (1981) used the Keller Box method for numerical solution of the nonsimilar partial differential equations for the cases of Chen and Eichhorn (1976). Their velocity and temperature profiles in the boundary layer were presented in graphical form. Numerical values for dimensionless wall heat transfer were not explicitly presented, but good agreement was claimed with the published values of Chen and Eichhorn. The temperature and velocity inversions shown in Figures 5-2, 5-3, 5-4, and 5-5 are also evident in the corresponding plots of Venkatachala and Nath.

The velocity inversions were also found by Eichhorn (1969), who used a series solution method to compute results for a Prandtl number of 6.0. Eichhorn (1969), however, does not predict velocity inversions for a Prandtl number of 0.7 using the series solution method. Venkatachala and Nath (1981) noticed a similar discrepancy between their results obtained with the Keller Box method and those of Eichhorn (1969) for a Prandtl number of 0.7. Venkatachala and Nath claim that the Keller Box method is more accurate, particularly at large values of the streamwise spatial coordinate, $\xi$.

A physical explanation (Jaluria, 1985) for a temperature inversion is that the ambient temperature decreases faster as a function of the streamwise distance for a cooled plate than the fluid inside the boundary layer can transfer heat to the wall, thereby creating the inversion. Jaluria also states that, in general, boundary layer

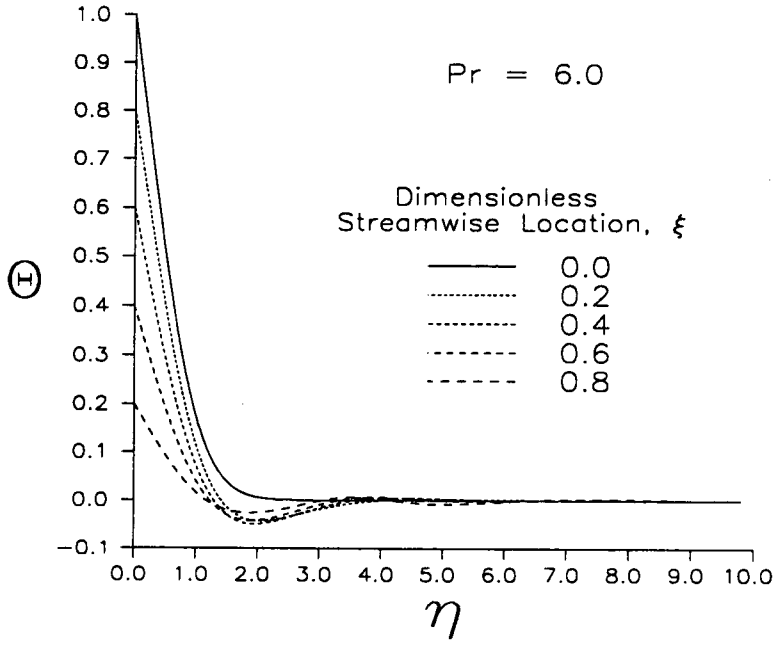


Figure 5-4. Temperature Profiles for Laminar Flow in a Linearly-Stratified Fluid with a Prandtl Number of 6.0.

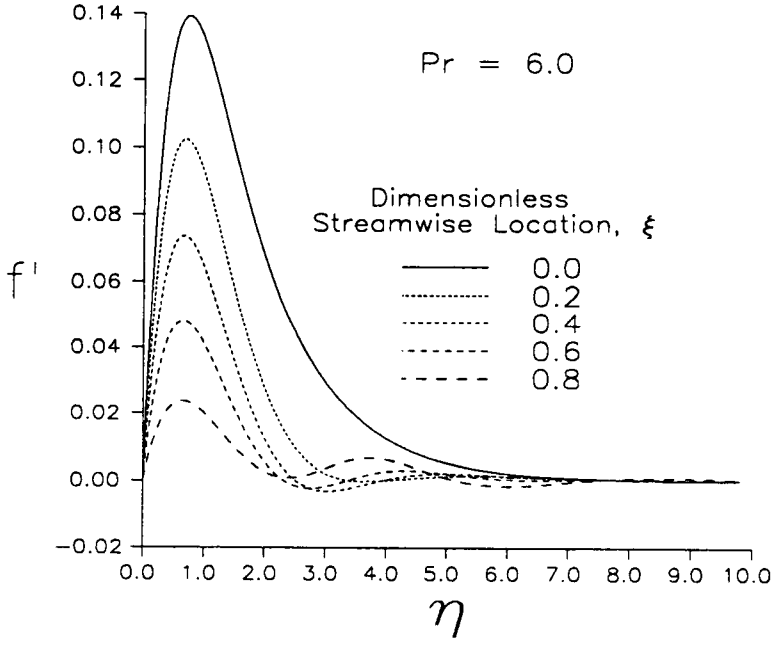


Figure 5-5. Velocity Profiles for Laminar Flow in a Linearly-Stratified Fluid with a Prandtl Number of 6.0.

theory might not be applicable when flow reversals occur and analysis of the full system of Navier-Stokes equations may be appropriate under such conditions. Also, these computed flow reversals may very well be physically unstable.

Such temperature and velocity inversions have also been observed experimentally. The data of Krane and Jessee (1983) clearly show the presence of both velocity and temperature inversions in laminar, natural convection boundary layers on the heated and cooled vertical walls of a square enclosure, which has a linearly-stratified core region. The Grashof and Prandtl numbers for this experiment are $10^5$ and 0.7, respectively.

At this point, it is sufficient to note that *all* of the numerical solutions of the analytical model faithfully reproduce the essential physical features of boundary layer flow in thermally-stratified fluids. Further experiments with the geometry of interest are recommended to determine which of the three solution methods yields the most accurate results.

### 5.2.4. Flows in which the gas participates in the thermal radiation process

The optically thick, or Rosseland, approximation for participating gas thermal radiation heat transfer is based on the assumption that the radiation emitted by a molecule is immediately absorbed by an adjacent molecule. This "diffusion approximation" makes an analogy between participating gas radiation heat transfer and thermal conduction heat transfer. As described in Section 4.2.2 and as shown in equation (4-13), the term representing participating gas thermal radiation in the conservation of energy equation resembles an enhanced thermal conductivity. When the difference in temperatures raised to the fourth power is linearized and the wall overheat ratio, $\lambda$, in equation (4-41) is equal to zero, the net effect of participating gas radiation heat transfer for the special case of the optically thick approximation is to effectively decrease the Prandtl number (Sparrow and Cess, 1966).

No references were found that report a computed or measured wall heat flux for the case of an optically thick, thermally participating medium radiating to an isothermal wall. Some references present studies of systems under similar circumstances, but are

not exactly applicable to the circumstances of interest here. Specifically, Cheng and Özisik (1972) present numerically determined dimensionless wall heat fluxes for an isothermal vertical plate, but not for optically thick conditions. Novotny and Yang (1967) present numerically determined dimensionless wall heat fluxes for an optically thick medium, but for a horizontal cylinder, instead of a vertical flat plate. Kennedy and Paszkowskyj (1970) do not present numerical results for the dimensionless wall heat flux, but do present results in graphical format that illustrate the effect on the wall heat flux as the radiation parameter, $M$, as defined in equation (4-38), and the wall overheat ratio, $\lambda$, as defined in equation (4-37), were varied.

The results from two previous investigations were used to validate the present model of participating gas radiation. Specifically, the study by Kuiken (1969) of natural convection on an isothermal wall immersed in a low Prandtl number fluid and the analytical study of Kennedy and Paszkowskyj (1970) of natural convection in a radiantly participating medium adjacent to an isothermal flat plate were used for validation purposes.

Kuiken (1969) performed a perturbation solution of the governing differential equations, since for low Prandtl numbers, a classical singular perturbation (small parameter multiplying the highest-order derivative) occurs in the energy equation. Kuiken compares his results to those of a similarity solution published by Sparrow and Gregg (1958) and shows agreement to the second significant digit for the dimensionless wall heat flux. In the absence of published values of wall heat flux for the specific case of radiation in an optically thick, participating medium, and based on the idea expressed above that in the optically thick limit, the net effect of the thermally participating medium is to effectively decrease the Prandtl number, Kuiken's data for low Prandtl number heat fluxes were used for verification of the present computational model. Kuiken reported his results for low Prandtl numbers in the form of the ratio:

$$\frac{Nu}{(RaPr)^{1/4}} = \frac{Nu}{Bo^{1/4}} = C_1 , \qquad (5-2)$$

where $C_1$ is a constant that Kuiken states should approach 0.60040 as the Prandtl number approaches zero and *Bo*, defined as the product of the Rayleigh and Prandtl numbers, is called the Boussinesq number by Bejan (1984). This ratio was computed using the Keller Box method and the Lentini-Pereyra technique in conjunction with the method of local nonsimilarity. These results are compared with those of Kuiken (1969) and Sparrow and Gregg (1958) in Table 5-7.

Table 5-7. Values of the Ratio $Nu/Bo^{1/4}$ for Natural Convection Boundary Layer Flows in a Radiatively Participating Fluid.

| Prandtl Number | Kuiken | Sparrow and Gregg | Present Investigation | |
|---|---|---|---|---|
| | | | Keller Box | Lentini and Pereyra |
| 0.003 | 0.5827 | 0.5827 | 0.5831 | 0.5832 |
| 0.008 | 0.5714 | 0.5729 | 0.5726 | 0.5730 |
| 0.020 | 0.5546 | 0.5582 | 0.5582 | 0.5583 |
| 0.030 | 0.5443 | 0.5497 | 0.5494 | 0.5497 |

As can be seen by inspection of Table 5-7, the values of the ratio $Nu/Bo^{1/4}$ computed with the present model agree with those of Kuiken and Sparrow and Gregg by less than one percent.

Kennedy and Paszkowskyj (1970) present a model for natural convection on an isothermal flat plate that includes the idealized approximations of the optically thick limit and the optically thin limit for participating gas thermal radiation. In the optically thick approximation, Kennedy and Paszkowskyj did not linearize the temperature dependence of the resulting effective thermal conductivity. They do not report the dimensionless heat flux at the plate, but do report in graphical form the resulting increase in convective heat transfer as a function of the ratio of the wall temperature to the fluid temperature far from the plate and also as a function of the parameter, *M*, defined in equation (4-38) that represents the ratio of heat transfer by conduction to that by optically thick radiation (Sparrow and Cess, 1966). Kennedy and Paszkowskyj

acknowledge that the temperature ratio, $T_w/T_\infty$, was sufficiently high in their calculations such that variable thermophysical properties might be expected to affect the solution. Thus, they report their results as being those for a highly idealized situation.

The Keller Box method and the Lentini and Pereyra method were both used compute the similarity solution for optically thick conditions as reported by Kennedy and Paszkowskyj for ranges of values of the parameters $M$ and $T_w/T_\infty$. Although the published results of Kennedy and Paszkowskyj were for heated walls only, the numerical methods of this dissertation will primarily be applied to cooled walls. The results computed with the Keller Box method are presented on Figure 5-6. These results agree to the fourth significant digit with the results computed with the Lentini and Pereyra method, which are not presented. The general trends of the dimensionless heat flux with $M$ and $T_w/T_\infty$ as shown in Figure 5-6 are also evident in the graphical results of Kennedy and Paszkowskyj (1970). The curve for a wall to fluid temperature ratio of unity can be considered as the curve representing linearized radiation. The effect of not linearizing the effective thermal conductivity for radiation due to a participating medium is, not surprisingly, dependent upon the relative wall temperature ratio. For heated walls, the heat transfer at the wall increases relative to the linearized case as the wall temperature is increased. For cooled walls, the heat transfer decreases relative to the linearized case as the wall temperature ratio decreases. However, the wall heat transfer increases for all wall temperature ratios as compared to the case of a non-participating medium. All curves approach the pure convection point on the ordinate as the radiation participation decreases, that is, as $M$ approaches infinity.

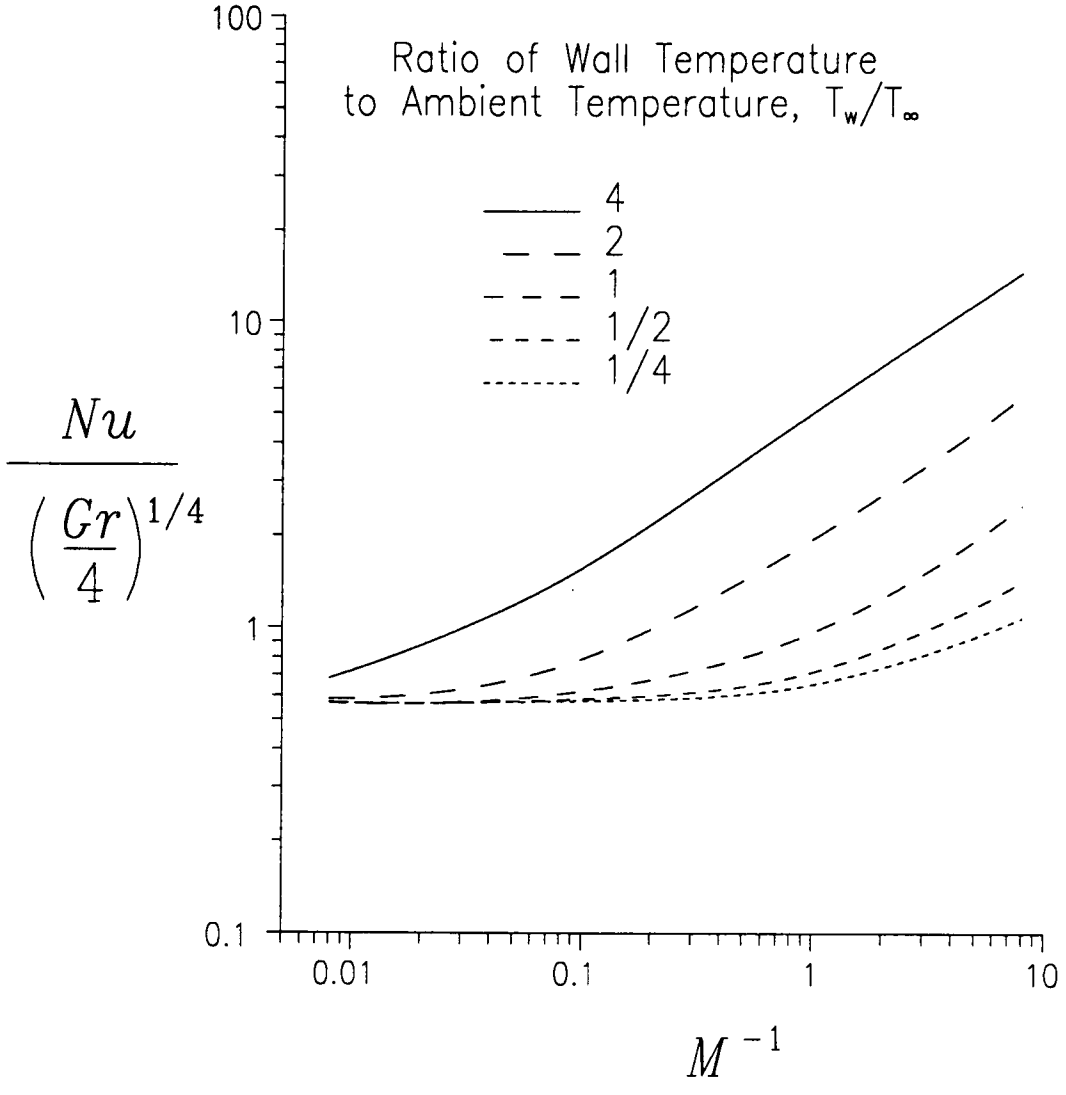


**Figure 5-6. Wall Temperature Ratio Effect on the Radiation Heat Transfer in a Natural Convection Boundary Layer Flow.**

## 5.3. Comparison of Results for Turbulent Flows

The functional relationships for turbulent diffusivities of momentum, heat, and particles were determined by comparison of computed values of the parameter $Nu/Ra^{1/3}$ to the experimental data of others, as listed in Section 5-1. Bayley (1955) developed a relationship for the turbulent natural convection flow on a vertical flat plate where the heat transfer coefficient is independent of length. The results of numerous other analyses, as discussed in Chapter 3, agree with Bayley's relationship. Some investigators, notably Seibers et al. (1985), also accounted for the effects of variable thermophysical properties and observed that the heat transfer coefficient remains independent of length.

### 5.3.1. Selection of a turbulent viscosity model

The relationships for the turbulent diffusivities in the inner and outer regions of the boundary layer are evaluated in this section. A value of the constant $A^+$ which appears in the expression for the turbulent diffusivity in the inner region of the boundary layer as presented in Section 4.3.2, and a value for the constant $\aleph$ that appears in the expression for turbulent diffusivity in the outer region as presented in Section 4.3.3, will be determined by comparison of computed results of the present model with the data of the investigations of Seibers et al. (1985) for the inner region and Mason and Seban (1973) for the outer region of the boundary layer.

With no prior knowledge that a higher-order method would be necessary to compute the velocity and temperature profiles accurately in the boundary layer, the local similarity, or first level of truncation, model of the nonsimilar boundary layer along with the finite-difference method of Lentini and Pereyra (1977) was used to perform the initial computations of the heat transfer in order to obtain a value of the constant $A^+$. The local similarity model was chosen for this purpose because of its simplicity and short numerical computation times. As is subsequently shown in this section, the first level of truncation model has sufficient accuracy for the levels of turbulence of interest in this investigation.

An iterative procedure was used to determine a value of $A^+$. First, the turbulent diffusivity model of Kato et al. (1968), as given by equation (4-20), or the turbulent diffusivity model of Reynolds (1976), as given by equation (4-21), was selected. Then an arbitrary value for $A^+$ was chosen and the heat transfer to the wall was computed. This procedure was repeated using different values of $A^+$ until the computed ratio $Nu/Ra^{1/3}$ agreed with the Seibers et al. value. For all computations, the thermophysical properties of air in the form of polynomial functions of temperature (Irvine and Liley, 1984) were used and the reference temperature was assumed to be that of the fluid far from the wall.

For the near wall turbulent diffusivity model of Reynolds, which is given by equation (4-21), the value of $A^+$ that gives agreement with the Seibers et al. data is 26. Similarly, for the model of Kato et al., given by equation (4-20), the value of $A^+$ that gives agreement with the Seibers et al. data is 34. The Reynolds model was chosen for performing the remainder of the turbulence calculations in this investigation because that model's predictions agree well with experimental results when a value of $A^+ = 26$ is used, which corresponds to the value of $A^+$ used in turbulent forced convection flow over a flat plate with no pressure gradient and no surface mass transfer. As reported by Kays and Crawford (1980), $A^+$ can be described as the dimensionless effective thickness of a laminar sublayer in which viscous effects damp out turbulent eddy fluctuations. Near the wall, it is anticipated that the fluid eddy movement is independent of the mechanism that moves eddies to the wall, that is, buoyancy forces, or inertial forces.

To and Humphrey (1986) used a turbulent Prandtl number of 0.9 for their sophisticated computational modeling of turbulence . When a turbulent Prandtl number of 0.9 is used in the Reynolds model of turbulence, $A^+$ increases from 26 to 29 in order to get good agreement with the Seibers data. Correspondingly, a turbulent Prandtl number of 0.9 in the Kato turbulence model requires $A^+$ to increase from 34 to 37 in order to obtain good agreement with the Seibers data. Since the data used by To and Humphrey (1986) to justify their choice of 0.9 for the turbulent Prandtl number could

also support the use of a value of 1.0, a value of unity was chosen for the turbulent Prandtl number because the corresponding value of $A^+$ agrees with the value for a flat plate in forced convection with no pressure gradient and no mass transfer at the wall.

The value of the constant $\aleph$ in the relationship for the eddy diffusivity of momentum in the outer region of the turbulent boundary layer, which is given by equation (4-29), was also determined by comparison with the results of Mason and Seban (1973), who used a more sophisticated turbulent kinetic energy and dissipation model. A value of $\aleph = 1$ results in computed values of the turbulent diffusivities of the same order of magnitude as those of Mason and Seban. The value of this constant can be varied from 0.5 to 1.5 with little resulting effect on the computed wall heat transfer. This is not surprising, since the heat transfer at the wall would be expected to be primarily affected by the conditions near the wall, such as the effective sublayer distance, rather than by conditions far from the wall. Values of the constant $\aleph$ less than 0.1, however, result in heat transfer rates at the wall resembling those for laminar flow conditions, which is simply due to the artificially low maximum value of turbulence given by the outer region model at such values of $\aleph$. Values of $\aleph$ greater than one result in apparent computational oscillations or numerical convergence failures. The use of the Klebanoff intermittency factor helps to achieve convergence for the solution of the two-point boundary-value problem without significantly affecting the computed wall heat transfer.

Hence, the turbulent viscosity relationship used for the turbulent calculations in the present work had one of the following forms:

$$\frac{\mu_t}{\mu} = 0.4y^+\left\{1-\exp\left[-\left(\frac{y^+}{26}\right)\right]\right\}^2, \qquad \text{(inner region)}, \qquad (5-3)$$

or

$$\frac{\mu_t}{\mu} = \xi^{1/2}Gr_L^{1/6}\left[1+5\left(\frac{y}{\delta}\right)^6\right]^{-1}, \qquad \text{(outer region)}. \qquad (5-4)$$

Both equations (5-3) and (5-4) are evaluated at each computational point within the boundary layer during the numerical iterations. The minimum value of the turbu-

lent viscosities computed using equations (5-3) and (5-4) is then used to determine whether the location at that distance from the wall is in the inner or outer region of the turbulent boundary layer.

### 5.3.2. Validation of the local similarity model for turbulent natural convection boundary layers

The results of computations using the method of local nonsimilarity for wall temperature to fluid temperature ratios of 1.19 and 2.40 and not including the temperature correction suggested by Seibers et al. (1985), are presented in Figure 5-7. The modified best-fit correlation of Seibers et al. (1985), which is given by equation (4-52), and the experimental data of Seibers et al. (1983) for five values of the wall to fluid temperature ratio, including uncertainties, are also presented in Figure 5-7. The results computed with the present model agree very well with Seibers et al. experimental data. These results show a slight decrease in Nusselt number as the wall temperature to fluid temperature ratio is increased.

Seibers suggests that the data should be modified by a slight temperature correction, as given by equation (4-52). The temperature-corrected Nusselt number results for the method of local nonsimilarity, the Seibers et al. (1985) correlation, and the Seibers et al. (1983) experimental data are presented in Figure 5-8. The agreement is quite good over a wide range of Rayleigh numbers and wall temperature to fluid temperature ratios.

Two additional methods were used for additional justification of the use of the local similarity model, or first level of truncation model of the method of local nonsimilarity, although favorable comparison of computed results with experimental data should suffice. Three different computations of the ratio $Nu/Ra^{1/3}$ at two different wall temperature to fluid temperature ratios were performed using both the first level of truncation and second level of truncation models along with the finite-difference procedure of Lentini and Pereyra (1977), and the Keller Box method. These results are presented in Table 5-8, along with the computed results of Seibers best fit correlation, which is given by equation (4-52).

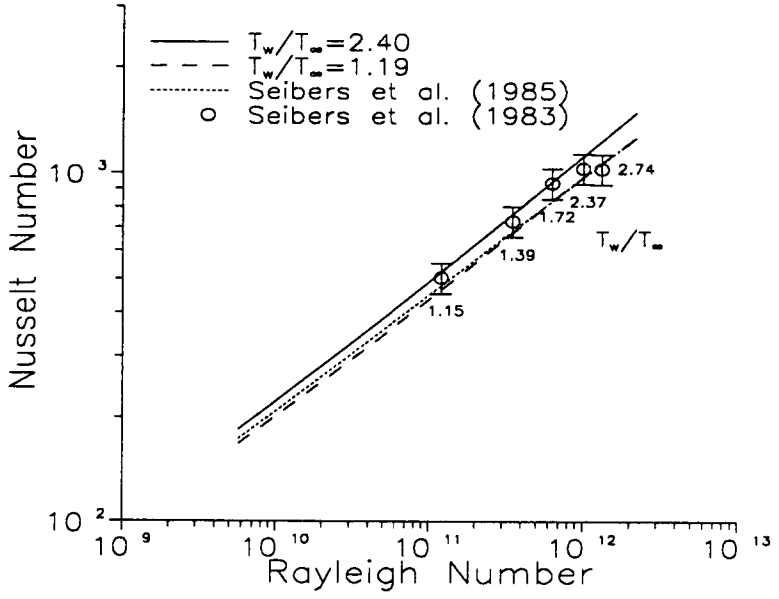


Figure 5-7. Turbulent Flow Correlation without Temperature Correction.

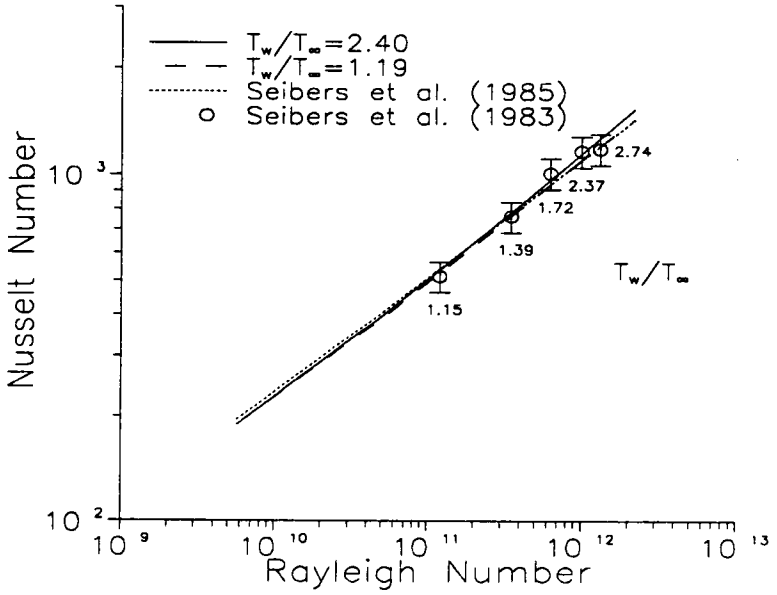


Figure 5-8. Turbulent Flow Correlation with Temperature Correction.

Table 5-8. Values of the Ratio $Nu/Ra^{1/3}$ for a Turbulent Natural Convection Boundary Layer.

| Rayleigh Number | modified Seibers correlation | Present Investigation | | |
|---|---|---|---|---|
| | | first level of truncation | second level of truncation | Keller Box |
| $T_w/T_\infty = 1.19$ | | | | |
| $5.7\times10^{9}$ | 0.1068 | 0.1032 | 0.1033 | 0.1031 |
| $4.6\times10^{10}$ | | 0.1043 | 0.1043 | 0.1081 |
| $1.5\times10^{11}$ | | 0.1063 | 0.1063 | 0.1098 |
| $3.7\times10^{11}$ | | 0.1084 | 0.1084 | 0.1120 |
| $7.2\times10^{11}$ | | 0.1104 | 0.1105 | 0.1140 |
| $T_w/T_\infty = 2.40$ | | | | |
| $5.7\times10^{9}$ | 0.0969 | 0.0936 | 0.0937 | 0.1020 |
| $4.6\times10^{10}$ | | 0.0934 | 0.0935 | 0.1044 |
| $1.5\times10^{11}$ | | 0.0945 | 0.0946 | 0.1064 |
| $3.7\times10^{11}$ | | 0.0958 | 0.0959 | 0.1085 |
| $7.2\times10^{11}$ | | 0.0972 | 0.0973 | 0.1105 |

As can be observed from Table 5-8, the ratio $Nu/Ra^{1/3}$ increases slightly with an increase in the Rayleigh number, which suggests a slight influence of length on the computed solution. This slight computed increase, however, is well within the experimental error limits as shown in Figure 5-7 and stated as ±10% by Seibers et al. (1983). The results computed using the Keller Box method are not as dependent on the wall temperature to fluid temperature ratio as are the results computed with the other methods. However, the computed results are in good agreement with each other, and are within the experimental limit of accuracy. Based upon these results, the first level of truncation model of the local nonsimilarity method, or the local similarity method, adequately predicts the heat transfer in a turbulent, natural convection boundary layer on a constant temperature flat plate immersed in an unstratified, semi-infinite fluid.

Additional justification for the use of the local similarity model is presented by comparison of the results computed with the model with the velocity and temperature profiles presented by George and Capp (1979). They developed relationships for natural convection velocity and temperature profiles near the wall using classical scaling arguments. Their velocity profile has a cubic dependence on the distance from the wall. Similarly, their temperature profile near the wall has reciprocal cube root dependence on the distance from the wall. George and Capp show that the temperature profile very near the wall should be linear. They present favorable comparisons of their derived relationships with the experimental data of others.

As additional justification for the use of the local similarity model (along with the chosen algebraic turbulence closure model) as solved by the finite-difference procedure of Lentini and Pereyra (1977), the computed results for the velocity and temperature profiles for wall to fluid temperature ratios of 1.19 and 2.40 are compared to the near-wall and very-near-wall relationships of George and Capp (1979). They suggest a length scale, $\eta_t$, for the inner region that is given by:

$$\eta_t = \left[\frac{(\nu/Pr)^2}{g\beta\Delta T}\right]^{1/3}. \qquad (5-5)$$

Seibers et al. (1985) suggest a temperature correction to this inner region length scale to account for property variations across the boundary layer. This correction has the following form:

$$\eta_t' = \eta_t\left(\frac{k_w}{k_\infty}\right)\left(\frac{T_w}{T_\infty}\right)^{0.14}. \qquad (5-6)$$

George and Capp (1979) also suggest an inner region velocity scale given by:

$$u_t = \left(\frac{g\beta\Delta T\nu}{Pr}\right)^{1/3}. \qquad (5-7)$$

The fluid velocity distribution in the near-wall region computed using the local similarity method with the thermophysical properties evaluated at the film temperature, which is defined as the average of the wall temperature and ambient fluid temperature, is presented on Figure 5-9 along with the correlations of To and Humphrey (1986), the correlation of George and Capp (1979), and the experimental data of Cheesewright and Ierokiopitis (1982) as taken from the graphical information presented in To and Humphrey. As can be seen in Figure 5-9, the cubic dependence of velocity on distance from the wall, manifested as straight lines, is evident in the near-wall region for all the plotted information.

The fluid temperature distribution in the near-wall region computed using the local similarity method with the thermophysical properties evaluated at the film temperature is presented in Figure 5-10 along with the correlation of Seibers et al. (1985) for the high wall temperature to fluid temperature ratios, the correlation of George and Capp (1979) for low wall temperature to fluid temperature ratios, and the experimental data of Seibers et al. (1983). As can be seen from this figure, the results of the Reynolds turbulence model and the local similarity method solved with the finite-difference procedure of Lentini and Pereyra (1977) compare very well with the results of the very complicated numerical procedure of To and Humphrey (1986) and the experimental data correlated by George and Capp (1979) and Seibers et al. (1983) for the heat transfer near the wall.

Based upon these results presented in Figures 5-7, 5-8, 5-9, and 5-10 and in Table 5-8, the first level of truncation model of the local nonsimilarity method, or the local similarity method, with the use of an algebraic turbulence closure as given by equations (5-3) and (5-4), adequately predicts the heat transfer, streamwise velocity, and temperature profile in a turbulent, natural convection boundary layer on a constant temperature flat plate immersed in an unstratified, semi-infinite fluid.

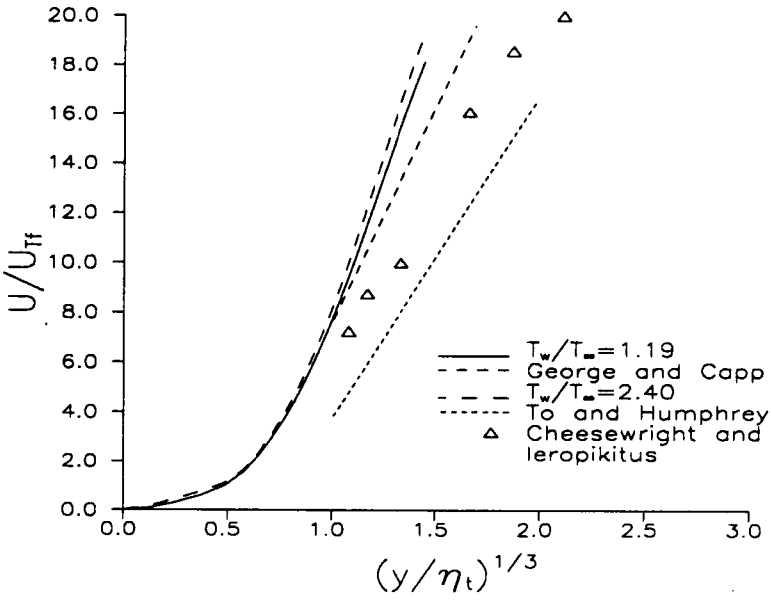


Figure 5-9. Velocity Distribution in a Turbulent Boundary Layer.

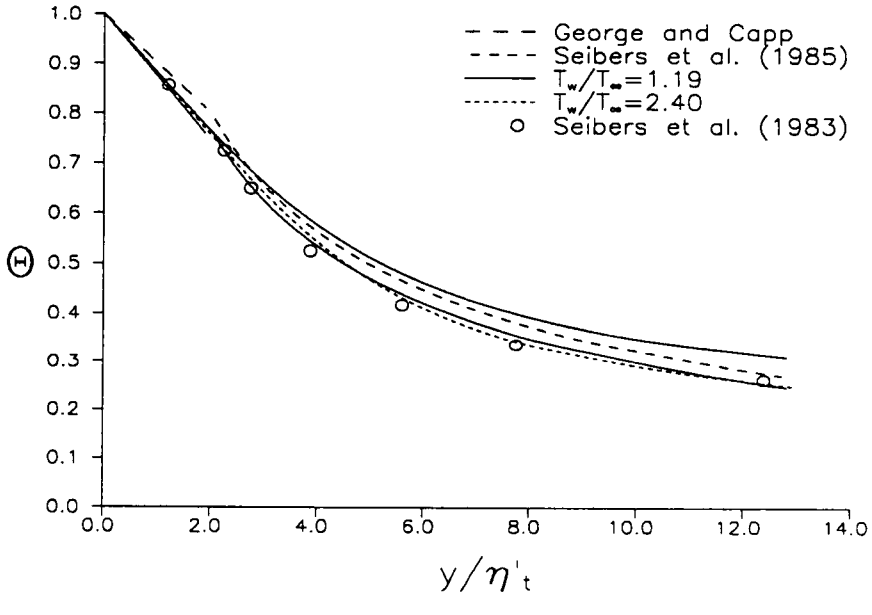


Figure 5-10. Temperature Distribution in a Turbulent Boundary Layer.

### 5.4. Comparison of Results for Flows with Volumetric Heat Sources

As mentioned in the literature search, Section 3.6, a number of experimental investigations of natural convection heat transfer with internal heat sources were focused on an enclosure with cooled vertical walls. Two investigations in which heat source strengths were sufficient to generate vertical boundary layers adjacent to the vertical cooled walls are those of Steinberner and Reineke (1978) and Greene (1982). Only Greene's investigation has sufficient information for comparison with the model of the present work.

Steinberner and Reineke (1978) present a limited amount of experimental and numerical heat transfer results for laminar and turbulent boundary layers adjacent to the cooled, vertical walls of an enclosed rectangular cavity. An observation in the lower portion of the vertical walls from the work of Steinberner and Reineke is not representative of the boundary layer on an isothermal, flat plate immersed in a fluid of semi-infinite extent. For the highest heat source strength, the Nusselt number increased noticeably with increasing length along the wall, contrary to the trend of the other two heat source strengths. A stationary secondary vortex was apparently generated at the highest value of heat source strength in the lower, turbulent portion of the vertical boundary layer. This vortex should not occur in the boundary layer flow over an isolated, vertical flat plate in a quiescent fluid. Due to the lack of reported temperature measurements or tabulated values of Nusselt and Rayleigh numbers, as well as a boundary layer that is not representative of that expected to occur in the geometry of the present work, no comparisons of the results of Steinberner and Reineke (1978) and the methods of the present work are presented.

Greene (1982) presents experimental data for a rectangular pool and analyses for the laminar boundary layer flow on a vertical flat plate in a quiescent, isothermal fluid of infinite extent. Greene's experimental apparatus allowed for a variable inclination of the isothermal, cooled wall. The heat transfer data generated in the vertical orientation only is compared in the following section with that of the model developed in the present work. Greene's heat transfer results are shown as having inadequate agreement with the

results of the present model. Some possible reasons for this disagreement are presented. Greene's analysis, however, which neglects the effect of a heat source term in the energy conservation equation for the boundary layer, is shown to be valid.

### 5.4.1. Flows in an open rectangular pool geometry

Greene (1982) performed an experiment with a volumetrically heated pool of aqueous salt solution that had a cooled isothermal vertical wall. In addition, Greene performed a scaling analysis for the boundary layer that also shows that the volumetric heat source term in the conservation of energy equation is negligible with respect to the other terms. A downward flow was observed adjacent to the cooled vertical wall that was claimed to be similar to flow in a vertical boundary layer from a cooled flat plate immersed in a fluid of semi-infinite extent. Greene states that the effect of a volumetric heat source in the experimental configuration was to maintain the difference in temperature between the cooled wall and the fluid far from the vertical wall. Greene presents the results in terms of a Nusselt number that is a function of a modified Rayleigh number based on the volumetric heat source. Greene's modified Rayleigh numbers were modified for presentation here by multiplying by the ratio of the Damköhler number, *Da*, as defined in equation (4-39) and computed from information presented by Greene, and Prandtl number in order to obtain a Rayleigh number based upon temperature difference. The data of Greene, as a function of Rayleigh number based on temperature difference, are plotted in Figure 5-11 where Greene's data set numbering convention is used in the graph legend. The correlation that Greene developed was not plotted, since the Rayleigh number in his correlation is based on volumetric heat source strength.

The results computed using the local similarity model with the Lentini-Pereyra technique are also plotted in Figure 5-11 for both laminar and turbulent flows. A Rayleigh number of $2\times10^9$ is used to divide the laminar and turbulent flow regimes. For each flow regime, a case with constant thermophysical properties and a case with variable thermophysical properties were computed. For the case of constant properties, all thermophysical properties were evaluated at the film temperature, which is defined as the average of the wall (345 K) and ambient fluid (366 K) temperatures. For the case

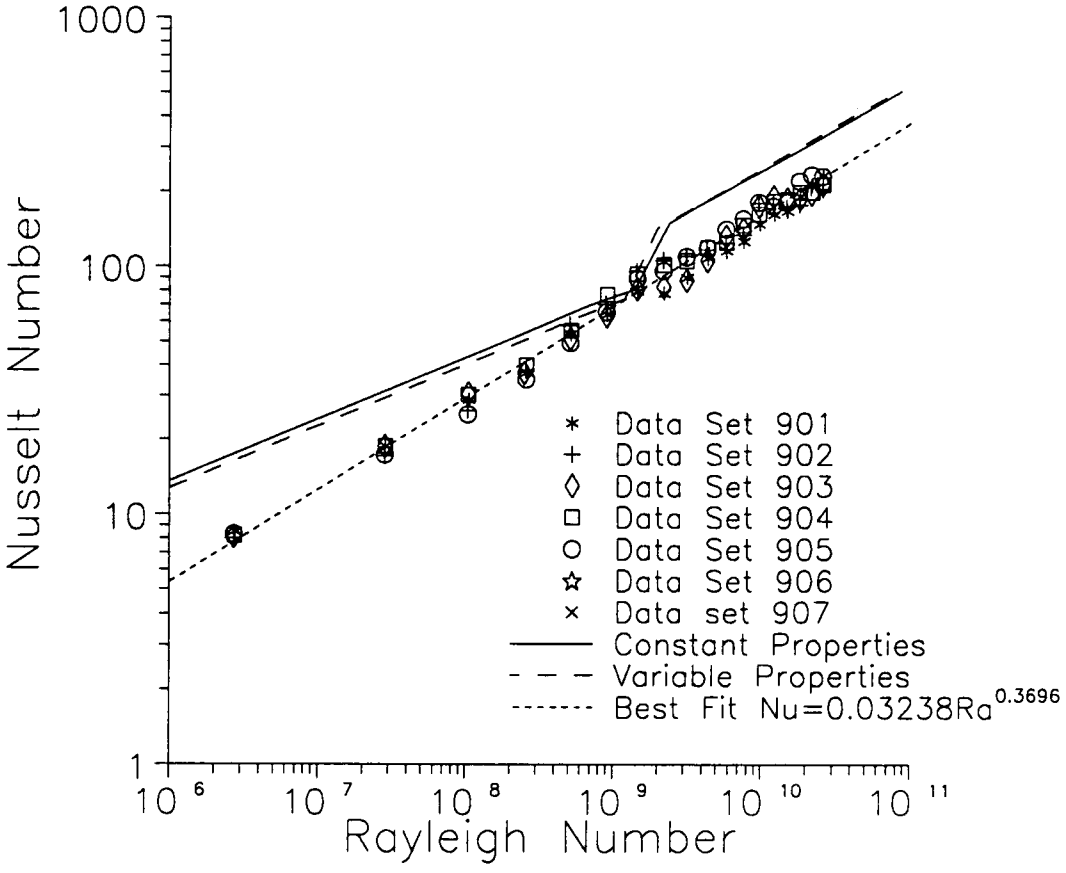


**Figure 5-11. Experimental Data of Greene (1982) for Heat Transfer.**

of variable thermophysical properties, the fluid temperature far from the vertical wall was used as a reference temperature. The computed effects of variable thermophysical properties as shown in Figure 5-11 are quite small, which is not surprising since the value of the wall overheat ratio, $\lambda \approx -0.06$, indicates a small temperature difference between the wall and ambient fluid, with a subsequent small variation of the thermophysical properties for the temperatures of interest in Greene's investigation.

From inspection of Figure 5-11, it may be concluded that the experimental results of Greene do not show any transition from laminar to turbulent flow over a range of Rayleigh numbers that would be expected to span such a transition for boundary layer flow on isolated, vertical flat plates. For Rayleigh numbers less than $2\times10^9$ where laminar flow would be expected on isolated, vertical flat plates, the Nusselt numbers measured by Greene are at least 10% lower than the results computed with the present model. The computed Nusselt number values in the laminar regime agree closely with those computed with the correlation of Churchill and Usagi (1972). For Rayleigh numbers greater than $2\times10^9$, where turbulent flow would be expected on isolated, vertical flat plates, the Nusselt numbers measured by Greene are at least 30% lower than Nusselt numbers computed with the local similarity method using the Lentini-Pereyra technique. These computed turbulent Nusselt numbers of the present work are in good agreement with the correlation of Saunders (1939), as given in equation (3-4), which was developed from an experimental investigation of a turbulent natural convection flow from an isothermal, isolated, vertical flat plate in water. The observed heat transfer results of Greene are not in good agreement with other experimental results of this present work for either turbulent or laminar natural convection flow on an isothermal, isolated, vertical flat plate.

One possible reason for this discrepancy is that Greene prescribed a boundary condition of zero velocity at the edge of the boundary layer. The value of the heat source strength used by Greene (1982) is approximately 200 times the value required to maintain a stable quiescent fluid far from the plate, as reported by Sparrow et al. (1963)

and discussed in Section 2.3. Thus, in Greene's experiments, the fluid far from the vertical wall must have had a non-zero vertical velocity, which Greene assumed as negligible and did not include in his analytical model.

Another possible reason for this discrepancy is due to outflow from the boundary layer at the bottom of the experimental apparatus. Greene's experiment was carried out in a pool of water with an aspect ratio of approximately unity with one cooled vertical wall and Joulean heating in the fluid. Even though a boundary layer was observed adjacent to the cooled isothermal wall, the measured Nusselt number results of Greene appear to be lower than those predicted with boundary layer equations that have been used to successfully match measured heat transfer results of many different investigations for flat plates immersed in a fluid of semi-infinite extent. This is not surprising, since the boundary layer in Greene's experiment must have had significant inflow at the top and significant outflow at the bottom in order to maintain the conservation of fluid mass in the pool. Greene's boundary layer is fundamentally different than the boundary layer on an isothermal flat plate immersed in a fluid of semi-infinite extent which has a very small amount of inflow into the boundary layer along the flow length and does not have outflow at all from the boundary layer at any flow length.

Bergholtz (1980) presents an analysis of the laminar flow in a enclosed rectangular cavity with cooled, isothermal vertical walls and adiabatic horizontal walls. Thin boundary layer regions adjacent to the cooled vertical walls and a core region were identified, as were matching conditions of temperature and heat flux at the interfaces between these regions. The cooled wall boundary layers have downflow and the core region has upflow. Thermal stratification is established in the core region, and is approximately linear with height. This stratification in the core region in rectangular cavities with natural convection flow driven by heating and cooling at the vertical walls, which are maintained at different temperatures, has been found experimentally by Elder (1965) and analytically by de Vahl Davis (1968). A slight temperature gradient ( $\approx$ 8 K/m) is evident in the core centerline temperature measured by Greene over 80% of the pool height and a much steeper temperature gradient ( $\approx$ 800 K/m) is evident over the remaining 20% of the pool height at the bottom of the pool. This situation indicates a

significant outflow of cold fluid from the wall boundary layer into the heated core region at the bottom of the pool. Additional analysis of Greene's data with the concepts of Bergholtz's cavity model is recommended.

Greene's analytical model neglected the volumetric heat source in the conservation of energy equation for the boundary layer. The scaling analysis of Appendix D shows that volumetric heat sources are significant when the Damköhler number, $Da$, is of the order of the product of the Prandtl number and the square root of the Grashof number. The absolute value of the Damköhler number for the experimental conditions of Greene (1982) is approximately 400, which is approximately three orders of magnitude lower than the product of the Prandtl number and the square root of the Grashof number, which is approximately $3\times10^5$. These heat source strengths and Grashof number conditions are within the range of interest for the present work. Computations were performed both with and without the volumetric heat source strength term included in the boundary layer equations. No difference (to the fourth significant digit) was computed for the ratio $Nu/Ra^{1/4}$ for laminar flows or $Nu/Ra^{1/3}$ for turbulent flows. Thus, for the heat source strengths and flow conditions of Greene, the effect of volumetric heat sources inside the boundary layer is negligible as presented in the scaling analysis of Appendix D.

Since Greene's heat transfer and fluid flow results are not representative of the geometry of interest in the present work as described in Section 2.1, the model developed in the present work does not adequately predict the heat transfer in this type of flow.

### 5.5. Comparison of Results for Flows with Thermophoretic Deposition of Particles on Cooled Surfaces

Goren (1977) and Batchelor and Shen (1985) developed a constant-property laminar flow relationship for the apparent wall concentration and the wall temperature ratio that is applicable when the Brownian layer is neglected. For the particular case of $KPr = 1$, the particle concentration equation in the absence of Brownian diffusion reduces to the energy conservation equation. Thus, the particle concentration has the same

solution (in terms of particle concentration, instead of temperature) as the energy equation. This exact solution for constant-property laminar flow was developed and expanded upon in Section 4.8 to include the case of turbulent flow with the constraint of identical turbulent Prandtl and Schmidt numbers, as well as certain thermophysical property variations for both laminar and turbulent flows.

Goren (1977) and Batchelor and Shen (1985) also assert that since the Brownian diffusion sublayer is very thin for large particle Schmidt numbers, the particle flux transported to the surface can be adequately computed by neglecting the Brownian diffusion sublayer. The scaling analysis presented in Appendix D also describes the circumstances when the particle flux due to Brownian diffusion is negligible with respect to the thermophoretic particle flux.

Since neglecting the Brownian layer is computationally advantageous in that it avoids requiring a very small mesh spacing very near the wall, the Keller Box method of this dissertation was developed to specifically take advantage of this approximation. The Lentini-Pereyra method is easily adapted to the models that either neglect or retain the Brownian sublayer. The Nachtsheim-Swigert method was not used in cases that consider thermophoretic particle deposition on the wall. The thermophoretic particle deposition results obtained from the numerical computations of this work are compared to the analytical results as presented in Section 4.8.

### 5.5.1. Exact solution results

Four circumstances were identified in Section 4.8 for which the equality of apparent wall particle concentration and wall temperature ratio were derived when $KPr = 1$. These circumstances result in the particle concentration equation reducing to the same form as the equation for conservation of energy. This equality of apparent wall particle concentration and wall temperature ratio was evaluated for both laminar and turbulent flows, with the Chapman-Rubesin parameter expression for variation of the thermophysical properties set to a constant equal to 0.9. A molecular Prandtl number of 0.8 is representative of steam at high temperature was used for these calculations along with an arbitrarily selected value of 0.8 for the wall temperature ratio. The values

of the wall particle concentration and the ratio $Nu/Ra^{1/3}$ computed with the Keller Box and the Lentini-Pereyra methods are presented in Table 5-9 for the case of turbulent Prandtl and Schmidt numbers equal to 1.0. The computed results for a second case in which the turbulent Prandtl number is equal to 0.9 and the turbulent Schmidt number is equal to 1.0 are presented in Table 5-10.

Inspection of Table 5-9 shows that the apparent wall particle concentration is equal to the wall temperature ratio for both laminar flow and turbulent flow with the same turbulent Prandtl and Schmidt numbers, as developed in Section 4.8. Inspection of Table 5-10 for the case of a slightly lower turbulent Prandtl number of 0.9 shows that the apparent wall particle concentration decreases by approximately 1.5% as the local Rayleigh number increases from $6.4\times10^{9}$ to $8.0\times10^{11}$. Comparison of the values of the ratio $Nu/Ra^{1/3}$ for these two cases shows that the heat transfer a turbulent Prandtl number of 0.9 is approximately 4.5% higher than that for the case in which the turbulent Prandtl number is 1.0 for both computational methods. Therefore, even though the apparent wall concentration decreases when the turbulent Prandtl number decreases from 1.0 to 0.9, the increase in heat transfer is proportionally higher, which results in higher particle deposition. Since thermophoresis is a phenomenon by which particle transfer is driven by a temperature gradient, additional heat transfer due to a higher temperature gradient results in an increase in particle deposition.

### 5.6. Errors Incurred by Neglecting the Brownian Diffusion Layer

The Brownian diffusion layer for high values of the particle Schmidt number was shown in Section 4.5 to be negligibly small. Neglecting the Brownian layer is computationally advantageous since a high Schmidt number flow would have a very thin particle concentration boundary layer lying within the thermal and velocity boundary layers. The impact of neglecting the Brownian diffusion layer on the computed value of the particle flux deposited on the wall is discussed below.

The Lentini-Pereyra method has the capability of resolving very thin boundary layers. Thus, the particle concentration profile, including the Brownian layer, was computed using this technique. The Lentini-Pereyra method was used to compute the

Table 5-9. Computed Values of the Apparent Particle Concentration at the Wall and the Ratio $Nu/Ra^{1/3}$ for $Pr_t = 1.0$ and $Sc_t = 1.0$.

| | Keller Box | | Lentini-Pereyra | |
|---|---|---|---|---|
| Rayleigh Number | Particle Concentration at the Wall | $Nu/Ra^{1/3}$ | Particle Concentration at the Wall | $Nu/Ra^{1/3}$ |
| Laminar | 0.8000 | 0.5494 | 0.8000 | 0.5242 |
| $6.4\times10^{9}$ | 0.8000 | 0.0986 | 0.8000 | 0.0959 |
| $2.1\times10^{10}$ | 0.8000 | 0.1086 | 0.8000 | 0.0959 |
| $5.1\times10^{10}$ | 0.8000 | 0.1085 | 0.8000 | 0.0965 |
| $1.0\times10^{11}$ | 0.8000 | 0.1104 | 0.8000 | 0.0973 |
| $1.7\times10^{11}$ | 0.8000 | 0.1111 | 0.8000 | 0.0981 |
| $2.7\times10^{11}$ | 0.8000 | 0.1126 | 0.8000 | 0.0990 |
| $4.1\times10^{11}$ | 0.8000 | 0.1134 | 0.8000 | 0.0999 |
| $5.8\times10^{11}$ | 0.8000 | 0.1146 | 0.8000 | 0.1008 |
| $8.0\times10^{11}$ | 0.8000 | 0.1156 | 0.8000 | 0.1016 |

Table 5-10. Computed Values of the Apparent Particle Concentration at the Wall and the Ratio $Nu/Ra^{1/3}$ for $Pr_t = 0.9$ and $Sc_t = 1.0$.

| | Keller Box | | Lentini-Pereyra | |
|---|---|---|---|---|
| Rayleigh Number | Particle Concentration at the Wall | $Nu/Ra^{1/3}$ | Particle Concentration at the Wall | $Nu/Ra^{1/3}$ |
| Laminar | 0.8000 | 0.5494 | 0.8000 | 0.5242 |
| $6.4\times10^{9}$ | 0.7949 | 0.1020 | 0.7903 | 0.0991 |
| $2.1\times10^{10}$ | 0.7896 | 0.1128 | 0.7898 | 0.0994 |
| $5.1\times10^{10}$ | 0.7889 | 0.1126 | 0.7895 | 0.1002 |
| $1.0\times10^{11}$ | 0.7891 | 0.1149 | 0.7893 | 0.1012 |
| $1.7\times10^{11}$ | 0.7888 | 0.1157 | 0.7892 | 0.1022 |
| $2.7\times10^{11}$ | 0.7887 | 0.1174 | 0.7891 | 0.1032 |
| $4.1\times10^{11}$ | 0.7886 | 0.1183 | 0.7890 | 0.1043 |
| $5.8\times10^{11}$ | 0.7886 | 0.1197 | 0.7890 | 0.1053 |
| $8.0\times10^{11}$ | 0.7886 | 0.1208 | 0.7890 | 0.1063 |

particle concentration profile, both with and without the Brownian layer for particle Schmidt numbers of $10^4$ and $10^6$, both laminar and turbulent flows with constant thermophysical properties, a wall temperature to fluid temperature ratio of 0.8, a Prandtl number of 0.8, and a thermophoretic coefficient, $K$, equal to the reciprocal of the Prandtl number. These computations were performed with and without an arbitrary value of Damköhler number ($Da$ = - 200) comparable to that expected for the conditions of the present work. The results for a particle Schmidt number of $10^6$ appear in Figure 5-12 and the results for a particle Schmidt number of $10^4$ are given in Figure 5-13 for the case in which the particles do not act as volumetric heat sources.

The curves shown in Figure 5-12 in which the particles act as volumetric heat sources are identical in shape to the curves for the case shown in Figure 5-13 for which the particles do not act as volumetric heat sources. The difference in thickness of the Brownian layer is strictly due to the different particle Schmidt numbers, where the thickness of the Brownian layer is of the order of $Sc^{-1}$, as shown in Section 4.5. The intent of these two Figures 5-12 and 5-13 is to show that there are no differences in particle concentration inside the Brownian diffusion layer, that is, the Brownian diffusion of particles that act as volumetric heat sources is no different than the Brownian diffusion of particles that do not act as volumetric heat sources. The scaling analysis of Appendix D shows that the Damköhler numbers of interest for the present work ($|Da| \leq 400$) for flows with Grashof numbers greater than $10^9$, are not sufficient to cause any heat source effects inside the thermal boundary layer. As might be expected, there are no heat source effects on the thermophoretic deposition of particles on the wall or on the shape of the particle concentration profile outside or inside the Brownian sublayer.

The points plotted in Figures 5-12 and 5-13 represent the adaptable mesh spacing generated by the Lentini-Pereyra method and are shown here only to demonstrate that aspect of the method. As can be seen from the increased frequency of the plotted points around the "knee" of the each particle concentration distribution, the Lentini-Pereyra method places additional mesh points in regions where the solution changes rapidly.

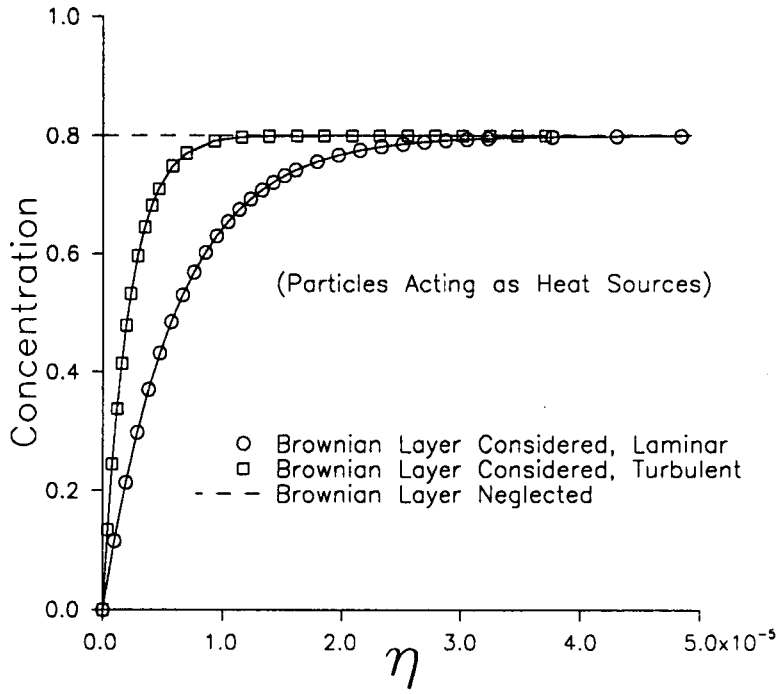


**Figure 5-12. Near Wall Particle Concentration for a Schmidt Number of $10^6$.**

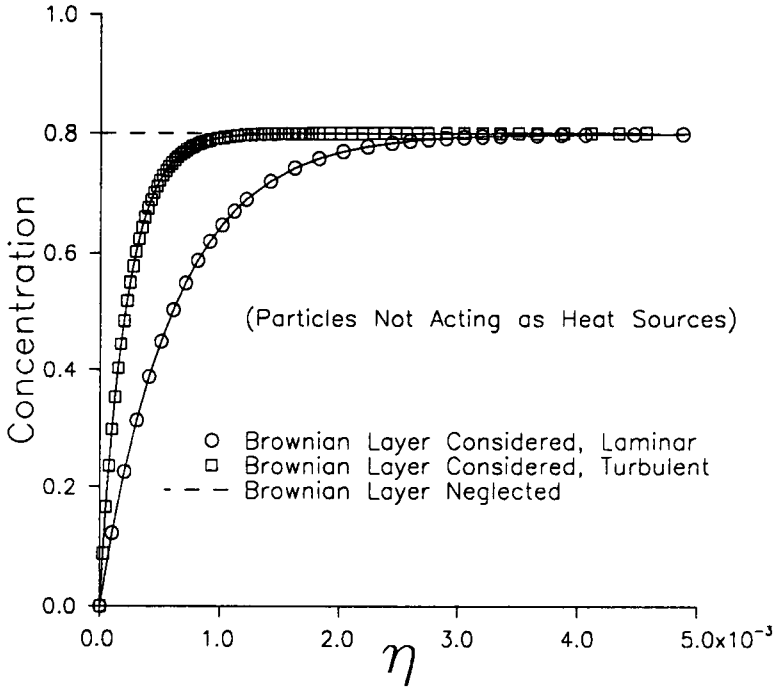


**Figure 5-13. Near Wall Particle Concentration for a Schmidt Number of $10^4$.**

Inspection of Figures 5-12 and 5-13 shows that the computed concentration profiles, sufficiently far from the wall, are not affected when the Brownian diffusion layer is neglected. The relative thickness of the Brownian layer is on the order of $Sc^{-1}$ for both laminar and turbulent flows. The computed thickness for laminar flow for Schmidt numbers of $10^4$ and $10^6$ correspond to those thicknesses computed by Walker et al. (1979) and Gökoglu and Rosner (1986) with an asymptotic expansion method for *forced* convection with Brownian diffusion and thermophoresis. Thus, it may be concluded that the Brownian layer thicknesses computed with the Lentini-Pereyra method match those in the literature for comparable conditions.

The dimensionless ratio of transfer coefficients, given by equation (4-60), was developed to permit the computation of the particle transfer coefficient corresponding to a given heat transfer coefficient without specifying a Schmidt number. However, the mass transfer from the fluid to the wall actually occurs by Brownian diffusion immediately adjacent to the wall. A "standard" Sherwood number for particle deposition at the wall, both with and without the Brownian layer, was developed to demonstrate that the thermophoretic particle flux to the wall computed by assuming the Brownian layer may be neglected is approximately equal to the particle flux directly at the wall in the limit of high Schmidt number.

A local Sherwood number is defined here by the following expression:

$$Sh = \frac{h_P x}{\mathcal{D}}, \qquad (5-8)$$

where $h_P$ is the particle transfer coefficient as given in equation (4-56), $x$ is the axial distance along the wall, and $\mathcal{D}$ is the Brownian diffusion coefficient.

An expression for the particle flux transferred to the wall by thermophoresis was developed in Section 4.8. The particle transfer coefficient is given by equation (4-56) as the ratio of the particle wall flux to the volumetric concentration of particles far from the wall. The expression for the particle transfer coefficient due to thermophoresis, given by equation (4-58), is repeated here as follows:

$$h_P = -\frac{\rho_w N_w}{\rho_\infty N_\infty} K \frac{\nu_w}{T_w}\left(\frac{\partial T}{\partial y}\right)_w . \qquad (5-9)$$

Assuming constant thermophysical properties, substituting equation (5-9) for the particle transfer coefficient into equation (5-8), which defines the local Sherwood number, and evaluating the wall heat flux in terms of the nonsimilarity variable transformations given by equations (4-33), (4-35), and (4-37) yields the following expression for the local Sherwood number for thermophoretic transport:

$$Sh_T = K\left(\frac{-\lambda\theta_w'}{1+\lambda}\right) n_w Sc\left(\frac{Gr}{4}\right)^{1/4} . \qquad (5-10)$$

Using Fick's Law to express the rate of particle deposition on the wall by Brownian diffusion enables the particle flux to be written as (Hidy and Brock, 1970):

$$j_B = -\mathcal{D}\left[\frac{\partial(\rho N)}{\partial y}\right]_w . \qquad (5-11)$$

With the assumption of constant thermophysical properties, the particle transfer coefficient for deposition at the wall by Brownian diffusion is given by the following expression:

$$h_B = -\frac{\mathcal{D}}{N_\infty}\left(\frac{\partial N}{\partial y}\right)_w . \qquad (5-12)$$

Substituting equation (5-12) and the nonsimilarity transformations given by equations (4-33) and (4-36) into equation (5-9) for the Sherwood number yields the Sherwood number for Brownian diffusion:

$$Sh_B = \frac{n_w'}{Sc} Sc\left(\frac{Gr}{4}\right)^{1/4} . \qquad (5-13)$$

The Sherwood numbers given by equations (5-10) and (5-13) were computed with the Lentini-Pereyra method for laminar constant property flow with a Prandtl number of 0.8, and a thermophoretic coefficient, $K$, of 0.1. The values of these Sherwood numbers, as divided by the product of the Schmidt number and the fourth root of the Grashof number divided by four, $Sc\,(Gr/4)^{1/4}$, are presented in Table 5-11 for a range of Schmidt numbers. Only one entry is shown for the case where Brownian diffusion is neglected, since the value of the Brownian diffusion coefficient and Schmidt number is immaterial for that case. The number of mesh points necessary to resolve the concentration profile is also presented in this table.

Table 5-11. Sherwood Numbers for Particle Deposition.

| | Brownian Layer Included | | Brownian Layer Neglected | |
|---|---|---|---|---|
| Schmidt Number | $\frac{n'_w}{Sc}$ | Mesh Points | $K\left(\frac{-\lambda\theta_w'}{1+\lambda}\right)n_w$ | Mesh Points |
| $10^0$ | 0.5887 | 20 | 0.0124 | 20 |
| $10^1$ | 0.1729 | 20 | | |
| $10^2$ | 0.0438 | 29 | | |
| $10^3$ | 0.0176 | 34 | | |
| $10^4$ | 0.0131 | 68 | | |
| $10^5$ | 0.0127 | 137 | | |
| $10^6$ | 0.0126 | 126 | | |

As can be seen from inspection of Table 5-11, the Sherwood numbers computed by including and neglecting the Brownian diffusion layer are considerably different for values of the Schmidt number less than $10^3$. For values of the Schmidt number greater than $10^3$, the thermophoretic and Brownian deposition are almost identical. The increased number of mesh points is indicative of the additional numerical effort necessary to resolve the Brownian sublayer for high Schmidt number circumstances.

Therefore for a sufficiently high Schmidt number greater than $10^3$, the particle deposition at the wall is computed with sufficient accuracy without consideration of the Brownian diffusion layer.

### 5.7. Summary and Conclusions of Model Validity

The analytical model developed in this work includes a number of extremely complex phenomena, such as turbulence, variable property effects, the thermophoretic transport of particulate matter that acts as a volumetric heat source, thermal stratification in the ambient fluid, and participation of the fluid in an exchange of thermal radiation. No single analytical or experimental investigation could be found in the open literature that includes *all* of the effects accounted for in the present work, necessitating validation of the model in a piecemeal fashion by comparison of computed results with the results of a number of different investigations, each of which is essentially focused on an exploration of only one of the many effects included in the present model. The analytical model has been validated by comparison with all of these investigations, except that involving a cavity flow with volumetric heat sources (Greene, 1982), which was shown as not having a natural convection boundary layer as that for flows on isothermal, vertical plates.

As shown in Section 5.2.1, the results for laminar flows compared very well with those from other investigations for constant thermophysical properties.

In Section 5.2.2, the results for laminar flows where the effects of variable thermophysical properties are considered gave the best agreement with the data of Cairnie and Harrison (1980) when polynomial functions of temperature were used to compute the fluid properties, as compared to approximating the properties as a constant Chapman-Rubesin parameter. There was no penalty of increased computation effort with the use of the polynomial functions of temperature.

In Section 5.2.3, laminar flows in a linearly-stratified temperature ambient fluid were considered. The best agreement for this nonsimilar flow is obtained with the use of the second-level model of the method of local nonsimilarity where the controversial terms, as indicated in Appendix A.1.2, were retained. The Lentini-Pereyra method of

integrating the two-point boundary layer differential equations was easily implemented and gave successfully converged solutions more frequently than the other methods. Because the model computes flow and temperature inversions observed by other investigators, the essential physical features of thermally-stratified flow are faithfully reproduced by the model.

No published results could be found for the optically thick limit of interest. Thus, the fact that in this limit, the term representing participating thermal radiation in the energy equation acts effectively like an increased thermal conductivity was exploited in section 5.2.4. This "diffusion approximation" allowed the results of the present model to be validated by comparison with low Prandtl number results reported in the open literature. Excellent agreement with these results was obtained. Computed trends of $Nu/Bo^{1/4}$ with the parameter, $M$, that represents the extent of radiation participation, and the wall temperature to fluid temperature ratio agree with those of Kuiken (1969) and Kennedy and Paszkowskyj (1970).

In Section 5.3, in order to keep the model as simple as possible, an algebraic turbulence closure for the turbulent diffusivity of momentum and the first-level of truncation model of the method of local nonsimilarity were chosen. After empirical constants were set, the model adequately predicts the heat transfer in a natural convection boundary layer, as reported by Seibers et al. (1983) for constant and variable fluid properties.

In Section 5.4, the heat transfer results computed with the present model did not adequately predict the heat transfer to a cooled vertical wall in an open pool with Joulean heating in the fluid, as measured by Greene (1982). This discrepancy is due to the fundamental difference in boundary layer structure that exists in Greene's experimental apparatus and that of the present analytical model. No effect due to the volumetric heat sources inside the boundary layer was observed, restricting the role of the heat source in the flow to provide the temperature difference between the wall and the fluid far from the wall only. No other published results were found in the open literature that concern the geometry and flow conditions of interest here, and experimental research is advised.

In Section 5.5, the deposition of particles by thermophoresis on a cooled wall was computed with the present model. The results compared favorably with exact analytical solutions that exist for a limited set of physical conditions when the neglect of the Brownian diffusion layer is valid.

Because of the fine computational detail required to resolve a very thin Brownian diffusion layer adjacent to the cooled plate, the accuracy of neglecting the Brownian layer was considered in Section 5.6. For particle Schmidt numbers greater than $10^3$, the flux of particles deposited on the wall by thermophoresis was adequately computed with both the Keller Box technique and the Lentini-Pereyra technique without resolving the Brownian layer as compared to the results computed with the Lentini-Pereyra technique that allows for resolution of the Brownian layer. Although the computation effort substantially increases when resolving the Brownian layer with the Lentini-Pereyra technique, it is not prohibitively increased. As also observed when computing the heat transfer in flows with a thermally-stratified temperature distribution in the ambient fluid, the Lentini-Pereyra technique was the easiest technique to implement and appeared to be the most robust under the widely varying conditions of the present investigation.

Thus, because of the detailed, favorable comparisons between the results computed with the present model and those given in the investigations listed in Section 5-1, the model is validated for the flows of interest and can adequately compute the heat transfer and thermophoretic particle deposition on cooled vertical walls immersed in heated fluids of semi-infinite extent.

# CHAPTER 6

# COMPUTATION OF THERMOPHORETIC PARTICLE DEPOSITION

## 6.1. Introduction

In this section, the dimensionless ratio of transfer coefficients is presented for the conditions likely to occur inside the Boiling Water Reactor (BWR). For the expected heat source strengths, the scaling analysis of Appendix D shows that the effects of the volumetric heat sources are negligible inside the boundary layer and that the presence of the volumetric heat sources only serve to set the temperature boundary conditions outside the boundary layer. The results for thermophoretic particle deposition presented in Section 5.6 that justify the neglect of the Brownian layer also show that the effects of the volumetric heat sources inside the Brownian layer are negligible. Consequently, the thermophoretic particle deposition results presented in this section specifically are computed without the heat source term inside the boundary layer. These results are reported in terms of the dimensionless ratio of transfer coefficients, equation (4-60). The heat transfer results are reported in terms of $Nu/Ra^{1/4}$ for laminar flow and $Nu/Ra^{1/3}$ for turbulent flow.

The method of local nonsimilarity with the Lentini-Pereyra integration method is used for computing the thermophoretic deposition results for the following flow conditions of interest:

1. Laminar and turbulent flow of steam, air, and hydrogen at a constant temperature and pressure far from the wall.
2. Stratified temperature of the ambient fluid far from the wall.
3. Participating gas thermal radiation.

## 6.2. Isothermal Conditions Far from the Wall

For the expected higher levels of volumetric heat source strengths, the fluid far from the wall could not be completely quiescent outside of the boundary layer since the stability criterion as developed by Sparrow et al. (1963) and described in Section 2.3

would be exceeded. Consequently, strong turbulent mixing would be expected to occur with a resulting uniform temperature distribution, as observed in the experimental results of Greene (1982).

As justified in Section 5.3, the local similarity model of the method of local nonsimilarity may be used to compute the heat transfer and particle deposition at the wall for both turbulent and laminar natural convection flows. A range of values of $KPr_-$ from 1.0 to 0.04 that covers the range of expected particle sizes and Knudsen numbers is used. The wall temperature ratios of 0.9, 0.7, and 0.5 are also used. Computations are presented for both constant and variable thermophysical properties.

For steam, a uniform temperature of 1000°C and pressure of 6.9 MPa are used to specify the conditions far from the wall. The Prandtl number for those conditions is 0.805. The effective dimensionless particle concentration at the wall, the dimensionless ratio of transfer coefficients, and the heat transfer are presented in Table 6-1 for laminar flow and in Table 6-2 for a turbulent flow that has a Rayleigh number of $2.4\times10^{12}$. Heat transfer and thermophoretic particle deposition results computed for both constant and variable thermophysical properties are also presented. The dimensionless ratio of transfer coefficients computed for steam is plotted in Figure 6-1.

Additional cases were computed for air and hydrogen assumed to be at atmospheric pressure and 1000°C temperature far from the wall. For air, the Prandtl number at the stated conditions is 0.710 and the Prandtl number for hydrogen is 0.726. The polynomial curve fits from Irvine and Liley (1984) are used to compute the thermophysical properties of air and hydrogen. The effective wall particle concentration, dimensionless ratio of transfer coefficients, and heat transfer for air are presented in Table 6-3 for laminar flows and in Table 6-4 for a turbulent flow having a Rayleigh number of $2.1\times10^{12}$. The effective wall particle concentration, dimensionless ratio of transfer coefficients, and heat transfer for hydrogen are presented in Table 6-5 for laminar flow and in Table 6-6 for a turbulent flow with a Rayleigh number of $2.2\times10^{12}$. The dimensionless ratio of transfer coefficients is presented of Figure 6-2 for air and in Figure 6-3 for hydrogen.

Table 6-1. Particle Deposition Results for Laminar Flows in Steam.

| | Constant Properties | | | Variable Properties | | | |
|---|---|---|---|---|---|---|---|
| $KPr_\infty$ | $n_w$ | $\rho_\infty C_\infty \frac{h_P}{h_H}$ | $\frac{Nu}{Ra^{1/4}}$ | $n_w$ | $\rho_\infty C_\infty \frac{h_P}{h_H}$ | $\frac{Nu}{Ra^{1/4}}$ | $\frac{\mu_w k_\infty}{\mu_\infty k_w}$ |
| $T_w/T_\infty$=0.9 | | | | | | | |
| 1.0 | 0.9000 | 0.1000 | 0.3914 | 0.9008 | 0.1084 | 0.3810 | 1.08 |
| 0.8050 | 0.9150 | 0.0818 | | 0.9157 | 0.0887 | | |
| 0.6038 | 0.9317 | 0.0625 | | 0.9322 | 0.0677 | | |
| 0.4025 | 0.9502 | 0.0425 | | 0.9505 | 0.0460 | | |
| 0.2013 | 0.9712 | 0.0217 | | 0.9710 | 0.0235 | | |
| 0.0805 | 0.9861 | 0.0088 | | 0.9859 | 0.0095 | | |
| 0.0403 | 0.9921 | 0.0044 | | 0.9919 | 0.0048 | | |
| $T_w/T_\infty$=0.7 | | | | | | | |
| 1.0 | 0.7000 | 0.3000 | 0.3914 | 0.7042 | 0.3600 | 0.3639 | 1.19 |
| 0.8050 | 0.7314 | 0.2524 | | 0.7346 | 0.3022 | | |
| 0.6038 | 0.7704 | 0.1993 | | 0.7716 | 0.2381 | | |
| 0.4025 | 0.8174 | 0.1410 | | 0.8168 | 0.1680 | | |
| 0.2013 | 0.8791 | 0.0758 | | 0.8766 | 0.0902 | | |
| 0.0805 | 0.9317 | 0.0321 | | 0.9285 | 0.0382 | | |
| 0.0403 | 0.9562 | 0.0165 | | 0.9534 | 0.0196 | | |
| $T_w/T_\infty$=0.5 | | | | | | | |
| 1.0 | 0.5000 | 0.5000 | 0.3914 | 0.5065 | 0.6308 | 0.3543 | 1.25 |
| 0.8050 | 0.5358 | 0.4313 | | 0.5403 | 0.5417 | | |
| 0.6038 | 0.5824 | 0.3516 | | 0.5839 | 0.4390 | | |
| 0.4025 | 0.6443 | 0.2593 | | 0.6416 | 0.3216 | | |
| 0.2013 | 0.7362 | 0.1481 | | 0.7280 | 0.1825 | | |
| 0.0805 | 0.8293 | 0.0667 | | 0.8167 | 0.0819 | | |
| 0.0403 | 0.8803 | 0.0354 | | 0.8662 | 0.0434 | | |

Table 6-2. Particle Deposition Results for a Turbulent Flow having a Rayleigh Number of $2.4\times10^{12}$ in Steam.

| | Constant Properties | | | Variable Properties | | | |
|---|---|---|---|---|---|---|---|
| $KPr_\infty$ | $n_w$ | $\rho_\infty C_\infty \frac{h_P}{h_H}$ | $\frac{Nu}{Ra^{1/3}}$ | $n_w$ | $\rho_\infty C_\infty \frac{h_P}{h_H}$ | $\frac{Nu}{Ra^{1/3}}$ | $\frac{\mu_w k_\infty}{\mu_\infty k_w}$ |
| $T_w/T_\infty$=0.9 | | | | | | | |
| 1.0 | 0.9000 | 0.1000 | 0.1198 | 0.9026 | 0.1086 | 0.1173 | 1.08 |
| 0.8050 | 0.9163 | 0.0819 | | 0.9185 | 0.0890 | | |
| 0.6038 | 0.9342 | 0.0626 | | 0.9358 | 0.0680 | | |
| 0.4025 | 0.9533 | 0.0426 | | 0.9544 | 0.0462 | | |
| 0.2013 | 0.9742 | 0.0217 | | 0.9747 | 0.0236 | | |
| 0.0805 | 0.9882 | 0.0088 | | 0.9884 | 0.0096 | | |
| 0.0403 | 0.9933 | 0.0044 | | 0.9934 | 0.0048 | | |
| $T_w/T_\infty$=0.7 | | | | | | | |
| 1.0 | 0.7000 | 0.3000 | 0.1198 | 0.7142 | 0.3650 | 0.1123 | 1.19 |
| 0.8050 | 0.7366 | 0.2541 | | 0.7489 | 0.3081 | | |
| 0.6038 | 0.7802 | 0.2019 | | 0.7902 | 0.2438 | | |
| 0.4025 | 0.8321 | 0.1435 | | 0.8392 | 0.1726 | | |
| 0.2013 | 0.8966 | 0.0773 | | 0.9001 | 0.0926 | | |
| 0.0805 | 0.9464 | 0.0327 | | 0.9474 | 0.0390 | | |
| 0.0403 | 0.9673 | 0.0167 | | 0.9675 | 0.0199 | | |
| $T_w/T_\infty$=0.5 | | | | | | | |
| 1.0 | 0.5000 | 0.5000 | 0.1198 | 0.5211 | 0.6491 | 0.1103 | 1.25 |
| 0.8050 | 0.5425 | 0.4367 | | 0.5619 | 0.5633 | | |
| 0.6038 | 0.5972 | 0.3606 | | 0.6141 | 0.4618 | | |
| 0.4025 | 0.6692 | 0.2693 | | 0.6825 | 0.3421 | | |
| 0.2013 | 0.7723 | 0.1554 | | 0.7804 | 0.1956 | | |
| 0.0805 | 0.8668 | 0.0698 | | 0.8705 | 0.0873 | | |
| 0.0403 | 0.9121 | 0.0367 | | 0.9142 | 0.0458 | | |

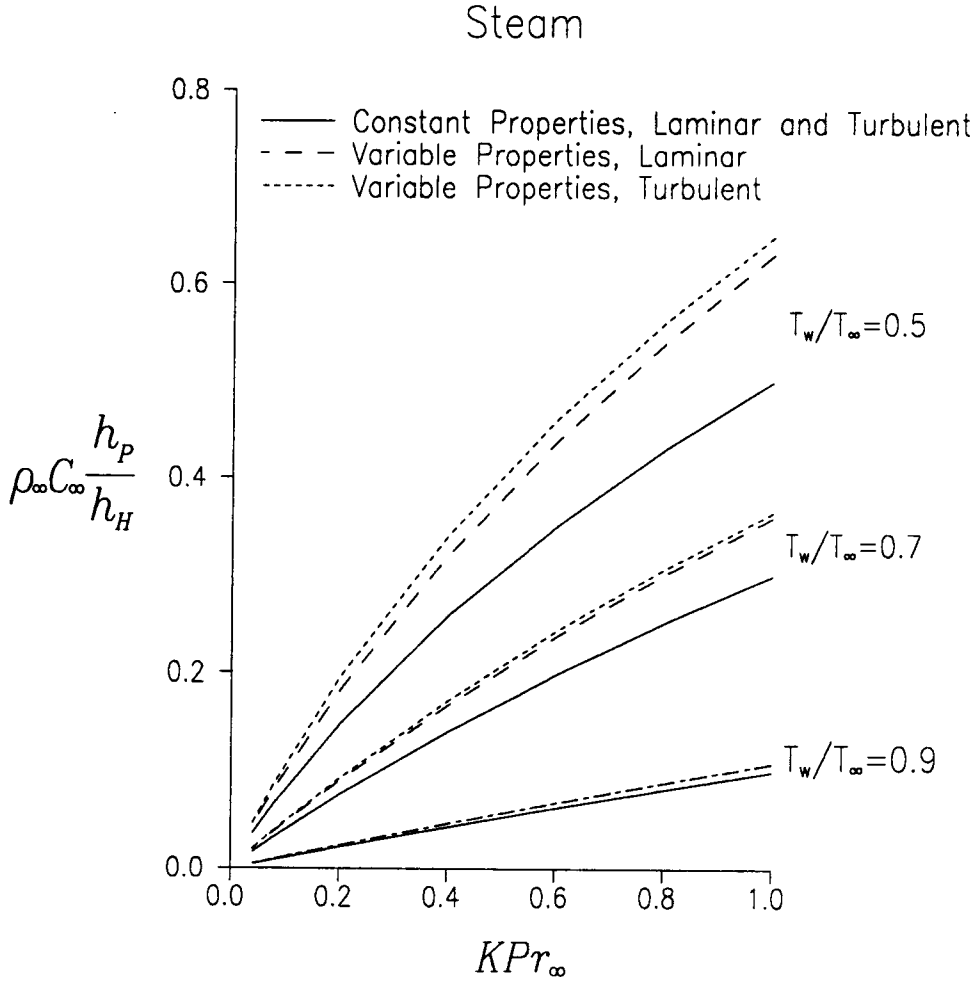


Figure 6-1. Dimensionless Ratio of Transfer Coefficients for Steam. The turbulent flow has a Rayleigh number of $2.4 \times 10^{12}$.

Table 6-3. Particle Deposition Results for Laminar Flows in Air.

| | Constant Properties | | | Variable Properties | | | |
|---|---|---|---|---|---|---|---|
| $KPr_\infty$ | $n_w$ | $\rho_\infty C_\infty \frac{h_P}{h_H}$ | $\frac{Nu}{Ra^{1/4}}$ | $n_w$ | $\rho_\infty C_\infty \frac{h_P}{h_H}$ | $\frac{Nu}{Ra^{1/4}}$ | $\frac{\mu_w k_\infty}{\mu_\infty k_w}$ |
| $T_w/T_\infty$=0.9 | | | | | | | |
| 1.0 | 0.9000 | 0.1000 | 0.3867 | 0.9005 | 0.1013 | 0.3881 | 1.01 |
| 0.7100 | 0.9229 | 0.0728 | | 0.9234 | 0.0737 | | |
| 0.5325 | 0.9381 | 0.0555 | | 0.9385 | 0.0562 | | |
| 0.3550 | 0.9549 | 0.0764 | | 0.9552 | 0.0381 | | |
| 0.1755 | 0.9740 | 0.0192 | | 0.9741 | 0.0194 | | |
| 0.0710 | 0.9874 | 0.0078 | | 0.9875 | 0.0079 | | |
| 0.0355 | 0.9928 | 0.0039 | | 0.9928 | 0.0040 | | |
| $T_w/T_\infty$=0.7 | | | | | | | |
| 1.0 | 0.7000 | 0.3000 | 0.3867 | 0.7036 | 0.3160 | 0.3916 | 1.05 |
| 0.7100 | 0.7495 | 0.2279 | | 0.7535 | 0.2401 | | |
| 0.5325 | 0.7861 | 0.1793 | | 0.7906 | 0.1890 | | |
| 0.3550 | 0.8302 | 0.1262 | | 0.8354 | 0.1331 | | |
| 0.1755 | 0.8869 | 0.0674 | | 0.8894 | 0.0709 | | |
| 0.0710 | 0.9345 | 0.0284 | | 0.9372 | 0.0299 | | |
| 0.0355 | 0.9565 | 0.0145 | | 0.9594 | 0.0153 | | |
| $T_w/T_\infty$=0.5 | | | | | | | |
| 1.0 | 0.5000 | 0.5000 | 0.3867 | 0.5062 | 0.5533 | 0.3953 | 1.09 |
| 0.7100 | 0.5568 | 0.3951 | | 0.5627 | 0.4364 | | |
| 0.5325 | 0.6027 | 0.3207 | | 0.6081 | 0.3537 | | |
| 0.3550 | 0.6631 | 0.2352 | | 0.6674 | 0.2588 | | |
| 0.1755 | 0.7518 | 0.1334 | | 0.7543 | 0.1462 | | |
| 0.0710 | 0.8404 | 0.0596 | | 0.8404 | 0.0652 | | |
| 0.0355 | 0.8883 | 0.0315 | | 0.8870 | 0.0344 | | |

Table 6-4. Particle Deposition Results for a Turbulent Flow having a Rayleigh Number of $2.1\times10^{12}$ in Air.

| | Constant Properties | | | Variable Properties | | | |
|---|---|---|---|---|---|---|---|
| $KPr_\infty$ | $n_w$ | $\rho_\infty C_\infty \frac{h_P}{h_H}$ | $\frac{Nu}{Ra^{1/3}}$ | $n_w$ | $\rho_\infty C_\infty \frac{h_P}{h_H}$ | $\frac{Nu}{Ra^{1/3}}$ | $\frac{\mu_w k_\infty}{\mu_\infty k_w}$ |
| $T_w/T_\infty$=0.9 | | | | | | | |
| 1.0 | 0.9000 | 0.1000 | 0.1174 | 0.9004 | 0.1013 | 0.1204 | 1.01 |
| 0.7100 | 0.9247 | 0.0729 | | 0.9251 | 0.0738 | | |
| 0.5325 | 0.9409 | 0.0556 | | 0.9413 | 0.0563 | | |
| 0.3550 | 0.9582 | 0.0378 | | 0.9585 | 0.0383 | | |
| 0.1755 | 0.9770 | 0.0193 | | 0.9772 | 0.0195 | | |
| 0.0710 | 0.9894 | 0.0078 | | 0.9896 | 0.0079 | | |
| 0.0355 | 0.9940 | 0.0039 | | 0.9941 | 0.0040 | | |
| $T_w/T_\infty$=0.7 | | | | | | | |
| 1.0 | 0.7000 | 0.3000 | 0.1174 | 0.7033 | 0.3159 | 0.1270 | 1.05 |
| 0.7100 | 0.7566 | 0.2301 | | 0.7603 | 0.2423 | | |
| 0.5325 | 0.7981 | 0.1820 | | 0.8017 | 0.1916 | | |
| 0.3550 | 0.8467 | 0.1287 | | 0.8502 | 0.1355 | | |
| 0.1755 | 0.9064 | 0.0689 | | 0.9093 | 0.0724 | | |
| 0.0710 | 0.9518 | 0.0289 | | 0.9539 | 0.0304 | | |
| 0.0355 | 0.9705 | 0.0148 | | 0.9723 | 0.0155 | | |
| $T_w/T_\infty$=0.5 | | | | | | | |
| 1.0 | 0.5000 | 0.5000 | 0.1174 | 0.5066 | 0.5537 | 0.1351 | 1.09 |
| 0.7100 | 0.5674 | 0.4026 | | 0.5754 | 0.4462 | | |
| 0.5325 | 0.6215 | 0.3307 | | 0.6305 | 0.3667 | | |
| 0.3550 | 0.6917 | 0.2454 | | 0.7016 | 0.2721 | | |
| 0.1755 | 0.7905 | 0.1402 | | 0.8007 | 0.1552 | | |
| 0.0710 | 0.8789 | 0.0624 | | 0.8878 | 0.0689 | | |
| 0.0355 | 0.9206 | 0.0327 | | 0.9278 | 0.0360 | | |

Table 6-5. Particle Deposition Results for Laminar Flows in Hydrogen.

| | Constant Properties | | | Variable Properties | | | |
|---|---|---|---|---|---|---|---|
| $KPr_\infty$ | $n_w$ | $\rho_\infty C_\infty \frac{h_P}{h_H}$ | $\frac{Nu}{Ra^{1/4}}$ | $n_w$ | $\rho_\infty C_\infty \frac{h_P}{h_H}$ | $\frac{Nu}{Ra^{1/4}}$ | $\frac{\mu_w k_\infty}{\mu_\infty k_w}$ |
| $T_w/T_\infty$=0.9 | | | | | | | |
| 1.0 | 0.9000 | 0.1000 | 0.3877 | 0.9008 | 0.1084 | 0.3810 | 1.01 |
| 0.7260 | 0.9214 | 0.0728 | | 0.9157 | 0.0887 | | |
| 0.5445 | 0.9369 | 0.0567 | | 0.9322 | 0.0677 | | |
| 0.3630 | 0.9539 | 0.0385 | | 0.9505 | 0.0460 | | |
| 0.1815 | 0.9732 | 0.0196 | | 0.9710 | 0.0235 | | |
| 0.0726 | 0.9866 | 0.0080 | | 0.9859 | 0.0095 | | |
| 0.0363 | 0.9920 | 0.0040 | | 0.9919 | 0.0048 | | |
| $T_w/T_\infty$=0.7 | | | | | | | |
| 1.0 | 0.7000 | 0.3000 | 0.3877 | 0.7042 | 0.3600 | 0.3639 | 1.02 |
| 0.7260 | 0.7464 | 0.2321 | | 0.7346 | 0.3022 | | |
| 0.5445 | 0.7833 | 0.1827 | | 0.7716 | 0.2381 | | |
| 0.3630 | 0.8279 | 0.1287 | | 0.8168 | 0.1680 | | |
| 0.1815 | 0.8853 | 0.0688 | | 0.8766 | 0.0902 | | |
| 0.0726 | 0.9335 | 0.0290 | | 0.9285 | 0.0382 | | |
| 0.0363 | 0.9558 | 0.0149 | | 0.9534 | 0.0196 | | |
| $T_w/T_\infty$=0.5 | | | | | | | |
| 1.0 | 0.5000 | 0.5000 | 0.3877 | 0.5065 | 0.6308 | 0.3543 | 1.03 |
| 0.7260 | 0.5534 | 0.4015 | | 0.5403 | 0.5417 | | |
| 0.5445 | 0.5992 | 0.3261 | | 0.5839 | 0.4390 | | |
| 0.3630 | 0.6593 | 0.2392 | | 0.6416 | 0.3216 | | |
| 0.1815 | 0.7473 | 0.1356 | | 0.7280 | 0.1825 | | |
| 0.0726 | 0.8343 | 0.0605 | | 0.8167 | 0.0819 | | |
| 0.0363 | 0.8810 | 0.0320 | | 0.8662 | 0.0434 | | |

Table 6-6. Particle Deposition Results for a Turbulent Flow having a Rayleigh Number of $2.2\times10^{12}$ in Hydrogen.

| | Constant Properties | | | Variable Properties | | | |
|---|---|---|---|---|---|---|---|
| $KPr_\infty$ | $n_w$ | $\rho_\infty C_\infty \frac{h_P}{h_H}$ | $\frac{Nu}{Ra^{1/3}}$ | $n_w$ | $\rho_\infty C_\infty \frac{h_P}{h_H}$ | $\frac{Nu}{Ra^{1/3}}$ | $\frac{\mu_w k_\infty}{\mu_\infty k_w}$ |
| $T_w/T_\infty=0.9$ | | | | | | | |
| 1.0 | 0.9000 | 0.1000 | 0.1178 | 0.9003 | 0.1008 | 0.1201 | 1.01 |
| 0.7260 | 0.9231 | 0.0744 | | 0.9235 | 0.0751 | | |
| 0.5445 | 0.9397 | 0.0568 | | 0.9400 | 0.0573 | | |
| 0.3630 | 0.9573 | 0.0386 | | 0.9576 | 0.0389 | | |
| 0.1815 | 0.9764 | 0.0197 | | 0.9767 | 0.0196 | | |
| 0.0726 | 0.9891 | 0.0080 | | 0.9893 | 0.0080 | | |
| 0.0363 | 0.9938 | 0.0040 | | 0.9940 | 0.0040 | | |
| $T_w/T_\infty=0.7$ | | | | | | | |
| 1.0 | 0.7000 | 0.3000 | 0.1178 | 0.7019 | 0.3079 | 0.1259 | 1.02 |
| 0.7260 | 0.7531 | 0.2342 | | 0.7555 | 0.2406 | | |
| 0.5445 | 0.7949 | 0.1854 | | 0.7975 | 0.1904 | | |
| 0.3630 | 0.8442 | 0.1312 | | 0.8468 | 0.1348 | | |
| 0.1815 | 0.9047 | 0.0703 | | 0.9070 | 0.0722 | | |
| 0.0726 | 0.9508 | 0.0296 | | 0.9527 | 0.0303 | | |
| 0.0363 | 0.9699 | 0.0151 | | 0.9713 | 0.0155 | | |
| $T_w/T_\infty=0.5$ | | | | | | | |
| 1.0 | 0.5000 | 0.5000 | 0.1178 | 0.5033 | 0.5173 | 0.1342 | 1.03 |
| 0.7260 | 0.5630 | 0.4085 | | 0.5679 | 0.4235 | | |
| 0.5445 | 0.6171 | 0.3358 | | 0.6236 | 0.3488 | | |
| 0.3630 | 0.6876 | 0.2495 | | 0.6957 | 0.2594 | | |
| 0.1815 | 0.7872 | 0.1428 | | 0.7965 | 0.1485 | | |
| 0.0726 | 0.8767 | 0.0636 | | 0.8855 | 0.0660 | | |
| 0.0363 | 0.9192 | 0.0335 | | 0.9266 | 0.0346 | | |

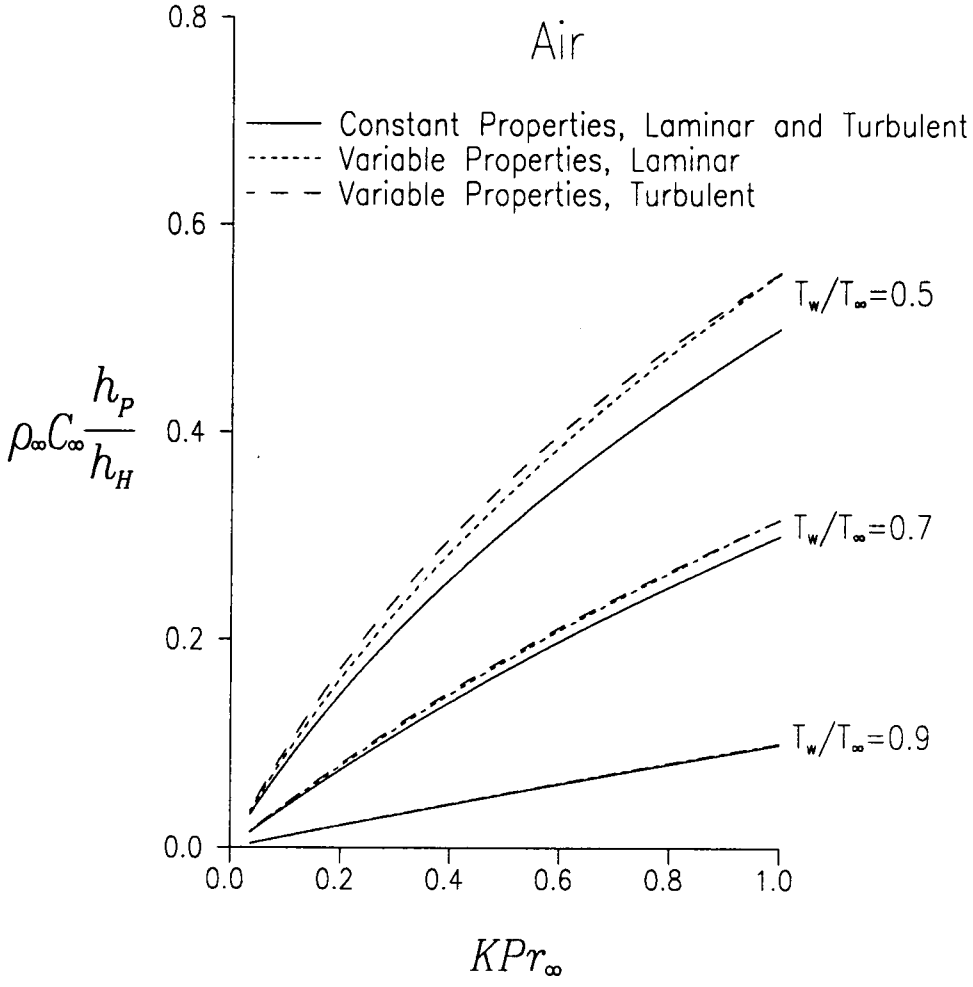


Figure 6-2. Dimensionless Ratio of Transfer Coefficients for Air.

The turbulent flow has a Rayleigh number of $2.1 \times 10^{12}$.

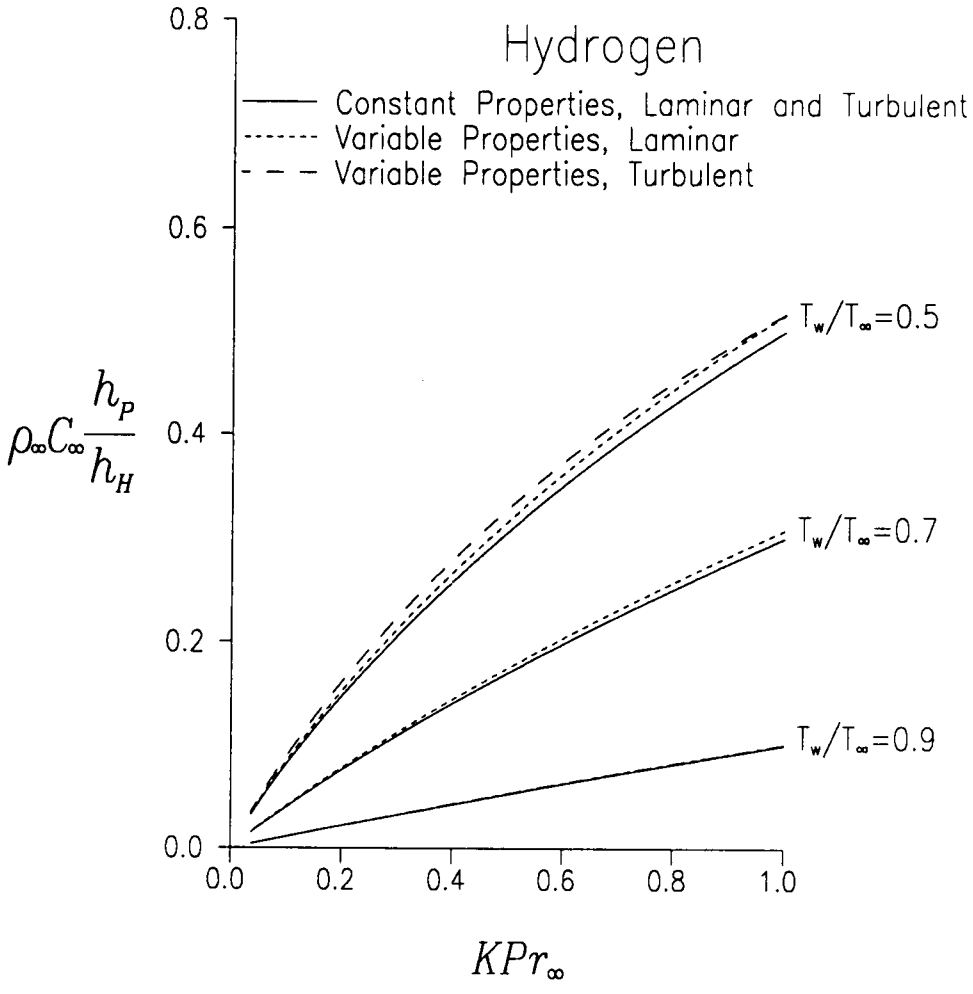


**Figure 6-3. Dimensionless Ratio of Transfer Coefficients for Hydrogen. The turbulent flow has a Rayleigh number of $2.2\times10^{12}$.**

Inspection of Tables 6-1 through 6-6 shows that the dimensionless ratios of transfer coefficients computed for constant property laminar and turbulent flows have differences in the third digit, which are considered to be negligible. The maximum difference of the computed dimensionless ratio of transfer coefficients at $T_w/T_\infty = 0.5$ between laminar and turbulent flows is less than 3% for all of the three gases.

Values of the term of $\mu_w k_\infty/\mu_\infty k_w$, which is the variable thermophysical property correction term in equation (4-60), are also presented in Tables 6-1 through 6-6. This term is dependent on the values of the temperatures at the wall and far from the wall. The variable-properties column for the dimensionless ratio of transfer coefficients reported in Tables 6-1 through 6-6 has this ratio included in accordance with equation (4-60). When the value of the dimensionless ratio of transfer coefficients for variable properties in Tables 6-1 through 6-6 is divided by the corresponding ratio of thermophysical properties $\mu_w k_\infty/\mu_\infty k_w$, the result is within approximately 4% of the value for the dimensionless ratio of transfer coefficients for constant properties. Thus, for natural convection flows where turbulence, thermophysical property variations, or both arise, an accurate estimate of the thermophoretic particle deposition can be made by multiplying the value of dimensionless ratio of transfer coefficients that was computed for laminar flow with constant properties by the thermophysical property ratio $\mu_w k_\infty/\mu_\infty k_w$.

Inspection of Figure 6-2 shows that for air the effects of variable thermophysical properties and turbulent conditions are not as large as those effects are for steam, as shown in Figure 6-1. Inspection of Figure 6-3 shows that the effects of variable properties and turbulent flow for hydrogen cause only slight perturbations from the constant-property laminar flow results. The thermophysical property ratios of $\mu_w k_\infty/\mu_\infty k_w$ for air and hydrogen presented in Tables 6-3 through 6-6 have comparable magnitudes at corresponding values of $T_w/T_\infty$.

The measure, $\omega$, of the computed dimensionless ratio of transfer coefficients, as developed in Section 4.9 and expressed in equation (4-93), is computed for all three gases and presented in Table 6-7. Inspection of Table 6-7 shows that the term $\omega$ varies from approximately 0.5 for $T_w/T_\infty = 0.5$ and values of $KPr_\infty$ close to unity to approximately 0.85 as $KPr_\infty$ decreases. Thus, the term $\omega$ appears to be a function of $T_w/T_\infty$ and $KPr_\infty$.

Table 6-7. Values of the Coefficient ω Appearing in Equation (4-93).

| | ω | | |
|---|---|---|---|
| $KPr_\infty$ | $T_w/T_\infty = 0.9$ | $T_w/T_\infty = 0.7$ | $T_w/T_\infty = 0.5$ |
| Steam | | | |
| 0.8050 | 0.8035 | 0.6370 | 0.5113 |
| 0.6038 | 0.8285 | 0.6777 | 0.5554 |
| 0.4025 | 0.8603 | 0.7275 | 0.6120 |
| 0.2013 | 0.9063 | 0.7996 | 0.6987 |
| 0.0805 | 0.9429 | 0.8715 | 0.7937 |
| 0.0403 | 0.9704 | 0.9103 | 0.8502 |
| Air | | | |
| 0.7100 | 0.8014 | 0.6537 | 0.5320 |
| 0.5325 | 0.8292 | 0.6934 | 0.5746 |
| 0.3550 | 0.8613 | 0.7412 | 0.6299 |
| 0.1755 | 0.9061 | 0.8068 | 0.7142 |
| 0.0710 | 0.9344 | 0.8788 | 0.8049 |
| 0.0355 | 0.9505 | 0.9105 | 0.8585 |
| Hydrogen | | | |
| 0.7260 | 0.7924 | 0.6507 | 0.5309 |
| 0.5445 | 0.8253 | 0.6884 | 0.5712 |
| 0.3630 | 0.8574 | 0.7360 | 0.6248 |
| 0.1815 | 0.8972 | 0.8023 | 0.7072 |
| 0.0726 | 0.9292 | 0.8687 | 0.7954 |
| 0.0363 | 0.9559 | 0.9043 | 0.8471 |

These values of the term ω indicate that a good approximation for the dimensionless ratio of transfer coefficients may be the upper limit as expressed in equation (4-92). Thus, instead of trying to determine a functional relationship between ω, $T_w/T_\infty$ and $KPr_\infty$, an *approximate* relationship for the dimensionless ratio of transfer coefficients was developed by using the binomial expansion of equation (4-94) with different levels of series truncation.

Retaining only the first term of the binomial expansion results in equation (4-91), which is the lower limit of the dimensionless ratio of transfer coefficients. Inspection of Figures 6-1, 6-2, and 6-3 shows that assuming a linear relationship between the dimensionless ratio of transfer coefficients and the product $KPr_\infty$ for any value of the wall temperature ratio would be inaccurate. Also, a linear relationship is inconsistent with the computed, non-zero value of the term ω, since a value for ω of zero would transform equation (4-93) into equation (4-91), which describes a linear relationship between the dimensionless ratio of transfer coefficients and the product $KPr_\infty$. Substituting the first two terms of the binomial expansion of equation (4-94) into equation (4-92) yields the following approximation for the dimensionless ratio of transfer coefficients:

$$\rho_\infty C_\infty \frac{h_P}{h_H} = \{(\lambda-1)(\lambda KPr_\infty)-(\lambda KPr_\infty)^2\}\left(\frac{\mu_w k_\infty}{\mu_\infty k_w}\right). \qquad (6-1)$$

Similarly, substituting a three-term expansion of the binomial series of equation (4-94) into equation (4-92) yields the following approximation for the dimensionless ratio of transfer coefficients:

$$\rho_\infty C_\infty \frac{h_P}{h_H} = \left\{(\lambda-\lambda^2-1)(\lambda KPr_\infty)+\left(\frac{3}{2}\lambda-1\right)(\lambda KPr_\infty)^2-\frac{1}{2}(\lambda KPr_\infty)^3\right\}\left(\frac{\mu_w k_\infty}{\mu_\infty k_w}\right). \qquad (6-2)$$

The dimensionless ratios of transfer coefficients computed with equations (6-1) and (6-2) are plotted, along with the results computed with the first-level of truncation model of the method of local nonsimilarity, for constant-property laminar flows in Figures 6-4, 6-5, and 6-6 for steam, air, and hydrogen, respectively.

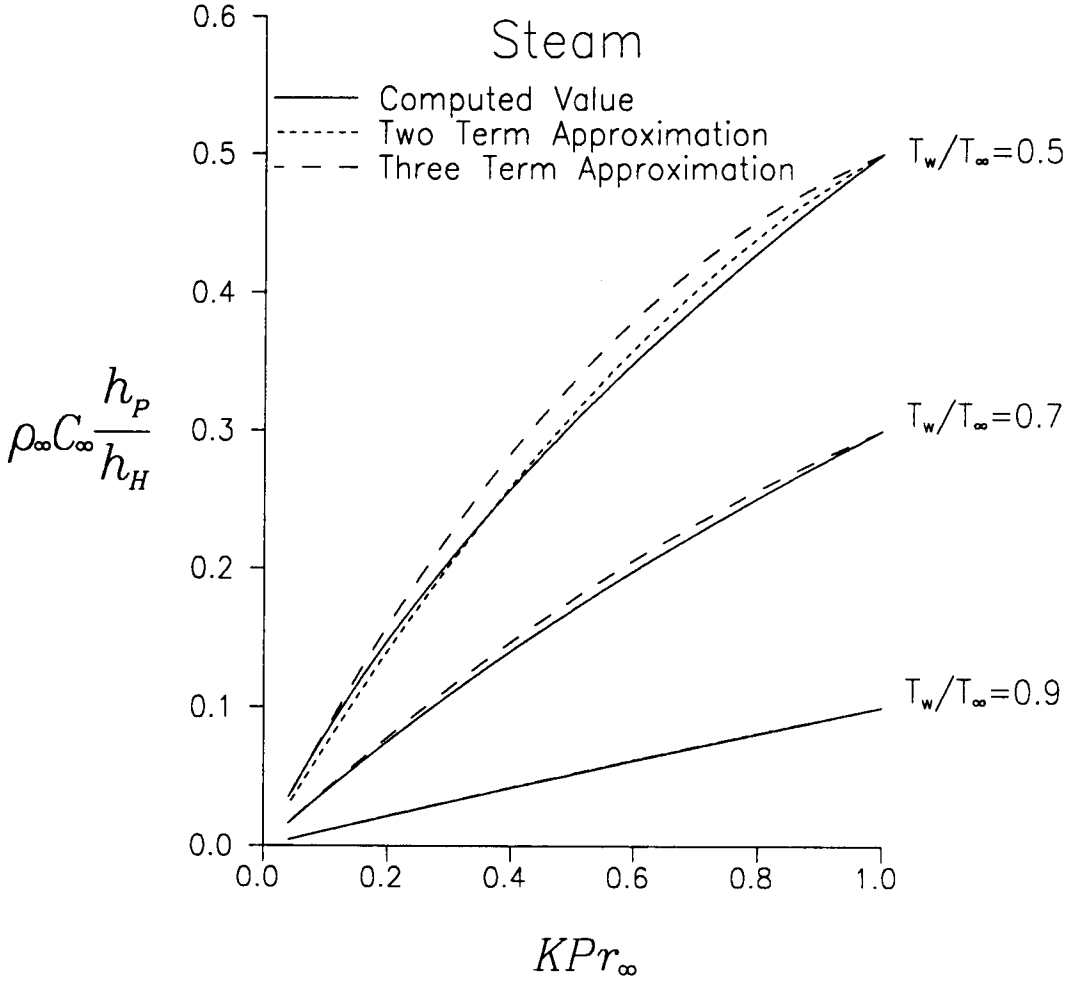


Figure 6-4. Approximate Dimensionless Ratio of Transfer Coefficients for Steam.

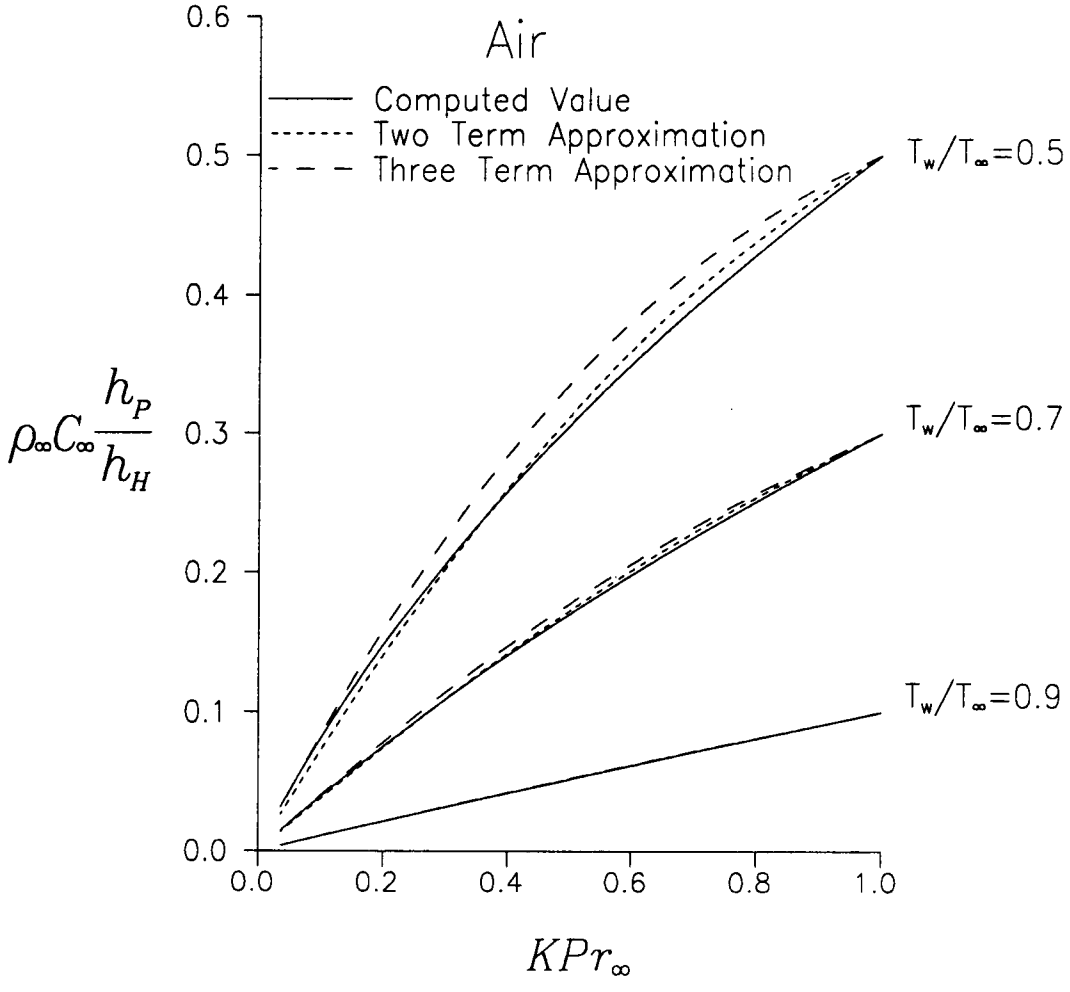


**Figure 6-5. Approximate Dimensionless Ratio of Transfer Coefficients for Air.**

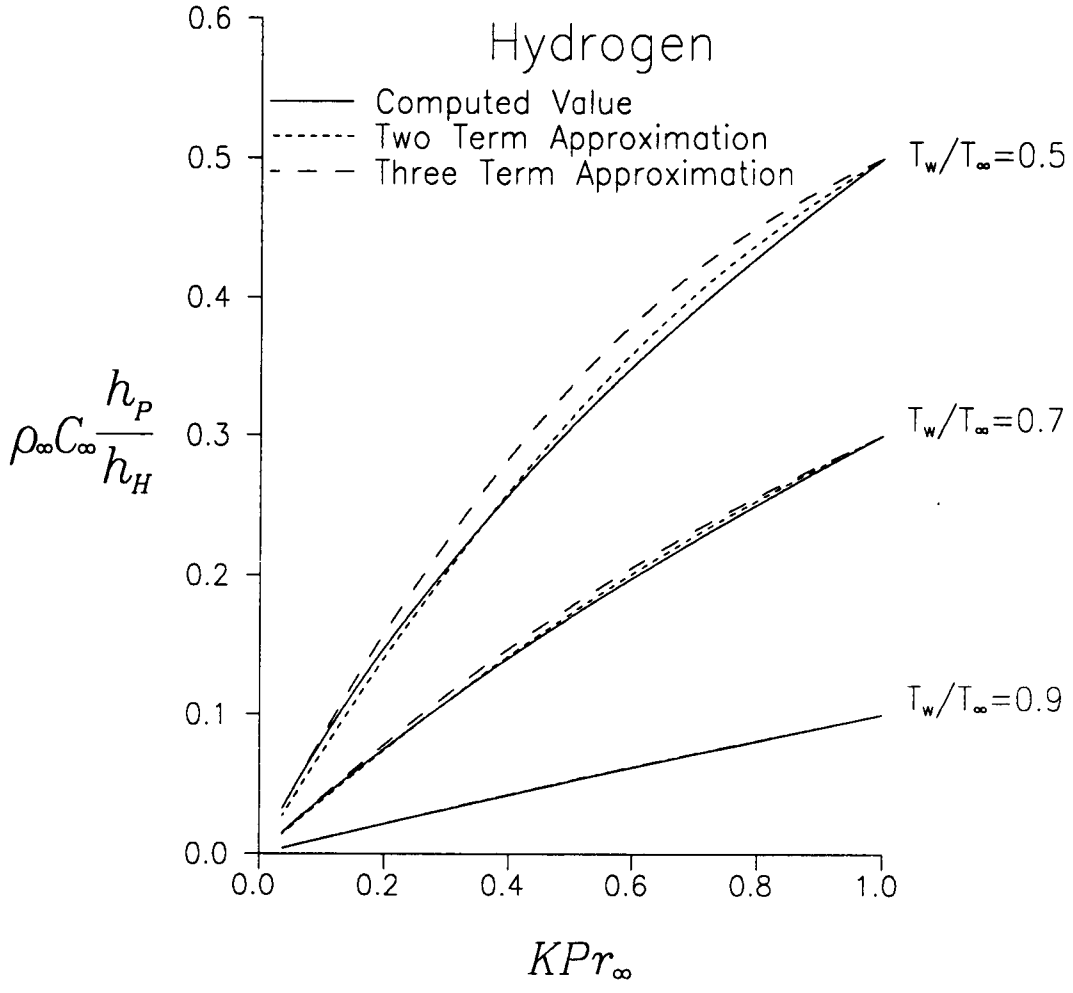


Figure 6-6. Approximate Dimensionless Ratio of Transfer Coefficients for Hydrogen.

Inspection of Figures 6-4, 6-5, and 6-6 shows that equation (6-1) yields the better approximation of the computed dimensionless ratio of transfer coefficients over the range of values of $KPr_\infty$ from 1.0 to 0.15 for all values of the wall temperature ratio, $T_w/T_\infty$. The maximum error of equation (6-1) in this range is on the order of 5% for $T_w/T_\infty = 0.5$ and is less than 1% for $T_w/T_\infty = 0.9$. Equation (6-2), however, yields a better approximation of the dimensionless ratio of transfer coefficients over the range of values of $KPr_\infty$ from 0.15 to 0.04 for all wall temperature ratios. The maximum error computed in this narrow range of $KPr_\infty$ is less than 5% for $T_w/T_\infty = 0.5$. These approximate results are consistent with the value for the term $\omega$, which was computed using equation (4-93) and is presented in Table 6-7.

Batchelor and Shen (1985) present an approximate relationship for the dimensionless particle concentration of a forced convection flow having a constant temperature and a uniform particle concentration far from the wall that is not expressly derived from the truncated binomial expansion given by (4-94). In deriving the dimensionless ratio of transfer coefficients given by equation (4-60) in Section 4.7.3.1, a convective heat transfer coefficient was defined, which is applicable in either forced or natural convection flow. Substitution of the approximate relationship developed by Batchelor and Shen for the effective dimensionless particle concentration at the wall in forced convection flow into equation (4-60) results in an equation for the dimensionless ratio of transfer coefficients that has the exact form of equation (6-1). Apparently, equation (6-1) may be applicable for forced as well as natural convection flows. The simplicity and reasonable accuracy of equation (6-1) over a fairly wide range of values of $KPr_\infty$ is noteworthy.

### 6.3. Stratified Fluid Temperature Far from the Wall

As shown by Sparrow et al. (1963) and described in Section 2.3, the ambient fluid temperature far from the wall cannot be stably stratified beyond a certain value of the volumetric heat source strength. For the steam conditions and geometry of interest in the present research, this value is of the order of 1 $nW/m^3$. This value is exceeded by the higher values of volumetric heat source strength expected in the upper plenum of a

BWR. However, situations where low heat source strengths per particle or low volumetric particle concentrations exist in the upper plenum of a BWR are also possible. These low heat source strengths will result in a stratified temperature distribution in the ambient fluid that is quadratic with respect to streamwise distance from the leading edge of the plate. The particle deposition on the wall due to thermophoresis from such a quadratically-stratified ambient fluid temperature is investigated below.

For a quiescent fluid with a vertical temperature difference between the leading edge and the trailing edge of the plate equal to the horizontal temperature difference between the leading edge of the plate and the fluid at the same elevation as the leading edge and far away from the wall, the vertical temperature distribution in the fluid is given by

$$\frac{T_{\infty,L} - T_{\infty}(x)}{T_w - T_{\infty,0}} = \frac{Da}{2}(\xi^2 - 1). \qquad (6-3)$$

The Damköhler number, $Da$, is equal to -2 when the fluid temperature at $L$ is equal to the wall temperature. From stability considerations alone, a fluid temperature at $L$ lower than the wall temperature is physically possible, but would be of no interest for this investigation of thermophoretic deposition, since a wall hotter than the fluid would repel particles (Talbot et al., 1980).

The Damköhler number is negative for cooled walls (wall temperature less than that of the fluid). The negative sign results from the nondimensionalization of the fluid temperature, as shown in equation (4-35), by the temperature difference between the wall and the fluid far from the wall. This temperature difference is negative for cooled walls and therefore the negative sign is simply a bookkeeping convention. A negative value of the Damköhler number for a cooled wall represents a volumetric heat source (i.e., heat addition) in the fluid.

As in the case of a constant-temperature fluid far from the wall, the heat source term of the conservation of energy equation inside the boundary layer is neglected for the quadratic temperature stratification given by equation (6-3). A wall temperature ratio of 0.9 (i.e., $\lambda$ = - 0.1) is chosen so that the Gray and Giorgini (1976) criterion for the

applicability of the Boussinesq approximation is satisfied. The purpose of this section is to focus on the effects of a thermally-stratified ambient fluid on thermophoretic deposition of particles and not on effects due to variable properties. For a fluid having a Prandtl number of 1.0, which is representative of steam at 400°C and 6.9 MPa, the following results are presented in Table 6-8: the ratio $Nu/Ra^{1/4}$, the dimensionless ratio of transfer coefficients given by equation (4-60), and the effective dimensionless wall particle concentration. The dimensionless particle concentration as a function of the pseudosimilarity variable, $\eta$, is presented in Figure 6-7 for the listed values of the streamwise coordinate, $\xi$.

For values of the normalized streamwise distance, $\xi$, greater than 0.6, the Lentini-Pereyra numerical scheme with the second-level of truncation model of the method of local nonsimilarity showed great difficulty in obtaining a converged solution of the dimensionless particle concentration differential equation. Since Chen and Eichhorn (1976) computed and experimentally observed stratified boundary layer flows detraining, or ejecting fluid, the velocity normal to the wall was examined, particularly at higher values of the streamwise coordinate, $\xi$. The computed effective particle wall concentration shown in Figure 6-7 merits further investigation, because it is noticeably decreasing for the higher values of $\xi$ and the computed particle concentration is greater than one for $\xi = 0.6$ at $\eta \approx 3$.

The fluid velocity normal to the wall is obtained by the substitution of the defining values for the pseudosimilarity variable, equation (4-33), and the dimensionless streamfunction, equation (4-34), into equation (4-31). The fluid velocity normal to the wall, the thermophoretic velocity, $V_T$, of equation (4-7), and the total velocity for a particle (the sum of these two transverse velocities) for the case of a quadratic temperature stratification are shown in Figure 6-8. Negative values of the ordinate denote flow directed towards the wall, as shown in Figure 2-2. (The negative, nonzero value of the particle velocity at the wall is actually at the edge of the Brownian layer, which is negligibly thin. The particle velocity at the wall must, of course, be zero.)

Table 6-8. Quadratic Stratification Results.

| $\xi$ | $\frac{Nu}{Ra^{1/4}}$ | $\rho_\infty C_\infty \frac{h_P}{h_H}$ | $n_w$ |
|---|---|---|---|
| 0.0 | 0.4011 | 0.1000 | 0.9000 |
| 0.1 | 0.3915 | 0.0997 | 0.8972 |
| 0.2 | 0.3868 | 0.0987 | 0.8897 |
| 0.3 | 0.3831 | 0.0972 | 0.8752 |
| 0.4 | 0.3746 | 0.0940 | 0.8458 |
| 0.5 | 0.3565 | 0.0858 | 0.7719 |
| 0.6 | 0.3263 | 0.0427 | 0.3847 |

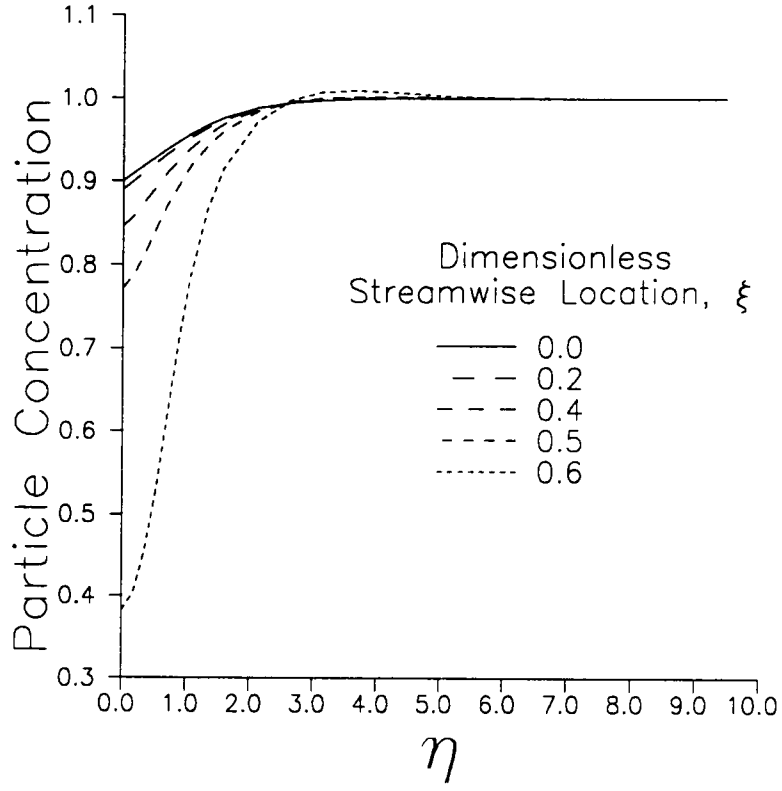


Figure 6-7. Particle Concentration Profile for Quadratic Stratification of the Ambient Fluid.

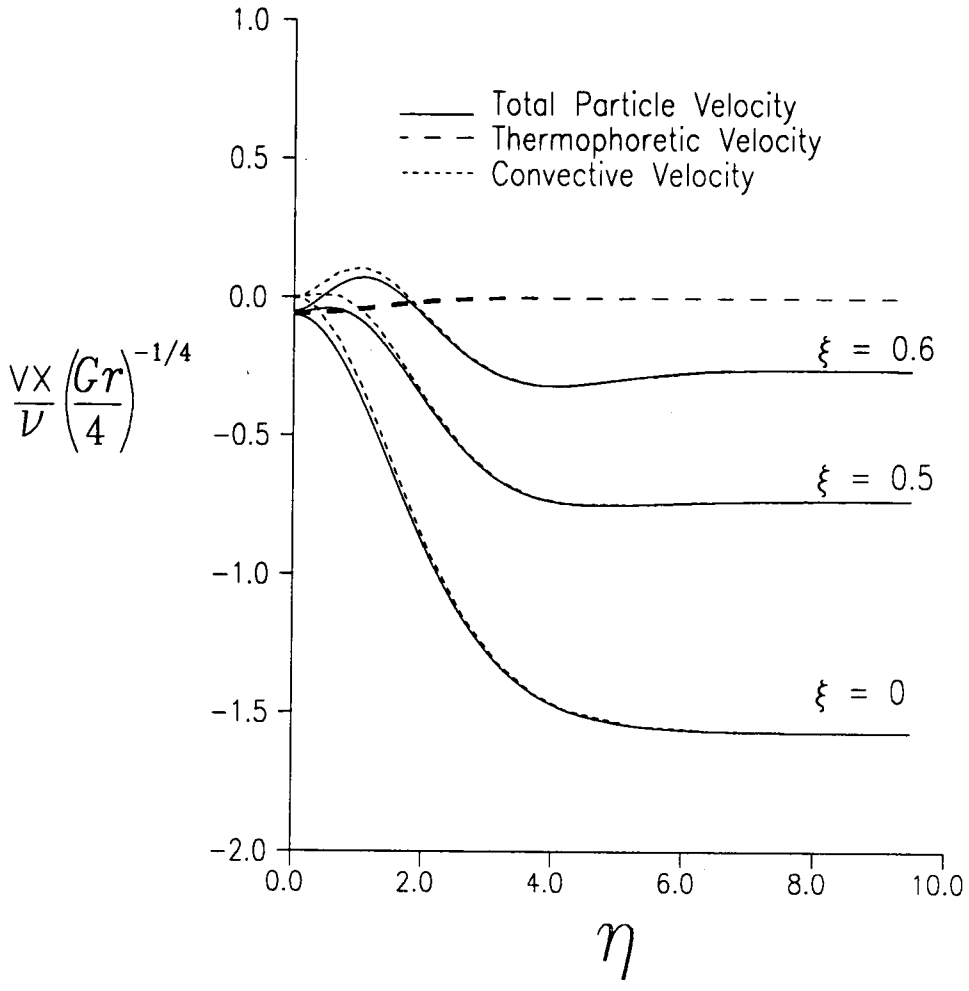


Figure 6-8. Transverse Velocities for Quadratic Stratification of the Ambient Fluid.

The normal velocities plotted in Figure 6-8 show that the convective motion of the fluid is *away from the wall* for values of $\eta$ less than $\approx 1$ at $\xi = 0.6$. The total transverse particle velocity is still towards the wall very near the wall at $\eta$ less than $\approx 0.5$, which indicates that some particles are being deposited on the wall by thermophoresis . At a value of $\eta$ slightly greater than 0.5, the total transverse particle velocity is zero, which indicates that the outward flow of the fluid due to the stratified temperature boundary condition in the ambient fluid is opposing the thermophoretic velocity and impeding any additional particles from depositing on the wall. Thus, at that streamwise station and for higher values of the streamwise distance, $\xi$, particles are swept downstream and are not deposited on the wall by thermophoresis.

The particle concentration greater than unity at the streamwise station $\xi = 0.6$ at a value of $\eta \approx 3$, which is shown in Figure 6-7, is due to a temperature lag in the boundary layer, which is characteristic of thermally stratified flows. This lag, or inversion, causes the thermophoretic movement of particles *away from the wall* and, thus, increases the particle concentration at an intermediate point in the boundary layer above the concentration far from the wall. These temperature inversions are shown in Figure 5-2 for an ambient fluid with a linearly-stratified temperature. Such inversions have been experimentally observed by Krane and Jessee (1983) in the laminar natural convection boundary layers on the heated and cooled vertical walls of a square enclosure, which has a linearly-stratified temperature core region.

As previously described, the Lentini-Pereyra method with the second-level of truncation had encountered numerical difficulties when attempting to compute concentration profiles for values of $\xi > 0.6$. To investigate the cause of these numerical difficulties at these relatively high values of $\xi$, the particle concentration equation (4-46) was rewritten neglecting Brownian diffusion and assuming constant thermophysical properties as follows:

$$\left[K\left(\frac{\lambda\theta'}{1+\lambda\theta}\right)+3f+4\xi f_{\xi}\right]n'+K\frac{\partial}{\partial\eta}\left(\frac{\lambda\theta'}{1+\lambda\theta}\right)n \;=\; 4\xi f' n_{\xi}\,. \qquad (6-4)$$

With the coefficients of the particle concentration gradient, $n'$, and the particle concentration, $n$, now specifically identified in equation (6-4), only the temperature and velocity profiles inside the boundary layer were computed for values of the streamwise coordinate greater than 0.6. The axial velocity and temperature profiles were similar to those presented in Section 5.2.3 in that temperature and velocity inversions in the boundary layer were computed. However, when the values for the dimensionless streamfunction, dimensionless temperature, and the partial derivative of the dimensionless streamfunction with respect to $\xi$ as functions of $\eta$ were substituted into the first term in brackets in the left-hand side of equation (6-4), a value of zero for the coefficient of the concentration gradient term occurred at $\eta \approx 0.5$, indicating a singularity in equation (6-4) for values of $\xi > 0.6$. The presence of this singularity is the apparent reason for the numerical difficulties encountered in solving the particle concentration equation for a quadratically-stratified ambient fluid temperature at values of $\xi > 0.6$.

One technique for solving the particle concentration equation at values of the streamwise parameter $\xi > 0.6$ would be to divide the solution domain at the singularity into the two computational domains of a near-wall region and a far-wall region. However, since the objective of the present research is to determine particle deposition on the wall from the fluid far from the wall, solving the particle concentration equation is unnecessary when this singular behavior arises in the differential equation. Physically, the particle concentration is zero somewhere in the boundary layer when this singularity occurs, and, therefore, deposition of particles on the wall from outside the boundary layer is impeded. Thus, at a point approximately halfway down the wall, particle deposition to the wall is inhibited by fluid detrainment from the boundary layer, which is due to the stratified temperature boundary condition far from the wall.

### 6.4. Participating Gas Thermal Radiation

Since one objective of this investigation is to investigate thermophoretic deposition of particles from steam at a high temperature and a high pressure, the effect of participating gas thermal radiation on particle deposition is investigated. Because the emission spectrum for steam, as well as many other gases, is transparent at some

wavelengths and not transparent at other wavelengths, use of the diffusion approximation will result in only an approximate value for particle deposition on the wall due to participating gas thermal radiation effects in steam. However, for the limited scope of this investigation, the simplifying Rosseland or diffusion assumption of Section 2.6 is used to approximate the participating gas radiation. Even though the diffusion approximation will not yield *accurate* results for the particle deposition, it will indicate the correct qualitative effects of the flow parameters on particle deposition.

The Lentini-Pereyra numerical method with the first-level of truncation model of the method of local nonsimilarity is used to compute the flow with a wall temperature ratio of 0.9, constant thermophysical properties, and constant fluid temperature far from the wall. Both laminar and turbulent flow conditions were investigated. As in the previous section, these conditions were chosen to focus attention solely on the effects of participating gas thermal radiation on particle deposition.

A range of values for the radiation parameter $M$ of equation (4-38) was chosen as representative (within the limitations of the Rosseland assumption) of the conditions under which the participating thermal radiation takes place in the steam. A thermophoretic coefficient $K$, assumed to be unaffected by the participating radiation heat transfer process, of 1.0 was used. For a temperature and pressure of 400°C and 6.9 MPa, steam has a Prandtl number of 1.0. The computed results, which are presented in Table 6-9 for laminar natural convection flows, include: the effective dimensionless wall particle concentration, $n_w$, the ratio $Nu/Ra^{1/4}$ that is representative of the heat transfer, and the dimensionless ratio of transfer coefficients as given by equation (4-60). The computed results, which are presented in Table 6-10 for a turbulent natural convection flow at a Rayleigh number of $3.0\times10^{12}$, include: the effective dimensionless wall particle concentration, $n_w$, the ratio $Nu/Ra^{1/3}$ that is representative of the heat transfer, and the dimensionless ratio of transfer coefficients as given by equation (4-60).

The total heat transfer at the wall has two components: convection and radiation. The total heat transfer and the convective component of the total heat transfer, which is given by $Nu/Ra^{1/3}$ for turbulent flows and $Nu/Ra^{1/4}$ for laminar flows, are presented in Tables 6-9 and 6-10. The dimensionless ratio of transfer coefficients, as derived in

Table 6-9. Particle Deposition and Heat Transfer Results for Laminar Flows with Participating Radiation.

| $M$ | $n_w$ | $\rho_\infty C_\infty \frac{h_P}{h_H}$ | $\frac{Nu_{convective}}{Ra^{1/4}}$ | $\frac{Nu_{total}}{Ra^{1/4}}$ |
|---|---|---|---|---|
| 100. | 0.9001 | 0.1000 | 0.3990 | 0.4029 |
| 1.0 | 0.9216 | 0.1024 | 0.3425 | 0.6399 |
| 0.1 | 0.9701 | 0.1078 | 0.1670 | 1.7899 |
| 0.01 | 0.9440 | 0.1104 | 0.0608 | 5.9746 |
| 0.001 | 0.9990 | 0.1110 | 0.0201 | 19.578 |

Table 6-10. Particle Deposition and Heat Transfer Results for a Turbulent Flow at a Rayleigh Number of $3.0\times10^{12}$ with Participating Radiation.

| $M$ | $n_w$ | $\rho_\infty C_\infty \frac{h_P}{h_H}$ | $\frac{Nu_{convective}}{Ra^{1/3}}$ | $\frac{Nu_{total}}{Ra^{1/3}}$ |
|---|---|---|---|---|
| 100. | 0.9005 | 0.1000 | 0.1230 | 0.1242 |
| 1.0 | 0.9348 | 0.1039 | 0.0894 | 0.1762 |
| 0.1 | 0.9853 | 0.1095 | 0.0319 | 0.3417 |
| 0.01 | 0.9985 | 0.1110 | 0.0071 | 0.6984 |
| 0.001 | 0.9998 | 0.1111 | 0.0019 | 1.8444 |

Section 4.7.3.1 and given by equation (4-60), is a dimensionless ratio of the particle transfer coefficient and the convective heat transfer coefficient. The dimensionless ratio of transfer coefficients depends only on the convective heat transfer and does not depend on the radiative portion of the heat transfer.

Inspection of Tables 6-9 and 6-10 shows that the effective dimensionless wall particle concentration is affected by the magnitude of the radiation as represented by the value of the parameter $M$. The exact solutions for the particle conservation equation for a $KPr_m$ of unity (as described in Section 4-8) are no longer applicable. The effective dimensionless wall particle concentration increases from 0.9 for the case of $M = 100$, which represents almost no participating thermal radiation, to almost unity for the case of $M = 0.001$, which represents a relatively large amount of thermal radiation. The dimensionless ratio of transfer coefficients increases by only 11% over this wide range of the parameter $M$. Negligible differences are computed between the effective wall particle concentration and the dimensionless ratio of transfer coefficients for laminar and turbulent flows. Similar observations were made in another computation in which a thermophoretic coefficient of $K = 0.5$ was used.

Further inspection of Tables 6-9 and 6-10 shows that the total heat transfer to the wall increases substantially as the level of the thermal radiation increases. However, the convective portion of the heat transfer decreases noticeably as the level of radiation participation increases. The convective heat transfer rates for laminar and turbulent flow are also presented in Figure 6-9. The decrease in convective heat transfer with an increasing level of radiation is striking.

Sparrow and Cess (1966) remark that for optically thick conditions, separation of the heat transfer at the wall into the convective and radiant components may prevent the correct computation of these components, although the total heat transfer is correctly computed. Kim and Viskanta (1984) used a more realistic band model of thermal radiation for steam at high temperature and pressure in a forced convection tube flow and concluded that the convective heat transfer may be greatly overpredicted for high pressure and high temperature steam at low velocities if the interaction between participating radiation and convection is neglected.

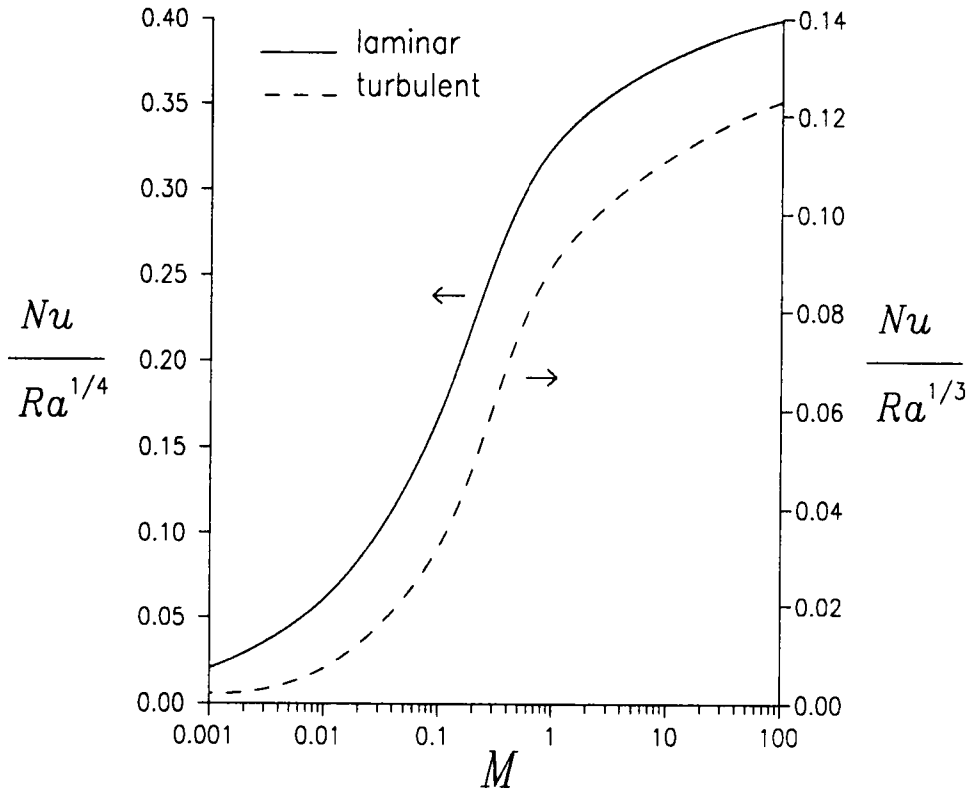


**Figure 6-9. Effect of Participating Radiation on Convective Heat Transfer.**

This substantial decrease in convective heat transfer would result in a correspondingly substantial decrease in the thermophoretic particle deposition on the wall as the level of radiation increases. Since participating gas thermal radiation is modeled as another mode of transferring heat by a diffusion process, the *effective* thermal conductivity increases as the level of radiation increases. This increased effective thermal conductivity results in a decreased effective Prandtl number and a decreased temperature gradient at the wall. For thermophoresis, the temperature gradient across a particle induces the thermal force that moves the particle in the direction opposite to the gradient. Thus, a decrease in the temperature gradient at the wall would result in a decrease in the thermophoretic particle deposition on the wall.

If, as assumed, the thermophoretic coefficient $K$ is not affected by the presence of participating gas thermal radiation, this would result in a decreased thermal force acting on the particle. This assumption must be considered as tentative and should be examined more closely in future investigations. The analysis for the thermal force given in Appendix C shows that the temperature gradient across the spherical particle, the interface conditions, and the thermal conductivities of the gas and particle are part of physical conditions that enter the derivation of the expression for the thermophoretic coefficient $K$. A derivation of an expression for $K$ in the presence of participating gas thermal radiation should specifically consider the temperature jump conditions at the interface between the particle and the surrounding fluid due to thermal radiation as well as the temperature jump conditions due to nonzero Knudsen number effects, and the effect (if any) of the increased effective thermal conductivity of the gas.

The temperature profiles both with and without participating gas thermal radiation effects for laminar and turbulent flows appear in Figure 6-10 for a radiation parameter of $M = 0.1$. Inspection of Figure 6-10 shows that the temperature gradient at the wall in the presence of participating gas thermal radiation is less than the temperature gradient at the wall without participating gas thermal radiation for laminar and turbulent flows. As should be expected, the temperature gradient for turbulent flow is greater than the temperature gradient for laminar flow for the corresponding cases with and without participating gas thermal radiation.

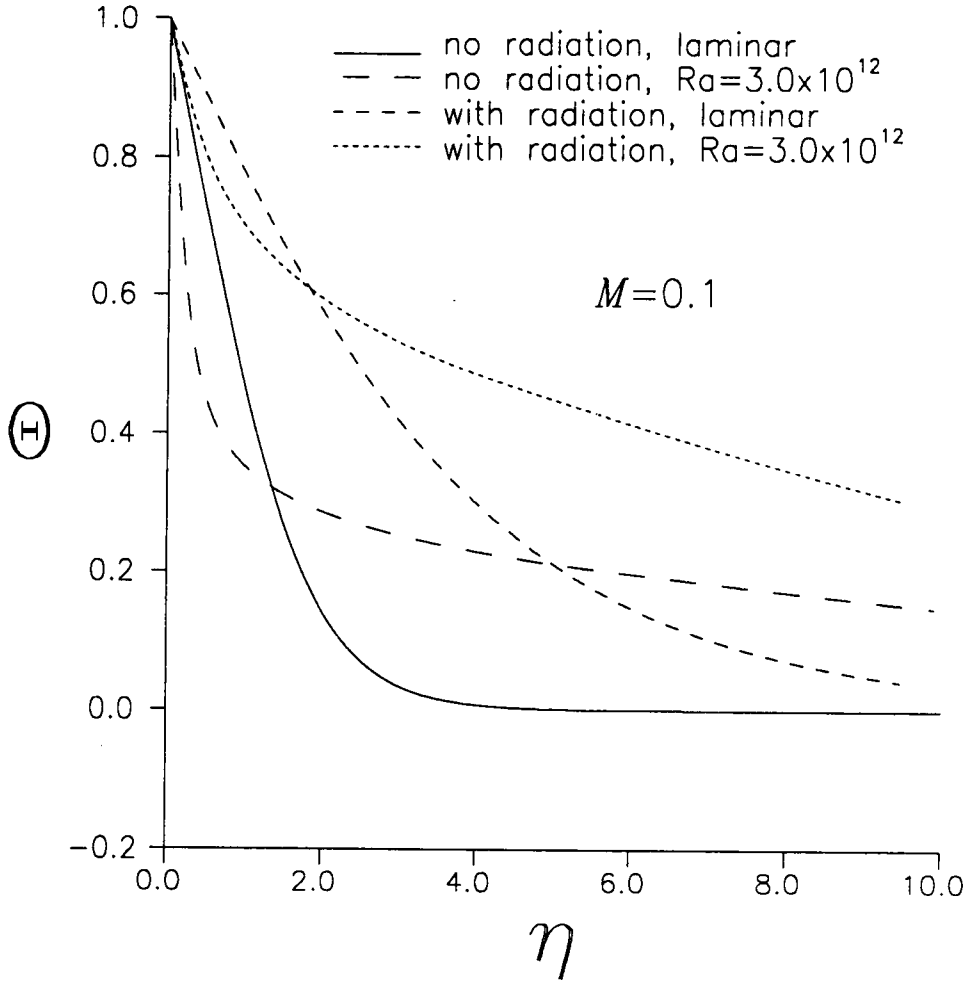


Figure 6-10. The Effect of Radiation on the Temperature Distribution.

Further inspection of Figure 6-10 shows that the thermal boundary layer thickness in laminar flow is increased when participating gas thermal radiation is included. This increased thermal boundary layer thickness in laminar flow is characteristic of low Prandtl number fluids.

Thus, for both laminar and turbulent natural convection flows, the effect of participating gas thermal radiation is to decrease the temperature gradient near the wall which results in a decrease of the thermophoretic deposition of particles on the wall, even though the dimensionless ratio of transfer coefficients presented in Tables 6-9 and 6-10 shows a slight increase as the level of radiation increases.

# CHAPTER 7

# CONCLUSIONS

Consideration of the results obtained in the present research suggests the following conclusions:

1. The presence of a volumetric heat source in a particle has a negligible effect on the thermophoretic transport of the particle. The temperature and flow distributions in the natural convection boundary layer on a cooled surface are not affected and the physics of thermophoresis are also not affected by the presence of volumetric heat sources with strengths expected in the Boiling Water Reactor subsequent to a severe accident.

2. The approximate dimensionless ratio of transfer coefficients, presented in Section 6.2, predicts thermophoretic particle deposition rates from a dilute suspension of single-sized particles for the three gases of steam, air, and hydrogen at a constant ambient temperature with acceptable accuracy. This approximate dimensionless ratio of transfer coefficients does not require the solution of the particle conservation equation and is independent of flow regime. Variable thermophysical properties, which are considered in the dimensionless ratio of transfer coefficients, result in increased particle deposition rates.

3. Particle deposition on the wall with a quadratically stratified ambient temperature is impeded on the lower half of the wall due to convective *outflow* from the boundary layer. Use of the dimensionless ratio of transfer coefficients with an average wall heat transfer coefficient in a fluid with a stratified ambient temperature distribution overpredicts the thermophoretic deposition rate.

4. Thermophoretic deposition of particles from gases that participate in the thermal radiation heat transfer process is less than that in gases that are transparent to thermal radiation. Use of the dimensionless ratio of transfer coefficients with a convective heat transfer coefficient in the presence of participating gas thermal radiation overpredicts the thermophoretic deposition rate.

# CHAPTER 8

## RECOMMENDATIONS FOR FURTHER RESEARCH

Consideration of the results obtained in the present research suggests that the following topics should be investigated:

1. Thermophoretic transport of particles should be investigated in an enclosed cavity, where the flow is driven by either internal heat sources in the fluid with cooled walls or by differing wall temperatures. A vertically stratified temperature distribution occurs in the central core of the cavity for these conditions. Stratified temperature conditions far from an isothermal wall are shown in Section 6.2 to block the thermophoretic transport of particles to the wall. Particle deposition on the walls of an enclosed cavity may be inhibited due to temperature stratification in the core region.

2. Thermal radiation effects on thermophoresis should be investigated in non-gray participating gases. The thermophoretic deposition of particles on a cooled wall is shown in Section 6.3 to decrease in the presence of an optically-thick participating gas. Thermophoretic deposition of aerosol particles may also decrease in media with spectral emission and absorption, such as steam, but perhaps not as much as that for optically-thick conditions. This decrease in thermophoretic deposition should be quantified for gases such as steam. In addition, participating gas thermal radiation effects on the thermophoretic force in the immediate vicinity of the particle and in the vicinity of the wall, similar to the analysis presented in Appendix C for the effect of volumetric heat sources on the thermal force, should also be investigated.

# LIST OF REFERENCES

## LIST OF REFERENCES

Abu-Romia, M. M., and Tien, C. L., 1967, "Appropriate Mean Absorption Coefficients for Infrared Radiation of Gases," *J. Heat Trans.*, Vol. 89, pp. 321-327.

Anderson, D. A., Tannehill, J. C., and Pletcher, R. H., 1984, *Computational Fluid Mechanics and Heat Transfer*, Hemisphere Publishing Corp., New York, p. 199.

Arpaci, V. S., 1966, *Conduction Heat Transfer*, Addison-Wesley, Reading, Massachusetts, Chapter 4.

Arpaci, V. S., 1968, "Effect of Thermal Radiation on the Laminar Free Convection From a Heated Vertical Plate," *Int. J. Heat Mass Trans.*, Vol. 11, pp. 871-881.

Arpaci, V. S., 1986, "Microscales of Turbulence and Heat Transfer Correlations," *Int. J. Heat Mass Trans.*, Vol. 29, pp. 1071-1078.

Arpaci, V. S., and Larsen, P. S., 1984, *Convection Heat Transfer*, Prentice-Hall, Englewood Cliffs, New Jersey, Chapters 2 and 12.

Ascher, U., and Russel, R. D., 1981, "Reformulation of Boundary Value Problems into 'Standard' Form," *SIAM Review*, Vol. 23, pp. 238-254.

Audunson, T., and Gebhart, B., 1972, "An Experimental and Analytical Study of Natural Convection with Appreciable Thermal Radiation Effects," *J. Fluid Mech.*, Vol. 52, pp. 57-95.

Aziz, A., and Na., T. Y., 1984, *Perturbation Methods in Heat Transfer*, Hemisphere Publishing, Washington, DC, Chapter 5, section 5.

Bakanov, S. P., and Roldughin, 1979, "On Two Methods in Large Aerosol Particle Thermophoresis Theory," *J. Coll. Int. Sci.*, Vol. 72, pp. 428-441.

Baker, A. J., 1983, *Finite Element Computational Fluid Mechanics*, Hemisphere Publishing Corp., New York.

Basset, A. B., 1888, *A Treatise On Hydrodynamics*, Vol. 2, Deighton, Bell & Co., Cambridge, p. 270; reprinted by Dover Publications, New York, 1961.

Batchelor, G. K., 1967, *An Introduction To Fluid Dynamics*, Cambridge University Press, London, Chapter 3.

Batchelor, G. K., 1974, "Transport Properties of Two-Phase Materials with Random Structure," *Annual Review Of Fluid Mechanics*, M. Van Dyke et al., ed., Annual Reviews, Inc., Palo Alto, California, Vol. 6, pp. 227-255.

Batchelor, G. K., and Shen, C., 1985, "Thermophoretic Deposition of Particles in Gas Flowing over Cold Surfaces," *J. Coll. Int. Sci.*, Vol. 107, pp. 21-37.

Bayley, F. J., 1955, "An Analysis of Turbulent Free Convection Heat Transfer," *Proc. Inst. Mech. Engrs.*, Vol. 169, pp. 361-370.

Bejan, A., 1984, *Convection Heat Transfer*, John Wiley and Sons, New York, Chapters 4 and 10.

Bergholtz, R. F., 1980, "Natural Convection of a Heat Generating Fluid in a Closed Cavity," *J. Heat Trans.*, Vol. 102, pp. 242-247.

Bird, R. B., Stewart, W. E., and Lightfoot, E. W., 1960, *Transport Phenomena*, John Wiley, New York, Chapter 18.

Boothroyd, R. G., 1971, *Flowing Gas-Solids Suspensions*, Chapman and Hall, London, Sections 2.7.5 and 10.4.

Boussinesq, J., 1877, "Théorie de l'écoulement Tourbillant," *Mem. Pres. Acad. Sci.*, Paris, Vol. 23, p. 46.

Bradshaw, P., 1978, "Introduction," *Turbulence, Topics In Applied Physics*, P. Bradshaw, ed., Springer-Verlag, New York, Vol. 12, p. 25.

Brenner, H., 1961, "The Slow Motion of a Sphere Through a Viscous Fluid Towards a Plane Surface," *Chem. Engr. Sci.*, Vol. 16, pp. 242-251.

Brock, J. R., 1962, "On the Theory of Thermal Forces Acting on Aerosol Particles," *J. Coll. Sci.*, Vol. 17, pp. 768-780.

Burden, R. L., Faires, J. D., and Reynolds, A. C., 1981, *Numerical Analysis, Second Edition*, Prindle, Weber, and Schmidt, Boston, Massachusetts, Chapter 10.

Byers, R. L., and Calvert, S., 1969, "Particle Deposition from Turbulent Streams by Means of Thermal Force," *I. E. C. Fundamentals*, Vol. 8, pp. 646-655.

Cairnie, L. R., and Harrison, A. J., 1982, "Natural Convection Adjacent to a Vertical Hot Plate with a High Surface-to-Ambient Temperature Difference," *Int. J. Heat Mass Trans.*, Vol. 25, pp. 925-934.

Cairnie, L. R., Harrison, A. J., and Morgan, P. A., 1981, "Autoignition in a Free Convection Boundary Layer," *Eighteenth Symposium (International) On Combustion*, The Combustion Institute, Pittsburgh, Pennsylvania, pp. 1799-1806.

Catchpole, J. P., and Fulford, G., 1986, "Dimensionless Groups," *CRC Handbook of Chemistry and Physics*, R. C. Weast, ed., CRC Press, Boca Raton, Florida, pp. F307-F324.

Cebeci, T., and Khattab, A., 1975, "Prediction of Turbulent Free Convective Heat Transfer From a Vertical Flat Plate," *J. Heat Trans.*, Vol. 97 pp. 469-471.

Cebeci, T. and Smith, A. M. O., 1974, *Analysis Of Turbulent Boundary Layers*, Academic Press, New York.

Cess, R. D., 1966, "The Interaction of Thermal Radiation with Free Convection Heat Transfer," *Int. J. Heat Mass Trans.*, Vol. 9, pp. 1269-1277.

Cheesewright, R., 1968,"Turbulent Natural Convection From a Vertical Plane Surface," *J. Heat Trans.*, Vol. 90, pp. 1-8.

Cheesewright, R., and Ierokiopitis, E., 1982, "Velocity Measurements in a Turbulent Natural Convection Boundary Layer," *Proceedings, Seventh International Heat Transfer Conference*, U. Grigull et al., ed., Hemisphere Publishing Corp., Washington, DC, Vol. 2, pp. 305-309.

Chen, C. C., and Eichhorn, R., 1976, "Natural Convection From a Vertical Surface to a Thermally Stratified Fluid," *J. Heat Trans.*, Vol. 98, pp. 446-451.

Cheng, E. H., and Özisik, M. N., 1972, "Radiation with Free Convection in an Absorbing, Emitting, and Scattering Medium," *Int. J. Heat Mass Trans.*, Vol. 15, pp. 1243-1252.

Chu, B-T, 1955, "Pressure Waves Generated By Addition of Heat in a Gaseous Medium," NACA TN 3411, National Advisory Committee for Aeronautics, Washington, DC.

Churchill, S. W., and Chu, H. H. S, 1975, "Correlating Equations for Laminar and Turbulent Free Convection from a Vertical Plate," *Int. J. Heat Mass Trans.*, Vol. 18, pp. 1323-1329.

Churchill, S. W., and Usagi, R., 1972, "A General Expression for the Correlation of Rates of Transfer and Other Phenomena," *AIChE J.*, Vol. 18, pp. 1121-1128.

Clausing, A. M., 1983, "Natural Convection Correlations for Vertical Surfaces Including Influences of Variable Properties," *J. Heat Trans.*, Vol. 105, pp. 138-143.

Coxson, M., and Parks, E. C., 1971, "Comment on "Local Nonsimilarity Boundary-Layer Solutions"," *AIAA J.*, Vol. 9, p. 1664.

Davies, C. N., 1966, "Deposition from Moving Aerosols," *Aerosol Science*, C. N. Davies, ed., Academic Press, London, pp. 393-446.

de Boer, P. C. T., 1984, "Thermally Driven Motion of Strongly Heated Fluids," *Int. J. Heat Mass Transfer*, Vol. 27, pp. 2239-2251.

de Vahl Davis, G., 1968, "Laminar Natural Convection in an Enclosed Rectangular Cavity," *Int. J. Heat Mass Trans.*, Vol. 11, pp. 1675-1693.

Deissler, R. G., 1964, "Diffusion Approximation for Thermal Radiation in Gases With Jump Boundary Condition," *J. Heat Trans.*, Vol. 86, pp. 240-246.

Depew, C. A., and Kramer, T. J., 1973, "Heat Transfer to Flowing Gas-Solid Mixtures," *Advances in Heat Transfer*, T. F. Irvine and J. P. Hartnett, ed., Vol. 9, Academic Press, Inc., New York, pp. 113-180.

Derjaguin, B. V., and Yalamov, Yu., 1965, "Theory of Thermophoresis of Large Aerosol Particles," *J. Coll. Sci.*, Vol. 20, pp. 555-570.

Derjaguin, B. V., and Yalamov, Yu., 1966, "Note," *J. Coll. Sci.*, Vol. 22, p. 195.

Derjaguin, B. V., Storozhilova, A. I., and Rabinovich, Ya. I., 1966, "Experimental Verification of the Theory of Thermophoresis of Aerosol Particles," *J. Coll. Int. Sci.*, Vol. 21, pp. 35-58.

Dresner, L., 1983, *Similarity Solutions of Nonlinear Partial Differential Equations, Research Notes in Mathematics 88*, Pitman Publishing, Marshfield, Massachusetts, Chapter 5.

Dutta, A., and Mashelkar, R. A., 1987, "Thermal Conductivity of Structured Fluids," *Advances in Heat Transfer*, T. F. Irvine and J. P. Hartnett, ed., Vol. 18, Academic Press, Inc., New York, pp. 161-239.

Dwyer, H. A., 1967, "Thirteen-Moment Theory of the Thermal Force on a Spherical Particle," *Phys. Fluids*, Vol. 10, pp. 976-984.

Eckert, E. R. G., and Soehnigen, E. E., 1948, *Studies on Heat Transfer in Laminar Free Convection with the Zender-Mach Interferometer*, Tech. Rep. No. 5747. A.T.I. No. 44580, Air Material Command (Dayton, Ohio).

Ede, A. J., 1967, "Advances in Free Convection," *Advances in Heat Transfer*, T. F. Irvine and J. P. Hartnett, ed., Vol. 4, Academic Press, Inc., New York, pp. 1-64.

Eichhorn, R., 1969, "Natural Convection in a Thermally Stratified Fluid," *Progress in Heat and Mass Transfer*, T. F. Irvine et al., ed., Pergamon Press, Vol. 2, pp. 41-53.

El-Wakil, M. M., 1962, *Nuclear Power Engineering*, McGraw-Hill, New York, pp. 222-223.

Elder, J. W., 1965, "Laminar Free Convection in a Vertical Slot," *J. Fluid Mechanics*, Vol. 23, pp. 77-98.

England, W. G., and Emery, A. F., 1969, "Thermal Radiation Effects on the Laminar Free Convection Boundary Layer of an Absorbing Gas," *J. Heat Trans.*, Vol. 91, pp. 37-44.

Epstein, M., Hauser, G. M., and Henry, R. E., 1985, "Thermophoretic Deposition of Particles in Natural Convection Flow From a Vertical Flat Plate," *J. Heat Trans.*, Vol. 107, pp. 272-276.

Epstein, P. S., 1929, "Zur Theorie des Radiometers," *Z. Phys.*, Vol. 54, pp. 537-563.

Etherington, H., 1958, *Nuclear Engineering Handbook*, McGraw-Hill, New York. Section 11, pp. 20-22.

Fairweather, G., and Vedha-Nayagam, M., 1987, "An Assessment of Numerical Software For Solving Two-Point Boundary-Value Problems Arising in Heat Transfer," *Numerical Heat Transfer*, Vol. 11, pp. 281-293.

Forsythe, G. E., Malcolm, M. A., and Moler, C.B., 1977, *Computer Methods For Mathematical Computations*, Prentice-Hall, Inc., Englewood Cliffs, New Jersey, pp. 129-147.

Fuchs, N. A., 1982, "Thermophoresis of Aerosol Particles at Small Knudsen Numbers: Theory and Experiment," *J. Aerosol Sci.*, Vol. 13, pp. 327-330.

Fujii, T., Takeuchi, M., and Morioka, I., 1974, "Laminar Boundary Layer of Free Convection in a Temperature Stratified Environment," *Proceedings of the Fifth International Heat Transfer Conference*, Tokyo, Vol. 3, pp. 44-48.

Galuska, M. J., Kim, K. H., and Choi, Y., 1986, "Laminar Natural Convection Heat Transfer to Non-Newtonian Fluids with Thermal Radiation Effects," *Proceedings of the Eighth International Heat Transfer Conference*, C. L. Tien et al., ed., Hemisphere Publishing Corp., Washington, DC, Vol. 2, pp. 779-783.

Gebhart, B., Jaluria, Y., Mahajan, R. L., and Sammakia, B., 1988, *Buoyancy-Induced Flows and Transport*, Hemisphere Publishing, Washington, DC.

George, W. K. Jr., and Capp, S. P., 1979, "A Theory for Natural Convection Turbulent Boundary Layers Next to Heated Vertical Surfaces," *Int. J. Heat Mass Trans.*, Vol. 22, pp. 813-826.

Gökoglu, S. A., 1987, "Discussion of Mills et al. on "The Effect of Wall Suction and Thermophoresis on Aerosol Deposition from a Laminar Boundary Layer on a Flat Plate"," *Int. J. Heat Mass Trans.*, Vol. 30, pp. 1559-1561.

Gökoglu, S. A., and Rosner, D. E., 1986, "Thermophoretically Augmented Mass Transfer Rates to Solid Walls Across Laminar Boundary Layers," *AIAA J.*, Vol. 24, pp. 172-179.

Goldhirsch, I., and Ronis, D., 1983a, "Theory of Thermophoresis. I. General Considerations and Mode-Coupling Analysis," *Phys. Rev. A*, Vol. 27, pp. 1616-1634.

Goldhirsch, I., and Ronis, D., 1983b, "Theory of Thermophoresis. II. Low Density Behavior," *Phys. Rev. A*, Vol. 27, pp. 1635-1656.

Goren, S. L., 1977, "Thermophoresis of Aerosol Particles in the Laminar Boundary Layer on a Flat Plate," *J. Coll. Int. Sci.*, Vol. 61, pp. 77-85.

Gray, D. G., and Giorgini, A., 1976, "The Validity of the Boussinesq Approximation for Liquids and Gases," *Int. J. Heat Mass Trans.*, Vol. 19, pp. 545-551.

Greene, G. A., 1982, *Experimental and Analytical Study of Natural Convection Heat Transfer of Internally Heated Liquids*, BNL-NUREG-51585, Brookhaven National Laboratory, Upton, New York.

Guceri, S. I., and Farouk, B., 1985, "Numerical Studies in Laminar and Turbulent Natural Convection," *Natural Convection: Fundamentals And Applications*, S. Kakaç et al., ed., Hemisphere Publishing Corp., Washington, DC, pp. 615-654.

Hales, J. M., Schwendiman, L. C., and Horst, T. W., 1972, "Aerosol Transport in a Naturally-Convected Boundary Layer," *Int. J. Heat Mass Trans.*, Vol. 15, pp. 1837-1850.

Hansen, A. G., 1964, *Similarity Analyses of Boundary Value Problems in Engineering*, Prentice-Hall, Englewood Cliffs, New Jersey, pp. 21-29.

Hidy, G. M., 1984, *Aerosols: An Industrial and Environmental Science*, Academic Press, Orlando, Florida, Chapter 2.

Hidy, G. M., and Brock, J. R., 1970, *The Dynamics Of Aerocolloidal Systems*, Pergamon Press, New York, Chapters 4 and 6.

Hindmarsh, A. C., 1977, *Solution of Block-Tridiagonal Systems of Linear Algebraic Equations*, UCID-30150, Lawrence Livermore National Laboratory, Livermore, California.

Hodge, S. A., 1988, March 17, Personal Communication, Oak Ridge National Laboratory, Oak Ridge, Tennessee.

Hoogendoorn, C. J., and Euser, H., 1978, "Velocity Profiles in the Turbulent Free Convection Boundary Layer," *Proceedings, Sixth International Heat Transfer Conference*, Hemisphere Publishing Corp., Washington, DC, Vol. 2, pp. 193-197.

Humphrey, J. A. C., Sherman, F. S., and To, W. M., 1985, *Numerical Simulation of Buoyant Turbulent Flow*, SAND-85-8180, Sandia National Laboratory, Livermore, California.

*IMSL Library, Edition 9*, 1982, IMSL, Inc., Houston, Texas.

Irvine, T. F., Jr., and Liley, P. E., 1984, *Steam and Gas Tables with Computer Equations*, Academic Press, Orlando, Florida, pp. 113-114, 146-147.

Ivchenko, I. N., and Yalamov, Yu. I., 1971, "A Hydrodynamic Method for the Calculation of the Rate of Thermophoresis of Moderately Large Involatile Aerosol Particles," *Russ. J. Phys. Chem.*, Vol. 45, pp. 317-322.

Jacobson, S., and Brock, J. R., 1965, "The Thermal Force on Spherical Sodium Chloride Aerosols," *J. Coll. Sci.*, Vol. 20, pp. 544-554.

Jaluria, Y, 1980, *Natural Convection Heat And Mass Transfer*, Pergamon Press, Elmsford, New York.

Jaluria, Y., 1985, "Convective Flow in a Stably Stratified Environment," *Natural Convection: Fundamentals and Applications*, S. Kakaç et al., ed., Hemisphere Publishing Corp., Washington, DC, pp. 413-442.

Jaluria, Y., and Torrance, K. E., 1986, *Computational Heat Transfer*, Hemisphere Publishing Corp., New York.

Jones, D. R., 1974, "Convective Effects in Enclosed, Exothermically Reacting Gases," *Int. J. Heat Mass Trans.*, Vol. 17, pp. 11-21.

Jones, W. P., and Launder, B. E., 1972, "The Prediction of Laminarization With a Two Equation Model of Turbulence," *Int. J. Heat Mass Trans.*, Vol. 15, pp. 301-314.

Kakaç, S., Atesoglu, O. E., and Yener, Y., 1985, "The Effects of the Temperature-Dependent Fluid Properties on Natural Convection - Summary and Review," *Natural Convection: Fundamentals and Applications*, S. Kakaç et al., ed., Hemisphere Publishing Corp., Washington, DC, pp. 729-773.

Kanki, T., Iuchi, S., Miyazaki, T., and Ueda, H., 1985, "On Thermophoresis of Relatively Large Aerosol Particles Suspended Near a Plate," *J. Coll. Int. Sci.*, Vol. 107, pp. 418-428.

Kato, H., Nishiwaki, M., and Hirata, M., 1968, "On the Turbulent Heat Transfer by Free Convection from a Vertical Plate," *Int. J. Heat Mass Trans.*, Vol. 11, pp. 117-125.

Kays, W. M., and Crawford, M. E., 1980, *Convective Heat and Mass Transfer, Second Edition*, McGraw-Hill, New York.

Kee, R. J., Landram, C. S., and Miles, J. C., 1976, "Natural Convection of a Heat Generating Fluid Within Closed Vertical Cylinders and Spheres," *J. Heat Trans.*, Vol. 98, pp. 55-61.

Keenan, J. H., Keyes, F. G., Hill, P. G., and Moore, J. G., 1969, *Steam Tables, Thermodynamic Properties Of Water Including Vapor, Liquid, And Solid Phases*, John Wiley, New York.

Keller, H. B., 1971, "A New Difference Scheme for Parabolic Problems," *Numerical Solution Of Partial Differential Equations*, B. Hubbard, ed., Academic Press, New York.

Keller, H. B., 1976, *Numerical Solution Of Two Point Boundary Value Problems*, Society for Industrial and Applied Mathematics, Philadelphia, Pennsylvania.

Keller, H. B., 1978, "Numerical Methods in Boundary Layer Theory," *Annual Review Of Fluid Mechanics*, M. Van Dyke et al., ed., Annual Reviews, Inc., Palo Alto, California, Vol. 10, pp. 417-433.

Keller, H. B., and Cebeci, T., 1972, "Accurate Numerical Methods for Boundary-Layer Flows. II: Two Dimensional Turbulent Flows," *AIAA J.*, Vol. 2, pp. 1193-1199.

Kennard, E. H., 1938, *Kinetic Theory Of Gases*, McGraw-Hill, New York, Chapter 8.

Kennedy, L. A., and Paszkowskyj, L. M., 1970, "Free Convection of an Absorbing-Emitting Gas From a Heated Vertical Plate," *ZAMP*, Vol. 21, pp. 901-909.

Kikuchi, Y., Shioyama, T., and Kawara, Z., 1986, "Turbulent Heat Transport in a Horizontal Fluid Layer Heated Internally and From Below," *Int. J. Heat Mass Trans.*, Vol. 29, pp. 451-461.

Kim, D. M., and Viskanta, R., 1984, "Interaction of Convection and Radiation Heat Transfer in High Pressure and Temperature Steam," *Int. J. Heat Mass Trans.*, Vol. 27, pp. 939-941.

Kousaka, Y., Okuyama, K., Nishio, S., and Yoshida, T., 1976, "Experimental Study of Thermophoresis of Aerosol Particles," *J. Chem. Eng. Japan*, Vol. 9, pp. 147-150.

Krane, R. J., and Jessee, J., 1983, "Some Detailed Field Measurements for a Natural Convection Flow in a Vertical Square Enclosure," *Proceedings, ASME/JSME Thermal Engineering Joint Conference*, Honolulu, Hawaii, Vol. 1, pp. 323-329.

Kreith, F., 1973, *Principles Of Heat Transfer, Third Edition*, Harper and Row, New York, p. 636.

Kreyszig, E., 1979, *Advanced Engineering Mathematics, Fourth Edition*, John Wiley and Sons, New York, pp. 554-557.

Kuiken, H. K., 1969, "Free Convection at Low Prandtl Numbers," *J. Fluid Mechanics*, Vol. 37, pp. 785-798.

Kulacki, F. A., and Richards, D. E., 1985, "Natural Convection in Plane Layers and Cavities with Volumetric Energy Sources," *Natural Convection: Fundamentals And Applications*, S. Kakaç et al., ed., Hemisphere Publishing Corp., Washington, DC, pp. 179-255.

Kutateladze, S. S., 1977, "The Model of Turbulent Free Convection Near a Vertical Heat Transfer Surface," *Heat Transfer And Turbulent Buoyant Convection*, D. B. Spalding and N. Afgan, ed., Hemisphere Publishing Corp., Washington, DC, Vol. 1, pp. 487-496.

Lamb, H., 1932, *Hydrodynamics, Sixth Edition*, Cambridge University Press, Cambridge, England; reprinted by Dover Publications, New York, 1945, pp. 602-604.

Launder, B. E., and Spalding, D. B., 1972, *Mathematical Models Of Turbulence*, Academic Press, London and New York.

Leal, L. G., 1977, "Macroscopic Transport Properties of a Sheared Suspension," *J. Coll. Int. Sci.*, Vol. 58, pp. 296-311.

LeFevre, E. J., 1956, "Laminar Free Convection from a Vertical Plane Surface," *Proc. 9th Intern. Congr. Appl. Mech.*, Brussels, Vol. 4, p. 168.

Lentini, M., and Pereyra, V., 1977, "An Adaptive Finite-Difference Solver for Nonlinear Two-Point Boundary-Value Problems with Mild Boundary Layers," *SIAM J. Numer. Anal.*, Vol. 14, pp. 91-111.

Lock, G. S. H., and Trotter, F. J. deB., 1968, "Observations on the Structure of a Turbulent Free Convection Boundary Layer," *Int. J. Heat Mass Trans.*, Vol. 11, pp. 1225-1234.

Loyalka, S. K., 1968, "Momentum and Temperature-Slip Coefficients with Arbitrary Accommodation at the Surface," *J. Chem. Phys.*, Vol. 48, pp. 5432-5436.

Loyalka, S. K., 1983, "Mechanics of Aerosols in Nuclear Reactor Safety: A Review," *Progress in Nuclear Energy*, Vol. 12, pp. 1-56.

Loyalka, S. K., and Ferziger, J. H., 1967, "Model Dependence of the Slip Coefficient," *Phys. Fluids*, Vol. 10, pp. 1833-1839.

Mason, H. B., and Seban, R. A., 1974, "Numerical Predictions for Turbulent Free Convection from Vertical Surfaces," *Int. J. Heat Mass Trans.*, Vol. 17, pp. 1329-1336.

Maxwell, J. C., 1873, *Electricity and Magnetism*, Clarendon Press, Oxford, p. 365.

Mayhew, Y. R., and Rogers, G. F. C., 1969, *Thermodynamic and Transport Properties of Fluids*, Oxford University Press, Oxford, England.

McAdams, W. H., 1954, *Heat Transfer, Third Edition*, McGraw-Hill, New York.

McCoy, D. D., and Hanratty, T. J., 1977, "Rate of Deposition of Droplets in Annular Two Phase Flow," *Int. J. Multiphase Flow*, Vol. 3, pp. 319-331.

Mills, A. F., and Wassel, A. T., 1975, "Aerosol Transport in a Thermally Driven Natural Convection Boundary Layer," *Lett. Heat Mass Trans.*, Vol. 2., pp. 159-168.

Mills, A. F., Hang, Xu, and Ayazi, F., 1984, "The Effect of Wall Suction and Thermophoresis on Aerosol Deposition from a Laminar Boundary Layer on a Flat Plate," *Int. J. Heat Mass Trans.*, Vol. 27, pp. 1110-1113.

Minkowycz, W. J., and Sparrow, E. M., 1966, "Free Convection Heat Transfer to Steam Under Variable Property Conditions," *Int. J. Heat Mass Trans.*, Vol. 9, pp. 1145-1147.

Minkowycz, W. J., and Sparrow, E. M., 1978, "Numerical Solution Scheme for Local Nonsimilarity Boundary-Layer Analysis," *Numerical Heat Trans.*, Vol. 1, pp. 69-85.

Miyamoto, M., Kajino, H., Kurima, J., and Takanami, I., 1982, "Development of Turbulence Characteristics in a Vertical Free Convection Boundary Layer," *Proceedings, Seventh International Heat Transfer Conference*, U. Grigull et al., ed., Hemisphere Publishing Corp., Washington, DC, Vol. 2, pp. 323-328.

Nachtsheim, P. R., and Swigert, P., 1965, *Satisfaction of Asymptotic Boundary Conditions in Numerical Solution of Systems of Nonlinear Equations of Boundary-Layer Type*, NASA TND3004, National Aeronautics and Space Administration, Washington, DC.

Novotny, J. L., and Yang, K-T., 1967, "The Interaction of Thermal Radiation in Optically Thick Boundary Layers," *J. Heat Trans.*, Vol. 89, pp. 309-312.

Novotny, J. L., Lloyd, J. R., and Bankston, J. D., 1974, "Local Nonsimilarity Applied to Free Convection Boundary Layers with Radiation Interaction," *Heat Transfer with Thermal Control Applications*, M. M. Yovanovich, ed., Progress in Astronautics and Aeronautics, Vol. 39, AIAA, New York, pp. 309-330.

Ostrach, S., 1953, *An Analysis of Laminar Free-Convection Flow and Heat Transfer About a Flat Plate Parallel to the Direction of the Generating Body Force*, NACA Report 1111, Washington, DC.

Ostrach, S., 1980, "Natural Convection With Combined Driving Forces," *Physicochemical Hydrodynamics*, Vol. 1, pp. 233-247.

Özisik, M. N., 1973, *Radiative Transfer and Interactions with Conduction and Convection*, Wiley-Interscience, New York.

Pai, S. I., 1956, *Viscous Flow Theory*, D. VanNostrand, Princeton, New Jersey.

Paolucci, S., 1982, *On the Filtering of Sound From the Navier Stokes Equations*, SAND82-8257, Sandia National Laboratory, Livermore, California.

Patankar, S. V., 1980, *Numerical Heat Transfer And Fluid Flow*, Hemisphere Publishing Corp., New York.

Prandtl, L., 1925, "Ueber die ausgebildete Turbulenz," *ZAMM*, Vol. 5, p. 136.

Prandtl, L., 1942, "Bemerkungen zur Theorie der freien Turbulenz," *ZAMM*, Vol. 22, pp. 241-243.

Prandtl, L., 1945, *Nachr. Akad. Wiss.*, Goettingen, Math-Phys. Klasse, p. 6.

Prodi, F., and Tampieri, F., 1988, "Problems in the Measurement of Thermophoretic Velocities of Aerosol Particles," *J. Aerosol Sci.*, Vol. 19, pp. 167-174.

Ramachandran, N., Armaly, B. F., and Chen, T. S., "Measurements and Predictions of Laminar Mixed Convection Flow Adjacent to a Vertical Surface," *J. Heat Trans.*, Vol. 107, pp. 636-641.

Randall, I. E., and Sesonske, A., 1959, "Effect of a Volume Heat Source on Free Convection Heat Transfer," *AIChE J.*, Vol. 5, pp. 150-154.

Reed, L. D., and Morrison, F. A., 1973, "Motion of an Aerosol Particle in an Unsteady Temperature Gradient," *J. Coll. Int. Sci.*, Vol. 42, pp. 358-365.

Reed, L. D., and Morrison, F. A., 1974, "Particle Interactions in Viscous Flow at Small Values of Knudsen Number," *J. Aerosol Sci.*, Vol. 5, pp. 175-189.

Reed, L. D., and Morrison, F. A., 1975, "Particle Interactions in Low Knudsen Number Thermophoresis," *J. Aerosol Sci.*, Vol. 6, pp. 349-365.

Rehm, R. G., and Baum, H. R., 1978, "The Equations of Motion for Thermally Driven Buoyant Flows," *J. Res. Natn. Bur. Stand.*, Vol. 83, pp. 297-308.

Reichardt, H., 1941, "Ueber eine neue Theorie der freien Turbulenz," *ZAMM*, Vol. 21, pp. 257-264.

Reynolds, W. C., 1976, "Computation of Turbulent Flows," *Annual Review of Fluid Mechanics*, Vol. 8, pp 183-208.

Reynolds, W. C., and Perkins, H. C., 1977, *Engineering Thermodynamics*, McGraw-Hill, New York, Chapter 8.

Reynolds, W. C., and Cebeci, T., 1978, "Calculation of Turbulent Flows," *Turbulence, Topics In Applied Physics*, P. Bradshaw, ed., Springer-Verlag, New York, Vol. 12, pp. 193-229.

Roache, P. J., 1976, *Computational Fluid Dynamics*, Hermosa Press, Albuquerque, New Mexico.

Rogers, D. F., 1974, "Further Comments on "Local Nonsimilarity Boundary-Layer Solutions"," *AIAA J.*, Vol. 12, pp. 1007-1008.

Rosner, D. E., and Fernandez de la Mora, J., 1982, "Small Particle Transport Across Turbulent Nonisothermal Boundary Layers," *J. Eng. Power*, Vol. 104, pp. 885-894.

Rosner, D. E., and Seshadri, K., 1981, "Experimental and Theoretical Studies of the Laws Governing Condensate Deposition From Combustion Gases," *Proceedings of the Eighteenth Symposium (International) on Combustion*, The Combustion Institute, Pittsburgh, Pennsylvania.

Rosseland, S., 1936, *Theoretical Astrophysics*, Oxford University Press, (Clarendon), London and New York.

Rouhiainen, P. O., and Stachiewicz, J. W., 1970, "On the Deposition of Small Particles From Turbulent Streams," *J. Heat Transfer*, Vol. 92, pp. 169-177.

Saffman, P. Q., 1965, "The Lift on a Small Sphere in a Slow Shear Flow," *J Fluid Mech.*, Vol. 22, pp. 385-400.

Saunders, O. A., 1939, "Natural Convection in Liquids," *Proc. R. Soc. London, Series A*, Vol. 172, pp. 55-71.

Schadt, C. F., and Cadle, R. D., 1961, "Thermal Forces on Aerosol Particles," *J. Physical Chem.*, Vol. 65, pp. 1689-1694.

Schaff, S. A., and Chambré, P. L., 1961, *Flow of Rarefied Gases*, Princeton University Press, Princeton, New Jersey, pp. 26-35

Schmidt, E. and Beckmann, W., 1930, "Das Temperatur-und Geschwindigkeitsfeld vor einer Waerme abgebenden senkrechter Platte bei natuerlicher Konvection," *Tech. Mech. u. Thermodynamik*, Bd. 1, Nr. 10, pp. 341; cont., Bd. 1, Nr. 11, pp. 391-406.

Segel, L. A., 1972, "Simplification and Scaling," *SIAM Review*, Vol. 14, pp. 547-571.

Seibers, D. L., 1979, *Natural Convection Heat Transfer From an External Receiver*, Sandia National Laboratory Report, SAND78-8276, Sandia National Laboratory, Livermore, California.

Seibers, D. L., Moffatt, R. F., and Schwind, R. G., 1985, "Experimental, Variable Properties Natural Convection From a Large, Vertical Flat Surface," *J. Heat Trans.*, Vol. 107, pp. 124-132.

Seibers, D. L., Schwind, R. G., and Moffatt, R. F., 1983, *Experimental Mixed Convection Heat Transfer From a Large, Vertical Surface In a Horizontal Flow*, SAND83-8225, Sandia National Laboratory, Livermore, California.

Siegel, R., and Howell, J. R., 1981, *Thermal Radiation Heat Transfer, Second Edition*, McGraw-Hill, New York.

Simpkins, P. G., Greenberg-Kosinski, S., and MacChesney, J. B., 1979, "Thermophoresis: The Mass Transfer Mechanism in Modified Chemical Vapor Deposition," *J. Appl. Phys.*, Vol. 50, pp. 5676-5681.

Soga, T., 1986, "A Kinetic Analysis of Thermal Force on a Spherical Particle of High Thermal Conductivity in a Monatomic Gas," *Phys. Fluids*, Vol. 29, pp. 976-985.

Sone, Y., 1972, "Flow Induced by Thermal Stress in Rarefied Gas," *Phys. Fluids*, Vol. 15, pp. 1418-1423.

Sparrow, E. M., 1971, "Reply by Authors to M. Coxon and E. K. Parks," *AIAA J.*, Vol. 9, p. 1664.

Sparrow, E. M., and Cess, R. D., 1966, *Radiation Heat Transfer*, Brooks/Cole Publishing Co., Belmont, California, Chapter 10.

Sparrow, E. M., and Gregg, J. L., 1958, "The Variable Fluid Property Problem in Free Convection," *Trans. Amer. Soc. Mech. Engrs.*, Vol. 80, pp. 879-886.

Sparrow, E. M., Goldstein, R. J., and Jonsson, V. K., 1963, "Thermal Instability in a Horizontal Fluid Layer: Effect of Boundary Conditions and Non-Linear Temperature Profile," *J. Fluid Mech.*, Vol. 18, pp. 513-528.

Sparrow, E. M., Quack, H., and Boerner, C. J., 1970, "Local Nonsimilarity Boundary-Layer Solutions," *AIAA J.*, Vol. 8, pp. 1936-1942.

Steinberner, U., and Reineke, H. H., 1978, "Turbulent Buoyancy Convection Heat Transfer With Internal Heat Sources," *Proceedings, Sixth International Heat Transfer Conference*, Hemisphere Publishing Corp., Washington, DC, Vol. 2, pp. 305-310 .

Talbot, L., 1980, "Thermophoresis-A Review," *Rarefied Gas Dynamics, Part 1*, S. S. Fisher, ed., Progress in Astronautics and Aeronautics, Vol. 74, pp. 467-488.

Talbot, L., Cheng, R. K., Schefer, R. W., and Willis, D. R., 1980, "Thermophoresis of Particles in a Heated Boundary Layer," *J. Fluid Mech.*, Vol. 101, pp. 737-758.

Tennekes, H., and Lumley, J. L., 1972, *A First Course In Turbulence*, The MIT Press, Cambridge, Massachusetts.

To, W. M., and Humphrey, J. A. C., 1986, "Numerical Simulation of Buoyant Turbulent Flow- 1. Free Convection Along a Heated, Vertical Flat Plate," *Int. J. Heat Mass Trans.*, Vol. 29, pp. 573-592.

Tyldesley, J. R., and Silver, R. S., 1968, "The Prediction of the Transport Properties of a Turbulent Fluid," *Int. J. Heat Mass Trans.*, Vol. 11, pp. 1325-1340.

Van Driest, E. R., 1956, "On Turbulent Flow Near a Wall," *J. Aero. Sci.*, Vol. 23, pp. 1007-1011 and 1036.

Venkatachala, B. J., and Nath, G., 1981, "Nonsimilar Laminar Natural Convection in a Thermally Stratified Fluid," *Int. J. Heat Mass Trans.*, Vol. 24, pp. 1848-1850.

Venkateshan, S. P., and Krishna Prasad, K., 1979, "Radiative Interactions in Boundary Layers," *J. Fluid Mech.*, Vol. 90, pp. 33-66.

Viskanta, R., 1966, "Radiation Transfer and Interaction of Convection with Radiation Heat Transfer," *Advances in Heat Transfer*, T. F. Irvine Jr. and J. P. Hartnett, ed., Academic Press, New York, Vol. 3, pp. 175-250.

Viskanta, R., and Grosh, R. J., 1962a, "Boundary Layer in Thermal Radiation Absorbing and Emitting Media," *Int. J. Heat Mass Trans.*, Vol. 5, pp. 795-806.

Viskanta, R., and Grosh, R. J., 1962b, "Effect of Surface Emissivity on Heat Transfer by Simultaneous Conduction and Radiation," *Int. J. Heat Mass Trans.*, Vol. 5, pp. 729-734.

Vliet, G. C., and Liu, C. K., 1969, "An Experimental Study of Turbulent Natural Convection Boundary Layers," *J. Heat Trans.*, Vol. 91, pp. 517-531.

Waldmann, L., and Schmitt, K. H., 1966, "Thermophoresis and Diffusiophoresis of Aerosols," *Aerosol Science*, C. N. Davies, ed., Academic Press, London, pp. 137-162.

Walker, K. L., Homsy, G. M., and Geyling, F. T., 1979, "Thermophoretic Deposition of Small Particles in Laminar Tube Flow," *J. Coll. Int. Sci.*, Vol. 69, pp. 138-147.

Wallis, G. B., 1969, *One-dimensional Two-phase Flow*, McGraw-Hill, New York, Chapters 2 and 8.

Warner, C. Y., and Arpaci, V. S., 1968, "An Experimental Investigation of Turbulent Natural Convection in Air at Low Pressure Along a Vertical Heated Flat Plate," *Int. J. Heat Mass Trans.*, Vol. 11, pp. 397-406.

White, F. M., 1974, *Viscous Fluid Flow*, McGraw-Hill Book Co., New York.

Wichner, R. P. et al., 1984, *Noble Gas, Iodine, and Cesium Transport in a Postulated Loss of Decay Heat Removal Accident at Browns Ferry*, ORNL/TM-9028, NUREG/CR-3617, Oak Ridge National Laboratory, Oak Ridge, Tennessee, pp. 92.

Wright, A. L., and Arwood, P. C., 1987, *Summary of Pretest Aerosol Code Results for LWR Aerosol Containment Experiment (LACE) LA1*, ORNL/TM-293, Oak Ridge National Laboratory, Oak Ridge, Tennessee.

Yang, R. J., and Aung, W., 1985, "Equations and Coefficients for Turbulence Modeling," *Natural Convection: Fundamentals And Applications*, S. Kakaç et al., ed., Hemisphere Publishing Corp., Washington, DC.

# APPENDICES

# APPENDIX A

# NUMERICAL TECHNIQUES

For the differential equations describing the problem of interest here, bounding conditions are prescribed at the wall and the edge of the boundary layer. This is called a boundary value problem, which is more difficult to solve than an initial value problem in which all the bounding conditions are prescribed at one location only. Two methods of solving the coupled, partial differential equations in this boundary value problem were used. The first technique is the local nonsimilarity method (Sparrow et al., 1970) in which the system of partial differential equations is transformed into an equivalent system of ordinary differential equations. The exact form of the transformed system of ordinary differential equations is described, specifically including terms that have caused some controversy in the literature. The second technique is a finite difference procedure called the Keller Box method (Keller, 1978).

Two numerical techniques were used to compute the solution to the transformed system of ordinary differential equations in the local nonsimilarity method. The first was a variant of the "shooting" method developed by Nachtsheim and Swigert (1965) and the second was a finite difference technique developed by Lentini and Pereyra (1977).

The Keller Box method is a systematic procedure for discretization of the partial differential equations that yields algebraic equations with a computationally desirable structure.

## A.1. The Method of Local Nonsimilarity

### A.1.1. General description of the method

The local nonsimilarity method of Sparrow et al. (1970), as described by Minkowycz and Sparrow (1978), was used for the numerical solution of the transformed partial differential equations. The independent variable $\eta$ is called a pseudosimilarity variable and is composed of a combination of both normal and streamwise spatial coordinates. For example, the pseudosimilarity variable used in the present work is given by:

$$\eta(x,y) = \frac{1}{L}\left(\frac{Gr_L}{4\xi}\right)^{1/4}\int_0^y \frac{\rho}{\rho_r}dy' . \qquad \text{(A-1)}$$

The intent of introducing this variable is to lessen the dependence of the solution upon the streamwise spatial coordinate in the same fashion as a similarity variable completely eliminates the solution dependence upon the streamwise spatial coordinate. The right hand sides of the transformed partial differential equations contain derivatives of the dependent variables with respect to the streamwise variable $\xi$, as well as those with respect to the pseudosimilarity variable, $\eta$. Retaining these derivative terms of $\partial f/\partial\xi$, $\partial\theta/\partial\xi$, and $\partial n/\partial\xi$ would require use of a numerical scheme suitable for *partial* differential equations in order to solve the system of equations. The retention of these derivative terms also couples the local solutions at adjacent streamwise stations, which precludes the possibility of finding a locally autonomous solution at any given streamwise station.

The computational task would be simplified by deletion of the streamwise derivative terms $\partial f/\partial\xi$, $\partial\theta/\partial\xi$, and $\partial n/\partial\xi$. This would result in a system of *ordinary* differential equations; however, the difference between the solution of this set of equations and that of the original set of equations is unknown. The coupling of streamwise stations is also severed in this approximation, resulting in a locally autonomous solution. This procedure is called the "local similarity method" and simply neglects the right hand sides of the governing equations with the assumption that they are sufficiently small. This assumption is good for very small values of the streamwise variable, but rapidly breaks down for increasing values of $\xi$. The resulting equations are ordinary differential equations, and the method of Nachtsheim and Swigert (1965) was used for their numerical solution. This local similarity method is called the "first level of truncation" in the method of local nonsimilarity.

The local nonsimilarity method retains *all* of the terms in the original set of governing equations, or at least approximations for all the terms containing streamwise derivatives. These terms are disguised by introducing new functions defined as

$$G \equiv \frac{\partial f}{\partial \xi}, \quad P \equiv \frac{\partial n}{\partial \xi}, \quad \text{and} \quad \Phi \equiv \frac{\partial \theta}{\partial \xi}. \tag{A-2}$$

Since these new functions represented additional unknowns, additional equations are needed to determine a unique solution. Subsidiary equations are generated by differentiating the system of partial differential equations and the boundary conditions with respect to the streamwise variable $\xi$. This generates terms of the form $\partial G/\partial \xi$, $\partial \Phi/\partial \xi$, and $\partial P/\partial \xi$. The second level of truncation of the local nonsimilarity method is performed by neglecting the streamwise derivatives of the functions $G$, $\Phi$, and $P$ *in the subsidiary equations*. Thus, the solution of the subsidiary set of equations provides approximations for the new variables, $G$, $\Phi$, and $P$.

This procedure results in a set of ordinary differential equations applicable at any streamwise station; that is, these equations may be solved directly at any streamwise location without performing any solutions at upstream locations. This "second level of truncation" retains all the terms of the original partial differential equations. The subsidiary equations and boundary conditions are of no direct interest but serve to close the system of equations including the new functions $G$, $\Phi$, and $P$. The intent of this procedure is to reduce the error incurred by neglecting the nonsimilar terms in a higher-order subsidiary equation instead of in the original set of equations, or the first set of subsidiary equations.

A third level of truncation could have been introduced by definition of the additional functions

$$H \equiv \frac{\partial G}{\partial \xi}, \quad \mathrm{X} \equiv \frac{\partial \Phi}{\partial \xi}, \quad \text{and} \quad Q \equiv \frac{\partial P}{\partial \xi}. \tag{A-3}$$

In this third level scheme, the second level subsidiary equations and boundary conditions would be differentiated with respect to the streamwise variable. The streamwise derivatives of these new functions $H$, X, and $Q$ would be neglected, resulting in still another set of ordinary differential equations that would be locally autonomous.

The method is usually considered to have converged if there is sufficient agreement between the second and third levels of truncation. The results of Sparrow and Yu (1971) and many other investigators have shown that the third level of truncation is rarely necessary for convergence. Thus, it has become a common practice to employ a second level of truncation scheme.

### A.1.2. Specific formulation of the second-level of truncation model

With the basic outline of the method as described in the previous section, the second-level of truncation model is applied to the differential equations of interest of the present work. The nonsimilar differential equations for Newton's Second Law, the conservation of energy, and the conservation of particles, as presented in Section 4.4 in equations (4-44), (4-45), and (4-46) are repeated as follows:

$$\frac{\partial}{\partial\eta}\left[\left(1+\frac{\mu_t}{\mu}\right)\left(\frac{\rho\mu}{\rho_r\mu_r}\right)f''\right]+3ff''-2(f')^2+\theta\left(\frac{T_{\infty,0}}{T_\infty}\right)=4\xi(f'f'_\xi-f''f_\xi)\,, \qquad \text{(A-4)}$$

$$\frac{1}{Pr_r}\left(\frac{C_r}{C}\right)\frac{\partial}{\partial\eta}\left\{\left(\frac{\rho k}{\rho_r k_r}\right)\left[1+\frac{k_t}{k}+\frac{4}{3M}(1+\lambda\theta)^3\right]\theta'\right\}+3f\theta'-4\xi f'\frac{\partial}{\partial\xi}\left(\frac{1}{\lambda}\right)+\frac{Da}{Pr_r}\left(\frac{C_r}{C}\right)\left(\frac{4\xi}{Gr}\right)^{1/2}n$$
$$=4\xi(f'\theta_\xi-\theta'f_\xi)\,, \qquad \text{(A-5)}$$

and

$$\frac{\partial}{\partial\eta}\left[\left(\frac{1}{Sc}+\frac{1}{Sc_t}\frac{\mu_t}{\mu}\right)\left(\frac{\rho\mu}{\rho_r\mu_r}\right)n'\right]+3fn'+K\frac{\partial}{\partial\eta}\left[\left(\frac{\rho\mu}{\rho_r\mu_r}\right)\left(\frac{\lambda\theta'}{1+\lambda\theta}\right)n\right]=4\xi(f'n_\xi-n'f_\xi)\,. \qquad \text{(A-6)}$$

The boundary conditions, as given by equation (4-43), are repeated as follows:

$$f(\xi,0)=\frac{\partial f(\xi,0)}{\partial\eta}=1-\theta(\xi,0)-\xi\frac{\partial\left(\frac{1}{\lambda}\right)}{\partial\xi}=n(\xi,0)=\frac{\partial f(\xi,\infty)}{\partial\eta}=\theta(\xi,\infty)=1-n(\xi,\infty)=0\,. \qquad \text{(A-7)}$$

As described in Section 4.4, the above set of equations is incomplete, since the turbulence quantities will be functions of $\eta$, the nondimensional distance from the wall, and the variable property terms may be functions of temperature, and hence must be prescribed in order to fully complete the set of differential equations. For the purposes

of describing the second-level of truncation model, the exact form of the turbulence quantities and the variable property relationships need not be specified. Participating thermal radiation and volumetric heat sources also need not be considered for simplicity in describing the method. The case of laminar, constant property flow with no participating thermal radiation or volumetric heat sources is therefore studied to describe the method of local nonsimilarity. The substitution of the disguised functions of equation (A-2) into equations (A-4), (A-5), and (A-6) for this specific case results in a set of equations of the following form:

$$f''' + 3ff'' - 2(f')^2 + \theta = 4\xi(f'G' - f''G), \tag{A-8}$$

$$\frac{1}{Pr}\theta'' + 3f\theta' - 4\xi f'\frac{\partial}{\partial\xi}\left(\frac{1}{\lambda}\right) = 4\xi(f'\Phi - \theta'G), \tag{A-9}$$

and

$$\frac{1}{Sc}n'' + 3fn' + K\frac{\partial}{\partial\eta}\left[\left(\frac{\lambda\theta'}{1+\lambda\theta}\right)n\right] = 4\xi(f'P - n'G). \tag{A-10}$$

The second-level of truncation model proceeds by taking the derivative of equations (A-8), (A-9), and (A-10) with respect to the streamwise coordinate, $\xi$. For the second-level of truncation model, the derivatives of the disguised functions with respect to $\xi$, as defined in equation (A-3), are neglected. Rearrangement results in the following set of subsidiary equations:

$$G''' + 3fG'' + 7f''G - 8f'G' + \Phi = 4\xi(G'^2 - G''G), \tag{A-11}$$

$$\frac{1}{Pr}\Phi'' + 3f\Phi' + 7G\theta' - 4f'\Phi - 4\left[f'\frac{\partial}{\partial\xi}\left(\frac{1}{\lambda}\right) + \xi G'\frac{\partial}{\partial\xi}\left(\frac{1}{\lambda}\right) + \xi f'\frac{\partial^2}{\partial\xi^2}\left(\frac{1}{\lambda}\right)\right] = 4\xi(G'\Phi - \Phi'G), \tag{A-12}$$

and

$$\frac{1}{Sc}P'' + 3fP' + 7Gn' - 4f'P + K\left[\frac{\partial^2}{\partial\eta\partial\xi}\left(\frac{\lambda\theta'}{1+\lambda\theta}\right)n + \frac{\partial}{\partial\eta}\left(\frac{\lambda\theta'}{1+\lambda\theta}\right)P + \frac{\partial}{\partial\xi}\left(\frac{\lambda\theta'}{1+\lambda\theta}\right)n' + \left(\frac{\lambda\theta'}{1+\lambda\theta}\right)P'\right]$$
$$= 4\xi(G'P - P'G). \tag{A-13}$$

The boundary conditions must also be differentiated with respect to $\xi$, with the resulting form:

$$G(\xi,0)=G'(\xi,0)=\Phi(\xi,0)+\frac{\partial\left(\frac{1}{\lambda}\right)}{\partial\xi}+\xi\frac{\partial^2\left(\frac{1}{\lambda}\right)}{\partial\xi^2}=P(\xi,0)=G'(\xi,\infty)=\Phi(\xi,\infty)=P(\xi,\infty)=0\,. \qquad \text{(A-14)}$$

The set of equations (A-8), (A-9), (A-10), (A-11), (A-12), and (A-13) with the boundary conditions (A-7) and (A-14) form a complete set. Special attention is focused on the terms in the right-hand side of the subsidiary equations, equations (A-11), (A-12), and (A-13). These terms arise from the differentiation of the terms inside the parentheses on the right-hand side of equations (A-8), (A-9), and (A-10) with respect to $\xi$. The inclusion or deletion of these terms in the method of local nonsimilarity has caused controversy in the literature. These terms were neglected in the original version of the method presented by Sparrow et al. (1970). The studies by Coxson and Parks (1971) and Chen and Eichhorn (1976) claim that retention of these terms is preferable, while the studies by Sparrow (1971) and Rogers (1974) claim that deletion of the terms is preferable. Based on the results presented in Section 5.2.3, these terms should be retained.

### A.1.3. Numerical solution techniques

The local nonsimilarity method transforms the system of partial differential equations into a system of ordinary differential equations which are numerically much easier to solve. However, the bounding conditions for the transformed set of differential equations are prescribed both at the wall and at the edge of the boundary layer. The numerical solution of this two-point boundary-value problem is more computationally involved than the numerical solution of an initial-value problem in which the system of differential equations has all of the necessary bounding conditions prescribed at only one point. Additionally, physical considerations require that the solution of the equations must exhibit asymptotic behavior at the edge of the boundary layer for the dependent variables representing fluid shear, temperature gradient, and particle concentration gradient. The first numerical technique used to compute the solution of

the transformed system of ordinary differential equations was a variant of the shooting method developed by Nachtsheim and Swigert (1965). The second technique was a finite difference procedure developed by Lentini and Pereyra (1977).

The shooting technique transforms the two-point boundary-value problem into a series of initial-value problems. Values are first assumed for the "missing" initial conditions, which are the desired solution parameters of the problem. For this problem, the missing initial values are the wall shear, the wall temperature gradient, and the wall particle concentration gradient. The assumed initial-value problem is then integrated across the boundary layer and the computed results at the edge of the boundary layer are compared to the actual boundary conditions specified by the original boundary-value problem. If the computed bounding value does not agree with the prescribed boundary condition within a specified amount, the assumed values for the missing initial conditions are corrected and the initial-value integration is performed again until the computed values at the edge of the boundary layer agreed with the prescribed boundary condition.

The name "shooting" was applied to this method because a gradient (elevation) is estimated at the beginning (shooter) of the integration interval (range) and the computed results are compared to the known boundary condition (target) at the other end of the interval. This procedure has the disadvantage of sensitivity to the value of the initial slope.

In a mathematical sense, the variable $\eta$ must vary from zero at the wall to infinity at the edge of the boundary layer. Practically, however, this infinite range of integration must be approximated by a finite range in order for the integration to be carried out on a digital computer. An asymptotic approach to a zero value of fluid shear, temperature gradient, and particle gradient is also required at the edge of the boundary layer. Nachtsheim and Swigert (1965) developed a method that modifies the shooting method so that a suitable finite approximation for the boundary-layer edge at infinity evolves as a part of the solution and that the asymptotic approach for some variables at the edge is achieved.

Solution of the third-order system of nonsimilar ordinary differential equations begins by reducing all equations to an equivalent set of first order equations. This step is necessary to use the Runge-Kutta integration routine RKF45 developed by Forsythe et al. (1977). The solution algorithm requires an initial guess for the location of the edge of the boundary layer, as well as guesses for the missing initial values.

The differential equations were also differentiated with respect to the missing initial values. This additional differentiation is necessary to compute the sensitivity of the computed solution at the boundary point of infinity to the guessed initial value. This computed information at the infinite boundary point is used to correct the initial guessed value. Details are found in Nachtsheim and Swigert (1965).

The integration across the boundary layer is then performed for all equations, including the differential equations representing the sensitivity with respect to the initial conditions. The difference between the computed and prescribed boundary conditions and the difference between the computed and expected asymptotic behaviors of the fluid shear, temperature gradient, and particle concentration gradient at the edge are then evaluated. These differences are squared and then summed to form the "error term." Corrections based upon the results of the sensitivity equations for the assumed initial values are then computed by a least-squares technique and the integration is done again. The solution is iterated in this fashion until the corrections in the initial values are less than a specified tolerance. If the computed error, given by the sum of the squared differences, at the edge of the boundary layer is not sufficiently small, the value for the location of the edge of the boundary layer is increased and further iterations are performed until the error is sufficiently small.

The integration routine, RKF45, was chosen because it is based on a robust, well tested algorithm, it is well documented, and the author was experienced in obtaining accurate solutions to nonsimilar boundary layer problems using this software. A detailed presentation of RKF45, including a listing, is found in Forsythe et al. (1977). The size of the integration step used in RKF45 is automatically chosen by the algorithm, so that a user-supplied local error criterion is satisfied. In this fashion, large integration steps are used when the solution is slowly varying, such as near the edge of the

boundary layer, and short steps are used when the solution is rapidly varying, such as near the wall. The use of this variable-step-size method tends to minimize the computer time necessary to solve the problem.

An additional technique for solving the nonsimilar boundary layer equations was developed. This technique is based on a finite-difference algorithm developed by Lentini and Pereyra (1977) as implemented in software by IMSL, Inc. (IMSL, 1982) in a subroutine called DVCPR. This finite-difference procedure also requires reducing the order of the original system of differential equations to an equivalent set of first-order equations. The code makes first-order difference approximations using the trapezoidal rule on an assumed finite-difference mesh for the entire integration interval over the boundary layer thickness. The coding automatically chooses a mesh spacing based upon satisfaction of a user-supplied local error criterion. Unlike the shooting method, the actual boundary conditions are supplied at both ends of the integration interval. The missing initial values evolve from the solution as do any other unknown interior values. No estimate of the missing initial conditions is necessary. Additional computer memory as compared to the shooting method may be required when using this method because of the potentially large coefficient matrix needed to store finite-difference values for the entire boundary layer.

A finite interval for integration is supplied to DVCPR by an estimate for the edge of the boundary layer. An error term is computed by squaring and summing the difference between the computed values and zero for the variables representing fluid shear, temperature gradient, and particle concentration gradient, which should asymptotically approach zero. If this error was not sufficiently small (on the order of $10^{-6}$), a larger value for the edge of the boundary layer is estimated and the computations are repeated until convergence.

The computed solutions are also plotted using computer software to insure that proper asymptotic behavior occurs as the edge of the boundary layer is approached. Physical considerations require that the solutions have a smooth asymptotic approach, instead of just a crossing point, as the edge of the boundary layer is reached.

The major advantage that this finite difference procedure has over the shooting method of Nachtsheim and Swigert is that the auxiliary differential equations for the computed solution sensitivity with respect to the guessed initial values are not needed. This procedure has fewer equations to integrate across the boundary layer, which results in a reduced possibility of programming errors. An additional advantage is that either: (1) the boundary condition at the wall for a particle concentration of zero when considering Brownian diffusion, or (2) the relationship between particle concentration and particle concentration gradient when neglecting Brownian diffusion is easily accommodated when using DVCPR. Because of the variable mesh spacing, the very steep concentration gradient at the wall that exists when considering Brownian diffusion does not cause the integration to fail as it might for any shooting method. The relationship between the particle concentration and the particle concentration gradient was easily incorporated when the Brownian layer was neglected.

### A.2. Keller Box Method

The Keller Box scheme (Keller, 1978) for boundary-value problems in partial differential equations has been used for solving many different problems arising in boundary layer flow (Keller and Cebeci, 1972). This method has many advantages, such as accuracy, adjustable mesh spacing, and the ability to consider some singularities at the endpoints. The accuracy is second order with respect to the mesh spacing. The finite-difference mesh spacing can have arbitrary size. The singular nature of the particle conservation equation when Brownian diffusion is negligible is easily accommodated in the solution scheme. Also, the thermophysical properties that are coefficients of the dependent variables need not be expressed as analytic functions of the independent variables.

The Keller Box scheme requires writing the coupled third-order system of partial differential equations as a coupled system of first-order partial differential equations. The solution domain is divided into rectangular subdomains (boxes), as shown on Figure A-1. The first order derivatives are approximated by central difference expressions and

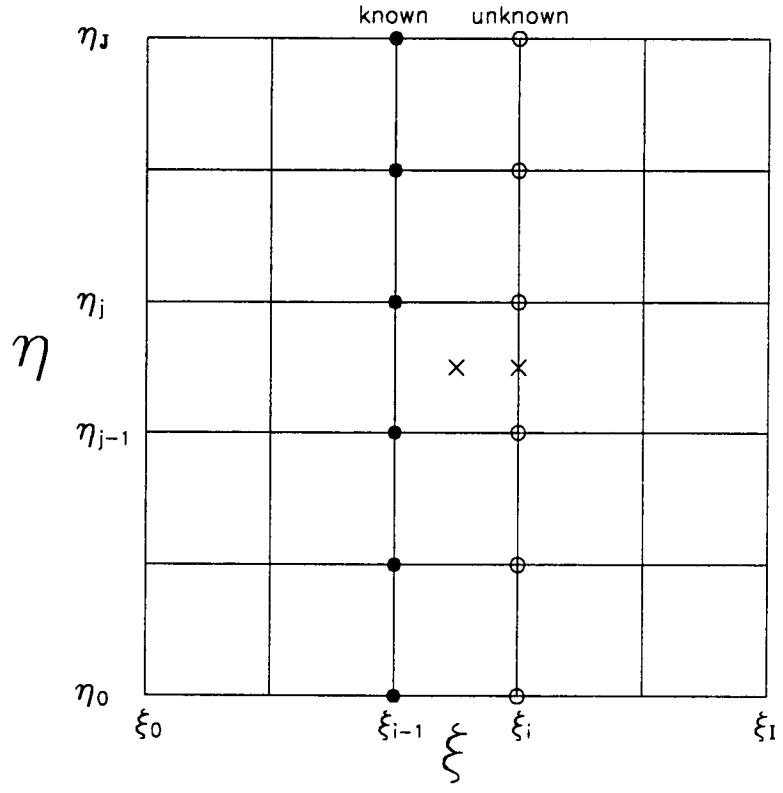


a. Representative Mesh

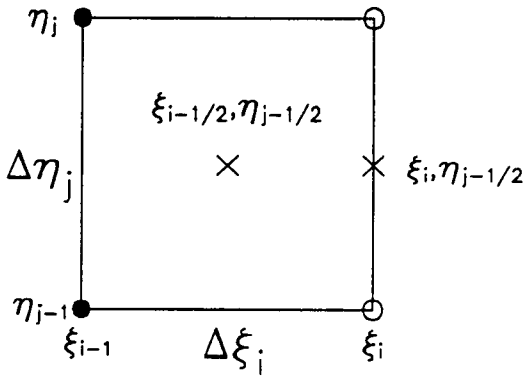


b. Mesh Details

Figure A-1. Keller Box Mesh Representation.

simple two-point averages using the function values at the corners of each box. The central difference expressions result in a numerical error on the order of the mesh spacing squared.

For demonstration purposes, the stream function $f$ was selected to represent one of the seven dependent variables. The numerical approximation to $f$ at mesh point $i$ and $j$ is denoted by $f_j^i$. The following notations are used for mesh averages and finite differences of the mesh quantity $f$. The fraction of one-half denotes the mid-point.

$$[f]_{j-1/2}^{i} \equiv \frac{1}{2}(f_j^i + f_{j-1}^i), \tag{A-15}$$

$$\left[\frac{\partial f}{\partial \xi}\right]_{j-1/2}^{i-1/2} \equiv \frac{1}{\Delta \xi_i}([f]_{j-1/2}^{i} - [f]_{j-1/2}^{i-1}), \tag{A-16}$$

$$\left[\frac{\partial f}{\partial \eta}\right]_{j-1/2}^{i} \equiv \frac{1}{\Delta \eta_j}(f_j^i - f_{j-1}^i), \tag{A-17}$$

$$\left[\frac{\partial f}{\partial \eta}\right]_{j-1/2}^{i-1/2} \equiv \frac{1}{2}\left(\left[\frac{\partial f}{\partial \eta}\right]_{j-1/2}^{i} + \left[\frac{\partial f}{\partial \eta}\right]_{j-1/2}^{i-1}\right), \tag{A-18}$$

and

$$[f]_{j-1/2}^{i-1/2} \equiv \frac{1}{2}([f]_{j-1/2}^{i} + [f]_{j-1/2}^{i-1}) = \frac{1}{4}(f_j^i + f_{j-1}^i + f_j^{i-1} + f_{j-1}^{i-1}). \tag{A-19}$$

For illustrative purposes, the Keller Box finite difference procedure is applied here to one of the nonsimilarity equations. The dimensionless conservation of energy equation for the simplest nonsimilarity case is shown here for turbulent natural convection flow with constant thermophysical properties over a constant temperature flat plate without a stratified freestream or thermophoresis. This equation is given by

$$\frac{1}{Pr}\frac{\partial}{\partial \eta}\left\{\left(1 + \frac{k_t}{k}\right)\theta'\right\} + 3f\theta' = 4\xi(f'\theta_\xi - \theta' f_\xi), \tag{A-20}$$

where a prime superscript represents a partial derivative with respect to the independent pseudosimilarity variable $\eta$ and a subscript $\xi$ represents a partial derivative with respect to the streamwise independent variable $\xi$. The term that represents turbulence is included to show the treatment of certain nonlinearities.

The corresponding finite difference equation is obtained by mesh averaging each of the terms of equation (A-20) at the center of the box. The mesh average of the products of dependent variables, such as the second term on the left hand side of equation (A-20), is used in the problem discretization instead of the product of the mesh averages of each dependent variable. This is done to minimize the amount of arithmetic manipulations and has no significant effect upon the accuracy or stability (Keller, 1978).

The mesh averaging operations for equation (A-20) are carried out according to the definitions expressed in equations (A-15) through (A-19). Performing the mesh operations on the energy equation yields the following expression.

$$\frac{1}{Pr\,2\Delta\eta_j}\left\{\left(1+\frac{k_t}{k}\right)_j^i \theta'^i_j + \left(1+\frac{k_t}{k}\right)_j^{i-1} \theta'^{i-1}_j - \left(1+\frac{k_t}{k}\right)_{j-1}^i \theta'^i_{j-1} - \left(1+\frac{k_t}{k}\right)_{j-1}^{i-1} \theta'^{i-1}_{j-1}\right\}$$

$$+\frac{3}{4}\{(f\,\theta')^i_j + (f\,\theta')^{i-1}_j + (f\,\theta')^i_{j-1} + (f\,\theta')^{i-1}_{j-1}\}$$

$$= 4\xi_{i-1/2}\left\{\frac{1}{4}(f'^i_j + f'^i_{j-1} + f'^{i-1}_j + f'^{i-1}_{j-1})\frac{1}{2\Delta\xi_i}(\theta^i_j + \theta^i_{j-1} - \theta^{i-1}_j - \theta^{i-1}_{j-1})\right.$$

$$\left.-\frac{1}{4}(\theta'^i_j + \theta'^i_{j-1} + \theta'^{i-1}_j + \theta'^{i-1}_{j-1})\frac{1}{2\Delta\xi_i}(f^i_j + f^i_{j-1} - f^{i-1}_j - f^{i-1}_{j-1})\right\}. \qquad \text{(A-21)}$$

As written, this system of algebraic equations is nonlinear. This system of nonlinear algebraic equations is solved using Newton's method as follows by writing the $(l+1)$-th iterate for the stream function as

$$f^{i,l+1}_j = f^{i,l}_j + \delta f^{i,l}_j\,, \qquad \text{(A-22)}$$

with similar linearizations for the other mesh functions.

In addition, the explicit definitions of the derivative function are written for the $i$-th line in the mesh such that

$$[f']^i_{j-1/2} = \left[\frac{\partial f}{\partial \eta}\right]^i_{j-1/2} = \frac{f^i_j - f^i_{j-1}}{\Delta\eta_j} = \frac{1}{2}[f'^i_j + f'^i_{j-1}] \tag{A-23}$$

and

$$[f'']^i_{j-1/2} = \left[\frac{\partial f'}{\partial \eta}\right]^i_{j-1/2} = \frac{f'^i_j - f'^i_{j-1}}{\Delta\eta_j} = \frac{1}{2}[f''^i_j + f''^i_{j-1}] \,. \tag{A-24}$$

The linearized dependent mesh functions are inserted into the nonlinear finite difference equations (A-21), as well as equations (A-23) and (A-24). After neglecting all quadratic and higher order terms for the Newton corrections, a linear system of algebraic equations with a block tridiagonal structure of the following form results.

$$A^{i,l}_j \delta^{i,l+1}_{j-1} + B^{i,l}_j \delta^{i,l+1}_j + C^{i,l}_j \delta^{i,l+1}_{j+1} = R^{i,l}_j \,, \tag{A-25}$$

where

$$\delta = (\delta f,\ \delta f',\ \delta f'',\ \delta\theta,\ \delta\theta')^T \,, \tag{A-26}$$

and

$$A^{i,l}_j,\quad B^{i,l}_j,\quad \text{and}\quad C^{i,l}_j \tag{A-27}$$

are square coefficient matrices of rank five for each normal grid position $j$ for the case of coupled momentum and energy equations. The coefficient matrices are of rank seven for the case of coupled energy, momentum, and particle conservation equations. The $\delta$ terms of equation (A-26) are called "Newton iterates."

The values of all grid functions for the $(i\text{-}1)$-th level are specified or have been computed from a previous streamwise position. These $(i\text{-}1)$ values are grouped into the right hand side residual vector of equation (A-25) and remain unchanged during the Newton iteration. The Newton iteration scheme is started with guessed values for the

grid functions at level $i$. These guessed values are typically the grid function value at the previous $(i\text{-}1)$-th level. These $i$-th level grid function values are also grouped into the right hand side residual vector and if the problem is nonlinear, also appear in the coefficient matrices on the left hand side.

Computation of the turbulence quantity in equation (A-21) requires a value for the dimensionless wall shear $f_0''$. Rather than linearize the turbulent diffusion coefficient term and complicate the solution, the previous value of the $(l\text{-}1)$-th iterate of $f_0''$ is used. Keller and Cebeci (1972) used a different turbulence model but made the same explicit representation for computation of the turbulence term.

The number of boundary conditions must equal the number of first-order differential equations that describe the problem. The boundary conditions at the position $J = 0$ and $J = J$ are incorporated into the coefficient matrices and residual right hand side terms by writing the specified relationships at the bounding point. For example, at the wall or $J = 0$, the stream function $f$ is defined as a constant equal to zero and the dimensionless wall temperature is defined as another constant equal to one for the case of no freestream stratification. Therefore, for the $l$-th iteration at position $j = 0$ and all $i$,

$$f_0^{i,l} = 0, \qquad \delta f_o^{i,l+1} = 0, \qquad \theta_0^{i,l} = 1, \quad \text{and} \quad \delta\theta_0^{i,l+1} = 0\,. \tag{A-28}$$

The value for the specified bounding grid function is used in the residual term or coefficient matrices whenever appropriate, according to the problem formulation. The equation for the Newton iterate is incorporated into the numerical method by inserting a unit coefficient into the appropriate position of the coefficient matrix for the Newton iterate. The residual term corresponding to that particular Newton iterate is zero. A similar expression is written for the other endpoint of the boundary layer.

The particle concentration inside the Brownian layer could have been computed with the Keller Box method by retaining the reciprocal Schmidt number in the formulation and specifying the particle concentration in the fluid at the wall as zero for the assumed perfectly absorbing wall. Since the thickness of the Brownian layer is very

small, as shown in Section 4.2, very small mesh spacing near the wall would be necessary to resolve the Brownian layer, which would require a great deal of computation effort. Since Brownian diffusion transport of particles is negligible with respect to thermophoretic transport except within the very thin Brownian layer as shown in Appendix D, the particle flux deposited on the wall can be computed without resolving the Brownian layer. Under these conditions, the extra work required to compute the particle concentration inside the Brownian layer is unnecessary, as shown in Section 5.6 where neglecting the Brownian layer had little effect on the deposited flux of particles on the wall when the Lentini and Pereyra (1977) method was used to resolve the Brownian layer.

The bounding condition for the particle concentration equation requires special treatment when neglecting the Brownian diffusion layer. This equation is repeated as follows:

$$\frac{\partial}{\partial\eta}\left[\left(\frac{1}{Sc}+\frac{1}{Sc_t}\frac{\mu_t}{\mu}\right)\left(\frac{\rho\mu}{\rho_r\mu_r}\right)n'\right]+3fn'+K\frac{\partial}{\partial\eta}\left[\left(\frac{\rho\mu}{\rho_r\mu_r}\right)\left(\frac{\lambda\theta'}{1+\lambda\theta}\right)n\right] = 4\xi(f'n_\xi - n'f_\xi)\,. \quad \text{(A-29)}$$

A bounding condition at the wall is imposed by writing the particle conservation equation at the wall with no diffusive terms and prescribing bounding conditions for the other known wall values of stream function ($f = 0$) and temperature ($\theta = 1$). For the case where the energy conservation and stream function are decoupled from the particle conservation equation, equation (A-29) reduces to the following expression.

$$n_w' - \frac{\lambda\theta_w'}{1+\lambda}n_w = 0\,. \quad \text{(A-30)}$$

Equation (A-30) relates the apparent particle concentration gradient at the wall to the apparent particle concentration in the fluid at the wall when Brownian diffusion is negligible with respect to thermophoretic transport. The Newton linearization of equation (A-30) is employed and the resulting expression is written in the form of a coefficient

matrix times the unknown Newton iterates and a residual right hand side term for incorporation (in a manner analogous to equation (A-28)) into the matrix equation (A-25). The linearized bounding condition is given by the following expression.

$$\delta n_w' - \frac{\lambda \theta_w'}{1+\lambda} \delta n_w = -n_w' + \frac{\lambda \theta_w'}{1+\lambda} n_w . \qquad \text{(A-31)}$$

The unknown values of particle concentration and particle concentration gradient in the fluid at the wall are determined as part of the solution in the identical fashion as the interior grid function values.

The particle concentration equation becomes singular at the wall when Brownian diffusion is neglected. The differential equation representing the particle concentration in the fluid at the wall is reduced from a second-order to a first-order differential equation because turbulent diffusion vanishes at the wall. Only one boundary condition can be satisfied by a first-order equation; in the case of the particle concentration equation, this condition must be satisfied at the boundary point of infinity, where the particle concentration must be one. However, away from the wall where turbulent diffusion is substantial, the particle conservation equation remains second-order and consequently requires two properly posed boundary conditions.

The Newton iteration is started at the streamwise position of $\xi$=0. All grid function variables are set to zero as an initial guess. The Newton iteration technique is used until the absolute values of the Newton iterates, equation (A-26), were all less than a specified tolerance, arbitrarily chosen as $10^{-5}$. Then for the nonsimilarity cases, where the streamwise partial derivatives were non-zero, a step in the streamwise direction is taken, and new values for the grid functions are then computed by the Newton iteration method.

In formulating the nonsimilarity boundary layer problem by transformation of variables, the edge of the boundary layer is transformed to infinity. A choice of a corresponding finite value of "infinity" must be made for computational purposes. For this problem, an arbitrary guess is made of $\eta$ = 10 for the edge of the boundary layer. This

is then the coordinate in the normal direction used to specify the boundary condition of zero streamwise velocity and zero temperature difference. The grid functions must approach these values smoothly in an asymptotic fashion. Physically, this means that a zero velocity at the edge of the boundary layer must also have a vanishing shear, and that a zero temperature difference must be accompanied by a vanishingly small heat flux.

For this problem, the sum of the squares of the two nondimensional variables representing fluid shear and heat flux at the edge of the boundary layer is monitored. If this sum is not sufficiently small, on the order of $10^{-6}$ or less, then a larger finite value for the edge of the boundary layer is chosen and the computations are repeated. This procedure is repeated until both the Newton iterates and the sum of the squares of the shear and temperature gradient at the edge of the boundary layer are within sufficiently small tolerances.

After Newton iteration convergence at each streamwise station, values of the solution are saved at all the mesh points. The solution is then plotted on a personal computer in order to insure proper asymptotic behavior of the solution. If proper asymptotic behavior of the solution near the edge of the boundary layer is not graphically observed, a larger finite value for the edge of the boundary layer is chosen and the computations are again repeated.

Ascher and Russel (1981) present an analysis that employs many methods of dealing with a semi-infinite computational domain. The method of arbitrarily assigning a sufficiently large value for the edge of the boundary layer, as described above, is the easiest of the methods presented by Ascher and Russel to incorporate but yields quite satisfactory results.

The Keller Box method has one disadvantage in that values for previous streamwise stations must be computed in order to advance the solution in the streamwise direction; that is, the method is not locally autonomous. The nonsimilarity method of Sparrow et al. (1972) is, however, locally autonomous, in that the computation for any particular streamwise station does not need information from any other streamwise station.

Three subroutines were necessary for any particular case of interest: a main driver subroutine which controls the Newton iteration scheme and provides output information, a subroutine that sets up the coefficient matrices and right hand side residual vector, and a subroutine for solving a block tridiagonal matrix that was developed by Hindmarsh et al. (1977). The Keller Box numerical solution is solved with a personal computer having an Intel 80286 central processor and an Intel 80287 numerical data processor. Typical cases take approximately one or two minutes for a solution to be obtained.

## APPENDIX B

## REYNOLDS AVERAGING OF THE GOVERNING EQUATIONS

The nonlinear Navier-Stokes equations, as developed for natural convection flow, are valid at any point in the fluid. When turbulence is observed, small macroscopic size "lumps" of fluid seem to move in an apparently random fashion. Exact solution of the governing equations under such conditions would require a great deal of computational resources in order to calculate the flow quantities at the fine level of detail required. According to White (1974), Reynolds (1895) proposed that the flow quantities be represented as a statistically-averaged mean value that slowly varies with respect to time and a fast-varying component that represents the instantaneous change with respect to time. For example, the velocity, $u$, in the streamwise direction is assumed to consist of two components as follows:

$$u = \overline{u} + u' \tag{B-1}$$

where $\overline{u}$ is defined as

$$\overline{u} = \frac{1}{\delta t}\int_{t}^{t+\delta t} u\,dt = (\text{mean value of } u) \tag{B-2}$$

and $\delta t$ is "sufficiently longer" than the relevant time period of the fluctuations. The mean value $\overline{u}$ may vary slowly over the time period of interest in any particular problem, although in this dissertation, only steady-state conditions are of interest and, therefore, time-varying mean turbulence conditions were not considered.

In a manner analogous to that used for the streamwise velocity, the other flow variables of interest, including the cross-stream velocity, the fluid temperature, and the particle concentration are decomposed into a mean value and a time-varying component as follows:

$$v = \overline{v} + v', \qquad T = \overline{T} + T', \quad \text{and} \quad n = \overline{n} + n'. \tag{B-3}$$

For simplicity, fast fluctuating components of the fluid thermophysical properties are not considered in this brief analysis. Humphrey et al. (1985) present a Reynolds averaging analysis for the turbulent natural convection equations in which a fluctuating component of the fluid density is considered. The resulting equations, as might be expected, are more complicated and show more coupling between the various equation components.

From the defining integral, the mean value of the fluctuating component must be zero, as shown here:

$$\overline{u'} = \frac{1}{\delta t}\int_t^{t+\delta t} u'dt = \frac{1}{\delta t}\int_t^{t+\delta t}(\overline{u}-u)dt = \overline{u}-\frac{1}{\delta t}\int_t^{t+\delta t} u dt = 0. \qquad \text{(B-4)}$$

Relationships for the product of any two turbulently fluctuating quantities may be developed from the defining integral relationship for a mean averaged quantity. For example, the product of the normal and streamwise velocities is developed in the following manner.

$$\overline{uv} = \frac{1}{\delta t}\int_t^{t+\delta t}(\overline{u}+u')(\overline{v}+v')dt = \overline{uv}+\overline{u'v'}. \qquad \text{(B-5)}$$

The following time averaging rules were similarly derived.

$$\overline{\overline{uv}} = \overline{uv}, \quad \overline{u'\overline{v}} = 0, \quad \overline{u+v} = \overline{u}+\overline{v}, \quad \text{and} \quad \overline{\frac{\partial u}{\partial x}} = \frac{\partial \overline{u}}{\partial x}. \qquad \text{(B-6)}$$

For the fluid continuity equation, the time averaging procedure results in the following relationship:

$$\frac{\partial \overline{u}}{\partial x}+\frac{\partial \overline{v}}{\partial y} = 0. \qquad \text{(B-7)}$$

The equation for Newton's Second Law as written in repeated indices notation for incompressible flow is time-averaged with the following results.

$$\rho\overline{u}_j\frac{\partial\overline{u}_i}{\partial x_j}+\rho\frac{\partial}{\partial x_j}(\overline{u_i'u_j'}) = \frac{\partial}{\partial x_j}\left[\mu\left(\frac{\partial\overline{u}_i}{\partial x_j}+\frac{\partial\overline{u}_j}{\partial x_i}\right)\right]-\frac{\partial\overline{P}}{\partial x_i}. \qquad (B-8)$$

The turbulent shear stress terms are written as if they were viscous stress terms by factorization of the spatial partial differential operator. The total apparent shear stress term is given by the following expression:

$$\tau_{ij} = \mu\left(\frac{\partial\overline{u}_i}{\partial x_j}+\frac{\partial\overline{u}_j}{\partial x_i}\right)-\rho\overline{u'_iu'_j}. \qquad (B-9)$$

The total apparent shear stress now consists of a laminar newtonian component plus an apparent turbulent component. The turbulent component is not only a function of fluid velocity, but also of geometry. Representation of this stress term is usually based upon empirical information. A turbulent eddy viscosity is defined in boundary layer analysis (Gebhart at al., 1988) for the largest (usually the normal) component of the turbulent shear stress in the following form:

$$\varepsilon_M = \frac{\mu_t}{\rho} = -\frac{\overline{u'v'}}{\partial\overline{u}/\partial y}. \qquad (B-10)$$

The total normal shear stress is then represented as the following:

$$\tau_{xy} = (\nu+\varepsilon_M)\frac{\partial\overline{u}}{\partial y}. \qquad (B-11)$$

The Reynolds averaging technique is also performed on the conservation of energy equation for steady-state incompressible flow with no heat sources or participating radiation heat transfer with the following result:

$$\rho C u_j\frac{\partial\overline{T}}{\partial x_j} = -\frac{\partial}{\partial x_j}(q_j)+\overline{\Phi}, \qquad (B-12)$$

where the turbulent viscous dissipation term is

$$\overline{\Phi} = \frac{\mu}{2}\overline{\left(\frac{\partial u_i}{\partial x_j}+\frac{\partial u_i'}{\partial x_j}+\frac{\partial u_j}{\partial x_i}+\frac{\partial u_j'}{\partial x_i}\right)^2}, \tag{B-13}$$

and the apparent total heat flux term is

$$q_j = -k\frac{\partial \overline{T}}{\partial x_j}+\rho C\overline{u_j'T'}. \tag{B-14}$$

The viscous heat generation term is quite complicated and is negligible with respect to the other terms in the conservation of energy equation under the conditions of interest here, as shown in Appendix D. White (1974) claims that for two-dimensional boundary layer flows, the viscous dissipation term reduces to the following expression:

$$\overline{\Phi} = \frac{\partial \overline{u}}{\partial y}\left(\mu\frac{\partial \overline{u}}{\partial y}-\rho\overline{u'v'}\right). \tag{B-15}$$

The equation for conservation of particles was also Reynolds time-averaged. In the absence of Brownian diffusion and for constant thermophysical properties, this equation may be written in cartesian coordinates in the following form:

$$\frac{\partial}{\partial x}(uN)+\frac{\partial}{\partial y}(vN)+\frac{\partial}{\partial y}(V_T N) = 0. \tag{B-16}$$

Equation (B-16) was Reynolds time-averaged and the following equation results:

$$\frac{\partial}{\partial x}(\overline{u}\overline{N})+\frac{\partial}{\partial y}(\overline{v}\overline{N})+\frac{\partial}{\partial y}(\overline{V}_T\overline{N})+\frac{\partial}{\partial x}(\overline{u'N'})+\frac{\partial}{\partial y}(\overline{v'N'})+\frac{\partial}{\partial y}(\overline{V'_T N'}) = 0. \tag{B-17}$$

As might be expected, there are terms that can be interpreted as representing the apparent turbulent diffusion of particles. There is also a term that Rosner and Fernandez de la Mora (1982) call "eddy thermophoresis." This additional Reynolds-averaged term results from the simultaneous fluctuation of the particle concentration and the thermophoretic velocity. Rosner and Fernandez de la Mora (1982) neglect eddy thermophoresis within the boundary layer with the argument that near the wall where

the thermophoretic velocity is high, the turbulence is small and that away from the wall where the turbulence is high, the thermophoretic velocity is small. They further argue that in boundary layer analysis, the turbulence term arising from the convective terms in the conservation equation is generally much larger than any other turbulence terms. Based on the lack of experimental justification that would verify the existence of eddy thermophoresis and the qualitative arguments of Rosner and Fernandez de la Mora (1982), eddy thermophoresis is neglected in the present work.

# APPENDIX C

# THERMOPHORESIS

## C.1. Introduction

Thermophoresis is defined as the phenomenon by which a small particle suspended in a gas moves in the direction opposite to that of an imposed temperature gradient. Although it exists only for flows with Knudsen numbers greater than zero and is, therefore, a rarefied flow phenomenon, thermophoresis can occur in practical engineering applications such as the deposition of combustion byproducts on cooled gas turbine blades and heat exchanger surfaces (Rosner and Seshadri, 1981). The thermophoretic deposition of aerosol particles on the order of one micrometer in diameter is of interest in this dissertation.

Maxwell (Kennard, 1938), while investigating the radiometer effect, became the first to successfully describe the physical principles of the thermal force which brings about thermophoresis. Epstein (1929) utilized those concepts of Maxwell and developed an expression for the thermophoretic force applicable for the slip flow regime for which the Knudsen number is in the range $0 < Kn < 0.25$ (Hidy and Brock, 1970). This expression of Epstein was found to reasonably predict the thermophoretic force on particles having relatively low thermal conductivities with respect to the thermal conductivity of the fluid. However, this Epstein expression was found to underpredict the thermophoretic force by a factor of thirty to fifty (Brock, 1962) for particles with relatively high thermal conductivities with respect to the thermal conductivity of the fluid.

Brock (1962) presents a derivation for the thermophoretic force by assuming that the fluid movement around the particle can be described by the classic creeping flow analysis of Stokes (Lamb, 1932) for a sphere in a very viscous fluid. This "hydrodynamic assumption" of particle movement, valid for the slip flow regime, resulted in an expression that predicts thermophoretic velocities that agree reasonably well with exper-

imental data for particles having relatively high thermal conductivities with respect to that of the fluid. Brock's expression reduces to Epstein's expression for particles with relatively low values of thermal conductivity.

Talbot (1980) presents a summary of three other methods of analysis for the thermal force, in addition to the hydrodynamic approach. These three other methods are based on higher order kinetic theory, irreversible thermodynamics, and solutions of the Boltzmann equation. The slip flow, or hydrodynamic, approach is the simplest method and apparently yields the most satisfactory results. The hydrodynamic approach of Brock is summarized below and then expanded upon to include the effect of a volumetric heat source on the thermophoretic velocity of the particle. The variation of the thermophoretic velocity with respect to temperature is also investigated.

## C.2. Development of an Expression for Thermophoretic Velocity

### C.2.1. Physical origin and rarefied flow parameters

Maxwell, as described in Kennard (1938), proposed a physical explanation for what was called the "radiometric force," which includes the effects of both thermophoresis and photophoresis. At a solid boundary in a nonuniformly heated gas, Maxwell showed that a "thermal creep" flow exists for flows with Knudsen numbers greater than zero.

Talbot (1980), in explaining Maxwell's derivation, states that a molecule obliquely striking the boundary delivers more tangential momentum to the boundary if the molecule originates in a hotter region of the gas than if it originates in a colder region, excluding specular reflection. Talbot proposed a thermal gradient in a gas inclined with respect to a wall as shown in Figure C-1, with forces caused by the rebounding molecules as shown in Figure C-2. For these two figures, $s$ is in a direction along the surface and $n$ is in a direction normal to the surface. Note that on a molecular scale, the surface will not be smooth and specular reflection cannot be expected.

As shown in Figure C-2, the incident molecule from the hotter region above the surface normal having velocity $u_h$ rebounds off the wall with velocity $u_h'$, losing some tangential momentum to the wall opposite to the direction of the thermal gradient. The incident molecule from the colder region below the surface normal having velocity $u_c$

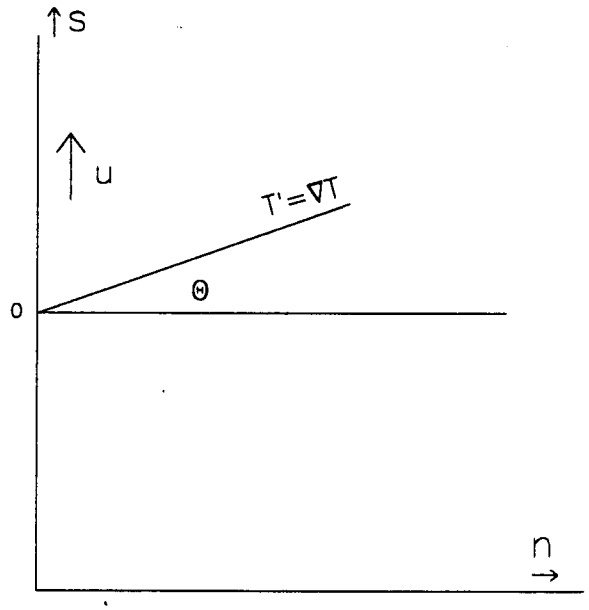


Figure C-1. Thermal Creep Flow Schema.

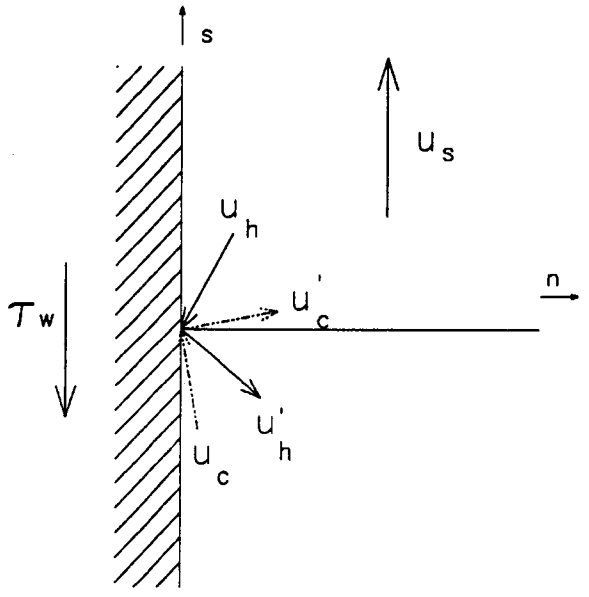


Figure C-2. Thermal Creep Force Balance.

would rebound with velocity $u_c'$, losing tangential momentum to the wall in the direction of the thermal gradient. Since, on the average, $u_h$ is greater than $u_c$, an unequal transfer of tangential momentum from the molecules in a fluid to the wall results in a shear stress $\tau_w$ on the wall in the direction of the thermal gradient. In order to maintain equilibrium, in the absence of a pressure gradient, velocity $u_s$ towards the hotter region is induced in the gas adjacent to the boundary.

Kennard (1938) presents an expression for the thermal creep velocity adjacent to a stationary boundary in a nonuniformly heated gas by integrating the Maxwell velocity distribution with the assumption that the net tangential momentum of molecules after reflection from the wall is balanced by momentum supplied by fluid movement and that the velocity distribution of the molecules is unchanged by the collision with the wall. The resulting thermal creep velocity of the gas is given by the following expression:

$$u_s = \frac{3}{4}\frac{\mu}{\rho T}\frac{\partial T}{\partial s}, \tag{C-1}$$

where $u_s$ is the thermal creep velocity and $s$ is the direction along the solid boundary.

Kennard (1938) also shows that a tangential slip velocity exists in an isothermal flow with a non-zero Knudsen number flows at a stationary wall. The total tangential slip velocity at the wall is the following expression (Talbot et al., 1980):

$$u_s = C_m \lambda \left(\frac{\partial u}{\partial n}\right)_w + C_s \frac{\mu}{\rho T}\left(\frac{\partial T}{\partial s}\right)_w, \tag{C-2}$$

where $n$ is in the direction normal to the solid boundary.

The term $\lambda$ is the mean free path based on viscosity, calculated as

$$\lambda = \frac{2\mu}{\rho \bar{c}} = \frac{2\mu}{\rho}\left(\frac{\pi}{8\mathcal{R}T}\right)^{1/2}, \tag{C-3}$$

where $\mu$ is the dynamic viscosity, $\rho$ is fluid density, and $\bar{c}$ is the mean molecular speed.

According to Talbot (1980), the first term on the right hand side of equation (C-2) represents a velocity slip condition where $C_m$ is called a momentum exchange coefficient, and the second term on the right hand side represented the contribution of temperature to the velocity slip at the interface, where $C_s$ is called a thermal slip coefficient. Both the coefficients $C_m$ and $C_s$ are of order unity and are dependent on molecular interaction of the gas and the wall. These coefficients are discussed below. Since the viscosity $\mu$ can be written in terms of the mean free path as defined in equation (C-3), both terms on the right hand side of equation (C-2) are directly proportional to the mean free path.

Another rarefied flow phenomenon existing at the interface between the wall and the fluid immediately adjacent is the temperature jump condition. According to Kennard (1938), Poisson postulated the existence of a temperature discontinuity at the interface of a solid boundary, analogous to the velocity slip at the interface. Smoluchowski (1898) experimentally confirmed this temperature jump. The temperature jump interface condition has the following form:

$$(T_f - T_w)_w = C_t \lambda \left( \frac{\partial T_f}{\partial n} \right)_w , \tag{C-4}$$

where $n$ is in the direction normal to the surface and $C_t$ is called the thermal accommodation coefficient. The value of thermal accommodation coefficient, which is dependent on the molecular interaction at the surface, is discussed below.

Values for the momentum exchange (or isothermal slip) coefficient, $C_m$, the thermal slip coefficient, $C_s$, and the temperature jump coefficient, $C_t$, are discussed by Talbot et al. (1980). A value of the thermal slip coefficient $C_s$ equal to three-fourths was originally derived by Maxwell under the assumption that the molecular velocity distribution was unchanged by the presence of the solid surface (Kennard, 1938), as can be seen in equation (C-1). According to Talbot (1980), Ivechenko and Yalamov (1971) present a more refined kinetic theory analysis and developed a value for $C_s$ of 1.17 for complete thermal accommodation.

Thermal accommodation, as defined by Kennard (1938), is a process that takes place at the solid surface such that any molecule that impacts on the surface has its mean energy adjusted, or "accommodated," to that of a gas at the surface temperature of the solid. The temperature jump coefficient, $C_t$, and the momentum exchange coefficient, $C_m$, were defined by Waldmann and Schmitt (1966) as follows:

$$C_t \equiv \left(\frac{15}{8}\right)\frac{2-\alpha_t}{\alpha_t} \quad \text{and} \quad C_m \equiv \frac{2-\alpha_m}{\alpha_m}. \tag{C-5}$$

$\alpha_t$ is defined as the thermal accommodation coefficient and $\alpha_m$ as the momentum accommodation coefficient. These coefficients have the following representations at the particle-gas interface:

$$\alpha_t \equiv \frac{E_i - E_r}{E_i - E_w} \quad \text{and} \quad \alpha_m \equiv \frac{G_i - G_r}{G_i}. \tag{C-6}$$

In equation (C-6), $E$ represents the molecular thermal energy, $G$ the molecular tangential momentum, the subscript $i$ stands for "incidence," the subscript $r$ represents "reflection," and the subscript $w$ stands for "wall conditions." The thermal accommodation coefficient represents the fraction of the energy retained by a reflected molecule in a surface collision. The momentum accommodation coefficient represents the fraction of the molecular tangential momentum retained by the surface in such a collision. Kennard (1938) remarks that the momentum accommodation coefficient could have a value greater than unity for the case of partial tangential reflection in which the direction of the molecule is reversed on reflection. Indeed, for the case of complete tangential reflection, the molecule is reflected directly backwards with no change in speed, which gives a momentum accommodation coefficient of two and a momentum exchange coefficient of zero that results in no momentum slip.

Waldmann and Schmitt (1966) did not elaborate on the derivation of equations (C-5). Kennard (1938) presents an analysis for the derivation of these equations based on a Maxwellian velocity distribution in the vicinity of the solid surface. Hidy and Brock (1970) present these coefficients in the following forms:

$$C_m = P_m\left(\frac{2-\alpha_m}{\alpha_m}\right) \quad \text{and} \quad C_t = P_t\left(\frac{2-\alpha_t}{\alpha_t}\right), \tag{C-7}$$

where $1.0 \le P_m \le 1.272$ and $1.875 \le P_t \le 2.48$.

Talbot et al. (1980) refer to previous investigations by Loyalka and Ferziger (1967) and Loyalka (1968), where a variational technique was used to solve the linearized Boltzmann equation that gives a value of 1.14 for $C_m$ and a value of 2.18 for $C_t$. Since the exact values of these slip flow parameters of $C_m$, $C_t$, and $C_s$ may require experiments with the actual aerosol geometry and the gas at the stated conditions of temperature and pressure, the values used for these slip flow parameters in this dissertation were those of Talbot et al. (1980).

### C.2.2. The hydrodynamic approximation for thermophoretic velocity

The slip-flow Knudsen number regime is of interest in this dissertation, which is $0 < Kn < 0.25$. The hydrodynamic approximation, originally suggested by Maxwell in 1890 (Hidy and Brock, 1970), consists of assuming that the Navier-Stokes equations of motion and the conservation of energy equation for the fluid are valid up to the wall, subject to slip-corrected boundary conditions. This assumption is questionable for Knudsen numbers larger than 0.25 (Hidy and Brock, 1970) where there is a large departure from continuum conditions, and, therefore, represents an upper limit for thermal force correlations based on the hydrodynamic approximation.

For large Knudsen numbers, the mean free path of a fluid molecule would be much longer with respect to the characteristic particle dimension and, therefore, the particle would have little influence upon the flow velocity and temperature fields. Hidy and Brock (1970) present analyses of the thermal force for the free molecular flow regime

($Kn \geq 10$) and for the transition regime ($Kn \approx 1$). Analysis of these two flow regimes generally requires solution of the Boltzmann equation (Schaff and Chambré, 1961) for the velocity distribution of the gas molecules.

Both Epstein (1929) and Brock (1962) solve for the thermal creep, or thermophoretic, velocity of a moving particle by using the hydrodynamic procedure. In this approach, the differential equations governing the temperature distribution in the particle and the velocity and temperature distributions in the fluid adjacent to the particle are each written separately. Matching boundary conditions at the surface of the particle are specified to close the system of differential equations. These analyses are summarized below. Both analyses use the Stokes approximation to obtain the velocity distribution in the fluid surrounding the particle and the same conservation of energy equation in the sphere, but differ in the conservation of energy equation for the fluid and the matching conditions at the sphere and fluid interface.

#### C.2.2.1. Analysis for velocity and temperature distributions

The particle geometry is assumed to be a sphere as shown on Figure C-3. The ambient temperature in the surrounding fluid far from the sphere is that corresponding to a constant temperature gradient $\nabla T_{\infty}$. The spherical coordinate system is positioned such that the origin is at the center of the spherical particle and the start of the azimuthal coordinate $\theta$ is in the direction of the uniform temperature gradient. Symmetry about the $\Phi$ axis is assumed so that derivatives with respect to $\Phi$ are zero. For the following analysis, the particle is stationary and all velocities of the fluid are relative to the origin at the center of the particle.

For steady-state conditions, the energy equation for the fluid is given by

$$\frac{1}{r^2}\frac{\partial}{\partial r}\left(r^2\frac{\partial T_f}{\partial r}\right)+\frac{1}{r^2\sin\theta}\frac{\partial}{\partial\theta}\left(\sin\theta\frac{\partial T_f}{\partial\theta}\right)=\frac{1}{\alpha}\left(\frac{u_\theta}{r}\frac{\partial T_f}{\partial\theta}+u_r\frac{\partial T_f}{\partial r}\right), \tag{C-8}$$

which expresses a balance between conduction and convection in the fluid.

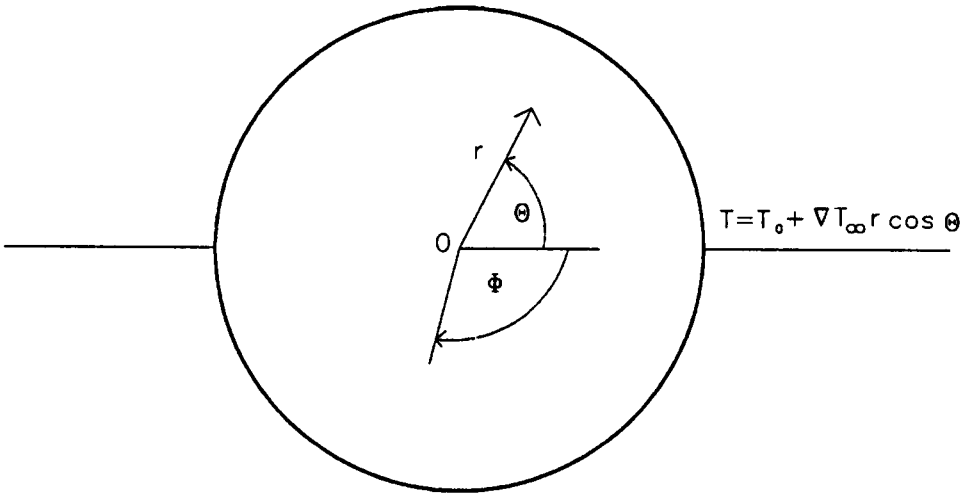


Figure C-3. Spherical Particle Geometry.

Also, for steady-state thermal conditions, in the absence of volumetric heat sources, the conduction heat transfer within the spherical particle is given by:

$$\frac{1}{r^2}\frac{\partial}{\partial r}\left(r^2\frac{\partial T_s}{\partial r}\right)+\frac{1}{r^2\sin\theta}\frac{\partial}{\partial\theta}\left(\sin\theta\frac{\partial T_s}{\partial\theta}\right)=0. \qquad \text{(C-9)}$$

A volumetric heat source and the effects of transient energy storage in the spherical particle are considered later in the analysis.

One interface, or matching, condition between the solution domains of the sphere and the fluid is the heat flux at the surface of the particle which may be expressed as:

$$k_f\left(\frac{\partial T_f}{\partial r}\right)_{r=R}=k_s\left(\frac{\partial T_s}{\partial r}\right)_{r=R}. \qquad \text{(C-10)}$$

Another interface condition is the rarefied flow temperature jump at the interface between the sphere and the fluid of equation (C-4). For the spherical coordinates of the present problem, the temperature jump interface condition has the following form:

$$(T_f - T_s)_{r=R} = C_t \lambda \left( \frac{\partial T_f}{\partial r} \right)_{r=R} . \tag{C-11}$$

The boundary condition on the fluid temperature distribution far from the sphere is of the following form:

$$T_f = T_0 + \nabla T_\infty r \cos\theta \quad \text{as} \quad r \to \infty . \tag{C-12}$$

This form for the bounding condition of the fluid temperature is chosen so that the thermal force on the particle is along the axis opposite to the direction of the temperature gradient. The temperature at the center of the sphere, $T_0$, need not be specified for the purposes of the present work, but must be finite. Note that although the fluid temperature seems to be unbounded as $r$ goes to infinity, the value for the angle $\theta$ remains unspecified. "Infinity" for the purposes of imposing a bounding condition on the fluid temperature far from the particle means simply that $r$ is sufficiently far from the particle so that the influence of the particle on the fluid temperature is negligible and not that the actual fluid temperature actually grows unbounded.

The Newton's Second Law equation for the fluid has the usual form in repeated indices notation (White, 1974):

$$\rho \frac{\partial u_i}{\partial t} + u_j \frac{\partial u_i}{\partial x_j} = \frac{\partial}{\partial x_j} \left[ \mu \left( \frac{\partial u_i}{\partial x_j} + \frac{\partial u_j}{\partial x_i} \right) \right] - \frac{\partial P}{\partial x_i} . \tag{C-13}$$

For the so-called Stokes approximation for very low Reynolds number flow, all inertial force terms, the left hand side of equation (C-13), may be neglected with respect to the viscous and pressure terms. The resulting equation is the following:

$$\frac{\partial}{\partial x_j}\left[\mu\left(\frac{\partial u_i}{\partial x_j}+\frac{\partial u_j}{\partial x_i}\right)\right] = \frac{\partial P}{\partial x_i}. \tag{C-14}$$

In spherical coordinates, equation (C-14) is written as the following two equations in the radial direction, $r$, and the tangential direction, $\theta$.

$$\mu\left[\frac{1}{r^2}\frac{\partial}{\partial r}\left(r^2\frac{\partial u_\theta}{\partial r}\right)+\frac{1}{r^2\sin\theta}\frac{\partial}{\partial\theta}\left(\sin\theta\frac{\partial u_\theta}{\partial\theta}\right)+\frac{2}{r^2}\frac{\partial u_r}{\partial\theta}-\frac{u_\theta}{r^2\sin^2\theta}\right] = \frac{1}{r}\frac{\partial P}{\partial\theta}. \tag{C-15}$$

$$\mu\left[\frac{1}{r^2}\frac{\partial}{\partial r}\left(r^2\frac{\partial u_r}{\partial r}\right)+\frac{1}{r^2\sin\theta}\frac{\partial}{\partial\theta}\left(\sin\theta\frac{\partial u_r}{\partial\theta}\right)-\frac{2u_r}{r^2}-\frac{2}{r^2\sin\theta}\frac{\partial(u_\theta\sin\theta)}{\partial\theta}\right] = \frac{\partial P}{\partial r}. \tag{C-16}$$

Conservation of mass for this flow yields:

$$\frac{\partial u_i}{\partial x_i} = 0. \tag{C-17}$$

In spherical coordinates, equation (C-17) is written as the following:

$$\frac{1}{r^2}\frac{\partial}{\partial r}(r^2u_r)+\frac{1}{r\sin\theta}\frac{\partial}{\partial\theta}(u_\theta\sin\theta) = 0. \tag{C-18}$$

In equations (C-15), (C-16), and (C-18), the fluid velocity is that relative to the particle, and therefore must vanish "sufficiently far away" from the spherical particle. The fluid continuity equation, equation (C-18), does not contain any terms representing evaporation or condensation of volatile gas species on the particle. A particle-gas interface condition of zero radial velocity at the surface of the sphere results from this requirement of no mass exchange between the particle and the fluid.

A streamfunction $\psi$ is defined in the usual manner so that the fluid continuity equation, equation (C-18), is identically satisfied as follows:

$$u_r \equiv \frac{1}{r^2 \sin\theta}\frac{\partial \psi}{\partial \theta} \quad \text{and} \quad u_\theta \equiv -\frac{1}{r \sin\theta}\frac{\partial \psi}{\partial r}. \tag{C-19}$$

The vector curl operator is applied to equation (C-14), or equivalently, equations (C-15) and (C-16) are cross-differentiated and then subtracted, and the identities of equation (C-19) are then substituted so that the equation for Newton's Second Law may be written in terms of the streamfunction as follows:

$$\left[\frac{\partial^2}{\partial r^2} + \frac{\sin\theta}{r^2}\frac{\partial}{\partial \theta}\left(\frac{1}{\sin\theta}\right)\frac{\partial}{\partial \theta}\right]^2 \psi = 0. \tag{C-20}$$

The solution to this fourth order partial differential equation of the biharmonic operator is obtained with the separation of variables method. The details of this solution are described in Lamb (1932). This solution is as follows:

$$\psi = \left(\frac{\hat{A}}{r} + \hat{B}r + \hat{C}r^2 + \hat{D}r^4\right)\sin^2\theta, \tag{C-21}$$

where $\hat{A}$, $\hat{B}$, $\hat{C}$, and $\hat{D}$ are arbitrary constants to be determined by the boundary conditions.

"Sufficiently far away" from the particle, the velocity must be zero. From inspection of the identities of equation (C-10), the streamfunction must be zero. This boundary condition requires that the two arbitrary constants $\hat{C}$ and $\hat{D}$ be zero. On substitution of the defining relations for the radial and angular velocities in terms of the streamfunction, the normal and tangential velocity components are the following:

$$u_r = \frac{2\cos\theta}{r}\left(\frac{\hat{A}}{r^2} + \hat{B}\right). \tag{C-22}$$

$$u_\theta = \frac{\sin\theta}{r}\left(\frac{\hat{A}}{r^2} - \hat{B}\right). \tag{C-23}$$

The bounding conditions on the particle are used to determine the remaining two constants. The requirement of zero normal velocity at the surface of the sphere is used to write one constant of equation (C-22) in terms of the other such that the velocities are written as follows:

$$u_r = \frac{2\hat{A}\cos\theta}{R^3}\left[\left(\frac{R}{r}\right)^3 - \frac{R}{r}\right]. \tag{C-24}$$

$$u_\theta = \frac{\hat{A}\sin\theta}{R^3}\left[\left(\frac{R}{r}\right)^3 + \frac{R}{r}\right]. \tag{C-25}$$

At this point in the analysis, the energy equation with the boundary condition at the sphere surface and the tangential velocity boundary condition at the sphere surface used by Epstein (1929) and Brock (1962) are different. The remaining constant, $\hat{A}$, is determined by evaluation of the tangential slip velocity at the interface. It is at this point that thermal creep flow is manifested as a rarefied flow phenomenon, since the no-slip velocity interface condition of continuum flow would result in a value of zero for $\hat{A}$ and a streamfunction equal to zero everywhere, signifying no flow.

#### C.2.2.2. The analysis of Epstein

Epstein (1929) neglects the right hand side of the energy conservation equation in the fluid, equation (C-8). This assumption of Epstein neglects convective effects on the temperature distribution in the fluid as compared to the conductive effects. This assumption is consistent with the neglect of the inertia terms of the equation of motion, equation (C-14), for the Stokes approximation of very low Reynolds number flows. The energy equation for both the sphere and the fluid surrounding it are the following:

$$\frac{1}{r^2}\frac{\partial}{\partial r}\left(r^2\frac{\partial T_s}{\partial r}\right)+\frac{1}{r^2\sin\theta}\frac{\partial}{\partial\theta}\left(\sin\theta\frac{\partial T_s}{\partial\theta}\right)=0\,,\qquad 0\le r\le R\,. \tag{C-26}$$

$$\frac{1}{r^2}\frac{\partial}{\partial r}\left(r^2\frac{\partial T_f}{\partial r}\right)+\frac{1}{r^2\sin\theta}\frac{\partial}{\partial\theta}\left(\sin\theta\frac{\partial T_f}{\partial\theta}\right)=0\,,\qquad R\le r\le\infty\,. \tag{C-27}$$

As shown by Kreyszig (1983), Laplace's equation in spherical coordinates may be solved with the separation of variables method. The general solution is the following infinite series in terms of the radius and the Legendre polynomials, $P_n$:

$$T(r,\theta)=\sum_{n=0}^{\infty}A_n r^n P_n(\cos\theta)+\sum_{n=0}^{\infty}\frac{B_n}{r^{n+1}}P_n(\cos\theta)\,,\quad n=0,1,\ldots \tag{C-28}$$

The Legendre polynomials can be found in Kreyszig (1983). Equation (C-28) is applied in the solution domains of the spherical particle and the surrounding fluid.

For the spherical particle, all the coefficients $B_n$ of equation (C-28) for the sphere must be zero in order to have a finite temperature at the center of the sphere. For the fluid, the temperature distribution far from the sphere is given by equation (C-12). The coefficient $A_0$ must therefore be the finite sphere center temperature $T_0$, the coefficient $A_1$ must be $\nabla T_\infty$, and all other coefficients $A_n$ for the fluid must be zero. The general solutions for the temperature distributions in the sphere and fluid reduce to the following.

$$T_s(r,\theta)=T_0+\sum_{n=1}^{\infty}A_n r^n P_n(\cos\theta)\,,\qquad n=1,2,\ldots \tag{C-29}$$

$$T_f(r,\theta)=T_0+\nabla T_\infty\, r\cos\theta+\sum_{n=0}^{\infty}\frac{B_n}{r^{n+1}}P_n(\cos\theta)\,,\qquad n=0,1,\ldots \tag{C-30}$$

Epstein does not consider the temperature jump condition of equation (C-11), but uses instead equal fluid and sphere temperatures at the interface. Equations (C-29) and (C-30) are matched at the radius $R$ to give the following:

$$\nabla T_{\infty} R\cos\theta + \sum_{n=0}^{\infty} \frac{B_n}{R^{n+1}} P_n(\cos\theta) = \sum_{n=1}^{\infty} A_n R^n P_n(\cos\theta)\,. \tag{C-31}$$

Equation (C-31) is rearranged to give:

$$\frac{B_0}{R} + \sum_{n=1}^{\infty} R^n P_n(\cos\theta)\left(A_n - \frac{B_n}{R^{2n+1}}\right) = \nabla T_{\infty} R\cos\theta\,. \tag{C-32}$$

Equation (C-32) yields the following relationships for the coefficients $A_n$ for the sphere and the coefficients $B_n$ for the fluid.

$$B_0 = 0\,, \tag{C-33}$$

$$A_1 - \frac{B_1}{R^3} = \nabla T_{\infty}\,, \tag{C-34}$$

$$A_n - \frac{B_n}{R^{2n+1}} = 0\,, \qquad n > 1\,. \tag{C-35}$$

Another interface condition used by Epstein was the heat flux interface condition of equation (C-10). Differentiating equations (C-29) and (C-30) with respect to $r$, evaluating at the radius $R$, and substituting into equation (C-10) gives the following:

$$k_s \sum_{n=1}^{\infty} n A_n R^{n-1} P_n(\cos\theta) = k_f\left[\nabla T_{\infty}\cos\theta - \sum_{n=1}^{\infty}(n+1)\frac{B_n}{R^{n+2}} P_n(\cos\theta)\right]. \tag{C-36}$$

Equation (C-36) is rearranged to the following form.

$$\sum_{n=1}^{\infty} R^{n-1} P_n(\cos\theta)\left[n A_n + \frac{k_f}{k_s}(n+1)\frac{B_n}{R^{2n+1}}\right] = \frac{k_f}{k_s}\nabla T_{\infty}\cos\theta\,. \tag{C-37}$$

Equation (C-37) establishes another relationship for the $A_n$ and the $B_n$ coefficients of the following form.

$$A_1 + 2\frac{k_f}{k_s}\frac{B_1}{R^3} = \frac{k_f}{k_s}\nabla T_\infty , \tag{C-38}$$

$$nA_n + (n+1)\frac{k_f}{k_s}\frac{B_n}{R^{2n+1}} = 0, \qquad n > 1 . \tag{C-39}$$

Equations (C-34), (C-35), (C-38), and (C-39) are sufficient to determine the value for each $A_n$ and $B_n$ coefficient. For $n = 1$, simultaneous solution of equations (C-34) and (C-38) yields the following expressions:

$$A_1 = \nabla T_\infty \left( \frac{3k_f}{2k_f + k_s} \right). \tag{C-40}$$

$$B_1 = R^3 \nabla T_\infty \left( \frac{k_f - k_s}{2k_f + k_s} \right). \tag{C-41}$$

For $n$ greater than 1, simultaneous solution of equations (C-35) and (C-39) yields the following general expression for the coefficients $B_n$.

$$B_n \left[ n + \frac{k_f}{k_s}(n+1) \right] = 0 . \tag{C-42}$$

Since the term in brackets of equation (C-42) is always positive for $n$ greater than one, all the coefficients $B_n$ for $n$ greater than one must be zero. The general solution for the temperature distribution in the sphere and the fluid reduces to the following expressions.

$$T_s(r,\theta) = T_0 + \left(\frac{3k_f}{2k_f + k_s}\right)\nabla T_\infty r\cos\theta\,. \tag{C-43}$$

$$T_f(r,\theta) = T_0 + \left[1 + \left(\frac{k_f - k_s}{2k_f + k_s}\right)\left(\frac{R}{r}\right)^3\right]\nabla T_\infty r\cos\theta\,. \tag{C-44}$$

Now with the temperature distribution in the fluid determined, Epstein then applies the thermal slip condition of equation (C-1) for the tangential velocity at the sphere surface in order to determine the last remaining undetermined constant for the streamfunction $\psi$. Taking the derivative of the fluid temperature of equation (C-44) with respect to $\theta$, evaluating the tangential velocity of equation (C-25) at the sphere radius, and solving for the remaining unknown constant of equation (C-25) yields the following equations for the tangential and radial fluid velocities:

$$u_\theta = -\frac{9}{8}\frac{\mu}{\rho T}\left(\frac{k_f}{2k_f + k_s}\right)\nabla T_\infty\left[\left(\frac{R}{r}\right)^3 + \frac{R}{r}\right]\sin\theta\,. \tag{C-45}$$

$$u_r = -\frac{9}{4}\frac{\mu}{\rho T}\left(\frac{k_f}{2k_f + k_s}\right)\nabla T_\infty\left[\left(\frac{R}{r}\right)^3 - \frac{R}{r}\right]\cos\theta\,. \tag{C-46}$$

The pressure distribution is readily obtained by integration of the equation for Newton's Second Law. Using the expressions for velocity of equations (C-45) and (C-46), integration of equation (C-16) yields the following pressure distribution:

$$P = P_\infty + \frac{9}{4}\frac{\mu^2}{\rho T}\left(\frac{k_f}{2k_f + k_s}\right)\frac{\nabla T_\infty}{r}\left(\frac{R}{r}\right)\cos\theta\,. \tag{C-47}$$

For a newtonian fluid, the viscous shear can be determined as follows:

$$\tau_{r\theta} = \mu\left(\frac{1}{r}\frac{\partial u_r}{\partial \theta} + \frac{\partial u_\theta}{\partial r}\right) = \frac{9}{8}\frac{\mu^2}{\rho T}\left(\frac{k_f}{2k_f + k_s}\right)\frac{\nabla T_\infty}{r}\left[5\left(\frac{R}{r}\right)^3 - \frac{R}{r}\right]\sin\theta\,. \qquad \text{(C-48)}$$

The net force in the direction of the imposed constant thermal gradient on the surface of the sphere caused by the thermal creep flow is determined by integration of the expressions for the pressure and shear stress as follows:

$$F_T = -\int_0^{\pi} (\tau_{r\theta}|_R \sin\theta + P|_R \cos\theta)\, dA\,, \quad \text{where} \quad dA = 2\pi R^2 \sin\theta\, d\theta\,. \qquad \text{(C-49)}$$

Evaluating equations (C-47) and (C-48) at the sphere radius $R$ and substituting into equation (C-49), Epstein obtains the following expression for the thermal force:

$$F_T = -9\pi R \frac{\mu^2}{\rho T}\left(\frac{k_f}{2k_f + k_s}\right)\nabla T_\infty\,. \qquad \text{(C-50)}$$

Brock (1962) claims that Epstein's expression underpredicts the thermal force by thirty to fifty times for aerosol particles with a large value of thermal conductivity as compared to the fluid thermal conductivity. From inspection of equation (C-50), as the particle thermal conductivity grows much larger than the fluid thermal conductivity, the thermal force predicted by equation (C-50) goes to zero. Schadt and Cadle (1961) report a value for thermophoretic force on sodium chloride particles approximately two orders of magnitude larger than that predicted by equation (C-50). Brock refined the hydrodynamic analysis of Epstein by inclusion of additional considerations as are shown in the following section.

#### C.2.2.3. The analysis of Brock

Brock (1962) refines the hydrodynamic analysis of Epstein (1929) by including additional slip flow interface boundary conditions between the particle and the adjacent fluid and specifically considers the convective movement of fluid around the particle in the conservation of energy equation. The analysis of Brock is summarized as follows.

The Stokes flow assumption for the flow of fluid around the particle is also invoked, that is, the inertial force terms in the equation for Newton's Second Law are neglected with respect to the viscous and pressure terms. The solution for the streamfunction develops as before, leaving the tangential and radial velocities in the fluid with one remaining arbitrary constant, as in equation (C-25), to be determined by evaluating the conservation of energy equations in the fluid and the sphere.

Brock (1962) includes two additional boundary conditions applicable in rarefied fluid flow. The first is the temperature jump interface condition of equation (C-4). For the geometry of the sphere in a fluid, this interface condition, as expressed in equation (C-11), is the following:

$$(T_f - T_s)_{r=R} = C_t \lambda \left( \frac{\partial T_f}{\partial r} \right)_{r=R} . \tag{C-51}$$

The second additional interface condition considered by Brock is the total slip-flow velocity at the particle surface of equation (C-2). For the spherical geometry, equation (C-2) is written in the following form.

$$u_\theta = C_m \lambda \left[ r \frac{\partial}{\partial r} \left( \frac{u_\theta}{r} \right) + \frac{1}{r} \frac{\partial u_r}{\partial \theta} \right]_{r=R} + C_s \frac{\mu}{\rho T} \frac{1}{R} \left( \frac{\partial T_f}{\partial \theta} \right)_{r=R} . \tag{C-52}$$

Brock uses the $C_s$ value of three-fourths, also used by Epstein, that was determined in Maxwell's derivation of equation (C-1). Since other analyses, such as the refined kinetic theory analysis by Ivchenko and Yalamov (1971), present different values for the thermal slip coefficient, the symbol $C_s$ is retained for the present description.

Brock also expands on the Epstein analysis by specifically addressing the effect of fluid convective movement around the sphere on the conservation of energy equation. The equations solved by Brock were those of Newton's Second Law, fluid mass continuity, conservation of energy in the fluid, and conservation of energy in the sphere. These are repeated here as the following:

$$\mu\left[\frac{1}{r^2}\frac{\partial}{\partial r}\left(r^2\frac{\partial u_\theta}{\partial r}\right)+\frac{1}{r^2\sin\theta}\frac{\partial}{\partial\theta}\left(\sin\theta\frac{\partial u_\theta}{\partial\theta}\right)+\frac{2}{r^2}\frac{\partial u_r}{\partial\theta}-\frac{u_\theta}{r^2\sin^2\theta}\right]=\frac{1}{r}\frac{\partial P}{\partial\theta}. \tag{C-53}$$

$$\mu\left[\frac{1}{r^2}\frac{\partial}{\partial r}\left(r^2\frac{\partial u_r}{\partial r}\right)+\frac{1}{r^2\sin\theta}\frac{\partial}{\partial\theta}\left(\sin\theta\frac{\partial u_r}{\partial\theta}\right)-\frac{2u_r}{r^2}-\frac{2}{r^2\sin\theta}\frac{\partial(u_\theta\sin\theta)}{\partial\theta}\right]=\frac{\partial P}{\partial r}. \tag{C-54}$$

$$\frac{1}{r^2}\frac{\partial}{\partial r}(r^2u_r)+\frac{1}{r\sin\theta}\frac{\partial}{\partial\theta}(u_\theta\sin\theta)=0. \tag{C-55}$$

$$\frac{1}{r^2}\frac{\partial}{\partial r}\left(r^2\frac{\partial T_s}{\partial r}\right)+\frac{1}{r^2\sin\theta}\frac{\partial}{\partial\theta}\left(\sin\theta\frac{\partial T_s}{\partial\theta}\right)=0, \qquad 0\le r\le R. \tag{C-56}$$

$$\frac{1}{r^2}\frac{\partial}{\partial r}\left(r^2\frac{\partial T_f}{\partial r}\right)+\frac{1}{r^2\sin\theta}\frac{\partial}{\partial\theta}\left(\sin\theta\frac{\partial T_f}{\partial\theta}\right)=\frac{1}{\alpha}\left(\frac{u_\theta}{r}\frac{\partial T_f}{\partial\theta}+u_r\frac{\partial T_f}{\partial r}\right), \qquad R\le r\le\infty. \tag{C-57}$$

Brock (1962) uses a perturbation expansion for solution of the above set of equations, equations (C-53) through (C-57), where the perturbation parameter, $\beta=C_s\frac{\mu}{\rho T}$, is suggested by its appearance in the interface thermal slip velocity condition, equation (C-52). These expansions are the following:

$$T_f=\sum_{i=0}\beta^iT_f^{(i)}. \tag{C-58}$$

$$T_s=\sum_{i=0}\beta^iT_s^{(i)}. \tag{C-59}$$

$$u_r=\sum_{i=0}\beta^{i+1}u_r^{(i+1)}. \tag{C-60}$$

$$u_\theta=\sum_{i=0}\beta^{i+1}u_\theta^{(i+1)}. \tag{C-61}$$

The following interface conditions at the sphere surface and boundary conditions sufficiently far from the sphere are applicable:

$$T_f^{(0)} = T_0 + \nabla T_\infty r\cos\theta, \qquad r \to \infty . \tag{C-62}$$

$$T_f^{(i)} = 0, \qquad i > 0, \qquad r \to \infty . \tag{C-63}$$

$$(T_f^{(i)} - T_s^{(i)})_{r=R} = C_t\lambda\left(\frac{\partial T_f^{(i)}}{\partial r}\right)_{r=R} . \tag{C-64}$$

$$k_f\left(\frac{\partial T_f^{(i)}}{\partial r}\right)_{r=R} = k_s\left(\frac{\partial T_s^{(i)}}{\partial r}\right)_{r=R} . \tag{C-65}$$

$$u_\theta^{(i+1)} = C_m\lambda\left[r\frac{\partial}{\partial r}\left(\frac{u_\theta^{(i+1)}}{r}\right) + \frac{1}{r}\frac{\partial u_r^{(i+1)}}{\partial\theta}\right]_{r=R} + \frac{1}{R}\left(\frac{\partial T_f^{(i)}}{\partial\theta}\right)_{r=R} . \tag{C-66}$$

$$u_r^{(i+1)} = 0, \quad r = R . \tag{C-67}$$

$$u_\theta^{(i+1)} = u_r^{(i+1)} = 0, \qquad r \to \infty . \tag{C-68}$$

Substitution for the expansion of the sphere temperature, equation (C-59), into the conservation of energy equation for the sphere, equation (C-56), and equating coefficients of equal powers of β, results in the following set of equations for the first two iterations:

$$\frac{1}{r^2}\frac{\partial}{\partial r}\left(r^2\frac{\partial T_s^{(0)}}{\partial r}\right) + \frac{1}{r^2\sin\theta}\frac{\partial}{\partial\theta}\left(\sin\theta\frac{\partial T_s^{(0)}}{\partial\theta}\right) = 0 . \tag{C-69}$$

$$\frac{1}{r^2}\frac{\partial}{\partial r}\left(r^2\frac{\partial T_s^{(1)}}{\partial r}\right) + \frac{1}{r^2\sin\theta}\frac{\partial}{\partial\theta}\left(\sin\theta\frac{\partial T_s^{(1)}}{\partial\theta}\right) = 0 . \tag{C-70}$$

Similar equations are written for the higher iterates.

Substitution of the expansion for the fluid temperature, equation (C-58), and the velocities, equations (C-60) and (C-61), into the conservation of energy equation for the fluid, equation (C-57), and equating equal powers of β, results in the following set of equations for the first three iterations:

$$\frac{1}{r^2}\frac{\partial}{\partial r}\left(r^2\frac{\partial T_f^{(0)}}{\partial r}\right)+\frac{1}{r^2\sin\theta}\frac{\partial}{\partial\theta}\left(\sin\theta\frac{\partial T_f^{(0)}}{\partial\theta}\right)=0. \tag{C-71}$$

$$\frac{1}{r^2}\frac{\partial}{\partial r}\left(r^2\frac{\partial T_f^{(1)}}{\partial r}\right)+\frac{1}{r^2\sin\theta}\frac{\partial}{\partial\theta}\left(\sin\theta\frac{\partial T_f^{(1)}}{\partial\theta}\right)=\frac{1}{\alpha}\left(\frac{u_\theta^{(1)}}{r}\frac{\partial T_f^{(0)}}{\partial\theta}+u_r^{(1)}\frac{\partial T_f^{(0)}}{\partial r}\right). \tag{C-72}$$

$$\frac{1}{r^2}\frac{\partial}{\partial r}\left(r^2\frac{\partial T_f^{(2)}}{\partial r}\right)+\frac{1}{r^2\sin\theta}\frac{\partial}{\partial\theta}\left(\sin\theta\frac{\partial T_f^{(2)}}{\partial\theta}\right)=\frac{1}{\alpha}\left(\frac{u_\theta^{(2)}}{r}\frac{\partial T_f^{(1)}}{\partial\theta}+u_r^{(2)}\frac{\partial T_f^{(1)}}{\partial r}\right). \tag{C-73}$$

Similar equations are written for the higher iterates.

Although Brock (1962) does not explicitly state that he used a streamfunction technique to facilitate determining the velocity distributions, it certainly could be used in an iterated fashion to obtain the *i*-th iterated solution for the velocity components. Since the boundary conditions sufficiently far from the sphere, equation (C-68), for both radial and tangential velocities and the radial velocity at the sphere interface, equation (C-67), are the same as those used in describing the derivation of Epstein, one remaining arbitrary constant for each iterated velocity component remains to be determined by the solution of the temperature distribution in the fluid through the interface slip flow condition of equation (C-66). The tangential and radial components of velocity for each iterated component of the solution can be written by inspection from equation (C-24) and equation (C-25) as follows:

$$u_r^{(i+1)}=\frac{2\hat{A}^{(i+1)}\cos\theta}{R^3}\left[\left(\frac{R}{r}\right)^3-\frac{R}{r}\right]. \tag{C-74}$$

$$u_\theta^{(i+1)}=\frac{\hat{A}^{(i+1)}\sin\theta}{R^3}\left[\left(\frac{R}{r}\right)^3+\frac{R}{r}\right]. \tag{C-75}$$

The zeroth level solution for the temperature distributions in the sphere and the fluid advances in a similar fashion to that for the Epstein solution, with the inclusion of the additional interface conditions of temperature jump, equation (C-64), and total

tangential slip, equation (C-66). The general solution of the Laplace equation for the zeroth temperature distribution in both the sphere and the fluid is equation (C-28), as presented previously for the Epstein solution.

Equation (C-28) is applied in the solution domains of the spherical particle and the surrounding fluid at each iterated level. For the sphere, in order to assure a finite temperature at the center, all the $B_n$ coefficients must be zero. For the purposes of this present work, the boundary condition at the center of the sphere is an unspecified, finite temperature of $T_0$. The general temperature solution in the sphere is given by the following expression for the zeroth level:

$$T_s^{(0)}(r,\theta) = T_0 + \sum_{n=1}^{\infty} A_n^{(0)} r^n P_n(\cos\theta), \tag{C-76}$$

where the coefficients $A_n^{(0)}$ remain to be determined at the sphere radius $R$.

Using the boundary condition far from the sphere, given by equation (C-62), the first two $A_n$ coefficients for the zeroth level solution are the following:

$$A_0^{(0)} = T_0 \qquad \text{and} \qquad A_1^{(0)} = \nabla T_\infty . \tag{C-77}$$

Thus, the general solution for the temperature distribution in the fluid surrounding the sphere may be written as

$$T_f^{(0)}(r,\theta) = T_0 + \nabla T_\infty r\cos\theta + \sum_{n=0}^{\infty} \frac{B_n^{(0)}}{r^{n+1}} P_n(\cos\theta), \tag{C-78}$$

where the $B_n^{(0)}$ coefficients must be determined by matching the temperature jump and heat fluxes at the particle-gas interface.

Application of the interface conditions of heat flux and temperature jump is used to evaluate the coefficients $A_n$ in equation (C-76) and the coefficients $B_n$ in equation (C-78) for the zeroth iterated solution. The temperature jump condition is evaluated by substitution of equations (C-76) and (C-78) into equation (C-64), which results in the equation:

$$\nabla T_{\infty} R\cos\theta + \sum_{n=0}^{\infty} \frac{B_n^{(0)}}{R^{n+1}} P_n(\cos\theta) - \sum_{n=1}^{\infty} A_n^{(0)} R^n P_n(\cos\theta)$$

$$= C_t\lambda\left(\nabla T_{\infty}\cos\theta - \sum_{n=0}^{\infty}(n+1)\frac{B_n^{(0)}}{R^{n+1}}P_n(\cos\theta)\right). \qquad \text{(C-79)}$$

Equation (C-79) is rearranged to get:

$$\frac{B_0^{(0)}}{R} + \sum_{n=1}^{\infty} R^n P_n(\cos\theta)\left\{\frac{B_n^{(0)}}{R^{2n+1}}\left[1+(n+1)C_t\frac{\lambda}{R}\right] - A_n^{(0)}\right\} = \nabla T_{\infty} R\cos\theta\left(C_t\frac{\lambda}{R} - 1\right). \qquad \text{(C-80)}$$

Equation (C-80) gives relationships between the $A_n$ and the $B_n$ coefficients for the zeroth level of the following form:

$$B_0^{(0)} = 0. \qquad \text{(C-81)}$$

$$\frac{B_1^{(0)}}{R^3}\left[1+2C_t\frac{\lambda}{R}\right] - A_1^{(0)} = \nabla T_{\infty}\left(C_t\frac{\lambda}{R} - 1\right). \qquad \text{(C-82)}$$

$$\frac{B_n^{(0)}}{R^{2n+1}}\left[1+(n+1)C_t\frac{\lambda}{R}\right] - A_n^{(0)} = 0, \qquad n > 1. \qquad \text{(C-83)}$$

Taking derivatives of equations (C-76) and (C-78) with respect to r, evaluating at the radius R, and substituting into the heat flux interface condition of equation (C-65) yields the following relationship:

$$k_s \sum_{n=1}^{\infty} n A_n^{(0)} R^{n-1} P_n(\cos\theta) = k_f\left[\nabla T_{\infty}\cos\theta - \sum_{n=1}^{\infty}(n+1)\frac{B_n^{(0)}}{R^{n+2}}P_n(\cos\theta)\right]. \qquad \text{(C-84)}$$

Equation (C-84) is rearranged as follows:

$$\sum_{n=1}^{\infty} R^{n-1} P_n(\cos\theta)\left[ nA_n^{(0)} + \frac{k_f}{k_s}(n+1)\frac{B_n^{(0)}}{R^{2n+1}}\right] = \frac{k_f}{k_s}\nabla T_\infty \cos\theta\,. \tag{C-85}$$

Equation (C-85) gives further relationships for the coefficients $A_n$ and $B_n$ for the zeroth level of the following form:

$$A_1^{(0)} + 2\frac{k_f}{k_s}\frac{B_1^{(0)}}{R^3} = \frac{k_f}{k_s}\nabla T_\infty\,. \tag{C-86}$$

$$nA_n^{(0)} + (n+1)\frac{k_f}{k_s}\frac{B_n^{(0)}}{R^{2n+1}} = 0\,, \qquad n > 1\,. \tag{C-87}$$

Equations (C-81), (C-82), (C-83), (C-86), and (C-87) are sufficient to determine the values for all $A_n$ and $B_n$ coefficients for the zeroth level. For $n = 1$, simultaneous solution of equations (C-82) and (C-86) yields the following expressions:

$$A_1^{(0)} = \frac{k_f}{k_s}\nabla T_\infty\left[\frac{3}{\left(1 + 2C_t\frac{\lambda}{R} + 2\frac{k_f}{k_s}\right)}\right]. \tag{C-88}$$

$$B_1^{(0)} = R^3\nabla T_\infty\frac{\left(\frac{k_f}{k_s} + C_t\frac{\lambda}{R} - 1\right)}{\left(1 + 2C_t\frac{\lambda}{R} + 2\frac{k_f}{k_s}\right)}. \tag{C-89}$$

For $n$ greater than 1, simultaneous solution of equations (C-83) and (C-87) yields the following general expression for the zeroth level coefficients $B_n$:

$$B_n^{(0)}\left\{n\left[1 + (n+1)\,C_t\frac{\lambda}{R}\right] + \frac{k_f}{k_s}(n+1)\right\} = 0\,, \qquad n > 1\,. \tag{C-90}$$

Since the term in braces in equation (C-90) is always positive for the permissible values of $n$ greater than one, all of the coefficients $B_n$ must be zero for $n$ greater than one

for the zeroth level. From equation (C-87), all the $A_n$ coefficients for $n$ greater than one must also be zero. Thus, the general solution for the temperature distributions in the sphere and the fluid reduces to the following forms:

$$T_s^{(0)}(r,\theta) = T_0 + \frac{k_f}{k_s}\left(\frac{3}{1+2C_t\frac{\lambda}{R}+2\frac{k_f}{k_s}}\right)\nabla T_\infty r\cos\theta\,. \tag{C-91}$$

$$T_f^{(0)}(r,\theta) = T_0 + \left[1+\left(\frac{\frac{k_f}{k_s}+C_t\frac{\lambda}{R}-1}{1+2C_t\frac{\lambda}{R}+2\frac{k_f}{k_s}}\right)\left(\frac{R}{r}\right)^3\right]\nabla T_\infty r\cos\theta\,. \tag{C-92}$$

The second term on the right hand side of equation (C-92) is the perturbation of the temperature distribution in the fluid due to the presence of the particle for the zeroth level, which represents negligible fluid convection energy transfer with respect to conduction. With the temperature distribution in the fluid determined for the zeroth level, the total slip velocity interface condition of equation (C-66) is invoked to determine the remaining unknown constant of equations (C-74) and (C-75) for the velocities. The resultant velocities are:

$$u_\theta^{(1)} = -\frac{3}{2}\frac{\nabla T_\infty\left(\frac{k_f}{k_s}+C_t\frac{\lambda}{R}\right)}{\left(1+2\frac{k_f}{k_s}+2C_t\frac{\lambda}{R}\right)\left(1+3C_m\frac{\lambda}{R}\right)}\left[\left(\frac{R}{r}\right)^3+\frac{R}{r}\right]\sin\theta\,. \tag{C-93}$$

$$u_r^{(1)} = -3\frac{\nabla T_\infty\left(\frac{k_f}{k_s}+C_t\frac{\lambda}{R}\right)}{\left(1+2\frac{k_f}{k_s}+2C_t\frac{\lambda}{R}\right)\left(1+3C_m\frac{\lambda}{R}\right)}\left[\left(\frac{R}{r}\right)^3-\frac{R}{r}\right]\cos\theta\,. \tag{C-94}$$

Now that the fluid temperature and velocity distributions are determined for the zeroth level of iteration, the next iteration level to solve for the fluid temperature distribution with convective terms is performed by substitution of equations (C-92), (C-93), and (C-94) into the first level conservation of energy equation, equation (C-72). The right hand side of the resultant equation is very lengthy, and, according to Brock (1962),

cannot meet the boundary condition of zero temperature far from the sphere for the first iteration level, equation (C-63). Since the fluid temperature distribution in the vicinity of the sphere is desired, the tangential and radial velocities of equations (C-93) and (C-94) are expanded with respect to the distance from the sphere in the vicinity of the sphere. The expansions used by Brock (1962) are the following:

$$\left(\frac{R}{r}\right)^3+\frac{R}{r}=2\left(\frac{R}{r}\right)^2+\sum_{n>2}a_n\left[\left(\frac{R}{r}\right)^n-\left(\frac{R}{r}\right)^{n+1}\right]. \tag{C-95}$$

$$\frac{R}{r}-\left(\frac{R}{r}\right)^3=\sum_{n>2}b_n\left[\left(\frac{R}{r}\right)^n-\left(\frac{R}{r}\right)^{n+1}\right]. \tag{C-96}$$

The expansion coefficients $a_n$ and $b_n$ need not be specified, since these expansions of equations (C-95) and (C-96) are taken only to first order in $(R/r)^2$.

The expansion of equation (C-96) taken to first order in $(R/r)^2$ is equivalent to neglecting the radial velocity of equation (C-94) in the vicinity of the sphere. Brock then solves the first iteration of the conservation of energy equation, equation (C-72). The resultant solution is rather lengthy with many terms representing temperature field perturbations caused by convective flow. Brock's result for the first perturbation level of temperature can be written as

$$T_f^{(1)}=f_1^{(1)}(r)+f_2^{(1)}(r)\cos^2\theta\,. \tag{C-97}$$

The resultant tangential velocity obtained by meeting the total slip condition of equation (C-66) can be written as

$$u_\theta^{(2)}=h_1^{(2)}(r)\sin\theta\cos\theta\,. \tag{C-97}$$

Brock additionally obtains a third-level iterated solution. The resultant fluid temperature and tangential velocity can be written as

$$T_f^{(2)} = f_1^{(2)}(r)\cos\theta + f_2^{(2)}(r)\cos^3\theta\,. \tag{C-98}$$

$$u_\theta^{(3)} = h_1^{(3)}(r)\sin\theta + h_2^{(3)}(r)\cos^2\theta\sin\theta\,. \tag{C-99}$$

Substituting the first three iterated solutions into the defining expansions of equations (C-58) and (C-61) yields the following:

$$T_f(r,\theta) = T_0 + \left[1 + \left(\frac{\frac{k_f}{k_s} + C_t\frac{\lambda}{R} - 1}{1 + 2C_t\frac{\lambda}{R} + 2\frac{k_f}{k_s}}\right)\left(\frac{R}{r}\right)^3\right]\nabla T_\infty\, r\cos\theta$$

$$+ \beta[f_1^{(1)}(r) + f_2^{(1)}(r)\cos^2\theta] + \beta^2[f_1^{(2)}(r)\cos\theta + f_2^{(2)}(r)\cos^3\theta] + \cdots\,. \tag{C-100}$$

$$u_\theta = -\frac{3}{2}\beta\frac{\nabla T_\infty\left(\frac{k_f}{k_s} + C_t\frac{\lambda}{R}\right)}{\left(1 + 2\frac{k_f}{k_s} + 2C_t\frac{\lambda}{R}\right)\left(1 + 3C_m\frac{\lambda}{R}\right)}\left[\left(\frac{R}{r}\right)^3 + \frac{R}{r}\right]\sin\theta$$

$$+ \beta^2[h_1^{(2)}(r)\sin\theta\cos\theta] + \beta^3[h_1^{(3)}(r)\sin\theta + h_2^{(3)}(r)\cos^2\theta\sin\theta] + \cdots\,. \tag{C-101}$$

With the tangential velocity of equation (C-101), the pressure distribution in the immediate vicinity of the sphere can be obtained by integrating the Newton's Second Law expression of equation (C-54). The fluid shear stress, as done in equation (C-48), may also be determined. The resulting expressions are:

$$P = P_\infty + 3\beta\frac{\left(\frac{k_f}{k_s} + C_t\frac{\lambda}{R}\right)}{\left(1 + 2\frac{k_f}{k_s} + 2C_t\frac{\lambda}{R}\right)\left(1 + 3C_m\frac{\lambda}{R}\right)}\frac{\nabla T_\infty}{r}\left(\frac{R}{r}\right)\cos\theta$$

$$+ \beta^2[\hat{h}_1^{(2)}(r)\cos^2\theta] + \beta^3[\hat{h}_1^{(3)}(r)\cos\theta + \hat{h}_2^{(3)}(r)\cos^3\theta] + \cdots\,. \tag{C-102}$$

$$\tau_{r\theta} = \frac{3}{2}\beta\frac{\left(\frac{k_f}{k_s}+C_t\frac{\lambda}{R}\right)}{\left(1+2\frac{k_f}{k_s}+2C_t\frac{\lambda}{R}\right)\left(1+3C_m\frac{\lambda}{R}\right)}\frac{\nabla T_\infty}{r}\left[3\left(\frac{R}{r}\right)^3+\frac{R}{r}\right]\sin\theta$$

$$+\beta^2[\hat{h}_1^{(2)}(r)\sin\theta\cos\theta]+\beta^3[\hat{h}_1^{(3)}(r)\sin\theta+\hat{h}_2^{(3)}(r)\cos^2\theta\sin\theta]+\cdots . \qquad \text{(C-103)}$$

As done for the Epstein derivation in Section C.2.2.2, the pressure distribution and the tangential shear stress are evaluated on the surface and then integrated to determine the total force on the sphere due to the thermal creep flow. Evaluating equations (C-102) and (C-103) at the sphere radius $R$ and substituting into the integral defined in equation (C-49) results in the following expression for the net thermal force:

$$F_T = -\beta\frac{12\pi\mu RC_s\left(\frac{k_f}{k_s}+C_t\frac{\lambda}{R}\right)}{\left(1+3C_m\frac{\lambda}{R}\right)\left(1+2\frac{k_f}{k_s}+2C_t\frac{\lambda}{R}\right)}\nabla T_\infty\int_0^\pi\left(\sin^3\theta-\frac{1}{2}\cos^2\theta\sin\theta\right)d\theta$$

$$+\beta^2\int_0^\pi(\hat{h}_1^{(2)}\sin^3\theta\cos\theta+\hat{h}_1^{(2)}\cos^3\theta\sin\theta)\,d\theta$$

$$+\beta^3\int_0^\pi(\hat{h}_1^{(3)}\sin^3\theta+\hat{h}_2^{(3)}\sin^3\theta\cos^2\theta+\hat{h}_1^{(3)}\cos^2\theta\sin\theta+\hat{h}_2^{(3)}\cos^4\theta\sin\theta)\,d\theta . \qquad \text{(C-104)}$$

The integral of the second perturbation term of equation (C-104) is zero. Contributions to the thermal force on the sphere appear only for the odd expansions. Since the second and subsequent perturbation solutions of the tangential velocity represent the effect of the fluid convective terms in the conservation of energy equation, equations (C-57) and (C-72), the contribution of thermal energy convection to the thermal force may be neglected to the second order in the expansion coefficient, $\beta$.

In this fashion, Brock showed that to the first order in the perturbation parameter for the temperature distribution and to the second order for the velocity distribution, the convective flow of energy around the sphere has no effect on the thermal force. Brock's expression for the thermal force, obtained by integrating equation (C-104) and substituting the expression for the expansion coefficient $\beta = C_s\frac{\mu}{\rho T}$, has the following form:

$$F_T = -\frac{12\pi\mu R C_s\left(\frac{k_f}{k_s}+C_t\frac{\lambda}{R}\right)}{\left(1+3C_m\frac{\lambda}{R}\right)\left(1+2\frac{k_f}{k_s}+2C_t\frac{\lambda}{R}\right)}\frac{\mu}{\rho T}\nabla T_\infty . \qquad \text{(C-105)}$$

In the above analysis for the thermal force on a sphere caused by thermal creep flow, the spherical particle is stationary and the calculated flow velocities are with respect to the stationary particle. Unless the particle is held in some manner by an external force, such as electromagnetism, the particle will move in the direction opposite to the thermal gradient with the thermal force balanced by a fluid drag force. In order to calculate a particle velocity due to thermal creep flow of fluid, the drag force on the particle must also be computed.

The Stokes problem (Schlichting, 1979) for the case of a sphere moving slowly relative to a viscous fluid with no effects due to nearby particles or solid boundaries results in a drag force on the sphere. Basset (1888), as described by Lamb (1932), corrects this Stokes drag result for Knudsen numbers less than 0.1 and obtains the following expression:

$$F_{drag} = 6\pi\mu R V\frac{\left(1+2C_m\frac{\lambda}{R}\right)}{\left(1+3C_m\frac{\lambda}{R}\right)}. \qquad \text{(C-106)}$$

With the assumption of steady-state flow and no other drag forces, Talbot (1980) adds the thermal force term of equation (C-105) and the drag term of equation (C-106), equates the sum to zero, and presents the following expression for the particle velocity due to the thermal force, which is called the "thermophoretic velocity:"

$$V_T = -\frac{2C_s\left(\frac{k_f}{k_s}+C_t\frac{\lambda}{R}\right)}{\left(1+2C_m\frac{\lambda}{R}\right)\left(1+2\frac{k_f}{k_s}+2C_t\frac{\lambda}{R}\right)}\frac{\mu}{\rho T}\nabla T_\infty . \qquad \text{(C-107)}$$

The sign of equation (C-107) is reversed so that the thermophoretic velocity $V_T$ is that of a particle moving relative to a stationary gas. Equation (C-107) for the thermophoretic velocity may be rewritten by grouping the thermal conductivity ratios and the rarefied flow terms and then defining the thermophoretic coefficient, K, as follows:

$$K = \frac{2C_s\left(\frac{k_f}{k_s}+C_t\frac{\lambda}{R}\right)}{\left(1+2C_m\frac{\lambda}{R}\right)\left(1+2\frac{k_f}{k_s}+2C_t\frac{\lambda}{R}\right)}. \tag{C-108}$$

Numerical values of $K$ are on the order of 0.1 for the sphere diameters and steam conditions of interest in the present work. The equation for the thermophoretic velocity may now be written in the following simplified form:

$$V_T = -K\frac{\mu}{\rho T}\nabla T_\infty. \tag{C-109}$$

Equation (C-109) for the thermophoretic velocity is used in the scaling analysis of Appendix D as well as in the development of the governing differential equations in Chapter 4.

#### C.2.2.4. Effect of volumetric heat source in the particle on thermophoretic velocity

Epstein (1929) and Brock (1962), as described in the previous sections, derive expressions for the thermal force of a particle without a volumetric heat source. For the present work, however, the particle may be emitting energy in a volumetric fashion. The effect of this heat source on the thermal force is shown to be zero in this section.

As stated previously for the case of a particle without a volumetric heat source, the second term in the brackets on the right-hand side of equation (C-92) is the perturbation of the temperature distribution in the fluid due to the presence of the particle. Since the tangential slip velocity at the particle surface, given by equation (C-52), depends on the angular derivative of the fluid temperature at the surface. Thus, the presence of volu-

metric heating in the particle could affect the thermophoretic force if the value of the temperature perturbation, or additional angular dependence of the gas temperature, is changed by the volumetric heat source in the particle.

For the case of a volumetric heat source in the particle having a strength $q'''$ that is constant and independent of position in the particle, the conservation of energy equation becomes

$$\frac{1}{r^2}\frac{\partial}{\partial r}\left(r^2\frac{\partial T}{\partial r}\right)+\frac{1}{r^2\sin\theta}\frac{\partial}{\partial\theta}\left(\sin\theta\frac{\partial T}{\partial\theta}\right)+\frac{q'''}{k_s}=0. \qquad \text{(C-110)}$$

This partial differential equation is non-homogeneous and, therefore, is not separable. The equation is linear, however, and superposition can be used to obtain a solution. Arpaci (1966) describes a procedure that assumes that the solution of the non-homogeneous problem described with one partial differential equation is the sum of a solution to a homogeneous partial differential equation and a solution to a one-dimensional differential equation where the constant volumetric heat source is formulated as a one-dimensional problem. Utilizing this procedure, which allows the use of separation of variables for the two-dimensional partial differential equation, the solution is assumed to have the following form:

$$T_s(r,\theta) = T_s^*(r,\theta)+T_s^+(r). \qquad \text{(C-111)}$$

Inclusion of the volumetric heat source term in the formulation of the one dimensional equation for $T_s^+(r)$ requires specification of boundary conditions. The boundary condition at the center of the sphere is an unspecified but finite temperature $T_c$. The boundary condition at the sphere radius, however, is still a matching condition for the solution domains in the sphere and in the surrounding fluid and requires evaluation of the temperature in the fluid as done above for the case of a particle without volumetric heating sources. The one-dimensional governing equation for the function $T^+(r)$ is given by:

$$\frac{1}{r^2}\frac{d}{dr}\left(r^2\frac{dT_s^+(r)}{dr}\right)+\frac{q'''}{k_s} = 0\,, \tag{C-112}$$

with boundary conditions of finite but as yet unspecified temperatures

$$T_s^+(0) = T_c \qquad \text{and} \qquad T_s^+(R) = T_R\,. \tag{C-113}$$

The solution of this equation is of the following form:

$$T_s^+(r) = T_c - \frac{q'''R^2}{6k_s}\left(\frac{r}{R}\right)^2. \tag{C-114}$$

Substituting the supposition of equation (C-111) into the conservation of energy equation (C-110) and recognizing equation (C-112), yields the following governing equation for $T_s^*$:

$$\frac{1}{r^2}\frac{\partial}{\partial r}\left(r^2\frac{\partial T_s^*}{\partial r}\right)+\frac{1}{r^2\sin\theta}\frac{\partial}{\partial\theta}\left(\sin\theta\frac{\partial T_s^*}{\partial\theta}\right) = 0\,. \tag{C-115}$$

Equation (C-115) is functionally identical to equation (C-9) and is amenable to solution by separation of variables. The boundary conditions, however, are different, as they must be. For this problem, the inhomogenous heat source term in equation (C-110) is transformed to appear at the matching point of the sphere-fluid interface. The solution of Laplace's equation in spherical coordinates was developed previously for equation (C-28) in terms of a series of Legendre polynomials. Using the supposition of equation (C-111), the individual solutions for $T^*$, equation (C-76), and $T^+$, equation (C-114), are added as follows:

$$T_s(r,\theta) = \sum_{n=0}^{\infty} A_n^* r^n P_n(\cos\theta)+T_c-\frac{q'''R^2}{6k_s}\left(\frac{r}{R}\right)^2. \tag{C-116}$$

The general solution for the temperature distribution in the fluid adjacent to the sphere is still given as equation (C-30). The temperature at the center of the sphere, however, is no longer $T_0$ (the center temperature with no heat source in the particle), but a higher temperature, $T_c$, due to the presence of the volumetric heat source.

The solutions must be matched at the solid-gas interface such that the heat flux and temperature jump conditions are satisfied. The heat flux interface condition results in the following relationship between the coefficients $A^*_n$ and $B_n$.

$$\sum_{n=0}^{\infty} R^{n-1} P_n(\cos\theta)\left[nA_n^* + (n+1)\frac{k_f}{k_s}\frac{B_n}{R^{2n+1}}\right] = \frac{k_f}{k_s}\nabla T_\infty \cos\theta + \frac{q'''R}{3k_s}. \qquad \text{(C-117)}$$

Inspection of equation (C-117) yields the following relationships:

$$B_0 = \frac{q'''R^3}{3k_f}. \qquad \text{(C-118)}$$

$$A_1^* + 2\frac{k_f}{k_s}\frac{B_1}{R^3} = \frac{k_f}{k_s}\nabla T_\infty \cos\theta. \qquad \text{(C-119)}$$

$$A_n^* + (n+1)\frac{k_f}{k_s}\frac{B_n}{R^{2n+1}} = 0, \qquad n > 1. \qquad \text{(C-120)}$$

The condition for the temperature jump at the interface results in the following relationship between the coefficients $A^*_n$ and $B_n$:

$$\sum_{n=0}^{\infty} R^n P_n(\cos\theta)\left\{\frac{B_n}{R^{2n+1}}\left[1 + (n+1)C_t\frac{\lambda}{R}\right] - A_n^*\right\}$$

$$= \nabla T_\infty R\cos\theta\left(C_t\frac{\lambda}{R} - 1\right) - \left(T_0 - T_c + \frac{q'''R^2}{6k_s}\right). \qquad \text{(C-121)}$$

The following relationships between the coefficients $A^*_n$ and $B_n$ are found from inspection of equation (C-121):

$$\frac{B_0}{R}\left(1+C_t\frac{\lambda}{R}\right)-A_0^* = -\left(T_0-T_c+\frac{q'''R^2}{6k_s}\right). \tag{C-122}$$

$$\frac{B_1}{R^3}\left[1+2C_t\frac{\lambda}{R}\right]-A_1^* = \nabla T_\infty\left(C_t\frac{\lambda}{R}-1\right). \tag{C-123}$$

$$\frac{B_n}{R^{2n+1}}\left[1+(n+1)C_t\frac{\lambda}{R}\right]-A_n^* = 0, \qquad n>1. \tag{C-124}$$

Since the value for the coefficient $B_0$ is determined from the heat flux interface condition of equation (C-118), the value for $A^*_0$ is uniquely determined by the following relationship:

$$A_0^* = T_0-T_c+\frac{q'''R^2}{6k_s}\left[2\frac{k_s}{k_f}\left(1+C_t\frac{\lambda}{R}\right)+1\right]. \tag{C-125}$$

which follows from equation (C-122) above.

The relationships for the values of the coefficients $A_n^*$ and $B_n$ when the index $n$ is greater than, or equal to, one are identical to those of equations (C-82), (C-83), (C-86), and (C-87). Hence, the coefficient $B_1$ is identical to the coefficient $B_1$ found for the case of no volumetric heating in the particle, equation (C-89), the $A_1^*$ coefficient is equal to the $A_1$ coefficient, and the coefficients $A_n^*$ and $B_n$ are zero for $n$ greater than one. The temperature distribution in the sphere and adjacent fluid are therefore given by the following expressions:

$$T_s(r,\theta) = T_0+\frac{q'''R^2}{6k_s}\left[2\frac{k_s}{k_f}\left(1+C_t\frac{\lambda}{R}\right)+1-\left(\frac{r}{R}\right)^2\right]+\frac{k_f}{k_s}\left(\frac{3}{1+2C_t\frac{\lambda}{R}+2\frac{k_f}{k_s}}\right)\nabla T_\infty r\cos\theta. \tag{C-126}$$

$$T_f(r,\theta) = T_0+\frac{q'''R^2}{3k_f}\left(\frac{R}{r}\right)+\left[1+\frac{\frac{k_f}{k_s}+C_t\frac{\lambda}{R}-1}{1+2C_t\frac{\lambda}{R}+2\frac{k_f}{k_s}}\left(\frac{R}{r}\right)^3\right]\nabla T_\infty r\cos\theta. \tag{C-127}$$

Note that the fluid temperature solution is unbounded as the distance from the particle along the direction of the temperature gradient increases. This seemingly unrealistic behavior is permissible under the initial problem statement that poses a uniform temperature gradient across the particle. "Infinity" for this problem is the distance "sufficiently far" from the particle so that the presence of the particle no longer affects the fluid temperature.

From inspection of equation (C-127), the angular variation of the fluid temperature is unaffected by the presence of a volumetric heat source in the spherical particle. Therefore, the derivative of the fluid temperature with respect to $\theta$ is completely unaffected by the presence of a heat source in the particle. The tangential slip velocity given by equation (C-52) is, therefore, unaffected by the presence of the volumetric heat source in the particle.

The radial variation of the fluid temperature, however, is affected by the presence of a volumetric heat source in the particle as, of course, is the derivative of the fluid temperature with respect to $r$. For the first level of the perturbation solution of Brock (1962), as described in the previous section, the derivative of the zeroth temperature solution in the fluid is taken with respect to $r$, as shown in the right-hand side of equation (C-72). The presence of a volumetric heat source in the particle might, therefore, affect the convective flow of energy in that governing equation. However, the radial velocity in the vicinity of the sphere is negligible, as shown by the expansion of equation (C-96) to first order in $(R/r)^2$ in equation (C-74). The tangential slip and pressure distribution around the sphere obtained from the perturbation solution of Brock are unchanged.

Since the tangential velocity distribution in the fluid and the effect of convective flow of energy are unchanged by the presence of a volumetric heat source in the particle, the pressure distribution given by equation (C-102) and viscous shear given by equation (C-103) are likewise unchanged. The thermal force given by equation (C-104) is, therefore, unchanged. Subsequently, the thermophoretic coefficient, $K$, given by equation (C-108) remains unchanged by the presence of a volumetric heat source in the particle.

### C.2.2.5. Effect of time-dependent particle temperature variation

For the above analyses, steady-state conditions are assumed, that is, the transient temperature variations of the sphere and fluid are neglected. Since the particle under the action of the thermal force will move from a hotter region of the fluid to a colder region, the matching temperature condition at the interface will change as the fluid temperature changes, giving rise to a time-dependent temperature distribution in the particle. The characteristic time for a transient temperature variation in the spherical particle is shown in this section to be negligible with respect to the characteristic time for thermophoretic particle movement.

Arpaci (1966) presents a characteristic time for conduction heat transfer in a sphere as follows:

$$t_s = \frac{R^2}{\alpha_s}, \tag{C-128}$$

where $R$ is the sphere radius and $\alpha_s$ is the thermal diffusivity of the particle.

A characteristic time for thermophoretic movement of the particle would be the time for a particle to move one diameter under the action of the thermal force at the thermophoretic velocity, $V_T$. This characteristic thermophoresis time has the following form:

$$t_T = \frac{2R}{V_T}. \tag{C-129}$$

Forming the ratio of these two characteristic times yields:

$$\varepsilon = \frac{t_s}{t_T} = \frac{R}{2\alpha_s} V_T. \tag{C-130}$$

Substitution of the thermophoretic velocity given by equation (C-109) and the definition of Prandtl number, the ratio of characteristic times is written in the following form:

$$\varepsilon = KPr\left(\frac{\alpha_f}{\alpha_s}\right)\left(\frac{R}{2}\right)\left(\frac{\nabla T_\infty}{T}\right). \tag{C-131}$$

The thermal gradient of the above equation is approximated by the ratio of the wall-to-fluid temperature difference and the characteristic distance, $\delta$. The final term on the right-hand side of equation (C-131) is therefore given approximately as

$$\frac{\nabla T_\infty}{T} = \frac{T_\infty - T_w}{T\delta}. \tag{C-132}$$

The boundary layer thickness for laminar flow conditions is approximated by the expression $\delta/L = Gr^{-1/4}$ (Jaluria, 1980). The thermal microscale $\delta/L = Gr^{-1/3}$ is used for turbulent flow conditions (Arpaci, 1986). $L$ is a characteristic flow length, which for this problem is the plate length of three meters. Substitution of the approximations for the thermal gradient normal to the wall in both laminar and turbulent flows given by equation (C-132) into equation (C-131) gives the following approximate forms for the ratio of characteristic times:

$$\varepsilon = KPr\left(\frac{\alpha_f}{\alpha_s}\right)\left(\frac{T_\infty - T_w}{T}\right)\left(\frac{R}{2L}\right)Gr^{1/4}. \tag{C-133}$$

$$\varepsilon = KPr\left(\frac{\alpha_f}{\alpha_s}\right)\left(\frac{T_\infty - T_w}{T}\right)\left(\frac{R}{2L}\right)Gr^{1/3}. \tag{C-134}$$

Equation (C-133) represents laminar flow conditions and equation (C-134) represents turbulent flow conditions. Since turbulent flows, where Grashof numbers are greater than $10^9$, give higher relative magnitudes in equation (C-134) as compared to equation (C-133), equation (C-134) will compute a greater magnitude for $\varepsilon$. This is physically realistic, since turbulent flows generally have a higher temperature gradient near the wall, and, therefore, would have higher thermophoretic velocities. The magnitudes of the individual terms of equation (C-134) are now considered.

The product of the thermophoretic coefficient $K$ and the Prandtl number of steam is on the order of one. For the present work, the fluid is steam and the particle is assumed to be stainless steel, which have comparable thermal diffusivities. The first term in parentheses on the right-hand side of equation (C-134) is, therefore, of order one. The value of the wall-to-fluid temperature difference divided by the fluid temperature varies from 0.1 to 0.5 for the present work, and will be considered as of order one. The particle radius $R$ is on the order of one micrometer and the plate length $L$ is three meters. The magnitude of the third bracketed term of equation (C-134) is, therefore, on the order of $10^{-6}$.

For the present work, turbulent flows with Grashof numbers on the order of $10^{12}$ are expected. The resultant value for $\varepsilon$ is, therefore, on the order of $10^{-2}$. This should be the largest value of the relative magnitude for the ratio of characteristic times $\varepsilon$ for the parameters of the present work. Thus, the transient temperature variation of the spherical particle as it is moved under the action of the thermophoretic force may be neglected with respect to the steady-state temperature distribution.

### C.3. Effect of Variable Properties on Thermophoretic Velocity

Since the effects of variable thermophysical properties are of interest, equation (C-109) was analyzed to examine these effects on the thermophoretic velocity. As will be shown, all of the terms in the coefficient of the temperature gradient are functions of temperature, including the thermophoretic coefficient $K$.

In general, the dynamic viscosity $\mu$ for gases varies with temperature as $T^n$ (Kays and Crawford, 1980). The exponent $n$ for air is approximately 0.7. For an ideal gas, the density varies inversely with the temperature. Therefore, if no temperature variation of the thermophoretic coefficient $K$ is assumed, the thermophoretic velocity would increase when the dynamic viscosity increased with increasing temperature. Thus, since the expression for the thermophoretic velocity was derived from a balance of thermal and viscous drag forces on the sphere, the thermal force must increase faster with respect to temperature than the viscous drag force.

The expression for the thermal force on the sphere, which is given by equation (C-105), was derived from the expression for the tangential slip velocity on the sphere, given by equation (C-101). As mentioned in Section C.2, both the viscous slip velocity and the thermal slip velocity are directly proportional to the mean free path. Since the mean free path depends on the dynamic viscosity as shown in equation (C-3), the mean free path must also vary directly with the temperature.

Substitution of the expressions for the temperature dependencies of the dynamic viscosity, mass density, and molecular speed in equation (C-3) shows the following dependence of the mean free path on the temperature.

$$\lambda \propto T^{n+1/2}. \tag{C-135}$$

For air, $n = 0.7$, and the mean free path would increase as $T^{1.2}$. Inspection of equation (C-101) shows that the tangential slip velocity is expected to increase as the temperature increases. The increase in the slip velocity would then cause an increase in the thermal force.

The resultant increase in the thermal force with an increase in temperature for a given temperature gradient is shown by equation (C-105). Equation (C-105) may be rewritten in the following form:

$$F_T = -\frac{12\pi R C_s\left(\frac{k_f}{k_s}+C_t\frac{\lambda}{R}\right)}{\left(1+3C_m\frac{\lambda}{R}\right)\left(1+2\frac{k_f}{k_s}+2C_t\frac{\lambda}{R}\right)}\frac{\mu^2}{\rho T}\nabla T_\infty . \tag{C-136}$$

Using the temperature variations found above, the term $\mu^2/\rho T$ in the coefficient of the temperature gradient varies as $T^{2n}$. Thus, for any positive exponent $n$, the thermal force increases as the temperature increases.

The temperature dependence of the fractional term involving the thermal conductivity ratio and the Knudsen number on the right-hand side of equation (C-136) is also determined. The values of interest for the thermal conductivity ratio and the Knudsen number are of the order of $10^{-2}$, and the rarefied flow parameters of $C_s$, $C_m$, and

$C_t$ are of the order of unity, as discussed in section C.2. Performing a binomial expansion of the denominator, and approximating the fractional term to first order in thermal conductivity ratio and Knudsen number yields the following expression:

$$\frac{12\pi RC_s\left(\frac{k_f}{k_s}+C_t\frac{\lambda}{R}\right)}{\left(1+3C_m\frac{\lambda}{R}\right)\left(1+2\frac{k_f}{k_s}+2C_t\frac{\lambda}{R}\right)} \approx 12\pi RC_s\left(\frac{k_f}{k_s}+C_t\frac{\lambda}{R}\right). \tag{C-137}$$

Inspection of equation (C-137) shows that this term from equation (C-136) increases with respect to temperature as the mean free path, assuming identical dependencies of the thermal conductivities of the gas and particle on temperature.

The variation of the thermal force with respect to temperature (to first order in the thermal conductivity ratio and Knudsen number) is given by:

$$F_T \propto T^{2n}(1+T^{n+1/2}). \tag{C-138}$$

The temperature variation of the viscous drag on a spherical particle moving at a given velocity can be determined from equation (C-106). Performing a binomial expansion of the denominator in equation (C-106) and retaining terms to first order in Knudsen number, the viscous drag on the sphere may be written as:

$$F_{drag} = 6\pi\mu RV\left(1-C_m\frac{\lambda}{R}\right). \tag{C-139}$$

Including the temperature dependencies of the dynamic viscosity and mean free path, the variation of the viscous drag with temperature, to first order in the Knudsen number and for a specified velocity, is given by:

$$F_{drag} \propto T^n(1-T^{n+1/2}). \tag{C-140}$$

The ratio of the thermal force to the viscous drag force may now be written as follows:

$$\frac{F_T}{F_{drag}} \propto T^n \frac{1+T^{n+1/2}}{1-T^{n+1/2}}. \tag{C-141}$$

This ratio increases with increasing temperature for any positive exponent $n$. In the absence of any other body forces acting on the sphere, this ratio represents the temperature dependence of the sphere velocity under the action of thermal force due to a thermal gradient.

# APPENDIX D

# SCALING ANALYSIS OF GOVERNING EQUATIONS

## D.1. Introduction

The complete set of governing equations and boundary conditions for the flows of interest in this research are, as shown in Chapter 4, extremely complicated. Numerical solutions of these equations are both difficult and expensive to achieve. Thus, any simplifications of these equations that can be performed without substantially changing the accuracy of their solutions are desirable. Identification of relatively small terms in the differential equations usually justifies neglecting these terms, which simplifies the numerical solution of the coupled equations without significantly affecting the accuracy of the solution. Care must be taken when neglecting small terms, however, to prevent the occurrence of singular perturbations.

The differential equations that describe the transient spatial distributions of the variables of interest for the different solution domains of solid and fluid have intrinsic reference quantities that describe the magnitude of the response to changes in operating conditions. These equations, including the interface conditions between the solid and fluid solution domains, are scaled such that the magnitude of the coefficient of each term indicates the relative importance of the particular effect represented by that term. This information is used to simplify the governing equations for appropriate ranges of the independent variables.

The intent of this analysis is to determine the relative magnitudes of the terms in each governing equation in order to simplify the numerical computations. After simplification, the actual computed values determined of the variables of interest should be little affected by deletion of the terms that are shown to be orders of magnitude smaller.

An important term that is used extensively in what follows is "unit order." This term is loosely defined to mean an absolute magnitude somewhere between 0.1 and 10.

The governing equations are recast in dimensionless variables such that each term in each differential equation, independent of its coefficient, is of unit order. Thus, the coefficient of each term represents the relative magnitude of that term. Each independent and dependent variable is replaced by a product of the form $T^* = T_c T$, where a star superscript denotes a physical variable, a subscript "*c*" represents a characteristic quantity, or "scale," and the remaining term without a subscript or superscript represents a dimensionless quantity of unit order. In this example, $T^*$ is the physical value of temperature, $T_c$ is a characteristic value of temperature valid over the range of interest, and $T$ is the dimensionless temperature of unit order.

These characteristic values are manipulated such that a nondimensional grouping of characteristic terms appears as the coefficient of a nondimensional term of unit order. Each such term of unit order denotes a different physical effect. Its coefficient, which is comprised of some combination of the characteristic quantities, indicates the *relative* importance of that effect. This procedure, as illustrated by Segel (1972), was applied to the coupled, conjugate heat and mass transfer problem of interest here. Each of the characteristic values was selected to correctly *scale* the equations, not to simply rewrite each equation in nondimensional form.

For this analysis, the solution domain for the problem is a thick-walled vertical plate and the adjacent fluid. This domain is split into two subdomains, one for the solid and one for the gas. The solutions in these two subdomains are matched by specifying the interface conditions on the wall temperature, heat flux, and velocity. These two solution subdomains form a conjugate heat transfer problem; that is, a problem in which the solutions in the subdomains are fully coupled.

### D.2. Development of the Governing Equations for the Particle-Fluid System

The differential equations to be solved are those for a compressible, newtonian mixture of fluid and particles as presented by Pai (1956), Bird et al. (1960), Batchelor (1967), and Kays and Crawford (1980). These equations express conservation of mass, Newton's Second Law, and conservation of energy for the fluid-particle system. The differential equations representing conservation of mass of the fluid, conservation of

mass of the particles, Newton's Second law for the fluid, and conservation of energy for the fluid are developed here. The maximum volumetric fraction of particles in the mixture for which effects due to the presence of particles on Newton's Second Law, conservation of energy, and the thermophysical properties may be neglected is determined in this section.

Viskanta (1966) states that radiation pressure effects are negligible for fluid systems, such as the one of interest in this investigation. Since the fluid of interest here is not a binary gas, Soret and Dufour effects cannot occur. However, Goldhirsch and Ronis (1983a) established that thermophoresis can be considered as a Soret effect for particle-gas systems. No references on effects in particle-gas systems comparable to the Dufour effect in binary gas systems could be found in the literature.

The governing equations are written in repeated index tensor notation as follows:

$$\frac{\partial \rho^*}{\partial t^*} + \frac{\partial}{\partial x_j^*}(\rho^* u_j^*) - \frac{\partial}{\partial x_j^*}(j_j^*) = 0\,, \tag{D-1}$$

$$\rho^* \frac{Du_i^*}{Dt^*} = \rho^* F_i^* + \frac{\partial}{\partial x_j^*}\left\{\mu^*\left(\frac{\partial u_i^*}{\partial x_j^*} + \frac{\partial u_j^*}{\partial x_i^*}\right)\right\} - \frac{2}{3}\frac{\partial}{\partial x_i^*}\left(\mu^* \frac{\partial u_j^*}{\partial x_j^*}\right) - \frac{\partial P^*}{\partial x_i^*}\,, \tag{D-2}$$

and

$$\rho^* \frac{De^*}{Dt^*} = -P^* \frac{\partial u_j^*}{\partial x_j^*} + Q^* - \frac{\partial q_j^*}{\partial x_j^*} + \mu^*\left\{\frac{\partial u_i^*}{\partial x_j^*}\left(\frac{\partial u_i^*}{\partial x_j^*} + \frac{\partial u_j^*}{\partial x_i^*}\right) - \frac{2}{3}\left(\frac{\partial u_j^*}{\partial x_j^*}\right)^2\right\}. \tag{D-3}$$

The term $D(...)/Dt^*$ represents the convective, or Stokes, derivative operator, which is also known as the substantial derivative. The symbol $j^*$ is used to represent the aerosol mass flux. The symbol $e^*$ denotes the internal energy of the mixture, the symbol $u^*$ represents the mass-averaged velocity (Bird et al., 1960), and the symbol $q^*$ denotes the sum of the conduction and the thermal radiation heat fluxes. All the dependent variables and the thermophysical properties represent a mixture of gas and particles. Equations (D-1) through (D-3) represent a system of five equations in the seventeen unknowns of $P$, $\rho$, $\mu$, $e$, $Q$, and of the velocities, particle fluxes, heat fluxes, and body forces in three directions. The number of unknowns is reduced to thirteen with the

assumption of two-dimensional flow, as shown in Figure 2-2. Constitutive relations, such as the Fourier law of heat conduction that relates the conductive heat flux to the temperature gradient and an equation of state for the fluid that relates the pressure to the density and temperature, will be employed such that the system of equations is closed.

The differential equation for the conservation of energy that governs the temperature distribution in the solid wall and in a particle, that is, the conduction equation, can be written by inspection from equation (D-3) by setting the convective, viscous dissipation, and compression work terms in the conservation of energy equation (D-3) to zero. Arpaci (1966) presents a derivation for the conduction equation, starting from a general control volume formulation that includes terms representing convective flow of energy that are later set to zero when the material is at rest. Arpaci's derivation results in an equation exactly in the form of equation (D-3) without the convective, viscous dissipation, or compression work terms.

For the conditions of interest of the present investigation, the ratio of the volume of the aerosol particles and the volume of the mixture of both particles and fluid is very small (on the order of $10^{-6}$), such that scaling the set of equations (D-1) through (D-3) will show that the presence of particles in the flow results in negligible effects on the fluid conservation equations and the thermophysical properties. Furthermore, the convection of energy by the particles will be shown to be negligible with respect to the energy convected by the fluid and thus, the conservation of energy equation can be written in a more familiar form for the fluid component only. This scaling effort will identify a maximum particle concentration for which the neglect of the particles in the conservation equations and thermophysical properties is valid.

First, the mass-averaged velocity of the particle-fluid mixture is determined, since it appears in all the conservation equations. In general, the velocity of a particle may be different than the velocity of the fluid. In the absence of thermophoresis and externally induced forces such as magnetism, particle motion relative to the fluid during a postulated transient period for the response of a particle initially at rest to a step change in fluid velocity is determined. Assuming that a spherical particle will experience Stokes

viscous drag during the transient period from the initial application of the step change in velocity, the time-dependent motion of the particle is described by Newton's Second Law as follows:

$$\frac{4}{3}\pi R^3 \rho_p^* \frac{du_p^*(t)}{dt} = 6\pi\mu^* R[u_f^* - u_p^*(t)] , \tag{D-4}$$

where the subscript "$f$" denotes the fluid (steam for the present investigation) and the subscript "$p$" denotes the aerosol particle. Equation (D-4) has the solution at time $t$, with an initial particle velocity of zero and a constant fluid velocity, $u_f^*$, applied at time zero, of

$$\frac{u_p^*(t)}{u_f^*} = 1 - \exp\left(-\frac{9}{2}\frac{\mu_f^*}{\rho_p^* R^2} t\right). \tag{D-5}$$

The time required for a particle at rest to be accelerated to velocity $u_p^*$ by the Stokes drag force caused by the fluid velocity $u_f^*$ is obtained from equation (D-5) and is designated as $t_{drag}$, so that

$$t_{drag} = -\left[\frac{2\rho_p^* R^2}{9\mu_f^*}\right] \ln\left(1 - \frac{u_p^*}{u_f^*}\right). \tag{D-6}$$

A characteristic time for the fluid flow would be the time for a fluid packet to move a characteristic flow distance at a characteristic fluid velocity. A characteristic velocity in a laminar, natural convection boundary layer, which can be considered as an expected maximum velocity (Jaluria, 1980), will be presented in Section D-4 and is given by equation (D-63). A characteristic flow time for the fluid to travel to travel the characteristic flow distance is given by

$$t_c = \frac{L}{U_c} = \frac{L^2}{\nu_f^*} Gr^{-1/2} . \tag{D-7}$$

The ratio of the particle drag time to the characteristic flow time is formed by dividing equation (D-6) by equation (D-7) to give

$$\frac{t_{drag}}{t_c} = -\frac{2}{9}\left(\frac{\rho_p^*}{\rho_f^*}\right)\left(\frac{R}{L}\right)^2 \ln\left(1-\frac{u_p^*}{u_f^*}\right) Gr^{1/2}. \qquad \text{(D-8)}$$

A particle is estimated to be essentially at the flow velocity when $u_p^*/u_f^* = 0.95$. For a carbon steel sphere, which has a density of 7800 kg/m$^3$, with a diameter of 1 μm in steam at 1000°C, which has a density of 11.8 kg/m$^3$, and in a flow having a Grashof number of $10^9$, the ratio of characteristic times as given by equation (D-8) is $4\times10^{-7}$. Thus, in the absence of thermophoresis or other external forces on a particle, the time required for the Stoke's drag force to equilibrate the particle and fluid velocities is *much less* than the time required for a typical fluid packet to traverse the low field. This is equivalent to saying that the particles essentially follow the flow with no velocity lag.

The term $q^*$ appearing in equation (D-3) represents the sum of the radiant and the conductive heat fluxes in the mixture. Since the particles may absorb and emit thermal radiation, the relative magnitude of the radiation heat flux emitted and absorbed by a particle with respect to the approximate conductive heat flux through a distance in the fluid equal to a particle radius is estimated by the following ratio (Hidy and Brock, 1970):

$$\frac{q_{radiation}}{q_{conduction}} = \frac{R\varepsilon_p\sigma(T_\infty^4 - T_w^4)}{k_f(T_\infty - T_w)}, \qquad \text{(D-9)}$$

where $\varepsilon_p$ is the emissivity of the particle and $\sigma$ is the Stefan-Boltzmann constant. For a steam temperature of 1000°C, a wall temperature of 300°C, and a particle diameter of 10 μm, the ratio of heat fluxes as given by equation (D-9) is less than $10^{-2}$. Thus, the radiation heat flux due to the presence of particles in the mixture is negligible with respect to the conductive heat flux in the fluid. The radiation heat flux in a *participating* medium, such as steam, however, may *not* be negligible with respect to the conductive heat flux. Participating media radiation heat transfer is discussed in Section D-4.

In order to analyze the conservation of energy equation (D-3) for effects due to the presence of particles, the density of the mixture is first examined for effects due to the presence of particles. The term $\rho^*$ represents the density of the steam-particle mixture. As illustrated by Wallis (1969), if $\alpha$ is defined to be the volumetric fraction of particles in the mixture, that is, the volume of the particles per unit volume of fluid-particle mixture, then the individual components of steam and aerosol contribute on a volumetric basis to the density of the mixture in the following fashion:

$$\rho^* = \alpha \rho_f^* + (1-\alpha)\rho_p^* . \tag{D-10}$$

Factoring the right-hand side of equation (D-10) yields the following expression for the density of the mixture:

$$\rho^* = \rho_f^* \left\{ 1 + \alpha \left( \frac{\rho_p^*}{\rho_f^*} - 1 \right) \right\} . \tag{D-11}$$

Assuming that the aerosol particles are carbon steel, which has a density of 7800 kg/m$^3$, and the fluid is steam, which has a minimum density of 11.8 kg/m$^3$ over the range of interest for this investigation, equation (D-11) can be written as the following:

$$\rho^* = \rho_f^* (1 + 690\alpha) . \tag{D-12}$$

The term $690\alpha$ represents the contribution of the carbon steel particles to the density of the particle-steam mixture. If it is arbitrarily assumed that this contribution is negligibly small when it is less than $10^{-2}$, equation (D-11) gives that the effects of particles on the mixture density are negligibly small if $\alpha$ is less than $1.5\times10^{-5}$.

The conservation of energy equation (D-3) has a term on the left-hand side that represents the mass-averaged internal energy of the mixture (Bird et al., 1960). This mass-averaged internal energy is written as:

$$\rho^* e^* = \alpha \rho_p^* e_p^* + (1-\alpha)\rho_f^* e_f^* . \tag{D-13}$$

Rearranging equation (D-13) yields the following expression:

$$\rho^{*}e^{*} = \rho_f^{*}e_f^{*}\left\{1+\alpha\left(\frac{\rho_p^{*}e_p^{*}}{\rho_f^{*}e_f^{*}}-1\right)\right\}. \tag{D-14}$$

The internal energy of an ideal gas can be written as the product of the specific heat at constant volume and the temperature and the internal energy of a solid particle can be written as the product of the specific heat and the temperature (Reynolds and Perkins, 1977). Defining the ratio of specific heats $\gamma$ as the ratio of the specific heat at constant pressure and the specific heat at constant volume, equation (D-14) can be written as the following:

$$\rho^{*}e^{*} = \rho_f^{*}e_f^{*}\left\{1+\alpha\left(\frac{\rho_p^{*}C_p^{*}}{\rho_f^{*}C_f^{*}}\gamma-1\right)\right\}. \tag{D-15}$$

For the conditions of interest of the present investigation (carbon steel particles in steam at 1000°C), equation (D-15) can be written as follows:

$$\rho^{*}e^{*} = \rho_f^{*}e_f^{*}(1+150\alpha). \tag{D-16}$$

The term $150\alpha$ represents the contribution of the carbon steel particles to the energy of the particle-steam mixture. If it is arbitrarily assumed that this contribution is negligibly small when it is less than $10^{-2}$, equation (D-16) gives the corresponding maximum volumetric fraction of the particles, $\alpha$, as $6.6\times10^{-5}$. This maximum volumetric fraction for the neglect of the internal energy of the particles in the flow is greater than the maximum volumetric fraction for the neglect of the effect of the particles on the mixture density. Thus, *the convection of internal energy by the particles is negligible with respect to the convection of internal energy by the fluid.* As illustrated by Arpaci and Larsen (1984), the use of thermodynamic identities and the Fourier law of heat conduction transforms the conservation of energy equation (D-3) into the following form:

$$\rho^{*}C^{*}\frac{DT^{*}}{Dt^{*}} = (\beta^{*}T^{*})\frac{DP^{*}}{Dt^{*}}+\frac{\partial}{\partial x_j^{*}}\left(k^{*}\frac{\partial T^{*}}{\partial x_j^{*}}\right)+Q^{*}-\frac{\partial q_{rj}^{*}}{\partial x_j^{*}}+\mu^{*}\left\{\frac{\partial u_i^{*}}{\partial x_j^{*}}\left(\frac{\partial u_i^{*}}{\partial x_j^{*}}+\frac{\partial u_j^{*}}{\partial x_i^{*}}\right)-\frac{2}{3}\left(\frac{\partial u_j^{*}}{\partial x_j^{*}}\right)^{2}\right\}. \tag{D-17}$$

Because the particles move at the fluid velocity and the presence of particles at low volume fractions causes negligible effects in the conservation of energy equation (D-3), equations (D-2) and (D-17) will be scaled as if the particles were not present in the fluid. Before this scaling can be performed, however, the remaining thermophysical properties of dynamic viscosity, thermal conductivity, and specific heat at constant pressure must also be examined for effects due to the presence of particles.

To compute the dynamic viscosity of a dilute mixture of particles in a fluid suspension, Wallis (1969) presents the Einstein equation which appears as follows:

$$\mu^* = \mu_f^*(1+2.5\alpha)\,, \tag{D-18}$$

where the term $2.5\alpha$ represents the contribution of the particles to the fluid dynamic viscosity in the mixture. Note that the viscosity of a dilute mixture of particles is greater than the viscosity of the fluid. If it is arbitrarily assumed that this contribution is negligibly small when it is less than $10^{-2}$, equation (D-18) gives that the effects of particles on the mixture density are negligibly small if $\alpha$ is less than $4\times10^{-3}$.

For a dilute suspension of noninteracting spherical particles, the effective thermal conductivity is identical in form to the effective electrical conductivity (Batchelor, 1974). Maxwell (1873) derives a relationship for the effective conductivity of a dilute suspension of spheres for which Dutta and Mashelkar (1987) present as the effective thermal conductivity for stagnant flow conditions. Leal (1977) describes additional considerations to determine the effective thermal conductivity of a moving suspension, such as particle rotations and a relative velocity between the particles and the fluid. Since the spheres are moving at the fluid velocity and the Magnus effect caused by particle rotation is negligible as described in Section 2.6, this stagnant model of effective thermal conductivity of a dilute suspension as derived by Maxwell (1873) is sufficient for the purposes of this scaling analysis. Thus, the effective thermal conductivity of the dilute suspension is given by the following expression:

$$\frac{k^*}{k_f^*} = \frac{k_p^*/k_f^* + 2 - 2\alpha(1-k_p^*/k_f^*)}{k_p^*/k_f^* + 2 + \alpha(1-k_p^*/k_f^*)}\,. \tag{D-19}$$

For a "sufficiently small" volumetric fraction (i.e., $\alpha < 1\times10^{-2}$), equation (D-19) may be approximated and rearranged to the following form:

$$k^* = k_f^*\left\{1+3\alpha\left(\frac{k_p^*/k_f^*-1}{k_p^*/k_f^*+2}\right)\right\}. \qquad \text{(D-20)}$$

The particles are assumed to be carbon steel, which has a thermal conductivity of 54 $W\cdot m^{-1}\cdot K^{-1}$. The minimum thermal conductivity of steam over the range of interest of this investigation occurs at 300°C and is equal to 0.06 $W\cdot m^{-1}\cdot K^{-1}$. With these values, equation (D-20) reduces to the following form:

$$k^* = k_f^*(1+3\alpha), \qquad \text{(D-21)}$$

where $3\alpha$ represents the contribution of the particles to the fluid thermal conductivity in the mixture. If it is arbitrarily assumed that this contribution is negligibly small when it is less than $10^{-2}$, equation (D-21) gives the corresponding maximum volumetric fraction of the particles, $\alpha$, as $3.3\times10^{-3}$.

Since the particles are moving with the fluid at the fluid velocity in the absence of thermophoresis, a mass-averaged specific heat at constant pressure can be defined as follows (Boothroyd, 1971):

$$\rho^* C^* = \alpha\rho_p^* C_p^* + (1-\alpha)\rho_f^* C_f^*. \qquad \text{(D-22)}$$

For a "sufficiently small" volumetric fraction, equation (D-22) reduces to the expressions for effective specific heat of a dilute suspension of particles presented by Wallis (1969) and Depew and Kramer (1973). To determine the maximum volumetric fraction so that the presence of particles does not significantly contribute to the specific heat of the mixture, equation (D-22) is rewritten in the following form:

$$\rho^* C^* = \rho_f^* C_f^*\left\{1+\alpha\left(\frac{\rho_p^* C_p^*}{\rho_f^* C_f^*}-1\right)\right\}. \qquad \text{(D-23)}$$

The particles are assumed to be carbon steel, which has a density of 7800 $kg \cdot m^{-3}$ and a specific heat of 465 $J \cdot kg^{-1} \cdot K^{-1}$. For the steam conditions of interest, the minimum product of density and specific heat occurs at 1000°C and has a value of 30 $kJ \cdot m^{-3} \cdot K^{-1}$. Substitution of these values into equation (D-23) yields the following relationship:

$$\rho^* C^* = \rho_f^* C_f^* (1 + 120\alpha), \tag{D-24}$$

where $120\alpha$ represents the contribution of the particles to the specific heat of the mixture. If it is arbitrarily assumed that this contribution is negligibly small when it is less than $10^{-2}$, equation (D-24) gives the corresponding maximum volumetric fraction of the particles, $\alpha$, as $8.3 \times 10^{-5}$. This value of the maximum particle volumetric fraction is greater than the maximum allowable value of the particle volumetric fraction for neglecting the effect of the particles on the mixture density. Thus, from equation (D-24), if the maximum particle volumetric fraction for the neglect of particles on the fluid density is satisfied, the specific heat at constant pressure of the mixture can be taken as that of the fluid alone.

From the above values derived for the maximum particle volumetric fraction allowable to neglect the effects due to the presence of particles on the thermophysical properties of density, dynamic viscosity, thermal conductivity, and specific heat at constant pressure, the least of these maximum particle volumetric fractions is that for density, which is $1.5 \times 10^{-5}$. As stated in Section 2.5, the maximum volumetric fraction of particles to be considered in the present investigation is $1.7 \times 10^{-6}$. Thus, *the thermophysical properties in the governing equations (D-2) and (D-17) can be taken as those of the steam alone* since the presence of the aerosol particles does not appreciably affect these values.

### D.3. Development of Dimensionless Groups

The governing equations (D-1), D-2), and (D-17), and the necessary initial conditions and boundary conditions to complete the problem description, will now be nondimensionalized, as described in Section D.1, by introducing the following set of nondimensional variables:

$$t \equiv \frac{t^*}{t_c} = \text{dimensionless time}, \tag{D-25}$$

$$x \equiv \frac{x^*}{X_c} = \text{dimensionless spatial coordinate}, \tag{D-26}$$

$$y \equiv \frac{y^*}{Y_c} = \text{dimensionless spatial coordinate}, \tag{D-27}$$

$$\rho \equiv \frac{\rho^*}{\rho_c} = \text{dimensionless density}, \tag{D-28}$$

$$F \equiv \frac{F^*}{F_c} = \text{dimensionless body force}, \tag{D-29}$$

$$\mu \equiv \frac{\mu^*}{\mu_c} = \text{dimensionless viscosity}, \tag{D-30}$$

$$P \equiv \frac{P^*}{P_c} = \text{dimensionless pressure}, \tag{D-31}$$

$$C \equiv \frac{C^*}{C_c} = \text{dimensionless specific heat}, \tag{D-32}$$

$$k \equiv \frac{k^*}{k_c} = \text{dimensionless thermal conductivity}, \tag{D-33}$$

$$Q \equiv \frac{Q^*}{Q_c} = \text{dimensionless volumetric heat source}, \tag{D-34}$$

$$q_r \equiv \frac{q_r^*}{q_{rc}} = \text{dimensionless radiant heat flux}, \tag{D-35}$$

$$u \equiv \frac{u^*}{U_c} = \text{dimensionless velocity}, \tag{D-36}$$

$$v \equiv \frac{v^*}{V_c} = \text{dimensionless velocity}, \tag{D-37}$$

$$T \equiv \frac{T^*}{T_c} = \text{dimensionless temperature}, \tag{D-38}$$

$$N \equiv \frac{N^*}{N_c} = \text{dimensionless particle concentration}, \tag{D-39}$$

$$K \equiv \frac{K^*}{K_c} = \text{dimensionless thermophoretic coefficient}, \tag{D-40}$$

and

$$\mathcal{D} \equiv \frac{\mathcal{D}^*}{\mathcal{D}_c} = \text{dimensionless diffusion coefficient}. \tag{D-41}$$

Substituting equation (D-10) for the effective density of the mixture into the continuity equation (D-1) yields the following relationship:

$$(1-\alpha)\left\{\frac{\partial \rho_f^*}{\partial t^*}+\frac{\partial}{\partial x_j^*}(\rho_f^* u_j^*)\right\}+\alpha\left\{\frac{\partial \rho_p^*}{\partial t^*}+\frac{\partial}{\partial x_j^*}(\rho_p^* u_j^*)-\frac{\partial j_j^*}{\partial x_j^*}\right\} = 0. \tag{D-42}$$

The terms in the first and second braces in equation (D-42) represent conservation of mass for the steam and for the particles, respectively. In order for this equation to be satisfied under all possible conditions, the terms in the braces must each be equal to zero. This requirement yields two separate equations: one for the conservation of mass of the steam and another for the conservation of mass of the particles. The relative importance of each component in equation (D-42) is determined by the value of the volumetric fraction, $\alpha$. If the particle behavior were not of interest, the mixture continuity equation (D-42) shows that mass flow rate of the particles can be neglected with respect to that of the fluid with a resulting error of the order of the volumetric fraction of the particles, $\alpha$, which is $10^{-6}$ for the conditions of interest of the present investigation. However, the particle behavior *is* of interest for this problem and the continuity equation allows decoupling the individual mixture components.

The requirement that the first term in braces of equation (D-42) be zero yields the following equation for conservation of mass of the steam:

$$\frac{\partial \rho_f^*}{\partial t^*} + \frac{\partial}{\partial x_j^*}(\rho_f^* u_j^*) = 0 . \tag{D-43}$$

Rewriting equation (D-43) for two-dimensional cartesian coordinates and in terms of the nondimensional variables gives:

$$\left(\frac{X_c}{t_c U_c}\right)\left[\frac{\partial \rho}{\partial t}\right] + \left[\frac{\partial(\rho u)}{\partial x}\right] + \left(\frac{V_c X_c}{U_c Y_c}\right)\left[\frac{\partial(\rho v)}{\partial y}\right] = 0 . \tag{D-44}$$

For the proper choice of the characteristic quantities, each term, independent of its coefficient, should be of unit order. Physically, the coefficient

$$\left(\frac{X_c}{t_c U_c}\right) \tag{D-45}$$

represents the ratio of a "flow time," or time which a fluid packet spends in the region of interest, to a characteristic time, $t_c$, for a transient to occur in the flow. The value of this ratio denotes the relative importance of transient effects on conservation of mass. The coefficient

$$\left(\frac{V_c X_c}{U_c Y_c}\right) \tag{D-46}$$

represents the relative importance of the net mass flow rate of steam in the $y$-direction with respect to that in the $x$-direction.

The characteristic values for the coefficient terms are left unspecified for now. For the remainder of this analysis, any term with dimensionless quantities enclosed in square brackets is assumed to be of unit order. The leading coefficient of each term is generally enclosed in parentheses and the order of magnitude of this coefficient indicates the relative importance of the following unit-order term.

The part of the mixture conservation equation (D-42) that represents conservation of particles may be written separately as

$$\frac{\partial \rho_p^*}{\partial t^*} + \frac{\partial}{\partial x_j^*}(\rho_p^* u_j^*) - \frac{\partial j_j^*}{\partial x_j^*} = 0 . \tag{D-47}$$

Denoting the number of particles per unit mass of fluid by $N^*$ and the mass of aerosol per particle by $M_p$, the aerosol particle density may be written as

$$\rho_p^* = \rho^* N^* M_p . \tag{D-48}$$

The total aerosol particle mass flux is the sum of the Brownian diffusion mass flux, the thermophoretic mass flux, and the gravitational settling mass flux (Hidy and Brock, 1970). The Brownian flux in the $x$-direction is determined from Fick's law to be the product of the Brownian diffusion coefficient, $\mathcal{D}$, and the aerosol density gradient in the $x$-direction. The thermophoretic mass flux is the product of the thermophoretic velocity $V_T$, as defined by equation (4-7), and the aerosol density. The gravitational settling mass flux is the product of the Stokes settling velocity (Hidy and Brock, 1970) and the aerosol particle density. The Stokes settling velocity, $V_g$, is given by the following expression:

$$V_g = \frac{2R^2}{9\nu^*}\left(\frac{\rho_p^*}{\rho_f^*} - 1\right) g . \tag{D-49}$$

Thus, the total aerosol mass flux in the $x$-direction is given by:

$$j_x^* = -\left\{\rho^* N^* K^* \frac{\nu}{T^*}\frac{\partial T^*}{\partial x^*} + \mathcal{D}^* \frac{\partial(\rho^* N^*)}{\partial x^*} + V_g \rho^* N^*\right\} . \tag{D-50}$$

Substitution of the expression for the particle mass flux in the $x$-direction, as given by equation (D-50), along with an analogous expression (without the gravitational settling term) for the particle mass flux in the $y$-direction, and the expression for the aerosol density given by equation (D-48) into equation (D-47), yields the following particle conservation equation:

$$\frac{\partial(\rho^* N^*)}{\partial t^*}+\frac{\partial}{\partial x^*}(\rho^* u^* N^*)+\frac{\partial}{\partial y^*}(\rho^* v^* N^*)+\frac{\partial}{\partial y^*}\left(\rho^* N^* K^* \frac{\nu}{T^*}\frac{\partial T^*}{\partial y^*}+\mathcal{D}^*\frac{\partial(\rho^* N^*)}{\partial y^*}\right)$$

$$+\frac{\partial}{\partial x^*}\left(\rho^* N^* K^* \frac{\nu}{T^*}\frac{\partial T^*}{\partial x^*}+\mathcal{D}^*\frac{\partial(\rho^* N^*)}{\partial x^*}+V_g\rho^* N^*\right)=0. \qquad \text{(D-51)}$$

Since only a monodisperse aerosol is assumed to be present, the mass of aerosol per particle is constant and, therefore, does not appear in equation (D-51).

Substitution of the product of the characteristic value and a dimensionless value for each quantity in equation (D-51) and division by the coefficient of the $x$-direction convective term yields the following equation:

$$\left(\frac{X_c}{t_c U_c}\right)\left[\frac{\partial(\rho N)}{\partial t}\right]+\left[\frac{\partial}{\partial x}(\rho u N)\right]+\left(\frac{V_c X_c}{U_c Y_c}\right)\left[\frac{\partial}{\partial y}(\rho v N)\right]$$

$$+\left(\frac{\nu_c}{U_c X_c}\right)\left(\frac{X_c}{Y_c}\right)^2\left[\frac{\partial}{\partial y}\left(K_c\left[\rho N K\frac{\nu}{T}\frac{\partial T}{\partial y}\right]+\left(\frac{\mathcal{D}_c}{\nu_c}\right)\left[\mathcal{D}\frac{\partial(\rho N)}{\partial y}\right]\right)\right]$$

$$+\left(\frac{\nu_c}{U_c X_c}\right)\left[\frac{\partial}{\partial x}\left(K_c\left[\rho N K\frac{\nu}{T}\frac{\partial T}{\partial x}\right]+\left(\frac{\mathcal{D}_c}{\nu_c}\right)\left[\mathcal{D}\frac{\partial(\rho N)}{\partial x}\right]\right)\right]+\left(\frac{V_g}{U_c}\right)\left[\frac{\partial(\rho N)}{\partial x}\right]=0. \qquad \text{(D-52)}$$

The values of the leading terms in parentheses are to be determined by analysis of the scaled versions of the other governing equations. Note that no characteristic value for particle concentration appears in equation (D-52). The scale for particle concentration is determined from evaluation of the boundary conditions for the particle concentration, as will be shown later in this section.

The equation for conservation of momentum in the $x$-direction, equation (D-2), is given by:

$$\rho^*\frac{\partial u^*}{\partial t^*}+\rho^* u^*\frac{\partial u^*}{\partial x^*}+\rho^* v^*\frac{\partial u^*}{\partial y^*}=\rho^* F_x^*-\frac{\partial P^*}{\partial x^*}+\frac{\partial}{\partial y^*}\left\{\mu^*\left(\frac{\partial u^*}{\partial y^*}+\frac{\partial v^*}{\partial x^*}\right)\right\}$$

$$+\frac{\partial}{\partial x^*}\left\{2\mu^*\frac{\partial u^*}{\partial x^*}-\frac{2\mu^*}{3}\left(\frac{\partial u^*}{\partial x^*}+\frac{\partial v^*}{\partial y^*}\right)\right\}. \qquad \text{(D-53)}$$

Rewriting this equation in terms of the dimensionless variables and dividing by the coefficient of the convective acceleration in the $x$-direction yields:

$$\left(\frac{X_c}{t_c U_c}\right)\left[\rho\frac{\partial u}{\partial t}\right]+\left[\rho u\frac{\partial u}{\partial x}\right]+\left(\frac{V_c X_c}{U_c Y_c}\right)\left[\rho v\frac{\partial u}{\partial y}\right]=\left(\frac{X_c F_{cx}}{U_c^2}\right)[\rho F_x]-\left(\frac{P_c}{\rho_c U_c^2}\right)\left[\frac{\partial P}{\partial x}\right]$$
$$+\left(\frac{\nu_c}{U_c X_c}\right)\left(\frac{X_c}{Y_c}\right)^2\left[\frac{\partial}{\partial y}\left\{\mu\left(\frac{\partial u}{\partial y}+\frac{V_c X_c}{U_c Y_c}\left(\frac{Y_c}{X_c}\right)^2\frac{\partial v}{\partial x}\right)\right\}\right]$$
$$+\left(\frac{\nu_c}{U_c X_c}\right)\left[\frac{\partial}{\partial x}\left\{2\mu\frac{\partial u}{\partial x}-\frac{2\mu}{3}\left(\frac{\partial u}{\partial x}+\frac{V_c X_c}{U_c Y_c}\frac{\partial v}{\partial y}\right)\right\}\right]. \qquad \text{(D-54)}$$

Similarly, rewriting the equation for conservation of momentum in the $y$-direction gives:

$$\rho^*\frac{\partial v^*}{\partial t^*}+\rho^* u^*\frac{\partial v^*}{\partial x^*}+\rho^* v^*\frac{\partial v^*}{\partial y^*}=\rho^* F_y^*-\frac{\partial P^*}{\partial y^*}+\frac{\partial}{\partial x^*}\left\{\mu^*\left(\frac{\partial u^*}{\partial y^*}+\frac{\partial v^*}{\partial x^*}\right)\right\}$$
$$+\frac{\partial}{\partial y^*}\left\{2\mu^*\frac{\partial v^*}{\partial y^*}-\frac{2\mu^*}{3}\left(\frac{\partial u^*}{\partial x^*}+\frac{\partial v^*}{\partial y^*}\right)\right\}. \qquad \text{(D-55)}$$

Rewriting this equation in terms of the nondimensional variables and dividing by the coefficient of the pressure gradient in the $y$-direction yields:

$$\left(\frac{\rho_c V_c Y_c}{t_c P_c}\right)\left[\rho\frac{\partial v}{\partial t}\right]+\left(\frac{\rho_c U_c V_c Y_c}{P_c X_c}\right)\left[\rho u\frac{\partial v}{\partial x}\right]+\left(\frac{\rho_c V_c^2}{P_c}\right)\left[\rho v\frac{\partial v}{\partial y}\right]=\left(\frac{\rho_c Y_c F_{yc}}{P_c}\right)[\rho F_y]$$
$$-\left[\frac{\partial P}{\partial y}\right]+\left(\frac{\mu_c U_c}{P_c X_c}\right)\left[\frac{\partial}{\partial x}\left\{\mu\left(\frac{\partial u}{\partial y}+\frac{V_c X_c}{U_c Y_c}\left(\frac{Y_c}{X_c}\right)^2\frac{\partial v}{\partial x}\right)\right\}\right]$$
$$+\left(\frac{\mu_c V_c}{P_c Y_c}\right)\left[\frac{\partial}{\partial y}\left\{2\mu\frac{\partial v}{\partial y}-\frac{2\mu}{3}\left(\frac{V_c X_c}{U_c Y_c}\frac{\partial u}{\partial x}+\frac{\partial v}{\partial y}\right)\right\}\right]. \qquad \text{(D-56)}$$

When equation (D-17) for conservation of energy is rewritten for a two-dimensional cartesian coordinate system and for constant dynamic viscosity and thermal conductivity, it is of the form:

$$\rho^*C^*\frac{\partial T^*}{\partial t^*}+\rho^*u^*C^*\frac{\partial T^*}{\partial x^*}+\rho^*v^*C^*\frac{\partial T^*}{\partial x^*} = (\beta^*T^*)\left(\frac{\partial P^*}{\partial t^*}+u^*\frac{\partial P^*}{\partial x^*}+v^*\frac{\partial P^*}{\partial y^*}\right)$$
$$+\frac{\partial}{\partial x^*}\left(k^*\frac{\partial T^*}{\partial x^*}\right)+\frac{\partial}{\partial y^*}\left(k^*\frac{\partial T^*}{\partial y^*}\right)+Q^*-\frac{\partial q^*_{rx}}{\partial x^*}-\frac{\partial q^*_{ry}}{\partial y^*}$$
$$+\mu^*\left\{2\left(\frac{\partial u^*}{\partial x^*}\right)^2+2\left(\frac{\partial v^*}{\partial y^*}\right)^2+\left(\frac{\partial u^*}{\partial y^*}+\frac{\partial v^*}{\partial x^*}\right)^2-\frac{2}{3}\left(\frac{\partial u^*}{\partial x^*}+\frac{\partial v^*}{\partial y^*}\right)^2\right\}. \qquad \text{(D-57)}$$

Rewriting this equation in terms of the nondimensional variables and dividing by the coefficient of the term representing the rate of convection in the $x$-direction gives:

$$\left(\frac{X_c}{t_cU_c}\right)\left[\rho C\frac{\partial T}{\partial t}\right]+\left[\rho uC\frac{\partial T}{\partial x}\right]+\left(\frac{V_cX_c}{U_cY_c}\right)\left[\rho vC\frac{\partial T}{\partial y}\right]$$
$$=\left(\frac{(\beta^*T^*)P_c}{\rho_cC_cT_c}\right)\left[\left(\frac{X_c}{t_cU_c}\right)\frac{\partial P}{\partial t}+u\frac{\partial P}{\partial x}+\left(\frac{V_cX_c}{U_cY_c}\right)v\frac{\partial P}{\partial y}\right]$$
$$+\left(\frac{k_c}{\rho_cU_cC_cX_c}\right)\left(\frac{X_c}{Y_c}\right)^2\left[\frac{\partial}{\partial y}\left(k\frac{\partial T}{\partial y}\right)+\left(\frac{Y_c}{X_c}\right)^2\frac{\partial}{\partial x}\left(k\frac{\partial T}{\partial x}\right)\right]$$
$$+\left(\frac{Q_cX_c}{\rho_cU_cC_cT_c}\right)[Q]-\left(\frac{q_{rc}}{\rho_cU_cC_cT_c}\right)\left(\frac{X_c}{Y_c}\right)\left[\left(\frac{Y_c}{X_c}\right)\frac{\partial q_{rx}}{\partial x}+\frac{\partial q_{ry}}{\partial y}\right]$$
$$+\left(\frac{\nu_cU_c}{C_cX_cT_c}\right)\left(\frac{X_c}{Y_c}\right)^2\left[2\mu\left(\frac{Y_c}{X_c}\right)^2\left\{\left(\frac{\partial u}{\partial x}\right)^2+\left(\frac{V_cX_c}{U_cY_c}\right)^2\left(\frac{\partial v}{\partial y}\right)^2\right\}\right.$$
$$\left.+\mu\left(\frac{\partial u}{\partial y}+\frac{V_cX_c}{U_cY_c}\left(\frac{Y_c}{X_c}\right)^2\frac{\partial v}{\partial x}\right)^2-\frac{2}{3}\left(\frac{Y_c}{X_c}\right)^2\mu\left(\frac{\partial u}{\partial x}+\frac{V_cX_c}{U_cY_c}\frac{\partial v}{\partial y}\right)^2\right]. \qquad \text{(D-58)}$$

Boundary conditions must be prescribed to complete the problem definition, and the values for the boundary conditions may possibly be used as scales. Boundary conditions for the fluid solution domain are required for the temperature, the fluid velocities, and the particle concentration, as prescribed in the problem definition. These boundary conditions are repeated below.

The boundary conditions on the fluid temperature are a known temperature distribution, $T_\infty(x)$, far from the wall and the interface condition that at the wall, the fluid temperature matches the wall temperature, $T_w$. Either temperature or the temperature difference could be used as a scale, $T_c$. This choice will be made in the next section.

The boundary conditions on the streamwise and transverse fluid velocity components at the wall are given by the no-slip condition and the requirement that there cannot be any flow through a solid surface; that is, both velocity components must be zero at the wall. Far from the wall, the streamwise velocity is specified as zero, which is appropriate for a quiescent fluid. An appropriate scale for the velocity in a natural convection flow is presented in the next section.

The boundary conditions for the particle concentration distribution in the flow are a specified concentration, $N_\infty$, far from the wall and a specified concentration of zero particles in the fluid immediately adjacent to the wall, that is, at zero distance from the wall. This boundary condition of zero particle concentration at zero distance from the wall is *mathematically convenient and the physical significance is debatable*, hence, its use is controversial. The specified concentration of particles far from the wall, as presented in Section 2.5, is on the order of $10^{11}$ particles per kilogram of steam. These prescribed particle concentrations vary over a range of several orders of magnitude. Indeed, the particle conservation governing equation (D-52) can admit *any* particle concentration scale, since no particle concentration scale appears in any of the terms of equation (D-52). Since the controversial requirement of zero particle concentration in the fluid at the wall arises from the consideration of Brownian diffusion, the scale for the particle concentration is chosen for convenience to be that of the particle concentration far from the wall, or $N_c = N_\infty$.

Several of the dimensionless parameters appear in the scaled equations (D-44), (D-52), (D-53), (D-56), and (D-58). Appropriate choices must now be made for the values of the characteristic quantities, or scales, and these values used to compute the values of the dimensionless parameters that appear in the scaled equations. The resulting values of the dimensionless parameters can then be used to systematically identify negligible terms in the equations. The effect of these choices in all five conservation

equations must be evaluated. In general, rescaling might be appropriate for different conditions or if a singular perturbation arises, although for the present investigation, rescaling was not necessary.

The characteristic time, $t_c$, is still undetermined for the coupled problem. There are two characteristic times, one representative of the temporal behavior of the solid plate and the other representative of the temporal behavior of the fluid. Although the spatial domains of the solid and the gas are different, they are joined across the face of the plate, where the local surface temperature and heat flux of the solid and fluid must match and the fluid velocity must be zero.

The equation for conservation of energy for the solid plate can be obtained by setting the convective, compression work, viscous work, volumetric heating, and radiation terms of the general, constant property, energy conservation equation (D-17) to zero. This yields the well-known transient conduction equation in physical variables

$$\rho^* C^* \frac{\partial T^*}{\partial t^*} = \frac{\partial}{\partial x^*}\left(k^* \frac{\partial T^*}{\partial x^*}\right) + \frac{\partial}{\partial y^*}\left(k^* \frac{\partial T^*}{\partial y^*}\right), \tag{D-59}$$

which is valid in the solid. Rewriting this equation in terms of the dimensionless variables yields:

$$\frac{\rho_s C_s Y_s^2}{k_s t_s}\left[\rho C \frac{\partial T}{\partial t}\right] = \left(\frac{Y_s}{X_s}\right)^2\left[\frac{\partial}{\partial x}\left(k \frac{\partial T}{\partial x}\right)\right] + \left[\frac{\partial}{\partial y}\left(k \frac{\partial T}{\partial y}\right)\right]. \tag{D-60}$$

Selection of the appropriate reference quantities, or scales, is performed in the following sections.

### D.4. Selection of the Reference Quantities for the Fluid Domain

The scaled fluid equations (D-43), (D-52), (D-54), (D-56), and (D-58) are examined below to select the appropriate values of the scales.

First, the characteristic values of the velocity, $U_c$, and of the spatial coordinate in the $x$-direction, $X_c$, will be determined. In a natural convection flow, a characteristic velocity is not as readily apparent as it is in a forced convection flow. Jaluria (1980) shows that when a buoyancy force due to density differences acts over a distance $L$ (such as the plate length), it increases the kinetic energy of the fluid. Thus, approximating the work done on a fluid packet by the buoyancy force to the change in kinetic energy of the packet gives:

$$\frac{\rho_c U_c^2}{2} \approx gL(\rho_\infty - \rho_c). \tag{D-61}$$

Viscous forces have been neglected in this estimate. Thus, this relationship represents an upper bound on the fluid velocity, $U_c$. Since a characteristic velocity must only be known to within an order of magnitude, the factor of 2 may be ignored, resulting in the following expression for the reference velocity:

$$U_c = \left( gL \frac{\rho_\infty - \rho_c}{\rho_c} \right)^{1/2}. \tag{D-62}$$

Rewriting this expression in terms of the Grashof number gives:

$$U_c = \frac{\nu_c}{L} Gr^{1/2}, \tag{D-63}$$

which is a valid estimate for the large Grashof number flows of interest in this present investigation.

The fluid transit time, $X_c/U_c$, may be taken as a characteristic time for the fluid. Thus, for high Grashof number flows, the expression

$$t_c = \frac{X_c}{U_c} = \frac{L^2}{\nu_c} Gr^{-1/2} \tag{D-64}$$

will be used as the estimate of the characteristic time for the fluid.

The coefficient, as expressed in equation (D-46), of the third term on the left-hand side of the fluid continuity equation (D-44) represents the relative importance of the net mass flow rate of fluid in the $y$-direction to that in the $x$-direction. The value of this coefficient is set to one, such that

$$\frac{V_c}{U_c} = \frac{Y_c}{X_c}. \tag{D-65}$$

One or both of the terms in parenthesis of equation (D-44) must be of unit order if the scaling is correct. This choice of characteristic quantities of equation (D-65) then indicates that the net mass rate of flow in the $y$-direction is just as important as that in the $x$-direction.

An appropriate characteristic pressure is the dynamic pressure, which is defined as follows:

$$P_c = \rho_c U_c^2. \tag{D-66}$$

A body force acting in the streamwise direction is the weight of the fluid in the boundary layer. The characteristic body force per unit fluid mass, $F_{cx}$, would simply be the acceleration of gravity, $g$, which acts in the negative $x$-direction. Substitution of the relationship between the characteristic velocities and lengths of equation (D-65) and the characteristic body force, characteristic pressure, characteristic velocity $U_c$, and characteristic plate length $L$ into equation (D-54) yields:

$$\left(\frac{L^2}{t_c \nu_c Gr^{1/2}}\right)\left[\rho\frac{\partial u}{\partial t}\right]+\left[\rho u\frac{\partial u}{\partial x}\right]+\left[\rho v\frac{\partial u}{\partial y}\right] = -\left(\frac{gL^3}{\nu_c^2 Gr}\right)[\rho F_x]-\left[\frac{\partial P}{\partial x}\right]$$
$$+\frac{1}{Gr^{1/2}}\left(\frac{X_c}{Y_c}\right)^2\left[\frac{\partial}{\partial y}\left\{\mu\left(\frac{\partial u}{\partial y}+\left(\frac{Y_c}{X_c}\right)^2\frac{\partial v}{\partial x}\right)\right\}\right]+\frac{1}{Gr^{1/2}}\left[\frac{\partial}{\partial x}\left\{2\mu\frac{\partial u}{\partial x}-\frac{2\mu}{3}\left(\frac{\partial u}{\partial x}+\frac{\partial v}{\partial y}\right)\right\}\right]. \tag{D-67}$$

In order to balance the viscous forces with the pressure and the buoyancy forces of equation (D-67) for steady-state conditions, the coefficient of the third term on the right-hand side must be of unit order. The ratio of transverse and streamwise lengths is then specified as

$$\frac{Y_c}{X_c} = \frac{\delta}{L} = Gr^{-1/4}, \tag{D-68}$$

where $\delta$ is the thickness of the boundary layer.

The thermodynamic pressure of the system is decomposed into the sum of the hydrostatic pressure and the motion pressure, which is the difference between the actual pressure at a point in the fluid and the pressure at that point if the fluid was at rest at the (uniform) reference conditions, or

$$P^* = P_h^* + P_m^* . \tag{D-69}$$

The streamwise pressure gradient is therefore given by:

$$\frac{\partial P^*}{\partial x^*} = \frac{\partial P_h^*}{\partial x^*} + \frac{\partial P_m^*}{\partial x^*} . \tag{D-70}$$

The hydrostatic pressure is that due to the weight of the fluid outside of the boundary layer as referenced to the origin. A characteristic hydrostatic pressure would therefore be $P_h^* = -\rho_\infty g L$, where the subscript "$\infty$" represents the density outside of the boundary layer so that the characteristic body force is representative of thermally-stratified as well as isothermal fluids. Substitution of the product of the characteristic value and a dimensionless value for each quantity in equation (D-70) yields:

$$\left[\frac{\partial P}{\partial x}\right] = \frac{P_{ch}}{P_c}\left[\frac{\partial P_h}{\partial x}\right] + \frac{P_{cm}}{P_c}\left[\frac{\partial P_m}{\partial x}\right] = -\frac{\rho_\infty g L}{\rho_c U_c^2}\left[\frac{\partial P_h}{\partial x}\right] + \frac{P_{cm}}{\rho_c U_c^2}\left[\frac{\partial P_m}{\partial x}\right] . \tag{D-71}$$

Substitution of equation (D-71), equation (D-68), and equation (D-65) into equation (D-67), and using the definition of Grashof number gives:

$$\left(\frac{L^2}{t_c \nu_c Gr^{1/2}}\right)\left[\rho\frac{\partial u}{\partial t}\right]+\left[\rho u\frac{\partial u}{\partial x}\right]+\left[\rho v\frac{\partial u}{\partial y}\right]=-\left(\frac{\rho_c}{\rho_\infty-\rho_c}\right)[\rho F_x]+\left(\frac{\rho_\infty}{\rho_\infty-\rho_c}\right)\left[\frac{\partial P_h}{\partial x}\right]$$
$$-\left(\frac{P_{cm}}{P_c}\right)\left[\frac{\partial P_m}{\partial x}\right]+\left[\frac{\partial}{\partial y}\left\{\mu\left(\frac{\partial u}{\partial y}+\frac{1}{Gr^{1/2}}\frac{\partial v}{\partial x}\right)\right\}\right]+\left(\frac{1}{Gr^{1/2}}\right)\left[\frac{\partial}{\partial x}\left\{2\mu\frac{\partial u}{\partial x}-\frac{2\mu}{3}\left(\frac{\partial u}{\partial x}+\frac{\partial v}{\partial y}\right)\right\}\right]. \qquad \text{(D-72)}$$

In order to evaluate the characteristic motion pressure, $P_{cm}$, the equation representing Newton's Second Law in the $y$-direction, equation (D-56), is now examined. First, since there obviously is no body force acting normal to the plate as shown in Figure 2-2, $F_{cy}$ is identically zero and there can be no hydrostatic contribution to the normal pressure gradient. The normal pressure gradient is therefore obtained by differentiating equation (D-69) with respect to the $y$-direction to give

$$\frac{\partial P^*}{\partial y^*}=\frac{\partial P_m^*}{\partial y^*}. \qquad \text{(D-73)}$$

Substitution of the of the characteristic values and dimensionless values for the motion pressure and the thermodynamic pressure yields:

$$\left[\frac{\partial P}{\partial y}\right]=\left(\frac{P_{cm}}{P_c}\right)\left[\frac{\partial P_m}{\partial y}\right]. \qquad \text{(D-74)}$$

Substitution of the characteristic velocity, $U_c$, of equation (D-63), and the ratio of the characteristic lengths, equation (D-65), into equation (D-56) gives:

$$\left(\frac{L^2}{t_c \nu_c Gr}\right)\left[\rho\frac{\partial v}{\partial t}\right]+\left(\frac{1}{Gr^{1/2}}\right)\left[\rho u\frac{\partial v}{\partial x}\right]+\left(\frac{1}{Gr^{1/2}}\right)\left[\rho v\frac{\partial v}{\partial y}\right]=-\left(\frac{P_{cm}}{P_c}\right)\left[\frac{\partial P_m}{\partial y}\right]$$
$$+\left(\frac{1}{Gr^{1/2}}\right)\left[\frac{\partial}{\partial x}\left\{\mu\left(\frac{\partial u}{\partial y}+\frac{1}{Gr^{1/2}}\frac{\partial v}{\partial x}\right)\right\}\right]+\left(\frac{1}{Gr^{1/2}}\right)\left[\frac{\partial}{\partial y}\left\{2\mu\frac{\partial v}{\partial y}-\frac{2\mu}{3}\left(\frac{\partial u}{\partial x}+\frac{\partial v}{\partial y}\right)\right\}\right]. \qquad \text{(D-75)}$$

Inspection of equation (D-75) shows that only the local acceleration forces may balance the convective acceleration and viscous forces. This occurs when the characteristic time, $t_c$, is given by

$$t_c = \frac{L^2}{\nu_c Gr^{1/2}}. \tag{D-76}$$

For steady-state conditions and for the Grashof number flows of interest ($Gr > 10^5$) in this present investigation, the normal pressure force term of equation (D-75) is not balanced with any other force term, and, thus, the derivative of the motion pressure with respect to the $y$-direction is identically zero. The pressure gradient across the boundary layer is given by

$$\frac{\partial P_m}{\partial y} = \frac{\partial P}{\partial y} = 0. \tag{D-77}$$

The pressure in the boundary layer is then constant with respect to the $y$-direction for the large Grashof number flows of interest in this present investigation and must be equal to the pressure outside the boundary layer. Since the motion pressure outside the boundary layer is constant everywhere, the gradient of the motion pressure with respect to the $x$-direction is also zero. Thus, the pressure in the boundary layer is constant.

The equation for Newton's Second Law in the $x$-direction, equation (D-72), for the Grashof number flows of interest ($Gr > 10^5$) in this present investigation reduces to:

$$\left(\frac{L^2}{t_c \nu_c Gr^{1/2}}\right)\left[\rho\frac{\partial u}{\partial t}\right] + \left[\rho u\frac{\partial u}{\partial x}\right] + \left[\rho v\frac{\partial u}{\partial y}\right] = -\left(\frac{\rho_c}{\rho_\infty - \rho_c}\right)[\rho F_x] + \left(\frac{\rho_\infty}{\rho_\infty - \rho_c}\right)\left[\frac{\partial P_h}{\partial x}\right] + \left[\frac{\partial}{\partial y}\left(\mu\frac{\partial u}{\partial y}\right)\right]. \tag{D-78}$$

The unit-order body force (weight) term and the unit-order hydrostatic pressure force term are representative of the force that drives the flow and are thus combined into a unit-order buoyant force term, $[B]$. Equation (D-78) reduces to the following form:

$$\left(\frac{L^2}{t_c \nu_c Gr^{1/2}}\right)\left[\rho\frac{\partial u}{\partial t}\right]+\left[\rho u\frac{\partial u}{\partial x}\right]+\left[\rho v\frac{\partial u}{\partial y}\right] = [B]+\left[\frac{\partial}{\partial y}\left(\mu\frac{\partial u}{\partial y}\right)\right]. \qquad \text{(D-79)}$$

The equation for Newton's Second Law in the $x$-direction is now scaled, except for an unknown scale for the fluid-flow time in the coefficient of the inertia force term. This fluid-flow time scale is shown in a subsequent section to be negligibly small with respect to a time scale for thermal conduction in the solid wall component. Also, inspection of equations (D-75) and (D-79) shows that the equation for Newton's Second Law in the $y$-direction is scaled with respect to the equation for Newton's Second Law in the $x$-direction by a factor of $Gr^{-1/2}$, such that for the high Grashof number flows of interest in this investigation, the equation for Newton's Second Law in the $y$-direction need not be solved.

The terms in the scaled conservation of energy equation (D-58) are now examined. The appropriate values for the isobaric expansion coefficient, $\beta$, the temperature, $T^*$, and the characteristic temperature, $T_c$, are now determined.

The first term on the right-hand side of equation (D-58) deals with the work done by pressure forces to deform the control volume ("compression work"). The product of the isobaric expansion coefficient, $\beta$, and the absolute temperature is identically one for an ideal gas. For the conditions of this present work, this value is acceptable.

The appropriate value for the characteristic temperature, $T_c$, is determined as follows. Inspection of the conservation of energy equation (D-57) in physical variables shows that the absolute temperature appears only in the coefficient of the compression-work term. For ideal gases, this term has already been considered in the above paragraph. Only derivatives of the temperature appear in all the other terms in the equation. The characteristic temperature $T_c$ could represent a temperature difference. However, the temperature of the reactor vessel wall, $T_w$, is a boundary condition for both the fluid and solid subdomains, as shown in Figure 2-2, and would be an appropriate value for the characteristic temperature. Hence, $T_c = T_w$.

A characteristic value for the radiant heat flux is the difference in the blackbody emissive powers of the wall and of the fluid far from the wall. This characteristic radiant heat flux is given by:

$$q_{cr} = \sigma(T_w^4 - T_\infty^4). \tag{D-80}$$

Substitution of these characteristic values for temperature and radiant heat flux, along with the previously determined values for the characteristic length scales and the characteristic velocity $U_c$, into equation (D-58) gives:

$$\begin{aligned}
&\left(\frac{L^2}{t_c \nu_c Gr^{1/2}}\right)\left[\rho C\frac{\partial T}{\partial t}\right]+\left[\rho u C\frac{\partial T}{\partial x}\right]+\left[\rho v C\frac{\partial T}{\partial y}\right] \\
&\quad=\left(\frac{gL}{\rho_c C_c}\right)\left(\frac{\rho_\infty-\rho_c}{T_w-T_\infty}\right)\left[\left(\frac{L^2}{t_c \nu_c Gr^{1/2}}\right)\frac{\partial P}{\partial t}+u\frac{\partial P}{\partial x}+v\frac{\partial P}{\partial y}\right] \\
&\quad+\frac{1}{Pr}\left[\frac{\partial}{\partial y}\left(k\frac{\partial T}{\partial y}\right)+\frac{1}{Gr^{1/2}}\frac{\partial}{\partial x}\left(k\frac{\partial T}{\partial x}\right)\right] \\
&\quad+\frac{1}{PrGr^{1/2}}\left(\frac{Q_c L^2}{k_c(T_w-T_\infty)}\right)[Q] \\
&\quad-\left(\frac{L\sigma}{\mu_c C_c Gr^{1/4}}\right)\left(\frac{T_w^4-T_\infty^4}{T_w-T_\infty}\right)\left[\frac{1}{Gr^{1/4}}\frac{\partial q_{rx}}{\partial x}+\frac{\partial q_{ry}}{\partial y}\right] \\
&\quad+\left(\frac{gL}{\rho_c C_c}\right)\left(\frac{\rho_\infty-\rho_c}{T_w-T_\infty}\right)\left[\frac{1}{Gr^{1/2}}2\mu\left\{\left(\frac{\partial u}{\partial x}\right)^2+\left(\frac{\partial v}{\partial y}\right)^2\right\}\right. \\
&\qquad\left.+\mu\left(\frac{\partial u}{\partial y}+\frac{1}{Gr^{1/4}}\frac{\partial v}{\partial x}\right)^2-\frac{2}{3}\frac{1}{Gr^{1/2}}\mu\left(\frac{\partial u}{\partial x}+\frac{\partial v}{\partial y}\right)^2\right].
\end{aligned} \tag{D-81}$$

For ideal gases, the leading coefficient in parentheses of the compression-work term and the viscous dissipation term is approximated as follows:

$$\left(\frac{gL}{\rho_c C_c}\right)\left(\frac{\rho_\infty-\rho_c}{T_w-T_\infty}\right)=\left(\frac{gL}{C_c T_\infty}\right)\left(\frac{\rho_\infty-\rho_c}{\rho_c}\right)\left(\frac{T_\infty}{T_w-T_\infty}\right)=\left(\frac{gL}{C_c T_\infty}\right)\left(\frac{\rho_\infty/\rho_c-1}{T_w/T_\infty-1}\right)\approx\frac{gL}{C_c T_\infty}, \tag{D-82}$$

which holds for an ideal gas, where the density is inversely proportional to the temperature such that $\rho_c \propto T_w^{-1}$. Substitution of known quantities into equation (D-82) yields:

$$\left(\frac{gL}{\rho_c C_c}\right)\left(\frac{\rho_\infty - \rho_c}{T_w - T_\infty}\right) \approx \frac{gL}{C_c T_\infty} \approx 10^{-6}. \tag{D-83}$$

The leading coefficient of the radiative heat flux is rewritten as follows:

$$\left(\frac{L\sigma}{\mu_c C_c Gr^{1/4}}\right)\left(\frac{T_w^4 - T_\infty^4}{T_w - T_\infty}\right) = \frac{1}{PrGr^{1/4}}\left(\frac{L\sigma(T_w + T_\infty)(T_w^2 + T_\infty^2)}{k_c}\right). \tag{D-84}$$

The dimensionless group in parentheses on the right hand side of equation (D-84) is the Stefan number, *St* (Catchpole and Fulford, 1986), which is indicative of the ratio of heat transfer by participating radiation to heat transfer by conduction. The Stefan number is defined as:

$$St = \frac{L\sigma(T_w + T_\infty)(T_w^2 + T_\infty^2)}{k_c}. \tag{D-85}$$

Substitution of known quantities of interest in the present investigation into equation (D-85) results in a value of approximately $10^3$ for the Stefan number. The leading coefficient of the dimensionless radiant heat flux term of equation (D-81) then is approximately

$$\frac{10^3}{PrGr^{1/4}}. \tag{D-86}$$

The value of this coefficient is on the order of one for the high Grashof numbers of interest ($10^{12}$) for this problem and would be greater than one for the lower Grashof numbers of interest ($10^9$). Thus, participating gas radiation heat transfer must be considered in the present investigation.

The dimensionless group in parentheses multiplying the unit-order heat source term of equation (D-81) is a Damköhler number, *Da* (Catchpole and Fulford, 1986), which is defined as:

$$Da \equiv \frac{Q_c L^2}{k_c(T_w - T_{\infty,0})} = \frac{\text{rate of energy generation}}{\text{rate of heat transfer by conduction}}. \qquad \text{(D-87)}$$

For the leading coefficient of the heat source term in equation (D-81) to be approximately one, the Damköhler number, *Da*, must be equal to the product of the Prandtl number, *Pr*, and the square root of the Grashof number, *Gr*. For the conditions in the present investigation of a maximum heat source strength of 5 kW/m$^3$, a characteristic flow length of 3 m, and a maximum temperature difference between the wall and ambient fluid (steam) of 700 K, the Damköhler number is of the order of $10^3$. The term $Da/(PrGr^{1/2})$, which is the leading coefficient of the heat source term in equation (D-81), is of order one for flows having a Grashof number of $10^6$ and is of order $10^{-2}$ for flows having a Grashof number of $10^{10}$. Thus, volumetric heat sources become important for low Grashof number flows and for high Damköhler number situations, which, according to equation (D-87), may occur at low values of the temperature difference between the wall and the ambient fluid.

From inspection of the coefficients of equation (D-87), the compression work, viscous dissipation, axial thermal conduction, and axial participating gas thermal radiation terms are at least three orders of magnitude less than the thermal convection, transverse thermal conduction, and transverse participating gas thermal radiation terms. Thus, the conservation of energy equation reduces to the form:

$$\left(\frac{L^2}{t_c \nu_c Gr^{1/2}}\right)\left[\rho C\frac{\partial T}{\partial t}\right]+\left[\rho u C\frac{\partial T}{\partial x}\right]+\left[\rho v C\frac{\partial T}{\partial y}\right] = \frac{1}{Pr}\left[\frac{\partial}{\partial y}\left(k\frac{\partial T}{\partial y}\right)\right]+\frac{Da}{PrGr^{1/2}}[Q]-\frac{St}{PrGr^{1/4}}\left[\frac{\partial q_{ry}}{\partial y}\right]. \qquad \text{(D-88)}$$

Note that acoustic phenomena are not important in equation (D-88) due to the absence of the pressure-work term.

The particle conservation equation (D-52) is scaled by substitution of the Stokes settling velocity, equation (D-49), the characteristic fluid velocity, equation (D-63), and the ratio of characteristic lengths, equation (D-65). The resulting equation is

$$\left(\frac{L^2}{t_c \nu_c Gr^{1/2}}\right)\left[\frac{\partial(\rho N)}{\partial t}\right]+\left[\frac{\partial}{\partial x}(\rho u N)\right]+\left[\frac{\partial}{\partial y}(\rho v N)\right] = \frac{2}{9}\left(\frac{\rho_p^*}{\rho_f^*}-1\right)\left(\frac{R}{L}\right)^2 \frac{T_\infty}{T_\infty - T_w} Gr^{1/2}\left[\frac{\partial(\rho N)}{\partial x}\right]$$

$$+\frac{1}{Gr^{1/2}}\left[\frac{\partial}{\partial x}\left(K_c\left[\rho N K \frac{\nu}{T}\frac{\partial T}{\partial x}\right]+\left(\frac{\mathcal{D}_c}{\nu_c}\right)\left[\mathcal{D}\frac{\partial(\rho N)}{\partial x}\right]\right)\right]$$

$$+\left[\frac{\partial}{\partial y}\left(K_c\left[\rho N K \frac{\nu}{T}\frac{\partial T}{\partial y}\right]+\left(\frac{\mathcal{D}_c}{\nu_c}\right)\left[\mathcal{D}\frac{\partial(\rho N)}{\partial y}\right]\right)\right] = 0. \qquad \text{(D-89)}$$

The coefficient of the first term on the right-hand side of equation (D-89) represents the relative importance of gravitational settling as a mechanism for removing particles from the flow. For the conditions of interest in the present investigation, the maximum value of this coefficient is approximately $10^{-5}$, indicating that Stokes settling is a negligible phenomenon. Further inspection of equation (D-89) shows that the remainder of the particle flux term in the $x$-direction is also negligible with respect to the convective terms and the particle flux term in the $y$-direction. The transient term in equation (D-89) has the same leading coefficient as the transient terms in the other fluid conservation equations. The importance of the transient term of the scaled particle conservation equation is considered in Section D.6 with the importance of the other transient terms of the governing equations.

The transverse particle flux term of equation (D-89) has two components, the thermophoretic particle flux and the diffusive particle flux. The leading coefficient of the scaled Brownian flux of unit order is the reciprocal Schmidt number of the particle in the fluid. The leading coefficient of the thermophoretic flux term is the characteristic value for the thermophoretic coefficient, $K$, which is of unit order. The particle Schmidt number is on the order of $10^4$ to $10^6$. These values indicate that the particle flux due to Brownian diffusion is negligible compared to the thermophoretic particle flux. As mentioned earlier in Section D-3, consideration of Brownian diffusion results in the

controversial boundary condition of zero particle concentration in the fluid at the wall. It is evident that *a singular perturbation does occur near the wall*, since a small parameter, $Sc^{-1}$, multiplies the highest order derivative. In order to meet this boundary condition, very steep concentration gradients occur near the wall resulting in a "boundary layer within a boundary layer." Near the wall, the Brownian diffusion term is not of order one, and equation (D-89) should be rescaled with a different characteristic value of particle concentration and spatial coordinate normal to the wall. This topic is discussed in Section 4.5 in great detail and will not be repeated here.

Apparent turbulent particle diffusion arose when formulating equations for the time-averaged turbulent flow as presented in Appendix B. For turbulent flows, the characteristic diffusion coefficient, $\mathcal{D}_c$, is on the order of the characteristic kinematic viscosity. Although analysis of equation (D-89) has shown that Brownian diffusion is negligible with respect to thermophoretic transport, the turbulent particle diffusion would not necessarily be negligible with respect to the thermophoretic transport.

The scaled diffusion term in brackets in equation (D-89) is manipulated further in order to scale the relative effect of individual density and particle concentration gradients. By use of the chain rule, the diffusive term in brackets is expanded as follows:

$$\left[\mathcal{D}\frac{\partial(\rho N)}{\partial y}\right] = \left[\rho\mathcal{D}\left\{\frac{\partial N}{\partial y}+\frac{N}{\rho}\frac{\partial \rho}{\partial y}\right\}\right] = \left[\rho\mathcal{D}\left\{\frac{\partial N}{\partial y}+N\frac{\partial \ln\rho}{\partial y}\right\}\right]$$

$$= \left[\rho\mathcal{D}\left\{\frac{\partial}{\partial y}(N+N\ln\rho)-\ln\rho\frac{\partial N}{\partial y}\right\}\right]. \qquad \text{(D-90)}$$

Since the dimensionless density, $\rho$, is of unit-order by definition, the logarithm of the dimensionless density, $\ln\rho$, in equation (D-90) must be of zero-order. The particle concentration, $N$, in equation (D-90) is also of unit-order by definition. The term $N\ln\rho$ must, therefore, be negligible with respect to the term $N$ and the term $\ln\rho\partial N/\partial y$ must be negligible with respect to the term $\partial N/\partial y$. Thus, inspection of equation (D-90) shows that the gradient of the product of the density and the particle concentration is approximately equal to the product of the density and the particle concentration gradient.

During the computations that were performed in the present investigation, the turbulent diffusion of momentum and energy was found to be approximately two orders of magnitude greater than the diffusion of momentum by viscous effects and diffusion of energy by thermal conduction. Since the particle was shown in Section 2.6 to be carried along with the turbulent eddy, turbulent diffusion of particles was found to dominate the particle transport in the turbulent region of the boundary layer. Thermophoresis was found to be important only when the temperature gradient became large, which for a turbulent flow occurs near the wall. Even though the relative importance of momentum, energy, and particle diffusion by turbulence compared to that by viscous diffusion, thermal conduction, and thermophoresis, was found to differ by two orders of magnitude across the boundary layer, no difficulties were encountered during numerical solution of the boundary layer equations. No advantage was seen in scaling the turbulence relationships and, therefore, scaling was not performed.

For the present investigation, the fluid density, the viscosity, the constant-pressure specific heat, and the thermal conductivity do not vary more than an order of magnitude over the range of expected conditions. This variance of thermophysical properties should therefore not affect the scales determined in this analysis.

The characteristic time for transient effects in the fluid and particle conservation equations has been left undetermined until now, when the transient heat transfer effects in the solid reactor vessel wall will be considered.

### D.5. Selection of the Reference Quantities for the Solid Domain

All characteristic quantities for the solid wall are representative of the reactor vessel material of carbon steel. The thermal diffusivity $\alpha_s$ is defined as:

$$\alpha_s = \frac{k_s}{\rho_s C_s}. \tag{D-91}$$

The length scale, $X_c$, must be the wall length, $L$, to be consistent with the fluid solution domain. The characteristic dimension of $Y_c$ is the thickness of the reactor

vessel wall, which is specified as 0.15 m. Writing the scaled conservation of energy equation for the solid wall, equation (D-60), in terms of the actual physical dimensions and values for the thermophysical properties yields:

$$\frac{Y_s^2}{\alpha_s t_s}\left[\rho C\frac{\partial T}{\partial t}\right] = (2.5\times 10^{-3})\left[\frac{\partial}{\partial x}\left(k\frac{\partial T}{\partial x}\right)\right]+\left[\frac{\partial}{\partial y}\left(k\frac{\partial T}{\partial y}\right)\right]. \tag{D-92}$$

Inspection of equation (D-92) shows that conduction of thermal energy in the $x$-direction is negligible with respect to the conduction of thermal energy in the $y$-direction. The characteristic time for the conservation of energy equation in the wall is then uniquely determined, since the leading coefficient of the transient term must be of order one to balance the conservation of energy equation governing the temperature in the reactor vessel wall. This characteristic time for the transient thermal response of the wall is

$$t_s = \frac{Y_s^2}{\alpha_s}. \tag{D-93}$$

### D.6. Selection of the Reference Quantities for the Coupled System

The governing differential equations of the fluid and wall could have been considered simultaneously, as this is a conjugate problem in which the heat flux and temperature must be matched at the interface. A final dimensionless parameter, $\varepsilon$, is defined as the ratio of the characteristic time for the fluid, equation (D-64), and the characteristic time for the solid wall, equation (D-93), such that

$$\varepsilon = \frac{t_c}{t_s} = \left(\frac{L}{Y_s}\right)^2\left(\frac{\alpha_s}{\nu_c}\right)\frac{1}{Gr^{1/2}}. \tag{D-94}$$

Introducing this parameter into the scaled equations of both solution domains, equations (D-44), (D-79), (D-88), (D-89), and (D-92), and by setting the solid wall characteristic time, $t_s$, as the time period of interest for solution of the coupled problem yields the following set of equations:

$$\text{(wall)} \qquad \left[\rho C \frac{\partial T}{\partial t}\right] = \left[\frac{\partial}{\partial y}\left(k \frac{\partial T}{\partial y}\right)\right], \tag{D-95}$$

$$\text{(fluid)} \qquad \varepsilon\left[\frac{\partial \rho}{\partial t}\right] + \left[\frac{\partial(\rho u)}{\partial x}\right] + \left[\frac{\partial(\rho v)}{\partial y}\right] = 0, \tag{D-96}$$

$$\text{(fluid)} \qquad \varepsilon\left[\rho \frac{\partial u}{\partial t}\right] + \left[\rho u \frac{\partial u}{\partial x}\right] + \left[\rho v \frac{\partial u}{\partial y}\right] = [B] + \left[\frac{\partial}{\partial y}\left(\mu \frac{\partial u}{\partial y}\right)\right], \tag{D-97}$$

$$\text{(fluid)} \qquad \varepsilon\left[\rho C \frac{\partial T}{\partial t}\right] + \left[\rho u C \frac{\partial T}{\partial x}\right] + \left[\rho v C \frac{\partial T}{\partial y}\right] = \frac{1}{Pr}\left[\frac{\partial}{\partial y}\left(k \frac{\partial T}{\partial y}\right)\right] + \frac{Da}{PrGr^{1/2}}[Q] - \frac{St}{PrGr^{1/4}}\left[\frac{\partial q_{r,y}}{\partial y}\right], \tag{D-98}$$

and

$$\text{(particles)} \quad \varepsilon\left[\frac{\partial(\rho N)}{\partial t}\right] + \left[\frac{\partial}{\partial x}(\rho u N)\right] + \left[\frac{\partial}{\partial y}(\rho v N)\right] + \left[\frac{\partial}{\partial y}\left(K_c\left[\rho N K \frac{\nu}{T}\frac{\partial T}{\partial y}\right] + \left(\frac{\mathcal{D}_c}{\nu_c}\right)\left[\rho \mathcal{D} \frac{\partial N}{\partial y}\right]\right)\right] = 0. \tag{D-99}$$

Substitution of the characteristic lengths and thermophysical properties of the fluid and wall into equation (D-94) yields the following expression for the ratio of characteristic times:

$$\varepsilon = \frac{10^3}{Gr^{1/2}}. \tag{D-100}$$

For Grashof numbers greater than $10^9$, the ratio of characteristic times is on the order of $10^{-2}$ or less. Considering only flows where the Grashof number is greater than $10^9$ allows all fluid transient terms to be neglected, which decouples the solid-wall

conservation of energy equation from the conservation equations for the particles and fluid. This decoupling allows specification of a constant wall temperature during the spatial integration of the fluid equations.

## APPENDIX E

## NOMENCLATURE

$A^+$ van Driest damping coefficient

$C$ Specific heat at constant pressure ($J \cdot kg^{-1} \cdot K^{-1}$)

$\mathcal{D}$ Diffusion coefficient ($m^2 \cdot s^{-1}$)

$F$ Body Force per unit fluid mass ($m \cdot s^{-2}$)

$H$ Paolucci criterion, equation (3-11)

$H_l$ Ratio of $Nu/Ra^{1/4}$, equation (4-48)

$H_t$ Ratio of $Nu/Ra^{1/3}$, equation (4-50)

$I$ Intensity

$K$ Thermophoretic coefficient

$L$ Plate length (m)

$M$ Conduction to radiation parameter, equation (2-6)

$M_p$ Aerosol particle mass (kg)

$N$ Number of particles per unit fluid mass ($kg^{-1}$)

$P$ Pressure (Pa)

$Q$ Volumetric heat strength ($W \cdot m^{-3}$)

$\mathcal{R}$ Ideal gas constant (8.3143 $kJ \cdot mol^{-1} \cdot K^{-1}$)

$R$ Particle radius (m)

$S^+$ Dimensionless stopping distance, equation (2-3)

$T$ Temperature (K)

$V_g$ Stokes settling velocity, equation (D-49) ($m \cdot s^{-1}$)

$V_T$ Thermophoretic velocity, equation (4-7) ($m \cdot s^{-1}$)

$d_p$ Particle diameter (m)

$f$ Dimensionless stream function, equation (4-34)

$g$ Gravitational acceleration constant (9.8 $m \cdot s^{-2}$)

$h_H$ Heat transfer coefficient, equation (4-53) ($W \cdot m^{-2}$)

$h_p$ Particle transfer coefficient, equation (4-56) ($m \cdot s^{-1}$)

$j^*$ Aerosol mass flux ($kg \cdot m^{-2} \cdot s^{-1}$)

$j_P$ Particle flux ($mol \cdot m^{-2} \cdot s^{-1}$)

$j_H$ Heat flux ($J \cdot m^{-2} \cdot s^{-1}$)

$k$ Thermal conductivity ($W \cdot m^{-1} \cdot K^{-1}$)

$n$ Dimensionless particle concentration, equation (4-36)

$t$ Time (s)

$u,v$ Streamwise and normal velocity ($m \cdot s^{-1}$)

$u^*$ Friction velocity ($m \cdot s^{-1}$)

$x,y$ Streamwise and normal position (m)

$y^+$ Dimensionless wall distance

**Greek Letters:**

$\alpha$ Accommodation coefficient, equation (C-6)

$\alpha$ Thermal diffusivity ($m^2 \cdot s^{-1}$)

$\alpha$ Volumetric fraction

$\beta$ Isobaric volumetric expansion coefficient ($K^{-1}$)

$$\beta = -\frac{1}{\rho}\left(\frac{\partial \rho}{\partial T}\right)_P$$

$\gamma$ Heat generation rate per particle (W)

$\gamma$ Klebanoff intermittency factor, equation (4-28)

$\delta$ Boundary layer thickness (m)

$\delta$ Thermal microscale (m)

$\varepsilon$ Characteristic time ratio, equation (D-94)

$\varepsilon$ Eddy diffusivity ($m^2 \cdot s^{-1}$)

$\eta$ Pseudosimilarity variable, equation (4-33)

$\theta$ Dimensionless fluid temperature, equation (4-35)

$\kappa$ Thermal radiation absorption coefficient ($m^{-1}$)

$\lambda$ Wall overheat ratio, equation (4-37)

$\lambda$ Mean free path (m)

$\mu$ Dynamic viscosity (Pa·s)

$\mu$ Gamma ray attenuation coefficient ($m^{-1}$)

$\nu$ Kinematic viscosity ($m^2 \cdot s^{-1}$)

$\xi$ Dimensionless streamwise variable, equation (4-32)

$\rho$ Density ($kg \cdot m^3$)

$\sigma$ Stefan-Boltzmann constant ($5.67 \times 10^{-8} W \cdot m^{-2} \cdot K^{-4}$)

$\tau$ Optical depth

$\tau$ Fluid shear stress (Pa)

$\psi$ Dimensional stream function, equation (4-31) ($m^2 \cdot s^{-1}$)

$\omega$ Bounding limit fraction, equation (4-93)

**Dimensionless Groups:**

*Bo* Boussinesq number, (*Ra*·*Pr*)

*Da* Damköhler number, equation (4-39)

*Gr* Grashof number

$$Gr = \frac{g(\rho_\infty - \rho_w)x^3}{\rho_\infty \nu^2}$$

*Kn* Knudsen number ($\lambda$ / *R*)

*Ma* Mach number ($u/u_{sonic}$)

*Nu* Nusselt number ($h_H x)/k$

$Ra^*$ Rayleigh number, equation (2-1)

*Ra* Rayleigh number (*Gr*·*Pr*)

*Sc* Schmidt number ($\nu/\mathcal{D}$)

*Sh* Sherwood number, equation (5-8)

*St* Stefan number, equation (D-85)

*Pr* Prandtl number ($\nu/\alpha$)

**Subscripts:**

$\infty$ Conditions far from the wall

$\infty$,0 Leading edge conditions far from the wall

*a* Aerosol

*B* Brownian

$c$ Characteristic

$f$ Fluid

$H$ Heat

$h$ Hydrostatic

$L$ Plate length (m)

$M$ Momentum

$m$ Motion

$p$ Particle

$r$ Reference value

$s$ Solid

$t$ Turbulent

$T$ Thermophoresis

$w$ Wall conditions

$x$ Local conditions

## VITA

James Charles Conklin was born on May 3, 1948 in Hartford, Connecticut. His father is Charles Edward Conklin and his mother is Faith Florence Conklin (nee Ringquist), both of whom reside in Newington, Connecticut. He attended the public schools of Newington, Connecticut, and was graduated with honors from Newington High School in 1966. He then attended the University of Connecticut and was awarded a Batchelor of Science in Engineering degree, with honors, in Mechanical Engineering in 1970. He then attended the Massachusetts Institute of Technology and was awarded a Master of Science in Nuclear Engineering degree in 1971.

He then reported on active duty in the U. S. Air Force at Cape Canaveral Air Force Station, Florida. Leaving the Air Force in 1974, he accepted employment at Oak Ridge National Laboratory (ORNL) in Oak Ridge, Tennessee, in 1975, and settled in Knoxville, Tennessee. He married Carol Ann Beavers on June 16, 1977.

He entered The Graduate School of The University of Tennessee in 1980 and attended classes part-time while employed at ORNL. Taking a leave of absence from ORNL in 1983, he devoted all his efforts towards his doctoral dissertation at The University of Tennessee until 1985, when he then returned to employment at ORNL. He is presently a development staff member at ORNL.